Atomic and Mass Spectrometry

METHOD DEVELOPMENT FOR ULTRA-TRACE ELEMENTAL AND ISOTOPIC ANALYSIS USING TANDEM ICP – MASS SPECTROMETRY (ICP-MS/MS)

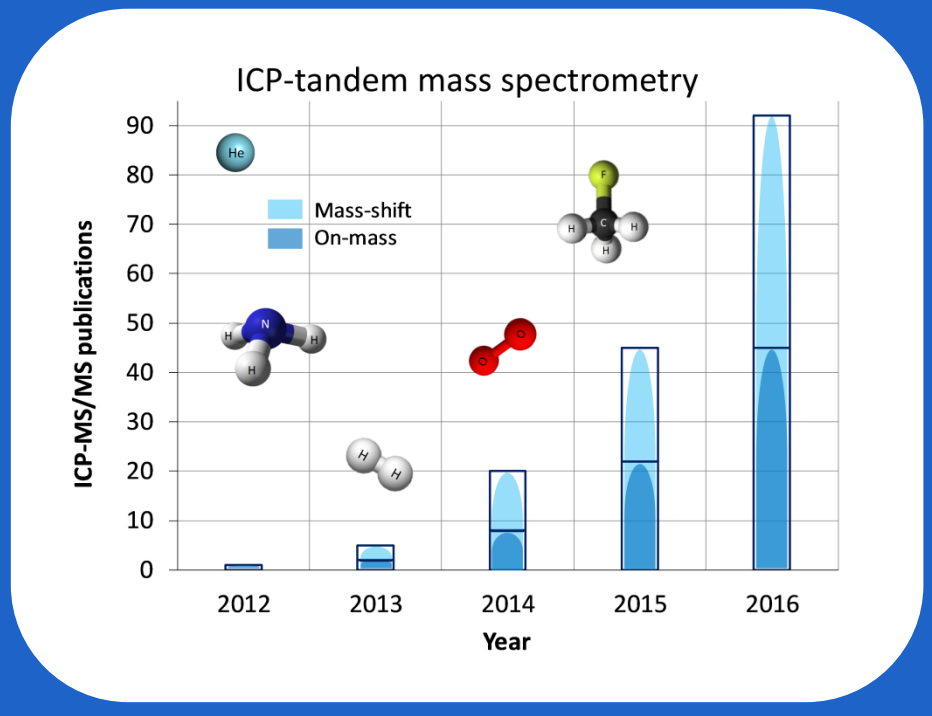

Eduardo Bolea Fernández

2017

Eduardo Bolea Fernández

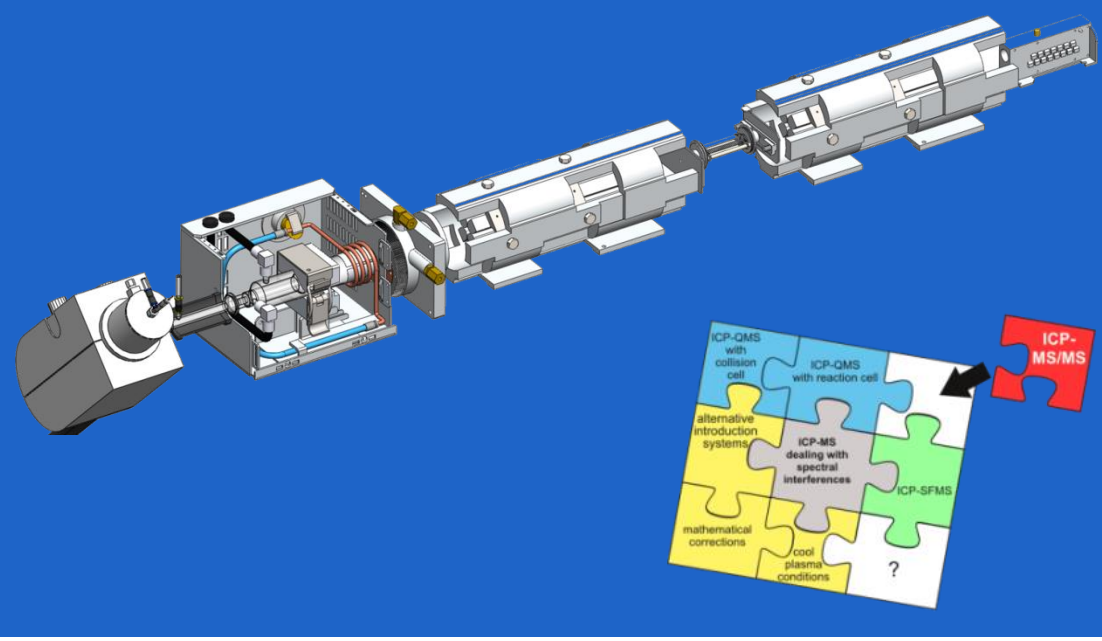

GHENT UNIVERSITY

FACULTY OF SCIENCES

SUPERVISORS:

Prof. Dr. Frank Vanhaecke

Prof. Dr. Martín Resano

Dr. Lieve Balcaen

FACULTY OF SCIENCES

DEPARTMENT OF ANALYTICAL CHEMISTRY
ATOMIC AND MASS SPECTROMETRY (A&MS)

METHOD DEVELOPMENT FOR ULTRA-TRACE ELEMENTAL AND ISOTOPIC ANALYSIS USING TANDEM ICP – MASS SPECTROMETRY (ICP-MS/MS)

Eduardo Bolea Fernández
Student number: 01209885

Supervisor(s): Prof. Dr. Frank Vanhaecke, Prof. Dr. Martín Resano, Dr. Lieve Balcaen

A dissertation submitted to Ghent University in partial fulfilment of the requirements for the degree of Doctor of Science: Chemistry

Academic year: 2016 – 2017

GHENT UNIVERSITY

Para mi familia

Para Ana

Contents

Abbreviations

amu	atomic mass unit
ANOVA	analysis of variance
AS	abundance sensitivity
BCR	Community Bureau of Reference
BEC	background – equivalent concentration
BOF-UGent	Ghent University Special Research Fund
CID	collision – induced dissociation
CRC	collision/reaction cell
CRM	certified reference material
DBS	dried blood spot
DRC	dynamic reaction cell
EBI	elemental bio-imaging
EDTA	ethylenediaminetetraacetic acid
EM	electron multiplier
ETAAS	electrothermal atomization atomic absorption spectrometry
eV	electronvolt
f	mass bias correction factor
F	value in a F-test of variances
FDNPP	Fukushima Daiichi nuclear power plant
FFF	field-flow fractionation
FWO	Flemish Research Foundation
GC	gas chromatography
GeoReM	geological and environmental reference materials database
HCT	hematocrit
HG	hydride generation

HPLC	high – performance liquid chromatography
HR	high resolution
IARC	International Agency for Research on Cancer
ICP	inductively coupled plasma
ICP-CRC-QMS	quadrupole based – inductively coupled plasma – mass spectrometry equipped with collision/reaction cell
ICP-MS	inductively coupled plasma – mass spectrometry
ICP-MS/MS	inductively coupled plasma – tandem mass spectrometry
ICP-OES	inductively coupled plasma – optical emission spectrometry
ICP-QQQ	triple quadrupole – inductively coupled plasma – mass spectrometry
ICP-QMS	quadrupole based – inductively coupled plasma – mass spectrometry
ICP-SIFT-MS	inductively coupled plasma selected-ion flow tube mass spectrometry
IDMS	isotope dilution mass spectrometry
KED	kinetic energy discrimination
LA	laser ablation
LC	liquid chromatography
LOD/LoD	limit of detection
LOQ/LoQ	limit of quantification
m	mass
MC-ICP-MS	multi-collector – inductively coupled plasma – mass spectrometry
MDL	method detection limit
MoM	metal-on-metal
MPI-DING	Max-Planck-Institut für Chemie, Germany
MQL	method quantification limit

MRI	magnetic resonance imaging
MS	mass spectrometry
MS/MS	mass/mass or double mass selection
m/z	mass-to-charge ratio
NBS	National Bureau of Standards, USA
NCR – CNRC	National Research Council Canada – Conseil National de Recherches Canada
NIST	National Institute of Standards and Technology
ORS	octopole reaction system
PGMs	Platinum group metals
PIS	product ion scanning
PN	pneumatic nebulization
PTFE	polytetrafluoroethylene
Q1	first quadrupole
Q2	second quadrupole
QC	quality control
QDs	quantum dots
QMS	quadrupole mass spectrometry
R	resolution
RMs	reference materials
RSD	relative standard deviation
s	standard deviation
SF-ICP-MS	sector-field – inductively coupled plasma – mass spectrometry
SQ	single quadrupole
S/N	signal-to-noise ratio
SRM	standard reference material

SSB	sample – standard bracketing approach
t	t-student
TIMS	thermal ionization mass spectrometry
UGent	Ghent University
USGS	United States Geological Survey, VA, USA
VAMS	volumetric absortive micro-sampling
VUB	Vrije Universiteit Brussel (Brussels free University)
WTO	wait time offset

Outlook and goals

Inductively coupled plasma – mass spectrometry (ICP-MS) is a widespread technique that can provide quantitative information on both the concentration and the isotopic composition of (ultra)traces of metals and metalloids in a large variety of sample types. Despite many advantages, the technique also suffers from drawbacks such as the occurrence of spectral and non-spectral interferences. Since the introduction of the first commercially available ICP-MS instrument in 1983, several instrumental developments have been made in order to tackle the problem of spectral overlap. Among the different improvements implemented over the years, the introduction of high-resolution sector-field ICP-MS (HR-SF-ICP-MS) instrumentation, and of collision/reaction cells into quadrupole-based ICP-MS (ICP-CRC-QMS) instruments, can be considered as the most powerful ones. However, the use of HR-SF-ICP-MS is typically accompanied by a significant reduction in sensitivity (1 - 2 orders of magnitude), whereas in ICP-CRC-QMS, the use of an inert collision gas in combination with kinetic energy discrimination (KED) also compromises sensitivity. The efficiency of the separation of analyte and interfering ions by using a reactive gas in ICP-CRC-QMS, on the other hand, is dependent on the availability of selective ion-molecule reactions within the CRC for the given combination of analyte and interfering ions.

In 2012, the gamut of quadrupole-based ICP-MS instruments was extended with the introduction of a tandem ICP – mass spectrometer (ICP-MS/MS). This instrument resembles a conventional ICP-CRC-QMS unit but with an additional quadrupole located before the CRC, thus leading to the configuration QMS-CRC-QMS. The ICP-MS/MS instrument has been specifically designed to deal with spectral overlap in a more effective way than the more conventional ICP-CRC-QMS systems. This novel set-up allows one to select ions with a specific mass-to-charge (m/z) ratio in the first quadrupole (Q1), while all interferences with m/z ratios different than the one of the target nuclide can be easily removed from the ion beam, before it enters the CRC. This leads to an enhanced control over the collisions and reactions taking place in the CRC, and consequently, more selective ion-molecule reactions with highly reactive gases, increasing the chances for highly accurate and interference-free determination of elemental concentrations and isotope ratios.

Although for a while high-resolution sector-field instruments have been considered far superior to quadrupole-based mass spectrometers, the recent introduction of tandem ICP – mass spectrometry is bridging the gap between instruments equipped with sector-field and quadrupole mass analyzers. It needs to be pointed out that ICP-MS/MS has been introduced very recently (2012) only. However, the fast increase in the number of scientific publications describing ICP-MS/MS-based applications over the last few years, already illustrates the enormous potential of this technique.

Since January 2013, the Atomic & Mass Spectrometry (A&MS) research group of Ghent University is housing such a tandem ICP – mass spectrometer (the first ICP-MS/MS unit installed in Belgium). The main goal of this PhD thesis was a characterization of this instrument and an exploration of the capabilities of this novel technique for a variety of applications, in order to evaluate the versatility of this type of instrumentation.

The first chapter of this PhD dissertation provides the reader with a general overview of the operating principles of tandem ICP – mass spectrometry, including a description of the instrument set-up, its different operation modes and scanning options as powerful tools for method development, as well as the most widely used approaches to deal with spectral overlap. In addition, some of the most demanding applications reported on in the literature to date are discussed in order to further illustrate the fundamental concepts.

Chapter 2 reports on the development of a novel method for the accurate determination of ultra-trace levels of Ti in human serum samples. Ti is frequently used in implants and prostheses, and their presence in the human body can lead to elevated Ti concentrations in body fluids. Until now, only SF-ICP-MS offered limits of detection that are sufficiently low for accurate determination of the basal levels of Ti in human serum. This work explores the capabilities of ICP-MS/MS using O_2 and NH_3/He reaction gases to overcome the spectral overlap.

In chapter 3, the performance of methyl fluoride (a mixture of 10% CH_3F and 90% He) as a reaction gas in ICP-MS/MS is evaluated in the context of the determination of ultra-trace concentrations of medically relevant metals (Al, Co, Cr, Mn, Ni, Ti and V) in blood serum and urine. While CH_3F is currently not one of the standard reaction gases recommended by the instrument manufacturer, earlier work in the

A&MS research unit and information available in the literature implied that this gas could provide good results. An optimized ICP-MS/MS method for single-element monitoring and a multi-element method under compromise conditions were developed. For validation purposes, the results thus obtained were compared with those of sector-field ICP-MS analysis of the same samples.

Chapter 4 describes the capabilities of ICP-MS/MS with CH_3F/He as a reaction gas for dealing with spectral overlap in the analysis of human blood, when using volumetric absorptive micro-sampling (VAMS) for sample collection. For validation purposes, a simple dilute-and-shoot approach (consisting of a 100-fold dilution) followed by ICP-MS/MS analysis has been developed for the accurate and sensitive determination of prosthesis-related metals (Al, Co, Cr, Ni, Sr, Ti, V and Zr) in whole blood.

Whereas chapters 2, 3 and 4 deal with the ultra-trace determination of metals in biofluids, i.e. urine, serum and whole blood, chapter 5 focuses on As and Se, two environmentally relevant elements that are strongly affected by Ar-based polyatomic interferences, i.e. $ArCl^+$ and Ar_2^+. The capabilities of the approach developed, which is based on a specific reaction pathway consisting of HF elimination after CH_3F addition, is evaluated by using synthetic matrices, containing elements that give rise to interfering ions, and a collection of reference materials from plant, animal and environmental origin, displaying a wide range of As and Se concentrations.

While the first part of this PhD thesis is devoted to ultra-trace elemental analysis, the capabilities of ICP-MS/MS in the context of isotopic analysis have been evaluated as well. For the work described in chapter 6, chemical resolution was used to avoid the isobaric overlap of ^{87}Rb and ^{87}Sr, enabling the accurate determination of the $^{87}Sr/^{86}Sr$ isotope ratio in geological materials. With such approach, no prior Rb/Sr separation is required as Rb and Sr show different reactivity towards the reaction gas. Next to spectral overlap, also mass discrimination and matrix effects can have a detrimental influence on the accuracy of the isotope ratio results. Both effects were studied and appropriate correction methods were selected.

Finally, in chapter 7, the use of a combination of laser ablation and tandem ICP – mass spectrometry (LA-ICP-MS/MS) is described for Sr isotopic analysis of solid samples with high Rb/Sr ratio. The approach described in chapter 6 is used in this

context to avoid the spectral overlap. Two sample introduction setups, leading to "dry" and "wet" plasma conditions, respectively, were evaluated and the figures of merit documented in detail. $^{87}Sr/^{86}Sr$ isotope ratio results were obtained for 7 glass-type geological reference materials, without the requirement of using closer matrix-matching for mass bias correction using a glass reference material (NIST SRM 610).

Nederlandstalige abstract

Inductief gekoppeld plasma - massaspectrometrie (ICP-MS) is een wijdverspreide techniek waarmee kwantitatieve informatie kan bekomen worden over de concentratie en de isotopische samenstelling van (ultra)sporen van metalen of metalloiden in een grote varieteit aan monstermaterialen. Naast de vele voordelen, kent de techniek ook enkele nadelen, zoals het voorkomen van spectrale en niet-spectrale interferenties. Sinds de introductie van het eerste commercieel beschikbare ICP-MS instrument in 1983, werden reeds verschillende instrumentele ontwikkelingen voorgesteld om het probleem van spectrale overlap aan te pakken. Hierbij kunnen de introductie van hoge resolutie sector-veld ICP-MS (HR-SF-ICP-MS) instrumentatie, en van botsings-/reactiecellen in quadrupool-gebaseerde ICP-MS (ICP-CRC-QMS) apparaten gezien worden als de meest krachtige methodes. Het gebruik van een hogere massaresolutie in HR-SF-ICP-MS gaat echter gepaard met een significante reductie in de gevoeligheid (1-2 grootteordes), terwijl in ICP-CRC-QMS het gebruik van een inert botsingsgas in combinatie met kinetische energiediscriminatie (KED) eveneens een negatieve invloed heeft op de gevoeligheid. Indien daarentegen een reactief gas aangewend wordt in ICP-CRC-QMS, is de efficiëntie van de scheiding van analietionen en interfererende ionen afhankelijk van de beschikbaarheid van selectieve ion-molecule reacties in de CRC voor deze specifieke combinatie van analiet- en interfererende ionen.

In 2012 werd het gamma aan quadrupool-gebaseerde ICP-MS instrumenten uitgebreid met een tandem ICP-massaspectrometer (ICP-MS/MS). Dit type apparaat vertoont grote gelijkenis met de traditionele ICP-CRC-QMS systemen, maar is uitgerust met een extra quadrupool tussen de interface en de reactiecel. De meerwaarde van de ICP-MS/MS apparatuur is te vinden in de meer efficiënte manier waarop kan omgegaan worden met spectrale overlap. In de eerste quadrupool kunnen immers alle interferenties met een m/z verhouding verschillend van deze van de analietnuclide reeds uit de ionenbundel verwijderd worden, nog voor deze in de CRC binnengeleid wordt. Op deze manier is een verhoogde controle mogelijk over de botsingen en reacties die plaatsvinden in de botsings-/reactiecel, zodat meer selectieve ion-molecule reacties met hoog reactieve gassen kunnen plaatsvinden en de mogelijkheden voor zeer accurate en interferentievrije bepaling van elementconcentraties of isotopenverhoudingen sterk toenemen. Daardoor mag algemeen gesteld worden dat tandem ICP-MS de kloof dicht tussen instrumenten

uitgerust met een sector-veld massaspectrometer en deze met (één) quadrupoolmassaspectrometer. Hoewel ICP-MS/MS pas geïntroduceerd werd in 2012, toont de snelle toename in het aantal publicaties over onderzoek dat gebruik maakt van deze techniek het grote potentieel ervan aan.

Sinds januari 2013 is een tandem ICP-MS apparaat in gebruik in de onderzoeksgroep Atoom- en MassaSpectrometrie (A&MS) van de Universiteit Gent (het eerste ICP-MS/MS apparaat dat geïnstalleerd werd in België). Het hoofddoel van dit doctoraatsonderzoek bestond erin dit instrument te karakteriseren en de mogelijkheden van deze nieuwe technologie te evalueren voor een grote verscheidenheid aan toepassingen.

Het eerste hoofdstuk van dit werk brengt een inleiding tot het werkingsprincipe van tandem ICP-MS en beschrijft de instrumentele set-up, de verschillende gebruikswijzes en scanmodi die beschikbaar zijn voor methode-ontwikkeling en de meest gebruikte methodes om spectrale overlap te verhinderen. Als illustratie van deze eerder fundamentele concepten, wordt daarnaast ook een overzicht gegeven van enkele veeleisende toepassingen die in de literatuur werden beschreven.

Hoofdstuk 2 behandelt de ontwikkeling van een nieuwe methode voor de accurate bepaling van ultrasporen Ti in menselijk serum. Ti wordt de laatste jaren frequent gebruikt in implantaten en de vraag rijst of de aanwezigheid van dergelijke implantaten in het menselijk lichaam aanleiding geeft tot verhoogde Ti concentraties in lichaamsvloeistoffen. Tot nog toe kon de spectrale overlap waardoor de bepaling van Ti in deze matrix gehinderd wordt enkel adequaat voorkomen worden met SF-ICP-MS, zodat enkel via deze techniek voldoende lage detectielimieten konden bereikt worden voor een accurate bepaling van de basale Ti gehaltes in menselijk serum. In dit werk werden de mogelijkheden van ICP-MS/MS onderzocht in deze context, met behulp van O_2 en NH_3/He als reactiegassen.

In hoofdstuk 3 worden de mogelijkheden beschreven van het gebruik van methylfluoride (mengsel van 10% CH_3F en 90% He) als reactiegas in ICP-MS/MS, in de context van de bepaling van ultrasporen van medisch relevante metalen (Al, Co, Cr, Mn, Ni, Ti en V) in bloedserum en urine. CH_3F werd niet aangeboden als één van de standaard reactiegassen door de instrumentleverancier, maar eerder werk binnen de A&MS onderzoeksgroep en informatie beschikbaar in de literatuur lieten vermoeden dat met behulp van dit reactieve gas goede resultaten zouden kunnen

bekomen worden. Voor de beschreven toepassing werden zowel mono-element methodes ontwikkeld (bepaling van elk element afzonderlijk onder de meest optimale instrumentele condities) als een multi-element methode voor de simultane bepaling van alle elementen onder compromisomstandigheden. Naast ICP-MS/MS analyses, werden tevens sector-veld analyses uitgevoerd van dezelfde stalen voor validatiedoeleinden.

Hoofdstuk 4 beschrijft de mogelijkheden van ICP-MS/MS met CH_3F/He als reactiegas voor de analyse van menselijk bloed wanneer gebruik gemaakt wordt van 'volumetric absorptive micro-sampling (VAMS)' voor monstername. Om de resultaten voor de VAMS-stalen te kunnen valideren, werd tevens een eenvoudige 'dilute-and-shoot' methode ontwikkeld voor de accurate en gevoelige bepaling van implantaat-gerelateerde metalen (Al, Co, Cr, Ni, Sr, Ti, V en Zr) in volbloed. Deze methode bestond uit een eenvoudige verdunning van het bloed (100x), en daaropvolgende ICP-MS/MS analyse.

Waar in hoofdstukken 2, 3 en 4 metalen in biologische matrices werden bepaald, focusseert het werk beschreven in hoofdstuk 5 zich op de bepaling van As en Se – twee elementen die belangrijk zijn in een milieu-context, en waarvan de ICP-MS bepaling sterk gehinderd wordt door spectrale overlap met onder andere Ar-gebaseerde polyatomische ionen zoals $ArCl^+$ en Ar_2^+. De aanpak die werd vooropgesteld is het gebruik van CH_3F/He in het ICP-MS/MS apparaat vermits As^+ en Se^+ ionen een specifiek reactiegedrag vertonen ten opzichte van CH_3F, namelijk CH_3F additie, met daaropvolgend HF eliminatie. De mogelijkheden van deze aanpak werden geïllustreerd door de studie van synthetische matrices die elementen bevatten die aanleiding geven tot interfererende ionen, en van een collectie referentiematerialen relevant in de context van milieu-onderzoek, die een brede range aan As en Se concentraties bestrijken.

Naast ultrasporen-elementanalyse werden ook de mogelijkheden van ICP-MS/MS voor isotopische analyse bestudeerd. In hoofstuk 6 wordt het gebruik van chemische resolutie (met CH_3F/He in de reactiecel) voor het verhinderen van de spectrale overlap van ^{87}Rb en ^{87}Sr beschreven, om accurate bepaling van de $^{87}Sr/^{86}Sr$ isotopenverhouding in geologische materialen mogelijk te maken, zonder voorafgaande afscheiding van Rb uit de matrix. Naast spectrale interferenties kunnen ook massadiscriminatie en matrixeffecten een nefaste invloed hebben op de

accuratesse van de resultaten van isotopische analyse. Beide effecten werden bestudeerd en geschikte correctiemethodes werden geselecteerd.

Tot slot wordt in hoofdstuk 7 de combinatie van laser ablatie met tandem ICP-MS (LA-ICP-MS/MS) beschreven voor de directe isotopische analyse van vaste materialen met een hoge Rb/Sr-verhouding. Hiervoor werd gebruik gemaakt van de methode die in hoofstuk 6 werd beschreven, maar diende extra aandacht besteed te worden aan de meest geschikte wijze van monsterintroductie. Twee verschillende opstellingen werden hierbij vergeleken, namelijk één leidend tot “droge” en één leidend tot “natte” plasmacondities. Na optimalisatie en selectie van de meest geschikte omstandigheden, werden $^{87}Sr/^{86}Sr$ isotopenverhoudingen bepaald voor 7 glasachtige geologische referentiematerialen, waarbij het gebruik van een glas referentiemateriaal (NIST SRM 610) volstond voor massadiscriminatie-correctie, en dus geen meer specifieke matrix-matching van de standaard noodzakelijk was.

Scientific impact

1. List of peer-reviewed scientific publications

1.1. Peer-reviewed scientific publications in international journals included in this PhD thesis

1. Lieve Balcaen, Eduardo Bolea-Fernandez, Martín Resano, Frank Vanhaecke. Accurate determination of ultra-trace levels of Ti in blood serum using ICP-MS/MS. Analytica Chimica Acta, 809 (2014) 1 – 8. Q1, IF: 4.513

2. Eduardo Bolea-Fernandez, Lieve Balcaen, Martín Resano, Frank Vanhaecke. Potential of methyl fluoride as a universal reaction gas to overcome spectral interference in the determination of ultratrace concentrations of metals in biofluids using Inductively Coupled Plasma – Tandem Mass Spectrometry. Analytical Chemistry, 86 (2014) 7969 – 7977. Q1, IF: 5.636

3. Eduardo Bolea-Fernandez, Lieve Balcaen, Martín Resano, Frank Vanhaecke. Interference-free determination of ultra-trace concentrations of arsenic and selenium using methyl fluoride as a reaction gas in ICP-MS/MS. Analytical and Bioanalytical Chemistry, 407 (2015) 919 – 929. Q1, IF: 3.125

4. Lieve Balcaen, Eduardo Bolea-Fernandez, Martín Resano, Frank Vanhaecke. Inductively coupled plasma – tandem mass spectrometry (ICP-MS/MS): A powerful and universal tool for the interference-free determination of (ultra)trace elements – A tutorial review. Analytica Chimica Acta, 894 (2015) 7 – 19. Q1, IF: 4.712.

5. Eduardo Bolea-Fernandez, Lieve Balcaen, Martín Resano, Frank Vanhaecke. Tandem ICP – mass spectrometry for Sr isotopic analysis without prior Rb/Sr separation. Journal of Analytical Atomic Spectrometry, 31 (2016) 303 – 310. Q1, IF: 3.379

6. Eduardo Bolea-Fernandez, Stijn J. M. Van Malderen, Lieve Balcaen, Martín Resano, Frank Vanhaecke. Laser ablation – tandem ICP – mass spectrometry (LA-ICP-MS/MS) for direct Sr isotopic analysis of solid samples with high Rb/Sr ratios. Journal of Analytical Atomic Spectrometry, 31 (2016) 464 – 472. Q1, IF: 3.379.

7. Eduardo Bolea-Fernandez, Kim Phan, Lieve Balcaen, Martín Resano, Frank Vanhaecke. Determination of ultra-trace amounts of prosthesis-related metals in whole blood using volumetric absorptive micro-sampling and tandem ICP – Mass spectrometry. Analytica Chimica Acta, 941 (2016) 1 – 9. Q1, IF: 4.712.

8. Eduardo Bolea-Fernandez, Lieve Balcaen, Martín Resano, Frank Vanhaecke. Overcoming spectral overlap via inductively coupled plasma-tandem mass spectrometry (ICP-MS/MS). A tutorial review. Journal of Analytical Atomic Spectrometry (2017) DOI: 10.1039/c7ja00010c. Q1, IF: 3.379.

1.2. Other peer-reviewed scientific publications in international journals

1. Martín Resano, Eduardo Bolea-Fernandez, Engracia Mozas, María R Flórez, Patricia Grinberg, Ralph E. Sturgeon. Simultaneous determination of Co, Fe, Ni and Pb in carbon nanotubes by means of solid sampling high-resolution continuum source graphite furnace atomic absorption spectrometry. Journal of Analytical Atomic Spectrometry, 28 (2013) 657 – 665. Q1, IF: 3.396.

2. María R. Flórez, Esperanza García-Ruiz, Eduardo Bolea-Fernandez, Frank Vanhaecke, Martín Resano. A simple dilute-and-shoot approach for the determination of ultra-trace levels of arsenic in biological fluids via ICP-MS using CH3F/He as a reaction gas. Journal of Analytical Atomic Spectrometry, 21 (2016) 245 – 251. Q1, IF: 3.379.

3. Ana Rua-Ibarz, Eduardo Bolea-Fernandez, Frank Vanhaecke. An in-depth evaluation of accuracy and precision in Hg isotopic analysis via pneumatic nebulization and cold vapor generation multi-collector ICP-mass spectrometry. Analytical and Bioanalytical Chemistry, 408 (2016) 417 – 429. Q1, IF: 3.125.

4. Balazs Klencsár, Eduardo Bolea-Fernandez, María R. Flórez, Lieve Balcaen, Filip Cuyckens, Frederic Lynen, Frank Vanhaecke. Journal of Pharmaceutical and Biomedical Analysis, 124 (2016) 112 – 119. Q1, IF: 3.169.

5. Ana Rua-Ibarz, Eduardo Bolea-Fernandez, Amund Maage, Sylvia Frantzen, Stig Valdersnes, Frank Vanhaecke. Assessment of Hg pollution released from a WWII submarine wreck (U-864) by Hg isotopic analysis of sediments and *Cancer pagurus* tissues. Environmental Science & Technology, 50 (2016) 10361 – 10369. Q1, IF: 5.396.

2. Conference proceedings

2.1. Presentations on international conferences

1. Eduardo Bolea-Fernandez, Lieve Balcaen, Martín Resano, Frank Vanhaecke. Methyl fluoride and inductively coupled plasma – tandem mass spectrometry (ICP-MS/MS): A universal solution to overcome spectral overlap in ICP-MS?. *2015 European Winter Conference on Plasma Spectrochemistry*. 22 – 26 February 2013, Münster, Germany. Oral presentation.

2. Eduardo Bolea Fernández, Stijn J.M. Van Malderen, Lieve Balcaen, Martín Resano, Frank Vanhaecke. Pneumatic nebulization (PN-ICP-MS/MS) and laser ablation tándem ICP-mass spectrometry (LA-ICP-MS/MS) as novel tools for straightforward strontium isotopic analysis. *2016 Winter Conference on Plasma Spectrochemistry*. 10 – 16 January 2016, Tucson, United States of America. Oral presentation.

3. Eduardo Bolea-Fernandez, Lieve Balcaen, Martín Resano, Frank Vanhaecke. Tandem ICP – mass spectrometry with chemical resolution: An ideal tool for the determination of ultra-trace concentrations of metals and metalloids in environmental samples. *18th International Conference on Heavy Metals in the Environment*. 12 – 15 September 2016, Ghent, Belgium. Oral presentation

2.2. Presentation on international conferences by other co-authors

1. Lieve Balcaen, Eduardo Bolea Fernández, Martín Resano, Frank Vanhaecke. Accurate determination of ultratrace levels of Ti in blood serum using ICP-MS/MS. *2014 Winter Conference on Plasma Spectrochemistry*. 6 – 11 January 2014, Florida, United States of America. Oral presentation.

2. Martín Resano Ezcaray, María R. Flórez García, Esperanza García-Ruiz; Eduardo Bolea-Fernández, Lieve Balcaen, Frank Vanhaecke. Atomic Techniques, Molecular Species. *13th Rio Symposium on Atomic Spectrometry.* 19 – 24 October 2014, Mérida, Yucatán, México. Oral presentation. Invited lecture.

3. Frank Vanhaecke, Yulia Anoshkina, Maite Aramendia, Lieve Balcaen, Eduardo Bolea-Fernandez, Marta Costas-Rodriguez, Joris Delanghe, Martín Resano, Stijn Van Malderen, Hans Van Vlierberghe. ICP–mass spectrometry as an emerging tool for medical diagnosis. *2015 European Winter Conference on Plasma Spectrochemistry.* 22 – 26 February 2015, Münster, Germany. Invited lecture.

4. Frank Vanhaecke, Yulia Anoshkina, Lieve Balcaen, Eduardo Bolea-Fernandez, Marta Costas-Rodriguez, Sara Lauwens, Lana Van Heghe, Stijn Van Malderen. Instrument evolution in ICP – mass spectrometry renders the technique ever more useful in biomedical analysis. *Colloquium Analytische Atomspektrometrie Canas.* 2015, 8 – 11 March 2015, Leipzig, Germany. Invited lecture.

5. Martín Resano, María R. Flórez, Esperanza García-Ruiz, Eduardo Bolea-Fernández, Frank Vanhaecke, Flavio Nakadi. Elemental analysis, atomic? Techniques. *Anakon 2015*. 23 – 26 March 2015, Graz, Austria. Invited lecture.

6. Lieve Balcaen, Eduardo Bolea-Fernandez, Martín Resano, Frank Vanhaecke. ICP-Tandem mass spectrometry (ICP-MS/MS) as a tool for the accurate determination of challenging elements in complex matrices. *2015 APWC 6th Asia-Pacific Winter Conference on Plasma Spectrochemistry*. 19 – 22 May 2015, Xiamen, China. Invited lecture.

7. Martín Resano Ezcaray, Esperanza García-Ruiz, Maite Aramendía, Eduardo Bolea-Fernandez, Frank Vanhaecke, Flavio Nakadi, Marcia Veiga. High-resolution for direct isotopic analysis. *SciX 2015 Conference*. 27 September – 2 October 2015, Providence, United States of America. Invited lecture.

8. Frank Vanhaecke, Lieve Balcaen, Eduardo Bolea-Fernandez, Patrick Degryse, Veerle Devulder, Axel Gerdes, Lara Lobo, Amund Maage, Martín Resano, Ana Rua-Ibarz. Extending the application range of provenance determination based on isotopic analysis. *Pacifichem 2015 International Chemical Congress of Pacific Basin Societies.* 15 – 20 December 2015, Honolulu, Hawaii. Invited lecture.

9. Esperanza García-Ruiz, María R. Flórez; Eduardo Bolea-Fernandez, Frank Vanhaecke, Martín Resano. A simple dilute-and-shoot ICP-MS method for As determination in blood. *2016 Winter Conference on Plasma Spectrochemistry*. 10 – 16 January 2016, Tucson, United States of America. Poster presentation.

10. Martín Resano Ezcaray, Esperanza García-Ruiz, Maite Aramendía, Eduardo Bolea-Fernandez, Lieve Balcaen, Frank Vanhaecke. High chemical resolution for elemental and isotopic analysis. *2016 Winter Conference on Plasma Spectrochemistry.* 10 – 16 January 2016, Tucson, United States of America. Invited lecture.

11. Balazs Klencsar, Eduardo Bolea-Fernandez, María R. Florez, Lieve Balcaen, Filip Cuyckens, Frederic Lynen, Frank Vanhaecke. Determination of the total drug-related chlorine and bromine contents in human blood plasma using high performance liquid chromatography – tandem ICP-mass spectrometry (HPLC-ICP-MS/MS). *HTC-14 14th International Symposium on Hyphenated Techniques in Chromatography and Separation Technology.* 27 – 29 January 2016, Gent, Belgium. Poster and oral presentations.

12. Frank Vanhaecke, Yulia Anoshkina, Lieve Balcaen, Tessa Buckle, Eduardo Bolea-Fernandez, Marta Costas-Rodriguez, Joris Delanghe, Sara Lauwens, Marijn Speeckaert, Stijn Van Malderen, Hans Van Vlierberghe, Thibaut Van Acker, Eva Vergucht, Laszlo Vincze. Novel clinical applications of ICP-mass spectrometry. *27th MassSpec Forum Vienna*. 23 – 24 February 2016, Vienna, Austria. Invited lecture.

13. Frank Vanhaecke, Andrea Bazzano, Marco Grotti, Ana Rua-Ibarz, Eduardo Bolea-Fernandez, Amund Maage. Improved insight into environmental issues via high-precision isotopic analysis by means of multi-collector ICP-MS (MC-ICP-MS). *ISEAC39 – International Conference on Environmental & Food Monitoring*. 19 – 22 July 2016 Hamburg, Germany. Invited lecture.

14. Ana Rua-Ibarz, Eduardo Bolea-Fernandez, Amund Maage, Sylvia Frantzen, Stig Valdersnes, Frank Vanhaecke. Mercury isotopic analysis via cold vapor generation – multi- collector – ICP-mass Spectrometry as a key tool for evaluating pollution in marine ecosystems. *18th International Conference on Heavy Metals in the Environment*. 12 – 15 September 2016, Ghent, Belgium. Oral presentation.

15. Balazs Klencsar, Eduardo Bolea-Fernandez, María R. Florez, Lieve Balcaen, Filip Cuyckens, Frederic Lynen, Frank Vanhaecke. Determination of the total content of drug-related chlorine and chlorine speciation in human blood plasma using high performance liquid chromatography – tandem ICP-mass spectrometry (HPLC-ICP-MS/MS). *2017 European Winter Conference on Plasma Spectrochemistry*. 19 – 24 February 2017, Sankt Anton am Arlberg, Austria. Intended for oral presentation.

16. Lieve Balcaen, Eduardo Bolea-Fernandez, Kim Phan, Martín Resano, Frank Vanhaecke. Determination of ultra-trace amounts of prosthesis-related metals in whole blood using volumetric absorptive micro-sampling and tandem ICP – Mass Spectrometry. *2017 European Winter Conference on Plasma Spectrochemistry*. 19 – 24 February 2017, Sankt Anton am Arlberg, Austria. Intended for oral presentation.

17. Martín Resano, Esperanza García-Ruiz, Diego Pereira Leite, Maite Aramendía, Luis Rello, Águeda Cañabate, José Luis Todolí, Eduardo Bolea-Fernández, Lieve Balcaen, Frank Vanhaecke, Sylvain Bérail, Christophe Pécheyran. New strategies for analysis of biological samples via ICP-MS. *2017 European Winter Conference on Plasma Spectrochemistry*. 19 – 24 February 2017, Sankt Anton am Arlberg, Austria. Invited lecture.

2.3. Presentations on other conferences

1. Lieve Balcaen, Eduardo Bolea-Fernandez, Glen Woods, Martín Resano, Frank Vanhaecke. ICP-MS/MS: an ideal technique for the accurate determination of challenging elements in complex matrices. *The analytical challenge*. 7 November 2013, Utrecht, Netherlands. Invited lecture.

2. Lieve Balcaen, Eduardo Bolea-Fernandez, Glen Woods, Martín Resano, Frank Vanhaecke. ICP-MS/MS: an ideal technique for the accurate determination of challenging elements in complex matrices. *Agilent ICP-QQQ Workshop*. 11 November 2013, Les Ulis, France. Invited lecture.

3. Frank Vanhaecke, Yulia Anoshkina, Lieve Balcaen, Marta Costas-Rodriguez, Eduardo Bolea-Fernandez, Ana Rua-Ibarz, Stijn Van Malderen. Mass Spectrometry in Food and Feed II, 15 September 2015, Ghent, Belgium.

4. Eduardo Bolea-Fernandez, Yulia Anoshkina, Lieve Balcaen, Marta Costas-Rodriguez, Sara Lauwens, Ana Rua-Ibarz, Frank Vanhaecke. ICP - mass spectrometry as a versatile tool for the determination of ultra-trace amounts

and isotopic analysis of metals and metalloids. 2016 Doctoraatssymposium. 17 March 2016, Gent, Belgium. Oral presentation.

5. Ana Rua-Ibarz, Eduardo Bolea-Fernandez, Amund Maage, Sylvia Frantzen, Stig Valdernes, Frank Vanhaecke. Assessment of Hg pollution released from a WWII submarine wreck by Hg isotopic analysis of sediments and Cancer pagurus tissues via cold vapor generation – multi collector ICP-mass spectrometry (CVG-MC-ICP-MS). 2016 Doctoraatssymposium. 17 March 2016, Gent, Belgium. Poster presentation.

6. Ana Rua-Ibarz, Eduardo Bolea-Fernandez, Amund Maage, Sylvia Frantzen, Stig Valdersnes, Frank Vanhaecke. Tracking mercury pollution in marine ecosystems. *Voorjaarsbijeenkomst Werkgroep Atoomspectrometrie*. 19 May 2016, Werkendam, Netherland. Invited lecture.

7. Lieve Balcaen, Eduardo Bolea-Fernandez, Glen Woods, Martín Resano, Frank Vanhaecke. (Ultra)traces of challenging elements in complicated matrices? ICP-MS/MS to the rescue!. *European Agilent ICP-QQQ User group meeting*. 6 – 7 October 2016, Barcelona, Spain. Invited lecture.

8. Lieve Balcaen, Eduardo Bolea-Fernandez, Ana Rua-Ibarz, Stijn Van Malderen, Frank Vanhaecke. Development and refinement of analytical methods based on ICP-mass spectrometry to meet the needs of contemporary chemical research. *Chemical Research in Flanders Symposium*. 24 – 26 October 2016, Blankenberge, Belgium. Invited lecture.

3. Teaching activities

1. Supervision of Isabel Maicas Gabas. Student from the Erasmus program between Ghent and Zaragoza Universities (6 months in 2013). *Determination of Titanium in human serum via the new Agilent 8800.*

2. Supervision of Elisabeth Nissen. Master thesis student during 1 academic year (2013 – 2014). *Interference-free determination of ultra-trace levels of Arsenic and Selenium using methyl fluoride as reaction gas in ICP-MS/MS.*

3. Guidance of a group of Bachelor students during a 1 month project (2014). *Evaluation of the capabilities of different reaction gases to avoid spectral interference in the determination of ultra-trace levels of Arsenic via ICP-MS/MS.*

4. Supervision of Thibaut Van Acker. Master thesis student during 1 academic year (2014 – 2015). *Method development for determination of platinum group metals using tandem ICP-mass spectrometry and application to measure their dispersion in urban areas.*

5. Supervision of Simone Braga da Silva. PhD student at the Federal University of Paraná. Research stay (March – December 2015). *Inductively coupled plasma – mass spectrometry (ICP-MS) and tandem inductively coupled plasma – mass spectrometry (ICP-MS/MS) for trace element analysis.*

6. Supervision of Kim Phan. Master thesis student 1 academic year (2015 – 2016). *Trace element analysis of blood via tandem ICP-mass spectrometry after volumetric absorptive microsampling.*

7. Supervision of Dylan De Block. Master thesis student 1 academic year (2016 – 2017). *Tandem ICP – mass spectrometry for Fe isotope ratio determination in the context of tracer experiments with enriched stable isotopes.*

CHAPTER 1

Inductively Coupled Plasma – Tandem Mass Spectrometry (ICP-MS/MS)

Adapted from Bolea-Fernandez et. al., J. Anal. At. Spectrom. (2017)
DOI: 10.1039/c7ja00010c

1.1. Theoretical section

1.1.1. Historical background

Inductively coupled plasma – mass spectrometry (ICP-MS) is one of the most powerful techniques for obtaining information on the concentration and isotopic composition of many elements in the most diverse sample matrices. However, since its commercial introduction in 1983, the scientific community was also aware of the drawbacks affecting ICP-MS, the occurrence of spectral overlap being the most important one.**[1]** Over the years, strong efforts from both academics and manufacturers have led to the development of different approaches that allow one to eliminate, or at least mitigate, spectral interference. Unfortunately, none of these approaches can be considered as universally applicable for interference-free analysis by means of ICP-MS. Although a review of these approaches can be considered to be beyond the scope of this chapter, it is important to provide a brief overview on the different currently existing options to deal with spectral overlap, aiming to better identify those situations for which ICP-MS/MS can be considered of particular interest.

Among the different options to deal with spectral interference, analyte/matrix separation, mathematical equations, and alternative sample introduction approaches, such as vapor generation systems,**[2,3]** have been used since the early years, in spite of the accompanying drawbacks, as for instance, lower sample throughput, added labor-intensiveness, loss of multi-element capabilities and/or higher level of uncertainty accompanying the measurement results. The introduction of cool plasma conditions, under which the signals for all Ar-containing ions are strongly decreased, was a first step towards a more general strategy, although this approach was also characterized by important limitations, such as a reduced element coverage (poor ionization efficiency for elements with a higher ionization energy), stronger matrix effects and an enhanced presence of other types of interfering ions (e.g., oxide ions).**[4]** The introduction of high-resolution (HR) sector-field ICP-MS (SF-ICP-MS) is generally considered a crucial breakthrough in this context.**[5]** However, an increase in mass resolution is accompanied by a significant drop in ion transmission efficiency, and thus in sensitivity (1 - 2 orders of magnitude), while also a fraction of the interferences (e.g., overlap of the signals from isobaric nuclides) cannot be overcome by using higher mass resolution.**[6]**

Furthermore, SF-ICP-MS instrumentation is more expensive than quadrupole based ICP-MS (ICP-QMS) instrumentation.

In 1997, manufacturers started to equip quadrupole-based ICP-MS (ICP-QMS) instruments with a multipole collision-reaction cell (CRC) system. For the first time, ICP-QMS could be considered a competitive approach to SF-ICP-MS for many of the most demanding applications.**[7]** The introduction of CRCs in ICP-QMS instrumentation (ICP-CRC-QMS) enabled various approaches to avoid spectral overlap by means of control over the collisions and reactions taking place in the cell, thus improving the selectivity of the technique.**[8,9]** In this way, analyte and interfering ions with the same (nominal) mass-to-charge (m/z) ratio can be separated from one another via gas phase ion-molecule processes.**[10]** Non-reactive gases (e.g., He) in combination with kinetic energy discrimination (KED) can be used to reduce the interferences produced by polyatomic ions.**[11]** Those ions show a larger collisional cross-section than do the atomic ions with the same mass, thus they collide more frequently and lose more energy than the analyte ions, such that they can be selectively denied entrance into the MS section via a decelerating potential.**[12,13]** However, for this process to be efficient, conditions are such that also a large fraction of analyte ions are removed, and thus, this compromises sensitivity. Therefore, especially for challenging situations, the use of a reactive gas (e.g., H_2, NH_3 or O_2) is usually preferred, although their use is not always self-evident. With chemical resolution based on selective ion-molecule reactions, spectral overlap from both atomic and molecular interfering ions with the same m/z as that of the corresponding analyte ion can be addressed.**[14]** The gas reacts either with the interfering ions, enabling the target element to be measured at the original m/z (on-mass), or with the analyte ion, resulting in a new reaction product ion that can be measured interference-free at another m/z (mass-shift). Selection of the best suited reaction gas is crucial, whereby it has to be taken into account that the more reactive the gas, the higher the efficiency of the reaction and thus, the expected sensitivity, but also the higher the possibility of creation of new spectral interferences, arising from ions that are formed via reactions between the reaction gas and concomitant matrix elements.**[15]** For conventional ICP-CRC-QMS instruments, the relatively poor control over the reaction cell chemistry in the context of mass-shift approaches has usually limited applications to gases giving rise to predictable reaction product ions and/or for on-mass approaches. In other

words, for the most demanding applications, the potential of ICP-CRC-QMS instruments has been trimmed down by the lack of control of the cell chemistry when using highly reactive gases.

In 2012, the introduction of a new type of quadrupole-based ICP-MS device (ICP – tandem mass spectrometer) has brought the concept of chemical resolution as a means to avoid spectral overlap to a higher level. ICP – tandem mass spectrometry (ICP-MS/MS) is a powerful and elegant approach for achieving interference-free conditions for elemental and isotopic analysis of elements suffering from strong spectral overlap. The superior capabilities for overcoming spectral overlap are provided by an improved control over the ion-molecule chemistry occurring within the CRC. Therefore, this chapter first provides a brief general introduction on the theoretical concepts of the in-cell chemical processes used in ICP-MS to overcome spectral overlap and subsequently describes the particularities of this novel instrumental set-up, the different modes of operation, the scanning options as key tools for method development for interference-free ultra-trace element determination, and a general overview of the most demanding applications.

1.1.2. Ion-molecule chemistry in a CRC

As indicated in the previous section, the introduction of CRC technology in 1997 was a significant breakthrough in ICP-QMS instrumentation. The first studies reporting on the use of ion-molecule chemistry within a pressurized multipole cell date from 1989. Rowan and Houk demonstrated that the use of reactions between plasma-generated ions and the molecules of different gases could be an effective approach to avoid spectral overlap in ICP-QMS.**[16]** However, getting an insight into the chemical processes occurring within a CRC is not always self-evident. One of the main challenges is the selection of an appropriate gas and the best suited reactions that enable interference-free conditions to be obtained. For this purpose, gas-phase ion-molecule processes has been extensively studied using different techniques (*e.g.*, ICP – selected-ion flow tube (SIFT) – MS).**[17,18]** However, the conditions in a pressurized multipole cell of an ICP-QMS instrument are such that the reactivity of a given ion towards a selected reaction gas is not always identical to that observed using other techniques. In other words, the selection of a reaction gas to remove a specific interference cannot only be based on the currently existing

databases (although they can be used as starting point). These differences can most likely be explained by the different conditions in which these reactions proceed, as typically the studies conducted to evaluate the reactivity have been carried out under thermal conditions. In absence of an external source of energy, only exothermic reactions can occur. However, in an ICP-CRC-QMS instrument, these requirements are not always fulfilled. In a CRC, the particles (i.e. ions and/or gas molecules) do not have a Maxwell-Boltzmann energy distribution with the same temperature in all degrees of freedom. This is related with the continuous introduction of gas and with the energy of the ions in the beam extracted from the plasma. Therefore, in the CRC, thermal conditions are not obtained.**[19, 20]** The introduction of a collision gas (*e.g.*, He) in a pressurized multiple cell can be used to thermalize the system by the so-called collisional-damping effect.**[21]** This effect has been used in ICP-QMS aiming at improving isotope ratio precision owing to the slowdown of the ion beam by means of collisions, *i.e.* the reduction in kinetic energy of the ions coming from the ICP aiding in obtaining near-thermal conditions in the CRC, and the mixing of ions sampled at slightly different moments in time from the ICP.**[11]** In addition, the collisional-damping effect has also been used for (*i*) increasing the residence time of the ions in the cell, thus enhancing the reaction rate of relatively slow reactions, and for allowing (*ii*) *termolecular* reactions that cannot proceed without involvement of a third particle that removes a certain amount of energy from an intermediate transition state.

Therefore, the selection of a selective ion-molecule process to avoid spectral overlap in ICP-CRC-QMS still remains a challenging task. The reaction selected needs to be thermodynamically and kinetically favorable. The difference in Gibbs free energy accompanying the process (ΔG) determines whether a reaction is thermodynamically allowed or not, but whether a given reaction is suitable for the analytical purpose intended is rather governed by its reaction rate (kinetics). However, even such a general statement has to be handled with care, as endothermic reactions can also occur in CRC systems under specific non-thermal circumstances, as occur at very high concentrations of the reactants and/or when additional sources of energy (e.g., owing to collisions) play a role, thus enabling the endothermicity of theoretically disallowed reactions to be overcome.**[9]**

From the above, it is clear that the use of ion-molecule processes occurring within a CRC aiming at overcoming spectral overlap have to be studied in detail

experimentally before this chemical resolution can be effectively applicable in an analytical context, and therefore, novel analytical tools able to increase our understanding of the in-cell chemistry processes may help in the development of new strategies to tackle the problem of spectral interferences in ICP-MS. The introduction of the novel ICP- tandem mass spectrometer can be seen as a powerful tool to study the reactions occurring within a CRC, thus providing additional means to avoid spectral overlap in ICP-QMS instruments.

1.1.3. Instrument set-up

The only ICP – tandem mass spectrometers currently available on the market are the Agilent 8800 (2012) and 8900 (2016). These instruments are often referred to as triple quadrupole ICP-MS or ICP-QQQ (Agilent Technologies – **Figure 1.1**). Therefore, for the description of the instrumental set-up, this specific instrumentation (Agilent 8800 due to the recently introduction of the Agilent 8900) needs to be referred to.

An ICP – tandem mass spectrometer can be seen as a conventional ICP-CRC-QMS unit with an additional quadrupole located before the CRC (Q1 – CRC – Q2). This configuration (MS/MS) provides an improved control over the cell chemistry, as in MS/MS mode, i.e. with both quadrupoles acting as a mass filter with an approx. 1 amu bandpass window, only ions of a given m/z – analyte ion and interfering ion(s) – are allowed to enter the CRC. Next to the possibility to use the previously mentioned collision and reaction gases, this improved control over the processes taking place in the CRC also simplifies the use of non-conventional, more reactive gases, that typically produce many different reaction product ions due to their high reactivity or more complex reaction behavior (e.g., CH_3F and NH_3), thus providing the user with additional means to deal with the spectral overlap.

ICP-MS/MS is a versatile technique, and next to the double mass selection approach (MS/MS) outlined before, the mass window of the first quadrupole can be adapted from approx. 1 amu to fully open, depending on the challenge posed by each specific application. This novel setup often provides LoDs comparable to what can be realized using a SF-ICP-MS instrument, even superior for target elements affected by spectral interferences requiring the use of the highest mass resolution in SF-ICP-MS instrumentation. However, also other factors, such as the necessity of

additional security measures owing to the use of reactive gases, have to be taken into account for cost-efficiency calculations. In the rest of this chapter, the mode with double mass selection will be termed MS/MS mode, that with the first quadrupole operated with a wider bandpass or "open" single quadrupole or SQ mode.

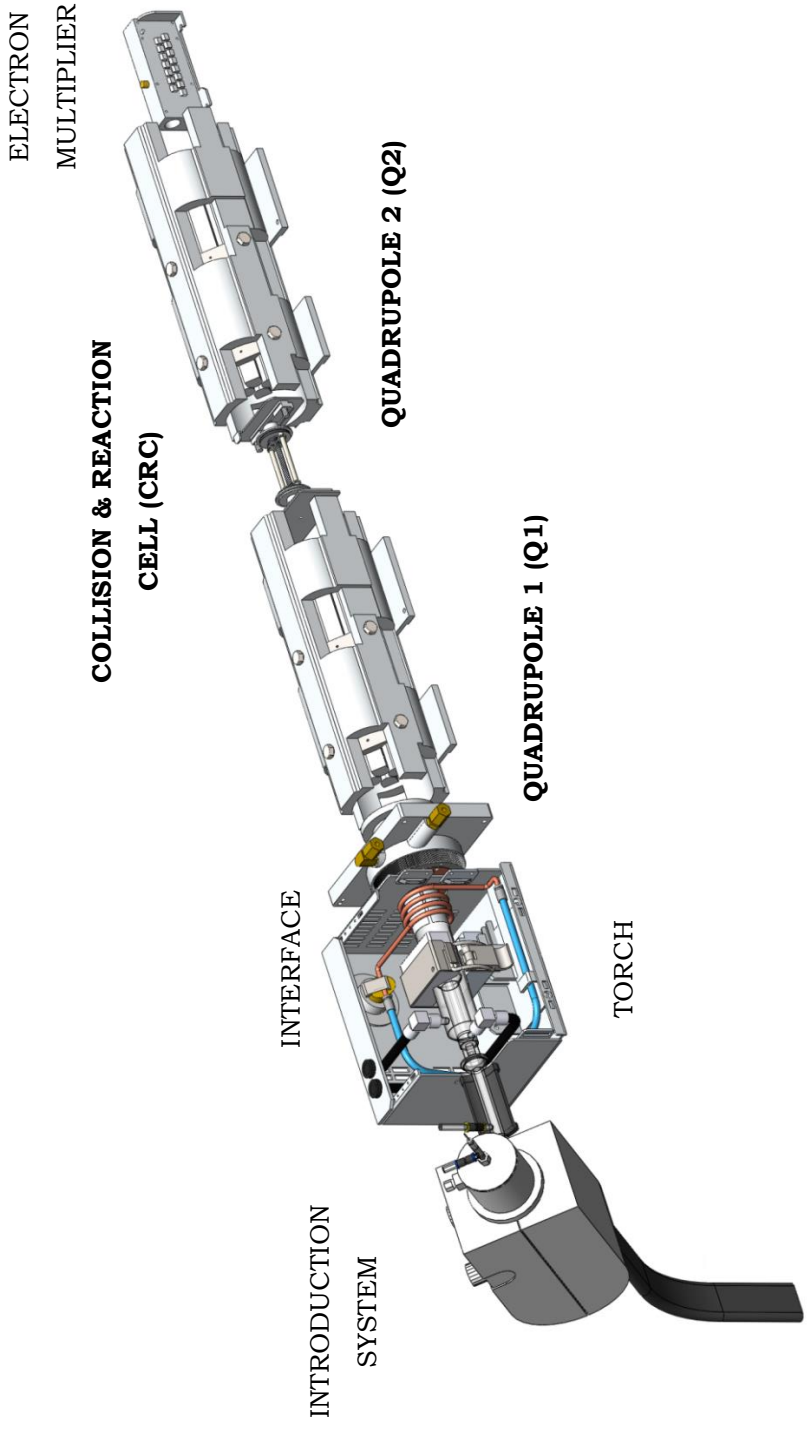

Figure 1.1. Graphical representation of an ICP – tandem mass spectrometer – based on the Agilent 8800 ICP-QQQ instrument (Agilent Technologies).

1.1.4. Operation modes: SQ vs MS/MS

The tandem configuration of ICP-MS/MS allows the mass spectrometer to be used in both SQ and MS/MS mode. When the instrument is working in SQ mode, Q1 can be operated as an ion guide only or as a bandpass mass filter. In the first case, Q1 is "fully open", thus all ions – the analyte ($^{m1}A^+$) ion and the interfering ions with the same m/z ($^{m1}I^+$), but also other concomitant ions with different m/z ($^{m2}C^+$) enter the CRC (**Figure 1.2**). This approach resembles the situation with a conventional ICP-CRC-QMS device and can be used in the case of less demanding applications, without the presence of interfering ions or in the case of simple matrices. By means of an appropriate selection of instrumental parameters, Q1 can also be used as a bandpass mass filter, thus only allowing those ions within a specific m/z range to reach the CRC. The bandpass mode resembles an ICP-QMS instrument equipped with a quadrupole-based CRC, typically termed dynamic reaction cell (ICP-DRC-QMS).

However, the true benefit of an ICP – tandem mass spectrometer is provided by the possibility of using double mass selection in the MS/MS mode, although it needs to be pointed out that the use of this mode involves a reduction in ion transmission efficiency, and thus sensitivity, in comparison to the SQ mode. In this approach, both Q1 and Q2 act as a real mass filter (1 amu bandpass), with both quadrupoles selecting the same m/z in the on-mass approach or different m/z's in the mass-shift approach, depending on whether the interfering or the analyte ion reacts with the selected reaction gas. In this MS/MS mode, a specific m/z (that of the target ion – ^{m1}A) is selected in Q1, such that only the analyte ion and the interfering ions with the same m/z ($^{m1}I^+$) are able to enter the CRC. All concomitant ions with different m/z ($^{m2}C^+$) are efficiently removed by Q1, which brings important advantages, *i.e.* (i) avoidance of unwanted product ions resulting from reactions between other ions and the reaction gas, (ii) a reduction of non-spectral interferences or matrix effects, affecting the reactions proceeding in the cell and (iii) an improvement in the ion-molecule chemistry occurring in the cell (see **Figure 1.2**).

These advantages result in higher capabilities for interference-free ultra-trace element determination and isotopic analysis, as enabled by using different reaction gases and adequate selection of the best reaction product ion to be monitored. Of course, this selection is not always self-evident, but some systematic approaches

can be relied on in order to find the best approach, leading to highest sensitivity and lowest detection limit. The next section (1.1.5) provides information on the use of different scanning options in the context of method development in ICP-MS/MS.

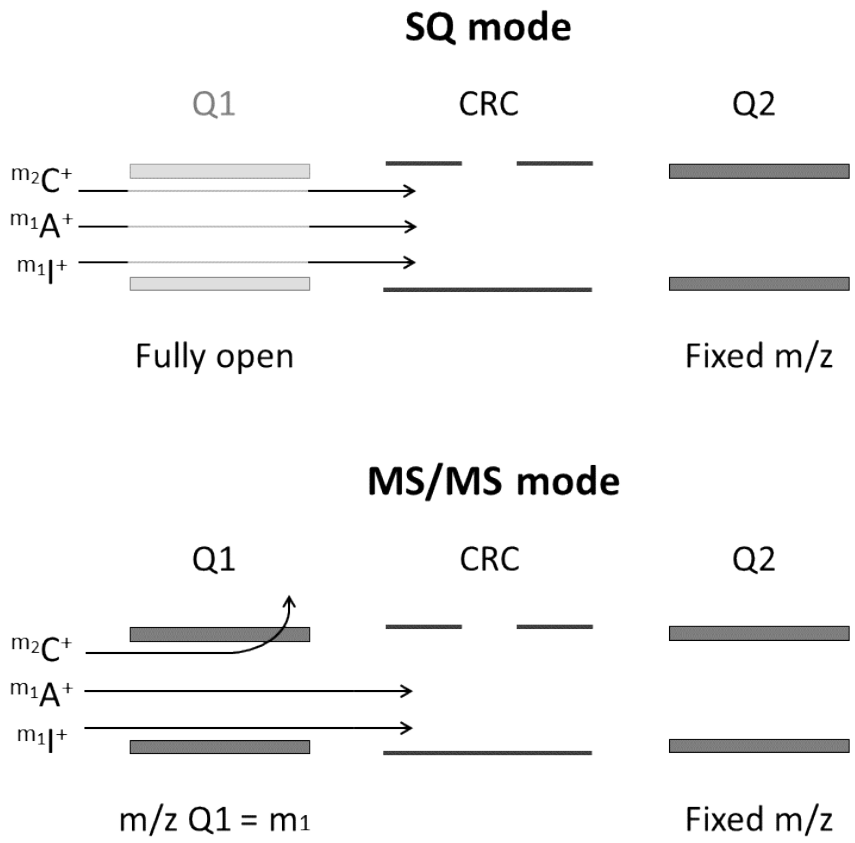

Figure 1.2. Schematic representation of both operation modes – SQ and MS/MS – in ICP – tandem mass spectrometry. A^+, C^+ and I^+ represent the analyte ion, the concomitant matrix ions with different m/z and the interfering ions with the same m/z, respectively.

1.1.5. Scanning options

In tandem mass spectrometry, different scanning options enable monitoring and identification of precursor and/or product ions. These scanning options can be seen as powerful tools allowing an enhanced insight into the potentially complex reactions taking place in the cell and thus, they facilitate the development of interference-free measurement methodologies. In this context, the MS/MS configuration of an ICP – tandem mass spectrometer enables product ion, precursor ion and neutral mass gain/loss scans.

1.1.5.1. Product ion scan

In ICP-MS/MS, the product ion scan is used for identification of the best suited reaction product ion after reaction between the original analyte ion and the reaction gas within the cell, aiming at obtaining interference-free conditions at the highest signal-to-background ratio. In order to perform a product ion scan, Q1 should be fixed at a specific nominal m/z, typically the one of the analyte ion of interest (^{m1}A), although it can also be used to evaluate the effect of a specific reaction gas on a potentially interfering ion. With the m/z of Q1 fixed at m_1 and the cell pressurized with the reaction gas (R), leading to different reaction product ions (e.g., $^{m1}A^{mR}R_x^+$), all product ions formed can be revealed by scanning Q2, thus covering the entire mass range (from 2 to 260 amu). From the product ion spectrum thus obtained (see **Figure 1.3**), the best suited reaction product ion (i.e., free from spectral overlap and with the highest signal-to-noise or S/N ratio) is selected for subsequent method development.

1.1.5.2. Precursor ion scan

As opposed to a product ion scan, a precursor ion scan is performed in order to obtain more insight into the origin of a specific product ion, resulting from a reaction between a so far unidentified ion and the reaction gas (R) within the cell, which might hinder interference-free determination of the analyte ion or reaction product ion thereof. Via precursor ion scanning, the m/z of the product ion selected is fixed by Q2, and with the cell pressurized with the reaction gas, a precursor ion spectrum is obtained upon scanning the entire mass range (2 – 260 amu) with Q1.

From the spectrum thus obtained (see **Figure 1.3**), precursor ions giving rise to spectral overlap at the m/z of interest can be identified, which might elucidate the origin of inaccurate results, resulting from a contribution of unexpected product ions to the signal intensity measured for the target analyte, if the system would be operated in SQ mode.

In addition, although in MS/MS mode Q1 only enables ions of a specific m/z reaching the cell (m_1), undesired interferences coming from reactions with ubiquitous elements present in the plasma source (e.g., Ar, C, N or O) cannot always be completely removed by means of Q1, giving rise to reaction product ions that are able to pass Q2 and interfere with the signal of the analyte ion at its

original m/z (on-mass) or at the m/z of the selected reaction product ion (mass-shift).

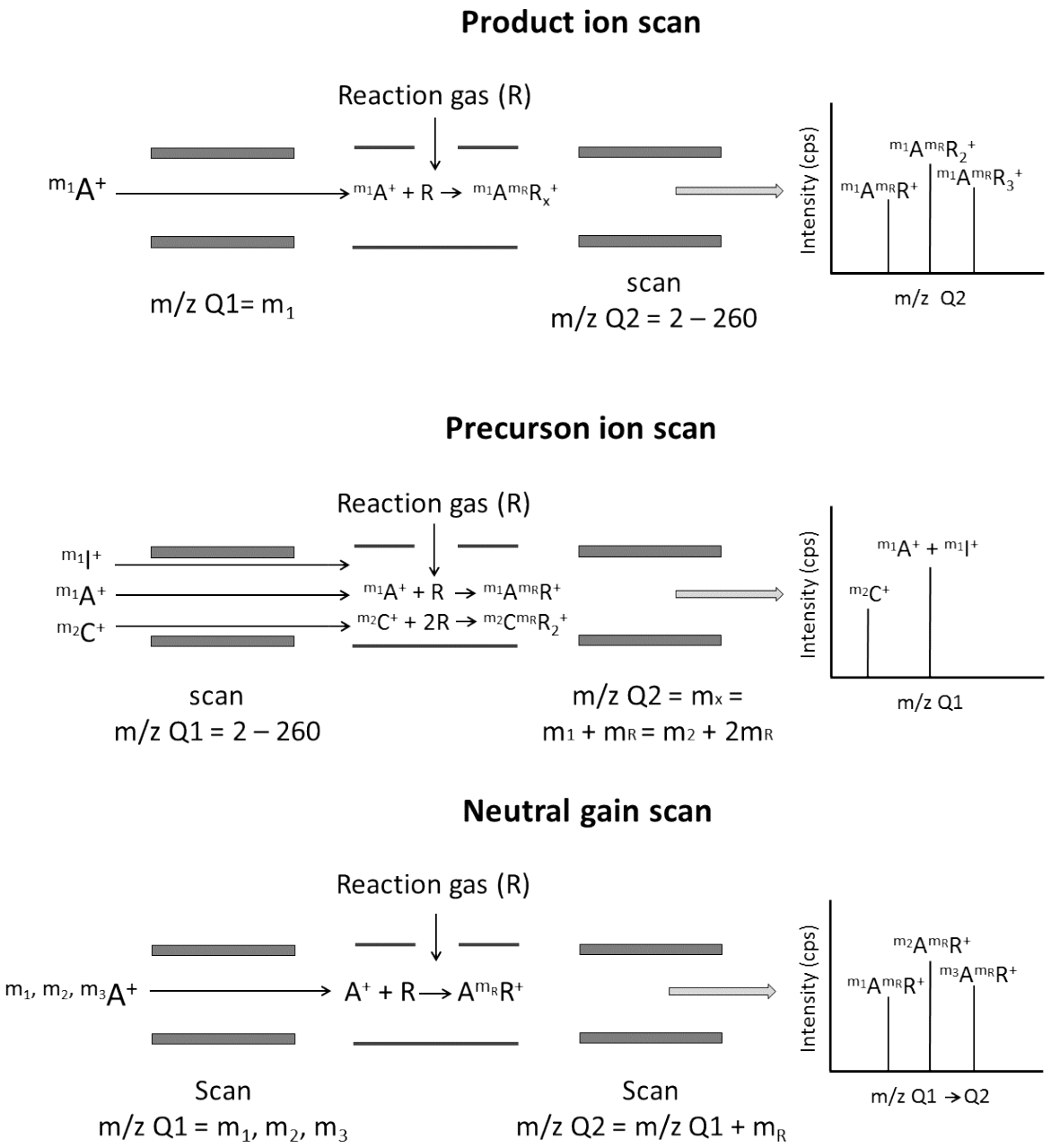

Figure 1.3. Schematic representation of the operating principles for the different scanning options available in ICP-MS/MS. A^+, C^+ and I^+ represent the analyte ion, the concomitant matrix ions with different m/z and the interfering ions with the same m/z, respectively.

1.1.5.3. Neutral mass gain/loss scan

Tandem mass spectrometry also allows neutral mass gain/loss scanning, in which both quadrupoles are used in scanning mode with a fixed difference in m/z between them, instead of keeping Q1 or Q2 fixed at a specific m/z. Both gain or loss of mass can be looked for, depending on whether the precursor ion is lower or higher in mass than the corresponding product ion. In molecular tandem mass spectrometry, where a precursor ion is fragmented by collision induced dissociation (CID), a neutral mass loss scan can be performed, e.g., to reveal which molecular ions lose a neutral fragment of given mass (e.g., H_2O) upon collision. However, in ICP-MS/MS, neutral mass gain scan is typically of greater interest as the precursor ions will most often be lighter. Such a neutral mass gain scan can be accomplished by synchronous scanning of Q1 and Q2, thereby maintaining a constant difference in m/z between both. This constant (K = m/z (Q2) - m/z (Q1)) has a value >0 in neutral mass gain scan and a negative one in neutral mass loss scan (K<0). The main goal of a neutral gain scan for ICP-MS is the study of the isotopic pattern of a target element of interest (A). As a general example, we assume an element with three isotopes ($^{m1,m2,m3}A$) and a reactive gas (R), reacting with the original analyte ions as follows: $^{m1,m2,m3}A^+ + {}^{mR}R \rightarrow {}^{m1,m2,m3}A^{mR}R^+$. The neutral gain scan can be used to evaluate if the set of reaction product ions $^{m1,m2,m3}A^{mR}R^+$ shows the same isotopic pattern than does the set of corresponding precursor ions. Thus, Q1 is selected at m/z = m_1,m_2 and m_3 and Q2 at m/z = m_1+m_R, m_2+m_R and m_3+m_R, respectively, so that K = m_R during the entire scanning process (see **Figure 1.3**). The neutral mass gain spectrum obtained in this way is a valuable tool for method development, especially in the context of isotopic analysis.

1.1.6. Abundance sensitivity

ICP-MS/MS also provides an improved abundance sensitivity (AS). By definition, AS is calculated as the ratio of the maximum ion current recorded at a specified m/z value to the maximum ion current arising from the same species recorded at a neighboring m/z value (m/z - 1 or m/z + 1). Thus, it is a measurement of the contribution of the peak tail of a spectral peak (with a certain m/z value) to the signal intensity at an adjacent m/z value. This value is dependent on the resolving power of the mass spectrometer.**[22]** For a quadrupole mass spectrometer (QMS),

the AS is in the order of ~10^7, which means that for a signal of 10^7 counts, at a specific m/z, there is a contribution of 1 count to the neighboring signals (at m/z - 1 and m/z + 1). An increase in AS was shown when operating the QMS at higher stability regions.**[23]** Additionally, the introduction of a non-reactive collision gas (e.g., He) in the CRC might lead to a slight improvement of the AS (10^8), although this is accompanied by a significant drop in sensitivity.**[24]** This improvement is a result of the reduction in the spread of the kinetic energy of the atomic ions.**[25]** While the contribution of a spectral peak to the intensity at neighboring m/z values, or even m/z values that are even further away, is very small, it can become meaningful in the determination of ultra-trace amounts of an analyte element in a matrix containing very high amounts of the adjacent element, or in the determination of extreme isotope ratios, whereby the nuclides considered show a pronounced difference in abundance, (e.g., $^{234}U/^{238}U$ or $^{236}U/^{238}U$). For an ICP – tandem mass spectrometer operated in MS/MS mode, both quadrupoles have an AS of ~10^7, thus the overall AS is the product of the AS for Q1 multiplied by that for Q2 ($AS_{ICP\text{-}MS/MS} = AS_{Q1} \times AS_{Q2}$). This leads to a theoretical AS of ~10^{14}, which suffices for the most demanding applications, and adds an additional benefit to ICP-MS/MS. However, because of the dynamic range of the detector this type of instrumentation is equipped with, it cannot be experimentally evaluated if an AS of 10^{14} is genuinely obtained, but the AS for ICP-MS/MS has been shown to be at least ~10^{10}.

1.1.7. Overcoming spectral overlap: on-mass and mass-shift approaches

Before starting with the description of some applications based on the use of ICP-MS/MS, and although the concepts of on-mass and mass-shift approaches as a means to overcome spectral overlap have been addressed very briefly in the previous sections already, it is worthwhile to describe both approaches into more detail. The difference between both lies in the strategy selected to circumvent the problem of spectral interference. For the on-mass approach (sometimes also called direct determination), both Q1 and Q2 are selected at the same m/z, *i.e.* that of the original analyte ion of interest (^{m1}A). The reaction between the reaction gas (R) and the interfering ion(s) ($^{m1}I^+$) is counted on for completely removing the contribution of

this (these) ion(s) to the signal intensity measured at this m/z. The newly formed reaction product ion(s) ($^{m1}I^{mR}R^{+}$) is (are) removed by means of Q2, while the analyte ion of interest is measured at its original m/z. This approach is also often relied on in conventional ICP-CRC-QMS, although it needs to be pointed out that enhanced control over the reaction cell chemistry is obtained in ICP-MS/MS due to the capability of Q1 to reject all concomitant ions with an m/z different from that of the analyte ion ($^{mR}C^{+}$). In this way, the formation of new, unwanted reaction product ions with the same m/z as that of the analyte ion and thus interfering with its determination can be avoided (see **Figure 1.4**). It is clear that the on-mass approaches have been further perfected with the introduction of ICP-MS/MS, however, quantitative conversion of the interfering ion into another species is required; this prerequisite is not always fulfilled.

In traditional ICP-CRC-QMS, the mass-shift approach (sometimes called indirect determination) is often hampered by the lack of control over the ion-molecule chemistry proceeding in the reaction cell. The introduction of ICP-MS/MS now allows one to fully exploit the capabilities of reaction gases as well. For such a mass-shift approach, Q1 is fixed at the original m/z of the analyte ion of interest ($^{m1}A^{+}$), such that only interfering ions with the same m/z ($^{m1}I^{+}$) are also able to reach the CRC, while all other ions with different m/z's ($^{mR}C^{+}$) are removed. The CRC is pressurized with a reaction gas, which has to show a high reactivity towards the analyte ion and no reactivity or a different behavior towards the interfering ion(s) (see **Figure 1.4**). In case several types of reaction product ions are formed, the best suited reaction one is selected and the Q2 is fixed at the corresponding m/z. Ions that interfere with the determination of the analyte ion at its original m/z enter the cell, but they are rejected by Q2 when they show no reactivity towards the reaction gas or react in a different way (show a different reactivity) towards the reaction gas.

It has to be mentioned that although a high conversion efficiency for the analyte ion is advantageous, quantitative conversion is not mandatory. Therefore, mass-shift seems to provide more versatility in avoiding spectral overlap, and that is why this strategy is typically preferred over the on-mass approach for obtaining interference-free conditions for elemental and isotopic analysis.

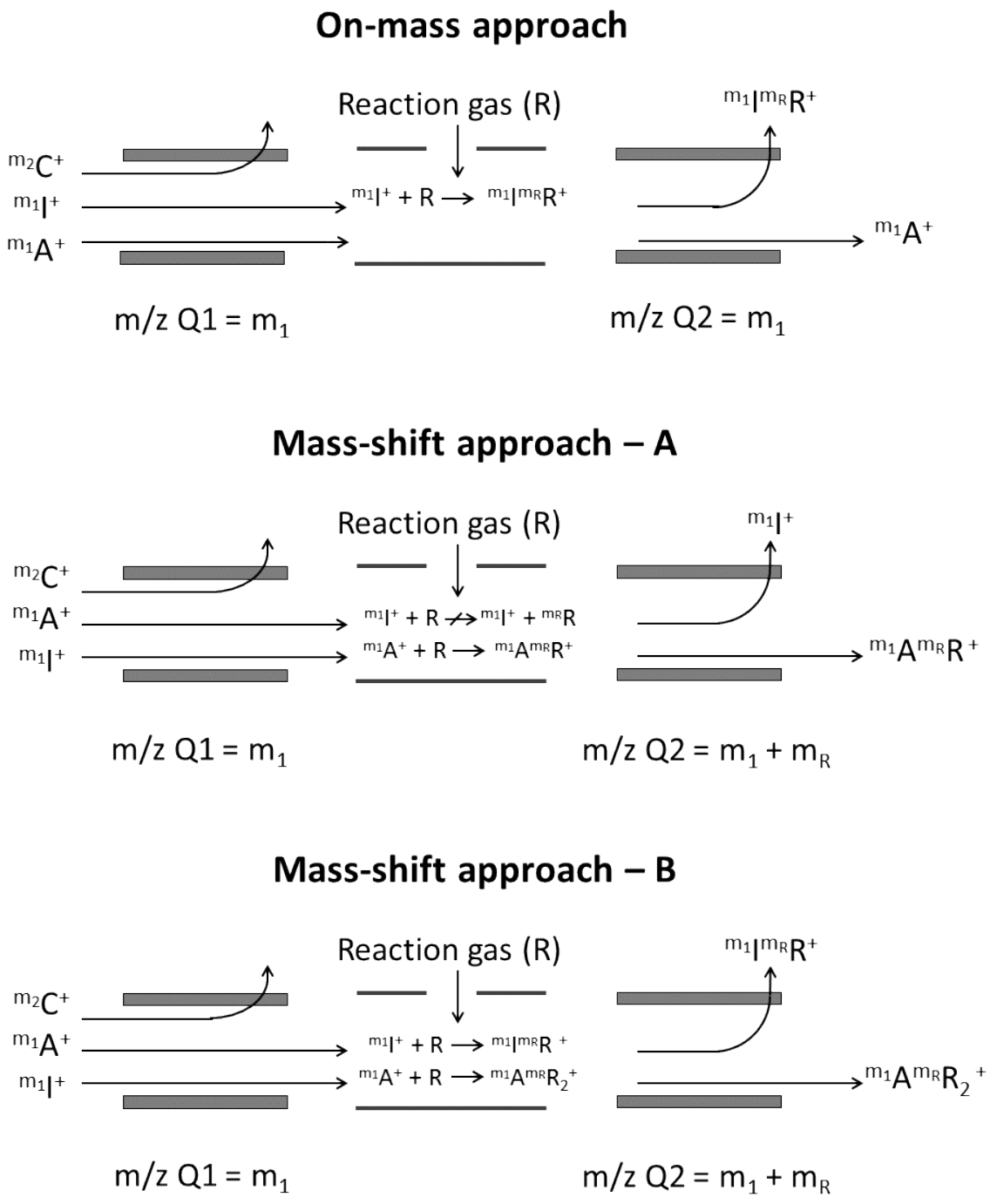

Figure 1.4. Schematic representation of both approaches used to overcome spectral overlap in ICP-MS/MS. Mass-shift approaches rely either on the absence of reaction for the interfering ion ($^{m1}I^+$) towards the reaction gas (R) – A, or a different reaction behavior between analyte ($^{m1}A^+$) and interfering ion ($^{m1}I^+$) towards R – B.

1.2. Applications

As stated above, ICP-MS/MS has only been introduced very recently. Nevertheless, several approaches reported on in the literature have already demonstrated the added value of this novel set-up. In this section, some of the applications described in the literature are summarized with the focus on the improvements obtained owing to the use of ICP-MS/MS, and paying attention to the different approaches and possible tools for method development, as described in preceding sections. Next to quantitative elemental analysis, also applications in the field of isotopic analysis have been selected, as well as examples of hyphenated set-ups, where an ICP – tandem mass spectrometer is used in combination with different introduction systems, including separation techniques.

1.2.1. Elemental analysis

Owing to the enhanced control over the reaction chemistry taking place in the reaction cell, the applicability of the mass-shift approach for dealing with spectral interferences has largely increased with the introduction of ICP-MS/MS. Oxygen (O_2) is one of the most frequently used reaction gases in ICP-CRC-QMS and its use has been widely described in the literature. Many elements show reactivity towards O_2, with O-atom transfer being the most common ion-molecule reaction. Thus, a target ion (M^+) is converted into a reaction product ion (MO^+) with a gain in m/z = 16. This reaction can be used both for on-mass and mass-shift approaches depending on whether the reaction takes place with the interfering or the analyte ion, respectively. The applicability of O_2 (as well as of other reaction gases) in conventional ICP-QMS or in ICP-MS/MS operated in SQ mode, might be limited by the formation of unwanted reaction product ions with the same m/z as that of the target analyte or the corresponding reaction product ion and/or by the presence of concomitant matrix elements with the same m/z as that of the reaction product ion selected (in mass-shift approaches). In this context, the addition of an extra quadrupole in the ICP – tandem mass spectrometer operating in MS/MS mode has been successfully used to overcome the spectral overlap in very diverse and challenging applications. For instance, it is well known that the determination of arsenic (^{75}As) is hampered by the occurrence of both non-spectral **[26]** and spectral interferences **[27]** (caused by the occurrence of, e.g., $^{40}Ar^{35}Cl^+$, $^{38}Ar^{37}Cl^+$, $^{40}Ca^{35}Cl^+$

and/or $^{59}Co^{16}O^+$ polyatomic ions, and of $^{150}Nd^{2+}$ and $^{150}Sm^{2+}$ doubly charged ions). By using O_2 as a reaction gas in ICP-MS/MS, $^{75}As^+$ ions are converted into the corresponding $^{75}As^{16}O^+$ reaction product ions (m/z = 91). While in SQ mode, the presence of ^{59}Co ($^{59}Co^+ + O_2 \rightarrow {}^{59}CoO^+$, $^{59}CoO^+ + O_2 \rightarrow {}^{59}CoO_2^+$; m/z = 91) and ^{91}Zr hinder the indirect measurement of $^{75}As^+$ as $^{75}AsO^+$, the use of Q1 in the MS/MS mode allows for an interference-free determination by removing all ions with m/z ≠ 75 (except when a significant amount of CoO^+ is formed already in the plasma as the result of a very high concentration of Co in the sample matrix). Another example is the work of Meyer *et al.*,**[28,29]** in which As was determined as the corresponding AsO^+ reaction product ion for the characterization of As-containing hydrocarbons (AsHCs), with the aim of evaluating the toxicity of these species during *in vitro* and *in vivo* studies.

Sulphur (S) is another element that suffers from strong spectral overlap, mainly from O-based polyatomic interferences. The reaction with O_2 leads to the formation of SO^+ product ions. However, as indicated in **Table 1.1**, SO^+ reaction product ions are not free from spectral interference, which limits the applicability of this approach for single quadrupole ICP-(CRC-)QMS systems. However, ICP-MS/MS operating in MS/MS mode enables interference-free measurement of S^+ as SO^+ owing to the capability of Q1 to efficiently get rid of ions with m/z ≠ 32,33 and 34, respectively. In this way, only those ions with m/z = 32, 33 and 34, respectively, can reach the cell and react with O_2.

Table 1.1. S-isotopes with their natural isotopic abundance and the most important potentially interfering ions hampering accurate S determination.**[30]**

Analyte	Abundance (%)	Ions causing spectral interference
$^{32}S^+$	95.04	$^{16}O^{16}O^+$, $^{14}N^{18}O^+$, $^{15}N^{16}O^1H^+$
$^{33}S^+$	0.75	$^{32}S^1H^+$, $^{16}O^{16}O^1H^+$, $^{16}O^{17}O^+$, $^{15}N^{18}O^+$, $^{14}N^{18}O^1H^+$
$^{34}S^+$	4.20	$^{33}S^1H^+$, $^{16}O^{18}O^+$
$^{32}S^{16}O^+$	95.04	$^{48}Ti^+$, $^{48}Ca^+$, $^{36}Ar^{12}C^+$
$^{33}S^{16}O^+$	0.75	$^{49}Ti^+$, $^{32}S^{17}O^+$
$^{34}S^{16}O^+$	4.20	$^{50}Ti^+$, $^{50}Cr^+$, $^{50}V^+$, $^{38}Ar^{12}C^+$, $^{36}Ar^{14}N^+$, $^{32}S^{18}O^+$, $^{33}S^{17}O^+$

The determination of S via reaction with O_2 in a mass-shift approach using ICP-MS/MS can be seen as one of the leading applications due to the relevance of S in many different contexts. For instance, a mono-element method for the direct quantification of sulfur dioxide (SO_2) in wine (food safety) was developed by Wang *et al.***[31]** The method developed was also successfully used for the quantification of other S-containing compounds. Other applications in which the determination of S is of high interest are described in the next sections.

The determination of trace amounts of selenium (Se) can also be accomplished in MS/MS mode with O_2 mass-shift approaches. Among others, the signals of the Se isotopes are affected by Ar-based polyatomic ions, Ar dimers being the most problematic ones. In this case, even the maximum resolution attained by present-day commercially available high resolution SF-ICP-MS instrumentation is not able to resolve the spectral overlap of the signals of $^{40}Ar_2^+$ and $^{80}Se^+$, the most abundant Se isotope (49.6 %). The conversion of Se^+ ions into the corresponding SeO^+ product ions in an ICP – tandem mass spectrometer allows for an interference-free determination by removing both polyatomic and doubly charged (Gd^{2+}) interfering ions. In the work of Bishop *et al.*,**[32]** Se was determined in the presence of a high concentration of Gd in serum samples, simulating the result of a Gd-based magnetic resonance imaging (MRI). A schematic diagram explaining the operating principles of MS/MS for the interference-free determination of Se using an on-mass (H_2) and mass-shift approach (O_2) is provided as **Figure 1.5** (from the work of Sugiyama *et al.***[33]**)

Although O_2 has been widely used, both in ICP-QMS and in ICP-MS/MS, two important drawbacks of this reaction gas need to be pointed out. On one hand, the O-atom transfer may impose difficulties to resolve isobaric overlap for those elements (analyte and interfering elements) with a similar affinity towards O_2. Those elements typically react in the same way and thus, the reaction product ions of the analyte and the interfering ions have the same m/z. Also for analyte signals that show spectral overlap with that of an O-based polyatomic interference i.e., m/z A^+ = m/z IO^+, the addition of O_2 in the cell might lead to the formation of the reaction product ions AO^+ and IO_2^+, the signals of which overlap at the new m/z.

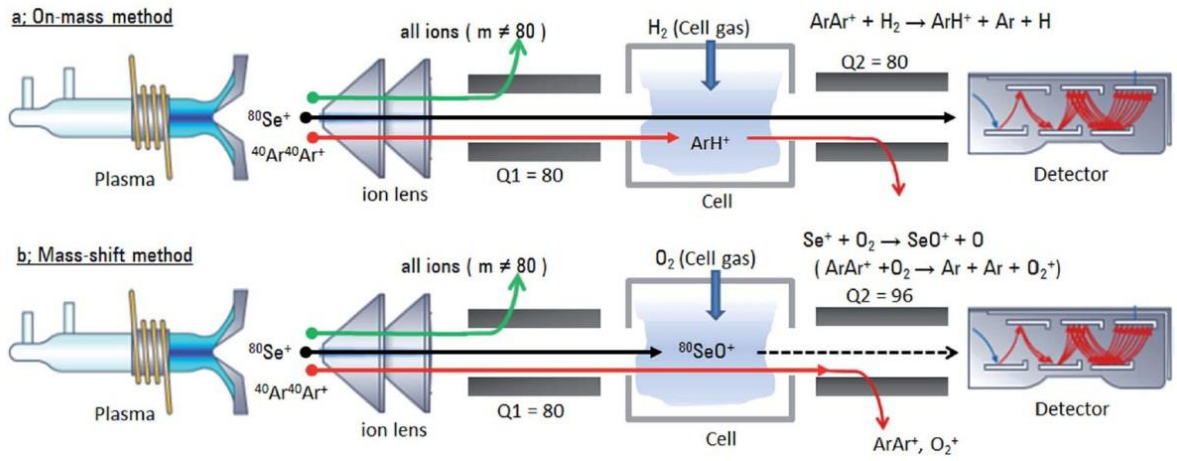

Figure 1.5. Example of on-mass (a) and mass-shift (b) approaches for the interference-free determination of ^{80}Se using ICP-MS/MS operated in MS/MS mode.**[33]**

The use of highly reactive gases, as for instance NH_3, can be seen as an elegant alternative to solve this kind of interferences. An example of this approach was shown by Balcaen *et al.*(Chapter 2)**[34]** This work aimed at the determination of ultra-trace levels of titanium (Ti) in blood serum in order to evaluate the condition of Ti-based implants in the human body. The capabilities of O_2 and NH_3 to resolve the spectral overlap for different Ti isotopes (caused by the occurrence of e.g., Ca^+, PO^+ and SO^+) were evaluated. The best suited reaction product ions were identified via product ion scanning (see **Figure 1.6**). The product ion scans for $^{48}Ti^+$ in the presence of $^{48}Ca^+$ using O_2 (**Figure 1.6A**) and NH_3 (**Figure 1.6B**) show the different behavior of those gases. TiO^+, and to a much lesser extent TiO_2^+, were formed by reaction with O_2, whereas for NH_3, higher order reaction product ions were also observed. The isobaric interference of $^{48}Ca^+$ and $^{48}Ti^+$ cannot be overcome by means of O_2, despite the reaction between Ca and O_2 being an endothermic process that should not occur in the cell. However, this reaction occurs to some extent as a result of the large excess of Ca in biological fluids. In the case of NH_3, the isobaric overlap of Ti and Ca can be overcome owing to the different reactivity towards the reaction gas. For Ti, a higher order reaction product ion ($Ti(NH_3)_6^+$) is formed, the signal of which is free from Ca-based spectral overlap. In addition, when using O_2, it was also demonstrated that the presence of high amounts of S and P in biofluids may give rise to spectral interferences for some Ti isotopes, due to the formation of SO^+ and PO^+ in the plasma source that are able to reach the cell and pass Q2 as

SO_2^+ and PO_2^+, overlapping with the signals of $^{47}TiO^+$ and $^{49}TiO^+$, respectively. A problem which can also be avoided by using NH_3. Thus, the mass-shift approach using NH_3 gas was considered more suitable for the determination of ultra-traces of Ti in biological samples, and instrumental LODs in the order of 10 ng L^{-1} have been reported on in this work.

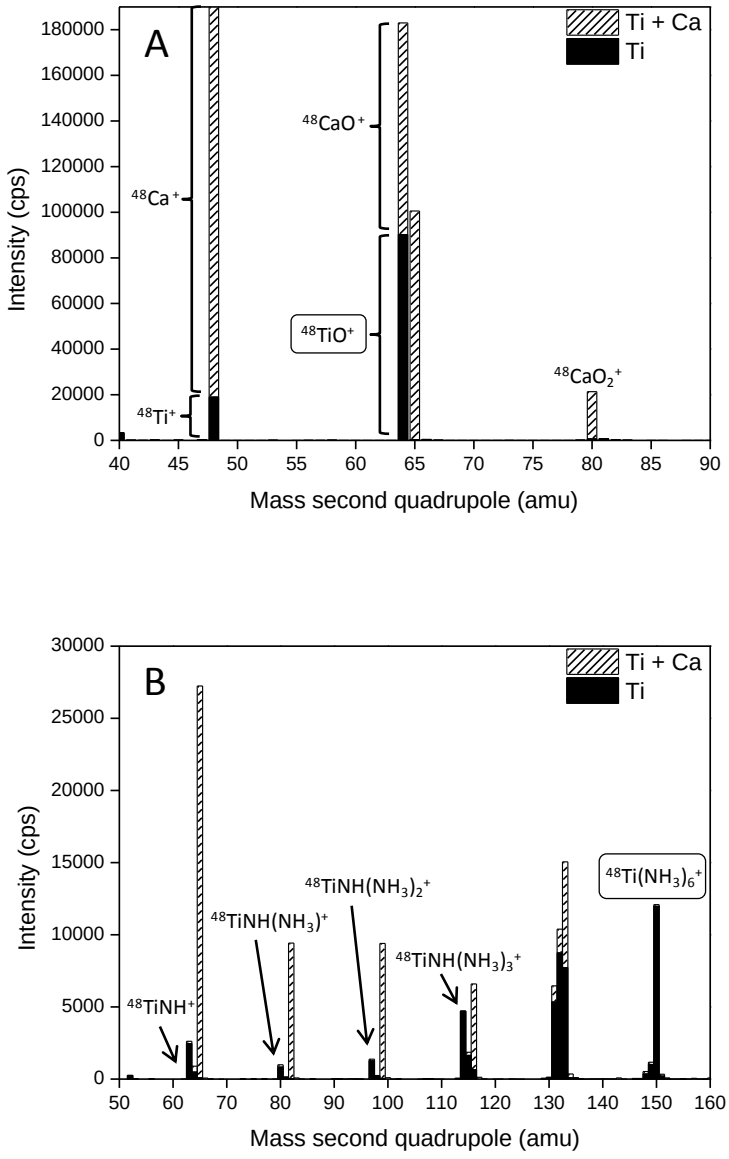

Figure 1.6. Product ion scans with Q1 fixed at m/z = 48 for a solution containing 1 µg L^{-1} Ti and a solution containing 1 µg L^{-1} Ti + 10 mg L^{-1} Ca. The reaction gas selected was O_2 (0.2 mL min^{-1} – A) and NH_3 (2 mL min^{-1} NH_3/He – B). Adapted from Balcaen *et al.***[34]**

In addition to the gases most commonly used in ICP-MS/MS, i.e., H_2, He, NH_3 and O_2, also methyl fluoride (CH_3F) has been evaluated for its capabilities as a reaction gas to avoid spectral overlap. This highly reactive gas has only been used scarcely in ICP-MS before,**[35,36]** but with the introduction of ICP-MS/MS, its application range has been extended. Like for NH_3, CH_3F reacts with the analyte ion (mass-shift approaches) in many different ways, to produce both simple and higher order reaction product ions. According to literature,**[37,38]** F-atom transfer (MF^+), CH_3F addition (MCH_3F^+) and CH_3F addition followed by HF (MCH_2^+) or H_2 ($MCHF^+$) elimination, are the most prevalent reaction pathways, but also the combination of those reactions to produce higher order reaction product ions has been reported on ($MF_a(CH_bF_c)_d^+$). Bolea-Fernandez *et al.*(Chapter 5)**[39]** describe the use of CH_3F (more accurately a mixture of 10 % CH_3F and 90 % He) for the mono-element determination of ultra-trace concentrations of As and Se. In this work, a selective reaction between the target nuclides ^{75}As and $^{77,78,80}Se$ takes place in the CRC to produce $^{75}AsCH_2^+$ (m/z = 89) and $^{77,78,80}SeCH_2^+$ (m/z = 91, 92 and 94, respectively). This reaction comprises the addition of CH_3F and the subsequent elimination of HF. These methods with different reaction gas flow rates for As and Se were successfully applied for the interference-free determination of As and Se in reference materials of plant, animal and environmental origin. Instrumental LODs of 0.2 ng L^{-1} for ^{75}As and ≤10 ng L^{-1} for $^{77,78,80}Se$ were obtained, which are according to the best of the authors' knowledge, the lowest LODs reported on in the literature for ICP-MS so far. However, despite of the benefits of CH_3F (e.g., highly reactive, but non-corrosive gas) as a reaction gas for ICP-MS/MS, also some disadvantages have to be noted, such as the requirement for additional safety measures and the fact that – currently – this gas is not part of the standard set of gases delivered with an ICP-MS/MS instrument.

While the specificity of some of the reactions taking place in the reaction cell may often be seen as an advantage, it may also be considered as a limitation for multi-element approaches. Generally seen, multi-element determination is an important advantage of ICP-MS over other analytical techniques. Simultaneous determination is especially relevant when aiming at high sample throughput, when the amount of sample is limited or when monitoring short transient signals. Below, specific applications aiming at ICP-MS/MS multi-element analysis are described. In the previous section, some of the capabilities and limitations of CH_3F, NH_3 and O_2

reaction gases have been discussed. In spite of the possibilities of other type of cell gases (e.g., H_2, He and N_2O) for the purpose of multi-elemental analysis, the applications selected comprise the use of those first three gases only.

O_2 has been widely used for the simultaneous determination of several analyte elements by means of ICP-MS/MS, usually making use of the combination of on-mass and mass-shift approaches within the same method. In this way, the determination of As, Cr, Hg and V in drinking water was accomplished by Amaral *et al.***[40]** O-atom transfer in a mass-shift approach was relied on to avoid the spectral overlap (e.g., $^{40}Ar^{35}Cl^+$, $^{35}Cl^{17}O^+$ and $^{35}Cl^{16}O^+$) affecting As, Cr and V via monitoring of the reaction product ions AsO^+, CrO^+ and VO^+, while Hg was determined on-mass under the same analytical conditions (owing to the absence of strong spectral interferences and to the low reactivity towards O_2). For this application, 0.3 mL min^{-1} of O_2 sufficed to avoid spectral overlap and LODs of 2, 3, 2 and 40 ng L^{-1} could be obtained for V (as $^{51}V^{16}O^+$), Cr (as $^{52}Cr^{16}O^+$), As (as $^{75}As^{16}O^+$) and Hg (as $^{202}Hg^+$), respectively.

The combination of on-mass and mass-shift approaches was also used by Diez Fernandez *et al.***[41]** for the determination of P/Ca, S/Ca and low B/Ca ratios in carbonates. The B/Ca ratios in carbonates are indicators of ocean acidification, but the determination of both elements is seriously hampered by spectral overlap. In this work, O-atom transfer was used for the determination of P and S as the corresponding PO^+ and SO^+ reaction product ions. However, special attention was also paid to the interferences affecting B and Ca, and to the way to resolve them. Firstly, because of the high concentration of Ca in comparison to B, the least abundant Ca isotope, i.e. ^{46}Ca, was selected in order to be able to detect both elements in pulse counting mode. The overlap of $^{46}Ti^+$ and $^{46}Ca^+$ was taken care of by converting ^{46}Ti ions into the corresponding $^{46}TiO^+$ ions, while $^{46}Ca^+$ can be measured on-mass due to the low reactivity of Ca towards O_2. For B, the situation is rather different, as the determination of ^{11}B is affected by the strong signal of the ubiquitous ^{12}C, potentially leading to inaccurate (biased high) results due to the overlap of the $^{12}C^+$ signal tail with the signal of $^{11}B^+$. The improvement in abundance sensitivity realized by operating the ICP – tandem mass spectrometer in MS/MS mode allowed for a full separation of the signals of ^{11}B and ^{12}C (see **Figure 1.7**), in contrast to conventional ICP-QMS or ICP-MS/MS operating in SQ mode, and thus

the method developed could be successfully applied to the measurement of low B/Ca ratios in samples with high C content.

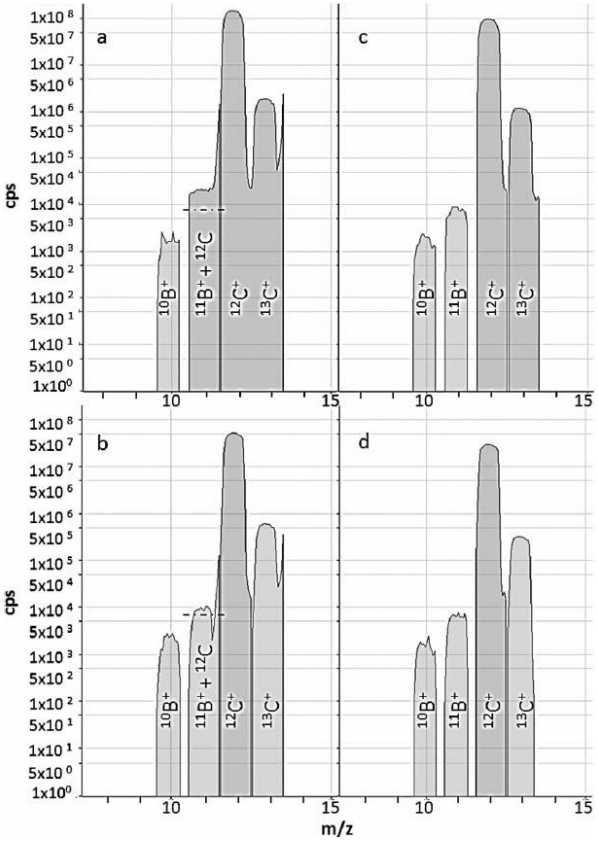

Figure 1.7. Example of the enhanced abundance sensitivity for ICP-MS/MS operated in MS/MS mode over SQ mode. The figure shows the mass spectra obtained for 0.5 ppb B using: SQ mode in (a) 1.3 and (b) 0.1 mg carbonate mL^{-1} solution and MS/MS mode in (c) 1.3 and (b) 0.1 mg carbonate mL^{-1} solution. Figure 7a and b show the influence of the $^{12}C^+$ signal tail on the signal of $^{11}B^+$.**[41]**

Amais *et al.***[42]** have made use of O_2 to avoid MoO^+ interferences in the determination of Cd in milk. As MoO^+ ions formed in the plasma source exhibit the same m/z as Cd ions, they enter the cell together. However, the introduction of 0.5 mL min^{-1} of O_2 enables to convert the MoO^+ ions into the corresponding MoO_2^+ ions, while Cd shows no reactivity towards O_2, thus allowing interference-free determination of Cd (on-mass approach) and of Mo (as MoO_2^+ – mass-shift approach). Next to O-atom transfer, another option to avoid spectral overlap with O_2 is the charge transfer reaction. The reaction mechanism involves the conversion of analyte or interfering ions into the corresponding neutral species, while O_2 is

converted into the O_2^+ ion (m/z = 32). This reaction can be used to avoid spectral overlap by neutralizing interfering ions, and measuring the analyte ion at its original m/z (on-mass approach). However, Böting *et al.***[43]** have evaluated the performance of this reaction for the indirect measurement of several target analytes (As, Au, B, Be, Br, Cl, I, P and Se). In such approach, Q1 was set at the m/z of the corresponding target ion, while Q2 was selected at m/z = 32 (O_2^+). These authors demonstrated using isotopically enriched O_2 that asymmetric charge transfer also occurs for elements with lower ionization energy (i.e, when the reaction is not likely to occur), and they have tentatively explained that the reaction proceeds through metastable ionic states. Further investigation is, however, required to fully explain the processes observed.

In contrast to O_2, the high reactivity of NH_3 leads to many simple and higher order reaction product ions, which renders it into a potentially powerful tool for multi-element method development. An example demonstrating the capabilities of NH_3 for multi-elemental analysis was provided by Sugiyama *et al.***[33]** in the context of the interference-free determination of noble metal elements – Ag, Au, Ir, Pd, Pt, Os, Rh and Ru. Noble metals comprise the platinum group metals (PGMs), Au and Ag, which are highly affected by several types of interferences. In this work, the high reactivity of NH_3 towards many of these interferences was used for avoiding spectral overlap. Ag, Pd, Rh and Ru show low reactivity with NH_3, so upon removing the interfering ions by reaction with NH_3, these analyte elements could be accurately measured at their original m/z (on-mass approach). In the case of Au, Ir, Os and Pt, high reactivity was shown for both analyte and interfering ions. Thus, the best suited reaction product ions were identified via product ion scanning. By means of the comparison of the corresponding product ion spectra for analyte and interfering ions, $Au(NH_3)_2^+$, $IrNH^+$, $OsNH^+$ and $Pt(NH_3)_2^+$ were selected for quantification purposes (mass-shift approach).

Next to NH_3, also CH_3F (mixture of 10% CH_3F and 90% He) has been evaluated for its capabilities for multi-elemental analysis. As described above, CH_3F can be involved in different reaction types, F-atom transfer and CH_3F addition being the most common ones. The potential of CH_3F in ICP-MS/MS was assessed by Bolea-Fernandez *et al.*(Chapter 3)**[44]** in the context of the determination of ultra-trace concentrations of light metals (m/z≤60) in biofluids. Al, Co, Cr, Mn, Ni, Ti and V were selected as the target elements in this work due to their relevance in

biomedical applications. It was observed that low CH_3F/He gas flow rates preferably lead to F-atom transfer (MF^+), while higher gas flow rates rather lead to CH_3F addition ($M(CH_3F)_x^+$) and/or higher order reaction product ions ($MF_a(CH3F)_b^+$). Via product ion scanning, the best reaction product ions were identified. Under compromise conditions (i.e. maximum CH_3F/He gas flow rate – 1mL min^{-1} with the mass flow controller calibrated for O_2), a multi-element method was developed for the simultaneous determination of all target elements. Accurate results were obtained, as well as instrumental LODs below 10 ng L^{-1}.

1.2.2. Isotopic analysis

As is widely known, ICP-MS is not only able to provide elemental, but also isotopic information. These isotope ratio measurements can even be affected by spectral interference to a larger extent, as for this type of analysis at least two isotopes of the same element need to be measured interference-free. The use of ICP-MS/MS for both the determination of natural variations in isotopic composition and for isotope dilution mass spectrometry (IDMS) have been reported on in literature.

1.2.2.1. Isotope dilution mass spectrometry

IDMS is considered as one of the most powerful methods for elemental assay with high accuracy.**[45]** The capabilities of ICP-MS/MS for IDMS determination of S in organic matrices were evaluated by Balcaen *et al.***[30]** As stated before, O_2 is a suited reaction gas to convert S^+ ions into the corresponding SO^+ reaction product ions by O-atom transfer. However, the presence of interfering ions at the m/z of the reaction product ions selected (Ca^+, Cr^+, Ti^+ and – in organic matrix – also ArC^+) traditionally hinders the accuracy of the determination. For evaluating the potential of ICP-MS/MS, 3 different modes were used: standard mode (no gas), bandpass mode (simulating ICP-DRC-QMS conditions) and MS/MS mode. It was clear from this work that only when using the MS/MS mode, accurate results can be obtained by means of IDMS. As a proof-of-concept, S was successfully determined in the NIST SRM 2773 (biodiesel) reference material. This work provided a general method for the accurate quantification of S in organic matrices, which is also applicable to S-speciation via reverse phase HPLC-ICP-MS/MS.

1.2.2.2. Natural variations in isotopic composition

Among the long list of challenges that characterizes isotopic analysis, the high precision required to see the often small natural variations in isotopic composition remains the most important one. For this reason, ICP-QMS has often been restricted to the study of induced changes in the isotopic composition of target elements in the context of tracer experiments with enriched stable isotopes or of IDMS. However, although limited to values of ~0.1% RSD, the precision attainable by means of quadrupole based ICP-MS instrumentation is fit-for-purpose for the study of natural variations in some specific applications, especially those dealing with elements with (a) radiogenic nuclide(s).

An ICP-MS/MS method for the accurate determination of $^{129}I/^{127}I$ isotope ratios was developed by Ohno *et al.***[46]** with the objective of investigating radioiodine released by the Fukushima Daiichi Nuclear Power Plant (FDNPP) accident. However, the ultra-trace concentrations of $^{129}I^+$ and the overlap of this signal with that of the isobaric $^{129}Xe^+$ and with the polyatomic ions $^{127}IH_2^+$ and $^{127}ID^+$ might hinder this determination. The use of 0.9 mL min^{-1} of O_2 in the reaction cell was sufficient to obtain a 1000-fold improvement in the background equivalent concentration (BEC) by means of the reduction of the isobaric overlap by $^{129}Xe^+$. In addition, the use of the MS/MS mode rejects all ions with different m/z than 129 by means of Q1, thus avoiding the formation of $^{127}IH_2^+$ and $^{127}ID^+$ in the reaction cell, while the low level of those interferences formed in the plasma can be corrected for by mathematical correction.

In the aftermath of the Fukushima accident, some works have focused on the determination of cesium (Cs) isotope ratios.**[47-49]** The accurate determination of $^{134}Cs/^{137}Cs$ and $^{135}Cs/^{137}Cs$ ratios is hampered by the overlap of the signals of Cs^+ with those of Ba^+ and of the oxides of Sb^+ and Sn^+. By means of ICP-MS/MS using nitrous oxide (N_2O) as a reaction gas, accurate isotope ratio results were obtained for different environmental samples. N_2O is a non-common reactive gas for ICP-MS/MS, for which O-atom transfer is the main reaction. In these works, isobaric interferences from $^{134,134,137}Ba$ were removed by means of reaction with N_2O ($Ba^+ + N_2O \rightarrow BaO^+ + N_2$), while Cs isotopes can be measured free from spectral overlap at the original m/z (on-mass approach). In addition, the ICP – tandem mass spectrometer operating in the MS/MS mode is able to reject Sb^+ and Sn^+ ions by means of Q1, thus avoiding the formation of the interfering ions SbO^+ and SnO^+ by

reaction with N_2O in the CRC. Thus, accurate isotopic analysis of Cs became feasible in spite of the different spectral interferences originally hindering this determination.

Another example of the use of ICP – tandem mass spectrometry for isotopic analysis is the measurement of strontium (Sr) isotope ratios. Sr shows relatively large natural variation in its isotopic composition as a result of the radiogenic character of ^{87}Sr, i.e. β^- decay of ^{87}Rb results in the formation of ^{87}Sr. However, ^{87}Rb shows isobaric overlap with ^{87}Sr, such that accurate isotope ratio results cannot be obtained except if Sr is chemically separated from Rb prior to the analysis. Bolea-Fernandez *et al.*(Chapter 6)**[50]** used ICP-MS/MS and CH_3F/He as a reaction gas to avoid the spectral overlap in the isotopic analysis of Sr, by means of the reaction between Sr^+ and CH_3F, leading to SrF^+, and the absence of reactivity in the case of Rb. Accurate $^{87}Sr/^{86}Sr$ isotope ratio results (measured as $^{87}SrF^+/^{86}SrF^+$) were obtained without matrix-matching of the external standard, and in the presence of interfering ions at the m/z of the reaction product ions selected, (owing to the ability of Q1 to reject all ions with an $m/z \neq 86$, 87 and 88). **Figure 1.8** shows the isotopic pattern for a standard solution of Sr and the same solution spiked with otherwise interfering elements i.e., Ag, Cd, Pd and Rb, using both SQ and MS/MS mode. It can be appreciated that there is spectral overlap when measuring on-mass using both modes and in mass-shift (SrF^+) in SQ mode, while in MS/MS mode, the isotopic pattern is preserved, thus allowing a direct isotopic analysis of Sr without prior Rb/Sr separation. In an earlier work performed with single quad ICP-DRC-QMS, matrix-matching of the standards used for mass bias correction was necessary.

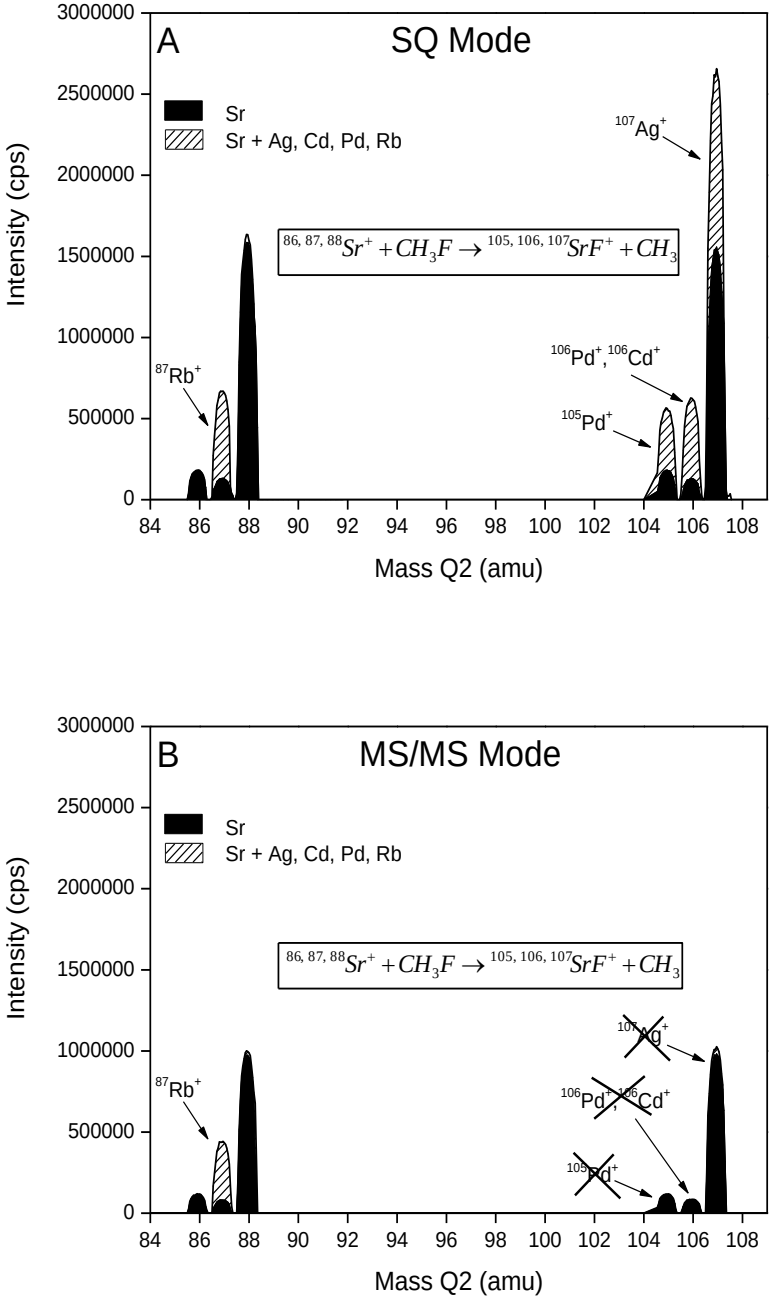

Figure 1.8. Mass spectrum showing the isotopic composition of Sr at the original m/z (86, 87 and 88) and at the m/z of the selected reaction product ion (SrF^{+}, 105, 106 and 107) for a standard solution of Sr (black) and for a standard solution of Sr doped with Ag, Cd, Pd and Rb (dashed lines) in both, SQ (A) and MS/MS (B) mode. Adapted from Bolea-Fernandez *et al.***[50]**

1.2.3. Hyphenated ICP-MS/MS applications

Like all ICP-MS devices, an ICP – tandem mass spectrometer can be coupled to other sample introduction systems or separation techniques to improve the performance for some specific and/or more demanding applications. A brief review of some of these hyphenated ICP-MS/MS applications is presented in this section.

1.2.3.1. Chromatography

When coupling LC or GC to ICP-MS, speciation analysis can be performed with highly sensitive detection, while the setup provides the advantage of structure-independent quantification. As many of the elements typically of interest in speciation studies (e.g., S, P, Cl, As, Se) are prone to spectral overlap in ICP-MS, the added value of using tandem mass spectrometry in this context is clear. Moreover, especially when combining LC and ICP-MS, the effluent of the LC system often contains a large fraction of organic solvents that may lead to additional interferences in the ICP-MS detection, which have to be tackled. Nelson *et al.***[51]** developed a new strategy for the determination of organo-Cl, -P and -S compounds in pesticides by means of gas chromatography ICP-MS/MS (GC-ICP-MS/MS). In this work, $^{31}P^+$ and $^{32}S^+$ were measured simultaneously using the MS/MS mode with O_2 as the reaction gas selected to avoid spectral overlap by means of O-atom transfer, producing the corresponding $^{31}PO^+$ and $^{32}SO^+$ reaction product ions (m/z = 47 and 48, respectively). Cl, however, could not be measured under the same conditions due to the different reactivity of Cl towards O_2 (charge transfer being the dominant process $Cl^+ + O_2 \rightarrow Cl + O_2^+$). Thus, Cl was measured upon reaction with H_2 in the CRC, according to the reaction pathway $Cl^+ + H_2 \rightarrow ClH_2^+$. It is important to stress that the chemical resolution of the spectral interferences affecting $^{35}Cl^+$ by reaction with H_2, with formation and detection of $^{35}ClH_2^+$, can only be accomplished successfully in MS/MS mode, otherwise there would be overlap of the signals of $^{35}ClH_2^+$ and $^{37}Cl^+$. Although also ^{37}Cl reacts with H_2 to form $^{37}ClH_2^+$, mass-shift reactions are typically not 100% efficient, such that part of the ^{37}Cl ions are still detected at their original m/z=37, as a consequence of which there is overlap with the $^{35}ClH_2^+$ signal. By using both methods, interference-free conditions for the measurement of P, S and Cl were obtained with LODs of 0.0005, 0.7 and 0.1 µg Kg^{-1}, respectively.

A similar method has been described by Diez Fernández *et al.***[52]** for the determination of ^{31}P and ^{32}S in the context of absolute quantitative proteomics and phosphoproteomics via HPLC-ICP-MS/MS with detection limits of 10 and 7 fmol for S and P, respectively.

HPLC-ICP-MS/MS has also been used for the speciation of different As-compounds at trace or ultra-trace levels. The method widely used in this context is O-atom transfer between O_2 and As^+ (m/z = 75 – Q1) and detection of As at the m/z of the AsO^+ reaction product ion (m/z = 91 – Q2), enabling interference-free determinations.**[53,54]** A similar approach using HPLC-ICP-MS/MS was also used by Musil *et al.***[55]** and compared with selective hydride generation (HG-ICP-MS/MS) for monitoring of inorganic As (iAs) in the context of food analysis. Using $NaBH_4$ at acidic conditions (high HCl concentration), the gaseous phase consisted of iAs only, while no volatile organoarsenic compounds were formed. This method was shown faster than HPLC-ICP-MS, without significant statistical difference for iAs concentration and with comparable LODs.

1.2.3.2. Asymmetric flow field-flow fractionation

Hyphenation of asymmetric flow field-flow fractionation to ICP-MS/MS (FFF-ICP-MS/MS) has been reported on in literature for nanoparticle analysis, i.e. separation and identification of nanoparticles. In the works of Menendez-Miranda *et al*,**[56,57]** a method for the interference-free determination of Cd, S, Se and Zn was developed for the assessment of the chemical composition of CdSe/ZnS quantum-dots populations (QDs). For such determination, a multi-element method was developed by combining on-mass and mass-shift approaches. It was shown that 0.35 mL min^{-1} of O_2 suffices to convert $^{32}S^+$ and $^{80}Se^+$ ions into the corresponding SO^+ and SeO^+ reaction product ions (m/z = 48 and 96, respectively), while $^{111}Cd^+$ an $^{66}Zn^+$ do not show reactivity towards O_2. An example of the fractogram obtained in this way is shown in **Figure 1.9**.

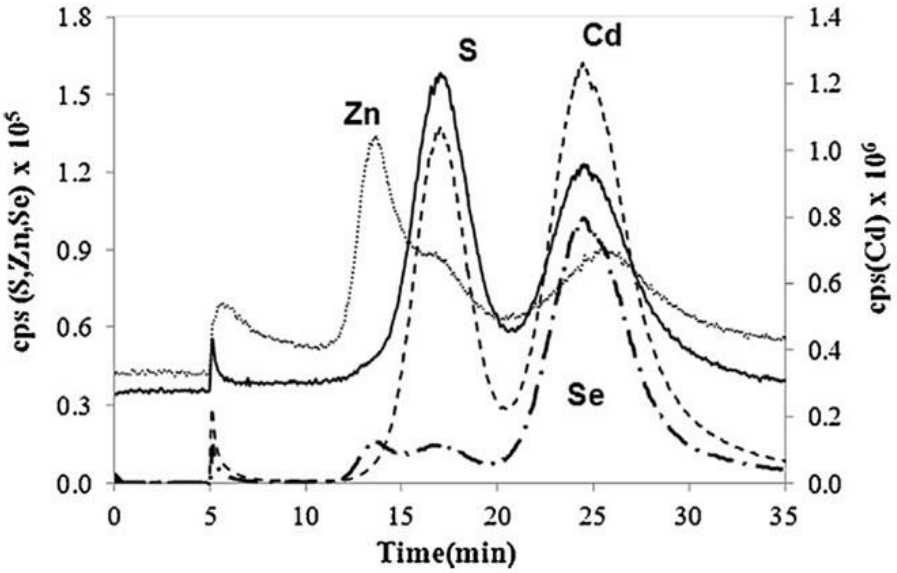

Figure 1.9. Fractogram of CdSe/ZnS quantum-dots population obtained using FFF-ICP-MS/MS. Nuclides measured: solid line: ^{32}S; dotted line: ^{66}Zn; dash-dot line: ^{80}Se; dashed line: ^{111}Cd. Adapted from Menendez-Miranda *et al.***[56]**

Another example on the use of FFF-ICP-MS/MS is the work of Aureli *et al.*,**[58]** who aimed at the development of easy, reliable and sensitive analytical methods for the determination of nano-sized silica, thus enabling the evaluation of possible effects of synthetic amorphous silica in nanomaterials on human health. Si was measured free from spectral interference after conversion of Si^+ ions into the corresponding SiO^+ reaction product ions by adding O_2 gas in the cell - m/z Q2 = 44, 45 and 46 for ^{28}Si, ^{29}Si and ^{30}Si, respectively). The method was successfully applied to the characterization of a reference material and a Si-suspension, containing particles with nominal diameters of 20 and 140 nm, respectively.

1.2.3.3. Laser ablation

The combination of laser ablation (LA) with ICP-MS detection is a powerful combination with as main advantages highly efficient and fast sample introduction, after limited sample preparation and with minimal sample damage. Moreover, by coupling LA to ICP-MS, the application range of ICP-MS is extended to spatially resolved analysis of selected sample regions. To date, only a few LA-ICP-MS/MS

papers have been published. This may be related to the fact that the LA unit provides transient signals, while – due to the double mass selection – ICP-MS/MS can be seen as a somewhat slower detector than single quadrupole ICP-MS instruments.

Bishop et al.**[59]** evaluated the capabilities of LA-ICP-MS/MS for elemental bio-imaging (EBI) of trace metal distributions in tissue sections. Different modes of operation were evaluated: no gas, bandpass (H_2 in the CRC) and MS/MS (O_2 in the CRC). The best conditions were found when using O_2 and such mode was used for evaluating the distribution of Zn (on-mass) within prostate cancer biopsy sample and of P and Se (mass-shift – PO^+ and SeO^+) in a mouse brain (**Figure 1.10**). This work was the first to demonstrate the potential of LA-ICP-MS/MS for EBI.

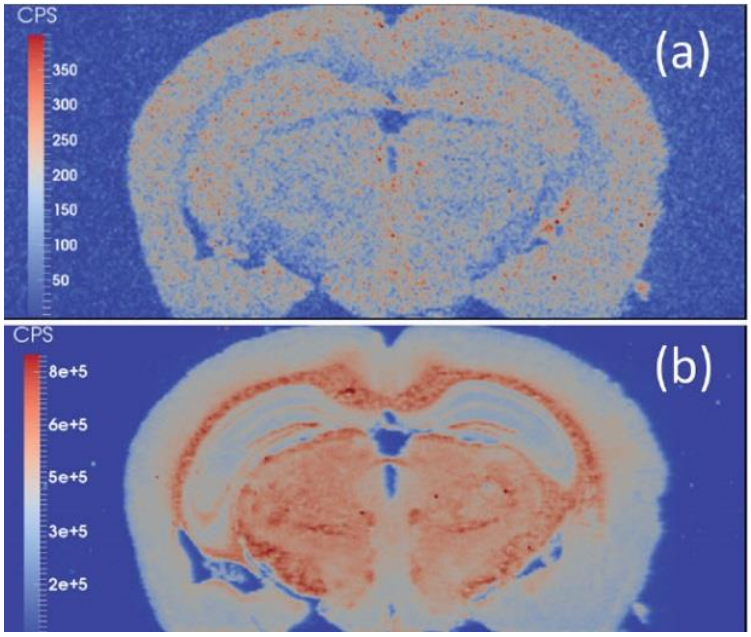

Figure 1.10. Image of a mouse brain obtained with LA-ICP-MS/MS (O_2 mode). (a) $^{80}Se^+ \rightarrow {}^{80}Se^{16}O^+$ and (b) $^{31}P^+ \rightarrow {}^{31}P^{16}O^+$. Adapted from Bishop *et al.***[59]**

Bolea-Fernandez *et al.*(Chapter 7)**[60]** reported on the use of LA-ICP-MS/MS for direct Sr isotopic analysis of solid samples with high Rb/Sr ratio. The approach used in this work involves chemical resolution of the isobaric overlap of the signals of ^{87}Rb and ^{87}Sr via reaction with CH_3F (as described in section 1.2.2.2 for digested materials), enabling accurate isotopic analysis of Sr without previous isolation of Rb

for samples showing high Rb/Sr ratio. The comparison of two different approaches, i.e., working under dry and wet plasma conditions, respectively, revealed that the use of wet plasma obtained by mixing of the LA aerosol with nebulized H_2O, provided the best results in terms of accuracy and precision (<0.05 % RSD) without the requirement of matrix-matching of the external standard for mass bias correction. The methodology developed in this work can be seen as a good and fast alternative for real-life applications in which the differences in isotopic composition between different samples are not too small, and for pre-screening and pre-selecting samples for higher-precision isotopic analysis, i.e. using thermal ionization mass spectrometry (TIMS) and/or multi-collector ICP-MS (MC-ICP-MS).

1.3. Summary and future perspectives

In this chapter, the operating principles of ICP – tandem mass spectrometry have been described with the focus on the differences between the tandem mass spectrometry configuration and conventional quadrupole-based ICP-MS. Furthermore, some demanding applications, covering a wide range of application fields, have been shortly reviewed. From this, the reader should have a clear view on the general capabilities and limitations of ICP – tandem mass spectrometry. However, the technique is still very recent and it may be expected that over the next years, many more application areas will benefit from the additional possibilities offered by ICP – tandem mass spectrometry. The use of ICP-MS/MS opens new possibilities to deal with spectral overlap by offering superior control over the cell chemistry, thus enhancing the possibilities of chemical resolution in ICP-QMS. The different scanning options are powerful tools for method development and for identification of the best suited reaction product ions, even or especially when using highly reactive gases. The fast increase in the number of ICP-MS/MS papers in literature illustrates these added values.

References

[1] R. F. J. Dams, J. Goossens, L. Moens, Mikrochim Acta, 119 (1995) 277 – 286.

[2] K. Sakata, K. Kawabata, Spectrochim Acta, Part B, 49 (1994) 1027 - 1038 .

[3] M. G. Minnich, R. S. Houk, J Anal At Spectrom, 13 (1998) 167 – 174.

[4] S. D. Tanner, J Anal At Spectrom, 10 (1995) 905 - 921.

[5] N. Jakubowski, L. Moens, F. Vanhaecke, Spectrochim Acta, Part B, 53 (1998) 1739 - 1763 (1998).

[6] L. Moens, N. Jakubowski, Anal Chem, 70 (1998) 251A - 256A.

[7] D. J. Douglas, Can J Spectrosc, 34 (1989) 38 - 49.

[8] S. D. Tanner, V. I. Baranov, At Spectrosc, 20 (1999) 45 – 52.

[9] S. D. Tanner, V. I. Baranov, D. R. Bandura, Spectrochim Acta, Part B, 57 (2002) 1361 - 1452.

[10] V. I. Baranov, S. D. Tanner, J Anal At Spectrom, 14 (1999) 1133 - 1142.

[11] N. Yamada, Spectrochim Acta, Part B, 110 (2015) 31 - 44.

[12] I. Feldmann, N. Jakubowski, D. Stuewer, Fresenius J Anal Chem, 364 (1999) 415 - 421.

[13] I. Feldmann, N. Jakubowski, C. Thomas, D. Stuewer, Fresenius J Anal Chem, 365 (1999) 422 - 428.

[14] S. D. Tanner, V. I. Baranov, U. Vollkopf, J Anal At Spectrom, 15 (2000) 1261 - 1269.

[15] S. D. Tanner, V. I. Baranov, J Am Soc Mass Spectrom, 10 (1999) 1083 - 1094.

[16] J. T. Rowan, R. S. Houk, Appl Spectroscopy, 43 (1989) 976 – 980.

[17] G. K. Koyanagi, V. I. Baranov, S. D. Tanner, D. K. Bohme, J Anal At Spectrom, 15 (2000) 1207 – 1210.

[18] D. K. Bohme, Int J Mass Spectrom, 200 (2000) 97 – 136.

[19] G. C. Eiden, C. J. Barinaga, D. W. Koppenaal, Rapid Commun Mass Spectrom, 11 (1997) 37 – 42.

[20] E. R. Denoyer, S. D. Tanner, U. Vollkopf, Spectroscopy, 14 (1999) 43 – 54.

[21] D. R. Bandura, S. D. Tanner, At Spectroscopy, 20 (1999) 69 – 72.

[22] K. K. Murray, R. K. Boyd, M. N. Eberlin, G. J. Langley, L. Li, Y. Naito, Pure Appl Chem, 85 (2013) 1515 - 1609.

[23] Z. Du, T. N. Olney, D. J. Douglas, J Am Soc Mass Spectrom, 8 (1997) 1230 - 1236.

[24] S. F. Boulyga, S. Becker, J Anal At Spectrom, 17 (2002) 1202 - 1206.

[25] K. Blaum, C. Geppert, P. Müller, W. Nörtershäuser, K. Wendt, B. A. Bushaw, Int J Mass Spectrom, 202 (2000) 81 - 89.

[26] J. Goossens, F. Vanhaecke, L. Moens, R. Dams, Anal Chim Acta, 280 (1993) 137 - 143.

[27] J. Darrouzès, M. Bueno, G. Lespès, M. Potin-Gautier, Talanta, 71 (2007) 2080 - 2084.

[28] S. Meyer, M. Matissek, S. M. Müller, M. S. Taleshi, F. Ebert, K. A. Francesconi, T. Schwerdtle, Metallomics, 6 (2014) 1023 - 1033.

[29] S. Meyer, J. Schulz, A. Jeibmann, M. A. Taleshi, F. Ebert, K. A. Francesconi, T. Schwerdtle, Metallomics, 6 (2014) 2010 - 2014.

[30] L. Balcaen, G. Woods, M . Resano, F. Vanhaecke, J Anal At Spectrom, 28 (2013) 33 - 39.

[31] X-W. Wang, J-F. Liu, X-Y. Wang, B. Shao, L-P. Liu, J. Zhang, Anal Methods, 7 (2015) 3224 - 3228.

[32] D. P. Bishop, D. J. Hare, F. Fryer, R. V. Taudte, B. R. Cardoso, N. Cole, P. A. Doble, Analyst, 140 (2015) 2842 - 2846.

[33] N. Sugiyama, Y. Shikamori, J Anal At Spectrom, 30 (2015) 2481 - 2487.

[34] L. Balcaen, E. Bolea-Fernandez, M. Resano, F. Vanhaecke, Anal Chim Acta, 809 (2014) 1 - 8.

[35] L. J. Moens, F. F. Vanhaecke, D. R. Bandura, V. I. Baranov, S.D. Tanner SD, J Anal At Spectrom, 16 (2001) 991 - 994.

[36] N. Nonose, M. Ohata, T. Narukawa, A. Hioki, K. Chiba, J Anal At Spectrom, 24 (2009) 310 - 319.

[37] X. Zhao, G. K. Koyanagi, D. K. Bohme, J Phys Chem A, 110 (2006) 10607 - 10618.

[38] P. Redondo, A. Varela-Álvarez, V. M. Rayón, A. Largo, J. A. Sordo, C. Barrientos, J Phys Chem A, 117 (2013) 2932 - 2943.

[39] E. Bolea-Fernandez, L. Balcaen, M. Resano, F. Vanhaecke, Anal Bioanal Chem, 407 (2015) 919 - 929.

[40] C. D. B. Amaral, R. S. Amais, L .L. Fialho, D. Schiavo, T. Amorim, A. R. A. Nogueira, F. R. P. Rocha, J. A. Nóbrega, Anal Methods, 7 (2015) 1215 - 1220.

[41] S. Diaz Fernández, J. R. Encinar, A. Sanz-Medel, D. Isensee, H. M. Stoll, Geochem, Geophys, Geosyst, 16 (2015) 2005 - 2014.

[42] R. S. Amais, A. Virgilio, D. Schiavo, J. A. Nóbrega, Microchem J, 120 (2015)64 - 68.

[43] K. Böting, S. Treu, P. Leonhard, C. Heiß, N. H. Bings, J Ana At Spectrom, 29 (2014) 578 - 582.

[44] E. Bolea-Fernandez, L. Balcaen, M. Resano, F. Vanhaecke, Anal Chem, 86 (2014) 7969 - 7977.

[45] P. Rodríguez-González, J. M. Marchante-Gayón, J. I. G. Alonso, A. Sanz-Medel, Spectrochim Acta, Part B, 60 (2005) 151 - 207.

[46] T. Ohno, Y. Muramatsu, Y. Shikamori, C. Toyama, N. Okabe, H. Matsuzaki, J Anal At Spectrom, 28 (2013) 1283 - 1287.

[47] T. Ohno, Y. Muramatsu, J Anal At Spectrom, 29 (2014) 347 - 351.

[48] J. Zheng, W. Bu, K. Tagami, Y. Shikamori, K. Nakano, S. Uchida, N. Ishii, Anal Chem, 86 (2014) 7103 - 7110.

[49] J. Zheng, K. Tagami, W. Bu, S. Uchida, Y. Watanabe, Y. Kubota, S. Fuma, S. Ihara, Environ Sci Technol, 48 (2014) 5433 - 5438.

[50] E. Bolea-Fernandez, L. Balcaen, M. Resano, F. Vanhaecke, J Anal At Spectrom, 31 (2015) 303 - 310.

[51] J. Nelson, H. Hopfer, F. Silva, S. Wilbur, J. Chen, K. S. Ozawa, P. L. Wylie, J Agric Food Chem, 63 (2015) 4478 - 4483.

[52] S. Diaz Fernández, N. Sugishama, J. R. Encinar, A. Sanz-Medel, Anal Chem, 84 (2012) 5851 - 5857.

[53] J. D. Palcic, J. S. Jones, E. L. Flagg, S. F. Donovan, J Anal At Spectrom, 30 (2015) 1799 - 1808.

[54] B. P. Jackson, J Anal At Spectrom, 30 (2015) 1405 - 1407.

[55] S. Musil, A. H. Pétursdóttir, A. Raab, H. Gunnlaugsdóttir, E. Krupp, J. Feldmann, Anal Chem, 86 (2014) 993 - 999.

[56] M. Menendez-Miranda, M. T. Fernandez-Arguelles, J. M. Costa-Fernandez, J. R. Encinar, A. Sanz-Medel, Anal Chim Acta, 839 (2014) 8 - 13.

[57] M. Menendez-Miranda, J. R. Encinar, J. M. Costa-Fernandez, A. Sanz-Medel, J Chromatogr A, 1422 (2015) 247 - 252.

[58] F. Aureli, M. D'Amato, A. Raggi, F. Cubadda, J Anal At Spectrom, 30 (2015) 1266 1273.

[59] D. P. Bishop, D. Clases, F. Fryer, E. Williams, S. Wilkins, D. J. Hare, N. Cole, W. Karst, P. A. Doble, J Anal At Spectrom, 31 (2016) 197 - 202.

[60] E. Bolea-Fernandez, S. J. M. Van Malderen, L. Balcaen, M. Resano, F. Vanhaecke, J Anal At Spectrom, 31 (2016) 464 - 472.

CHAPTER 2

Accurate determination of ultra-trace levels of Ti in blood serum using ICP-MS/MS

Adapted from Balcaen et. al., Anal. Chim. Acta, 809 (2014) 1 – 8

2.1. Introduction

The determination of low levels of Ti in biological fluids has become a hot topic in the last 10 to 15 years, mainly because of the increased use of Ti in prostheses and dental implants and the awareness that metallic joint replacement devices can interact with the surrounding body fluids and tissues. As all metallic implants are subject to wear over time, increased serum and urine metal concentrations and, eventually, local and systemic metal storage may be the result.**[1-7]** Moreover, Ti is also widely used – often under the form of TiO_2 nanoparticles - as a white pigment in paints, coatings, plastics, food, toothpaste or in sunscreen.**[8]** In 2006, the International Agency for Research on Cancer (IARC) has classified TiO_2 dust as an IARC Group 2B carcinogen, which means that it is possibly carcinogenic to humans.**[8]** So far, there is no real evidence on the clinical consequences and potential adverse effects of Ti, released in the human body, but there is a clear need for more systematic research on this topic.**[9]**

Over the years, many authors have reported on the basal Ti levels in human body fluids, with values ranging between 0.200 µg L^{-1} and 200 µg L^{-1}.**[5, 6, 10-13]** The very large spread on these results indicates that there is a lot of confusion about the actual basal levels of Ti, which makes it also difficult to obtain reliable information on the possible release of additional Ti in the body. This controversy finds its origin in the fact that most of the analytical methods typically used for trace element determination – such as ETAAS (electrothermal atomization atomic absorption spectrometry),**[14, 15]** ICP-OES (inductively coupled plasma - optical emission spectroscopy) **[16]** or ICP-QMS (inductively coupled plasma - quadrupole-based mass spectrometry) **[3, 17]** – are not sensitive and/or selective enough to allow for an accurate quantification of the ultra-trace levels of Ti in complex matrices, such as human blood (serum). Although, owing to its sensitivity, ICP-MS can generally be seen as the method of choice for the determination of ultra-trace metals in clinical samples, the specific problem for Ti is the occurrence of spectral overlap affecting all Ti isotopes (**Table 2.1**) when samples with high Ca, P, S, C and Cl contents (such as clinical samples) have to be analyzed.

Nowadays, the most general way of dealing with spectral interferences is the use of a suited collision/reaction gas in a quadrupole-based ICP-MS instrument (chemical resolution), or of double-focusing sector field (SF)-ICP-MS (higher mass resolution).

Table 2.1. Titanium isotopes with their natural isotopic abundance [18] and the most important isobaric and polyatomic interferences [19] (non-restrictive list).

Analyte	Abundance (%)	Isobaric interferences	Polyatomic Interferences
$^{46}Ti^+$	8.25	Ca^+ (0.004[a])	$^{32}S^{14}N^+$, $^{14}N^{16}O_2^+$, $^{15}N_2{}^{16}O^+$
$^{47}Ti^+$	7.44	---	$^{32}S^{14}N^1H^+$, $^{30}Si^{16}O^1H^+$, $^{32}S^{15}N^+$, $^{33}S^{14}N^+$, $^{15}N^{16}O_2^+$, $^{14}N^{16}O_2{}^1H^+$, $^{12}C^{35}Cl^+$, $^{31}P^{16}O^+$
$^{48}Ti^+$	73.72	Ca^+ (0.187[a])	$^{32}S^{16}O^+$, $^{34}S^{14}N^+$, $^{33}S^{15}N^+$, $^{14}N^{16}O^{18}O^+$, $^{14}N^{17}O_2^+$, $^{12}C_4^+$, $^{36}Ar^{12}C^+$
$^{49}Ti^+$	5.41	---	$^{32}S^{17}O^+$, $^{32}S^{16}O^1H^+$, $^{35}Cl^{14}N^+$, $^{34}S^{15}N^+$, $^{33}S^{16}O^+$, $^{14}N^{17}O_2{}^1H^+$, $^{14}N^{35}Cl^+$, $^{36}Ar^{13}C^+$, $^{36}Ar^{12}C^1H^+$, $^{12}C^{37}Cl^+$, $^{31}P^{18}O^+$, $^{31}P^{17}O^1H^+$
$^{50}Ti^+$	5.18	Cr^+ (4.345[a]), V^+ (0.25[a])	$^{32}S^{18}O^+$, $^{32}S^{17}O^1H^+$, $^{36}Ar^{14}N^+$, $^{35}Cl^{15}N^+$, $^{36}S^{14}N^+$, $^{33}S^{17}O^+$, $^{34}S^{16}O^+$, $^{35}Cl^{14}N^1H^+$, $^{34}S^{15}N^1H^+$

[a] Isotopic abundance (%) for isobaric interferences

Sarmiento-González *et al.* showed that the interferences affecting the Ti isotopes could not be overcome by using H_2 or He as collision/reaction gases in an ICP-QMS instrument, equipped with an octopole collision/reaction cell (or octopole reaction system ORS).**[17]** Up to now, only by using a double-focusing SF-ICP-MS instrument, operated at a higher mass resolution (R=3000), a method detection limit of < 100 ng L^{-1} could be obtained.**[20]** From the above, it must be clear that the shortness in suitable analytical methodologies severely hinders the research concerning Ti release in the body of people with Ti-based implants, particularly considering that the superior robustness and cost-efficiency of quadrupole-based ICP-MS devices makes these instruments to be more prevalent in routine labs than SF-ICP-MS devices.

The introduction of tandem ICP-mass spectrometry (ICP-MS/MS) offers superior potential to deal with spectral overlaps (Chapter 1).**[21, 22]** Such instrument should therefore offer improved possibilities for the determination of Ti, although the number of publications reporting on the performance of this spectrometer is still very low and, to the best of the authors' knowledge, no papers reporting on Ti monitoring have been published yet.

Therefore, the main goal of this work is to explore the capabilities of an ICP-QQQ device and develop a novel analytical method that is both sensitive and selective enough to allow for the accurate determination of Ti concentrations in blood serum of non-exposed and exposed individuals.

2.2. Experimental

2.2.1. Instrumentation

All measurements were carried out with an Agilent 8800 triple-quadrupole ICP-MS instrument (ICP-QQQ / Agilent Technologies, Japan), equipped with a MicroMist nebulizer and a Peltier-cooled (2 °C) scott-type spray chamber for sample introduction. This instrument contains an octopole-based collision/reaction cell, located in-between two quadrupole mass analyzers. The octopole cell can be vented or pressurized with a collision gas (typically He) or a reaction gas (typically H_2, O_2 or NH_3/He), or a mixture of both (**Figure 2.1**).

In this work, the possibilities of using O_2 and NH_3/He as reaction gases for the interference-free determination of Ti in a blood serum matrix, were evaluated. As the width of the first quadrupole bandpass can be varied from “fully open” down to “single mass width”, an enhanced control over the chemical reactions taking place in the octopole cell is enabled (compared to other collision/reaction cell based instruments). This offers good prospects for the determination of elements which traditionally suffer from spectral interferences when measured with a quadrupole-based ICP-mass spectrometer. Typical instrumental settings and measurement parameters used throughout the experiments can be found in **Table 2.2**.

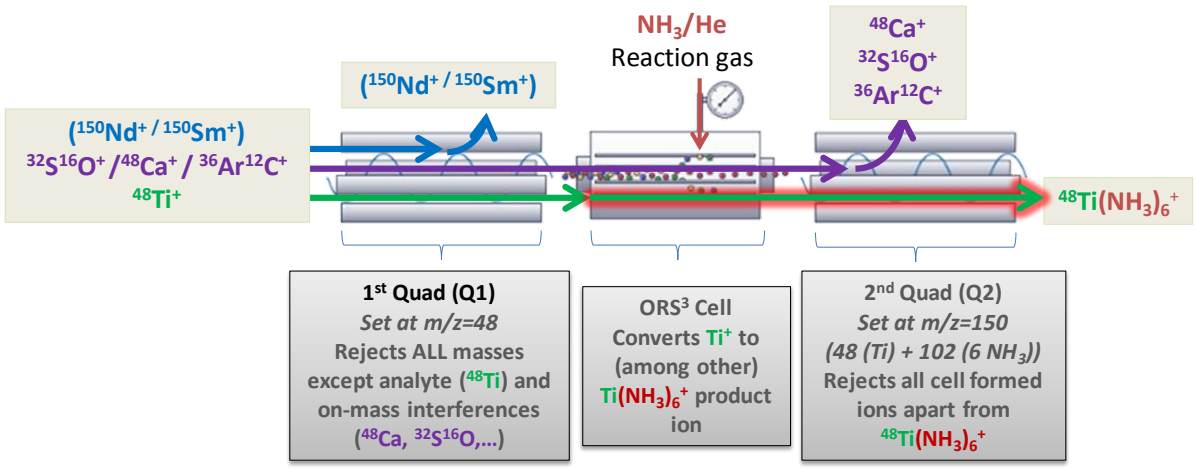

Figure 2.1. Schematic representation of the operating principle of the ICP-QQQ system, functioning in MS/MS mode, leading to an interference-free determination of ^{48}Ti (as $^{48}Ti(NH_3)_6^+$). (same principle for other Ti-isotopes)

To validate the results obtained by means of ICP-MS/MS, all samples have also been analyzed by means of sector field ICP-MS, which – until now – can be seen as the method of choice for the determination of low levels of Ti in biological materials. For these analyses, a Thermo Element XR sector field ICP-MS instrument (ThermoScientific, Germany) was used, under the conditions specified in **Table 2.2**.

2.2.2. Samples and reagents

All standard solutions that were used for optimization, internal standardization and calibration were prepared by dilution of commercially available single element standard solutions (1 g L^{-1} – Instrument Solutions, The Netherlands) with 0.14 M HNO_3. Only high-purity reagents were used for sample preparation. Water was purified by means of a Direct Q-3 Milli-Q system (Millipore, USA), while HNO_3 (14 M, pro analysis, ChemLab, Belgium) was further purified by sub-boiling distillation.

For external calibration, a set of 5 standard solutions with concentrations ranging between 0 and 5 µg L^{-1} Ti (0, 0.5, 1, 2.5 and 5 µg L^{-1} Ti) was used. For validation of the method, Seronorm™ Trace Elements Serum, Level 1 (Ref. 9067 - Sero, Norway) was used. For this material, the Ti concentration is not certified, but an indicative value of 11.2 µg L^{-1} Ti is provided on the certificate of analysis.

Table 2.2. Instrumental settings for the Agilent 8800 ICP-QQQ and the Thermo Element XR SF-ICP-MS instruments.

Agilent 8800			**Element XR**	
	NH_3/He (10/90)	**O_2**		
Scan type	MS/MS		Scan type	EScan
Plasma mode	Low Matrix		Resolution	Medium
RF power	1550 W		RF power	1200 W
Carrier gas flow rate	1.08 L min^{-1}		Carrier gas flow rate	0.975 L min^{-1}
Reaction gas flow rate	2 mL min^{-1} [a]	0.2 mL min^{-1}		
Q1 bias	-1 V		Mass window	100%
Octopole bias	-5 V		Search window	70%
Energy discrimination	-8 V		Integration window	60%
Q2 bias	-13 V		Sample time	0.010 s
Q2 axis offset	-0.18	-0.01	Samples/peak	20
Q1 –> Q2 masses	46 –> 148 47 –> 149 48 –> 150 49 –> 151 50 –> 152 71 –> 71	46 –> 62 47 –> 63 48 –> 64 49 –> 65 50 –> 66 71 –> 71	Nuclides monitored	^{47}Ti, ^{49}Ti, ^{71}Ga
Wait Time Offset	2 ms			
Total analysis time / sample	128 s		Total analysis time / sample	90 s

[a] Combined with 1 mL min^{-1} He gas

The real human serum samples were obtained from the Miguel Servet Universitary Hospital (Zaragoza, Spain). For this study, in addition to four control samples taken from healthy patients, four patients with metallic implants were selected. These

patients all have the same type of hip prosthesis, gamma® intramedullary nail (Stryker Trauma GmbH, Germany), which is made of a titanium alloy (Ti-6Al-4V) and designed to address stable and non-stable intertrochanteric fractures. In all cases, the prosthesis was implanted more than 4 years prior to blood collection.

2.2.3. Sample preparation

As for non-exposed people, Ti concentrations in body fluids are expected to be very low, special precautions have to be taken for contamination control. Different types of recipients and cleaning procedures have been tested. Finally, for preparing sample dilutions and standard solutions, only metal-free tubes (15 or 50 mL polypropylene centrifuge tubes, VWR, Belgium) – pre-cleaned with 0.42 M HNO_3 – were used throughout the experiments.

Prior to analysis, the freeze-dried Seronorm™ reference material was reconstituted following the procedure provided by the manufacturer and the resulting solutions were diluted 10-fold to reduce the amount of serum matrix introduced into the plasma. In this way, matrix effects can be limited and clogging of the nebulizer, torch and cone apertures can be avoided.**[17]**

Human serum samples were collected in 6 mL trace element analysis Vacutainer® tubes (royal blue cap) from Becton Dickinson, reference 368380. To avoid metal contamination during blood extraction, blood samples were withdrawn from a forearm vein using a Becton Dickinson Vacutainer® Push Button Blood Collection Set, equipped with a stainless-steel needle surrounded by an inert plastic cannula. After permitting clot retraction, the tube was centrifuged at 1500g for 10 min and the serum obtained was transferred to 4.5 mL cryogenic tubes (cryotubes, reference 363452, Nunc®, Roskilde, Denmark) and stored at -20°C until analysis. Prior to analysis, only a 10-fold dilution with 0.14 M HNO_3 was required. To all samples and standards, Ga was added as internal standard (final concentration: 0.1 μg L^{-1}). All samples were analyzed within 24 hours after sample preparation, to ensure the stability of the solutions and to minimize the risk of sample contamination.

2.3. Results and discussion

2.3.1. Optimization of ICP-MS/MS protocol for the determination of Ti in serum

2.3.1.1. Selection of the reaction gas and quadrupole mass settings

In a complex sample, such as human blood serum, containing high levels of matrix elements such as C, Ca, Cl, Mg, P and S, the interference-free determination of ultra-trace levels of Ti is a challenging task. It has been shown before **[17]** that the use of a collision gas, such as He, or a reactive gas, such as H_2, in an ORS-ICP-QMS system, is not sufficient to remove all interferences and that such an approach is therefore not suited for this kind of application. However, instead of removing the interfering ions, in some cases it is also possible to convert the target ions into reaction product ions that can be measured interference-free at another mass-to-charge ratio (m/z) (mass-shift). For this particular approach, the use of the recently introduced ICP-QQQ instrumentation has demonstrated to be particularly suitable (e.g., for determination of S as SO^+ **[21,22]** and of P as PO^+ **[21]**). Thus, this strategy was evaluated in the present work.

Based on the information on reaction efficiencies available in the literature,**[23]** it was decided to evaluate the use of O_2 and NH_3/He (mixture of 10% NH_3 in He) as reaction gases for the determination of Ti in human serum. For both reaction gases, a product ion scan was recorded for a 1 µg L^{-1} Ti standard solution (**Figure 2.2**, see grey line patterned signal). In a product ion scan, the m/z of the first quadrupole Q1 is set at a fixed value (m/z of the original analyte ion), while the second quadrupole Q2 scans over (nearly) the entire mass range. These product ion scans can be seen as a fast and easy way to obtain information on the reaction products formed in the reaction cell, when only ions with one specific m/z-ratio enter the cell.

From **Figure 2.2**, it can be seen that the use of O_2 results in a rather simple product ion pattern, while NH_3/He definitely gives rise to a more complex cluster ion formation. When aiming at a maximum signal intensity (maximum sensitivity), it seems logical to select mass-to-charge ratios of, respectively, x ($^xTi^+$) and x+16 ($^xTi^{16}O^+$) for Q1 and Q2 when using O_2, and of x ($^xTi^+$) and x+102 ($^xTi(^{14}N^1H_3)_6^+$) when

using NH_3/He as a reaction gas. As the signals obtained for TiO^+ are ~ 10 times higher than the $Ti(NH_3)_6^+$-signals, it could be concluded that O_2 is the preferred reaction gas.

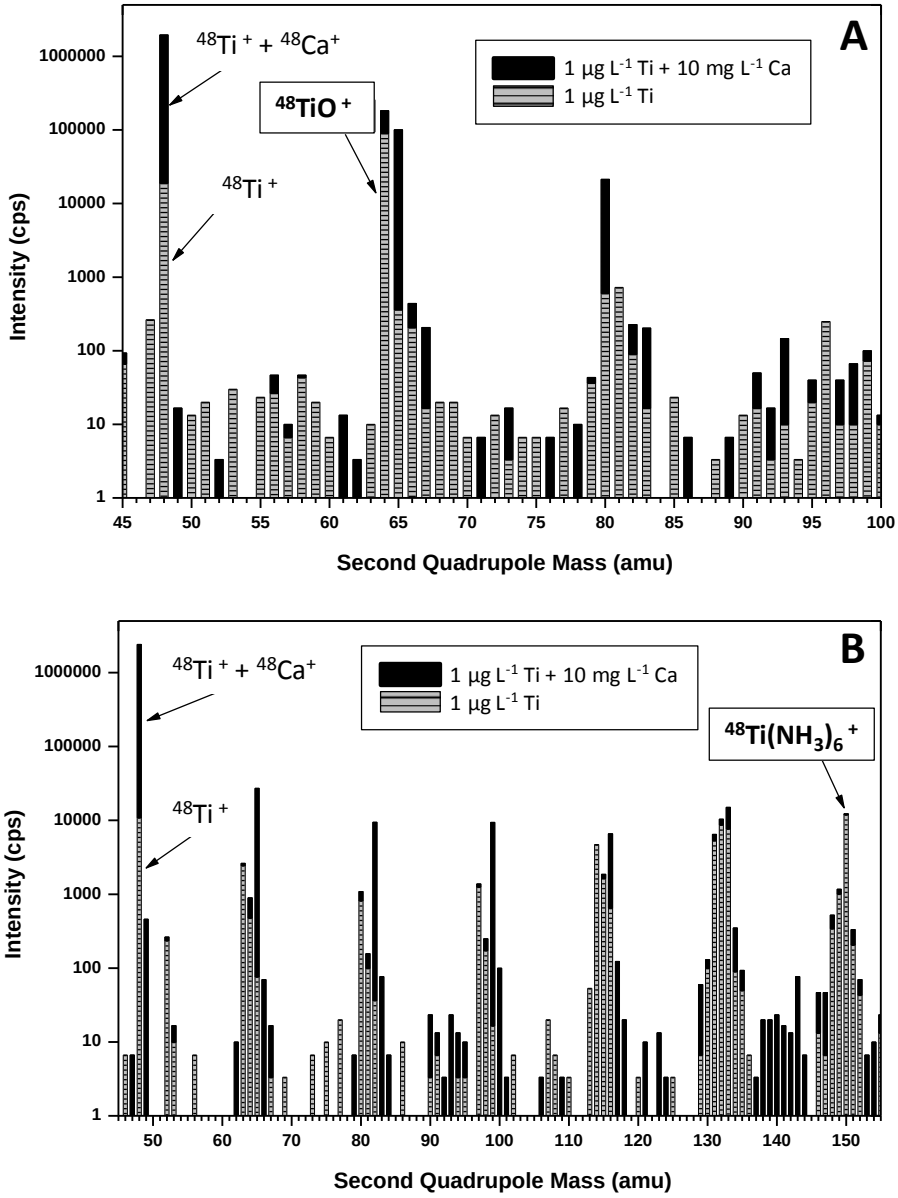

Figure 2.2. Product ion scans (Q1: 48 – Q2: scanned) for a solution containing 1 µg L^{-1} Ti (grey – line pattern) and a solution containing 1 µg L^{-1} Ti + 10 mg L^{-1} Ca (black – solid fill), with (A) O_2 and (B) NH_3/He as reaction gas

However, maximum sensitivity is only one aspect, and definitely, also (matrix-related) background signals should be taken into account before drawing final

conclusions. Therefore, the most important matrix elements, typically present in human blood serum, were added to a Ti standard solution and a product ion scan was also performed for these solutions. Although many matrix elements and all Ti isotopes were studied, for the sake of clarity, **Figure 2.2** only shows the results of a product ion scan with Q1 set at m/z=48, for a 1 µg L^{-1} Ti solution, with 10 mg L^{-1} Ca added. This choice has been made, because of the fact that (i) ^{48}Ti is the most abundant Ti isotope, (ii) the signals of $^{48}Ti^+$ and $^{48}Ca^+$ show isobaric overlap and (iii) there is a large excess of Ca compared to Ti in a serum matrix (Ti/Ca-ratio in this study ~ Ti/Ca-ratio in the Seronorm Trace Elements Serum L-1 reference material = 0.000117).

From **Figure 2.2A**, it is immediately clear that the problem of isobaric overlap of the $^{48}Ti^+$ and $^{48}Ca^+$ signals cannot be entirely solved by using O_2 as a reaction gas, because of the reaction between Ca and O_2, with formation of, among other, CaO^+. This may be surprising, as the O-atom transfer reaction between Ca and O_2 is an endothermic process, and typically endothermic reactions do not occur easily/rapidly in a reaction cell under appropriate lens and cell conditions.**[23]** Nevertheless, due to the large excess of Ca in the serum matrix under consideration, even with a very limited O-atom transfer reaction efficiency, the contribution of CaO^+ to the total signal intensity at m/z=64 seems to be substantial and would definitely lead to erroneous results. Also for the less abundant isotopes of Ti, several interfering ions contributed to the total signal at the m/z of the reaction product ions (**Table 2.3**).

While many of these interfering ions can be excluded by using the MS/MS mode (e.g., the isobaric interferences), those interferences that find their origin in O-atom transfer reactions between ions passing Q1 (*e.g.*, Ca^+ at m/z=46; PO^+ at m/z=47 and 49; SO^+ at m/z=48, 49 and 50, respectively) and the O_2 gas in the reaction cell, cannot be entirely removed. Based on these findings, it can be concluded that conversion of Ti^+ into TiO^+ is not the best approach for dealing with interferences in clinical samples, although it could be a useful approach for samples without or with only low concentrations of matrix elements that can give rise to interfering ions.

In contrast, the situation with NH_3/He as a reaction gas is much more promising, as can be seen from the product ion scans in **Figure 2.2B**. While for the $Ti(NH_3)_z$ clusters with $z < 6$, a clear increase of the signals can be noticed when a large amount of Ca is added to the solution, the $Ca(NH_3)_6$ cluster does not seem to be

formed, which makes the determination of Ti^+ as $Ti(NH_3)_6^+$ feasible, even in the presence of a large amount of Ca. Although not shown in this chapter, also the product ion scans performed with the Q1 set at m/z=46, 47, 49 and 50, give no evidence of possible interfering ions at the corresponding m/z for the $Ti(NH_3)_6^+$ cluster ions. Based on these results, it was decided to focus further on the use of NH_3/He as reaction gas and to determine the Ti concentrations in the serum samples via $Ti(NH_3)_6^+$ cluster ions in the m/z-range from 148 to 152.

Table 2.3. Reaction product ions formed upon reaction of Ti with O_2 in the reaction cell, together with the most important isobaric and polyatomic interferences at the m/z of the product ions (non-restrictive list). It has to be noted that most (but not all) of these interferences can be overcome by using the MS/MS mode.

Product Ion	Q1 (amu)	Q2 (amu)	Isobaric interferences	Polyatomic Interferences
$^{46}Ti^{16}O^+$	46	62	Ni^+ (3.63 [a])	$^{46}Ca^{16}O^+$, $^{36}Ar^{26}Mg^+$
$^{47}Ti^{16}O^+$	47	63	Cu^+ (69.15 [a])	$^{31}P^{16}O_2^+$, $^{16}O^{12}C^{35}Cl^+$, $^{40}Ar^{23}Na^+$, $^{23}Na^{40}Ca^+$, $^{46}Ti^{16}O^1H^+$, $^{14}N^{12}C^{37}Cl^+$
$^{48}Ti^{16}O^+$	48	64	Zn^+ (48.27 [a])	$^{48}Ca^{16}O^+$, $^{32}S^{16}O_2^+$, $^{31}P^{16}O^{17}O^+$, $^{32}S_2^+$, $^{36}Ar^{14}N_2^+$
$^{49}Ti^{16}O^+$	49	65	Cu^+ (30.85 [a])	$^{33}S^{16}O_2^+$, $^{32}S^{16}O^{17}O^+$, $^{32}S^{16}O_2{}^1H^+$, $^{31}P^{16}O^{18}O^+$, $^{40}Ar^{25}Mg^+$, $^{36}Ar^{14}N_2{}^1H^+$, $^{32}S^{33}S^+$, $^{12}C^{16}O^{37}Cl^+$, $^{12}C^{18}O^{35}Cl^+$,
$^{50}Ti^{16}O^+$	50	66	Zn^+ (27.98 [a])	$^{50}Cr^{16}O^+$, $^{50}V^{16}O^+$, $^{34}S^{16}O_2^+$, $^{32}S^{16}O^{18}O^+$, $^{33}S^{16}O^{17}O^+$, $^{33}S^{16}O_2{}^1H^+$, $^{32}S^{17}O_2^+$, $^{32}S^{34}S^+$, $^{33}S_2^+$

[a] Isotopic abundance (%) for isobaric interferences

It has to be noted that Q2 is typically calibrated for the detection of mono-atomic ions. Mono-atomic ions with a mass between 148 and 152 show a negative mass defect when referred to the nominal mass. However, as lighter ions such as N and H rather show a positive mass defect, the exact mass of the $Ti(NH_3)_6^+$ cluster ions is higher than that of the mono-atomic ions typically measured in that mass range. In order to ensure an accurate and precise measurement of the cluster ion, a recalibration of the Q2 axis offset was performed, resulting in a shift of -0.01 to -0.18.

2.3.1.2. Optimization of the reaction gas flow rate

The NH_3/He reaction gas flow was optimized for a minimal BEC (background-equivalent concentration) value, *i.e.*, the best compromise between low background and high sensitivity. Based on the signals obtained for a 0.14 M HNO_3 blank and a 1 µg L^{-1} Ti solution (**Figure 2.3**), a value of 2 mL min^{-1} was selected as the optimal NH_3/He flow rate. It should be noted that the gas flow rate in the Agilent MassHunter software for a gas connected on the 3rd cell gas line, can only be set in %. With the mass flow controller "fully open" (100%), the corresponding gas flow rate for the NH_3/He-mixture (10% NH_3 / 90% He) is 10 mL min^{-1}. In this work, the optimal performance was obtained at a cell gas flow rate of 20%, which corresponds to an actual NH_3/He flow rate of 2 mL min^{-1}.

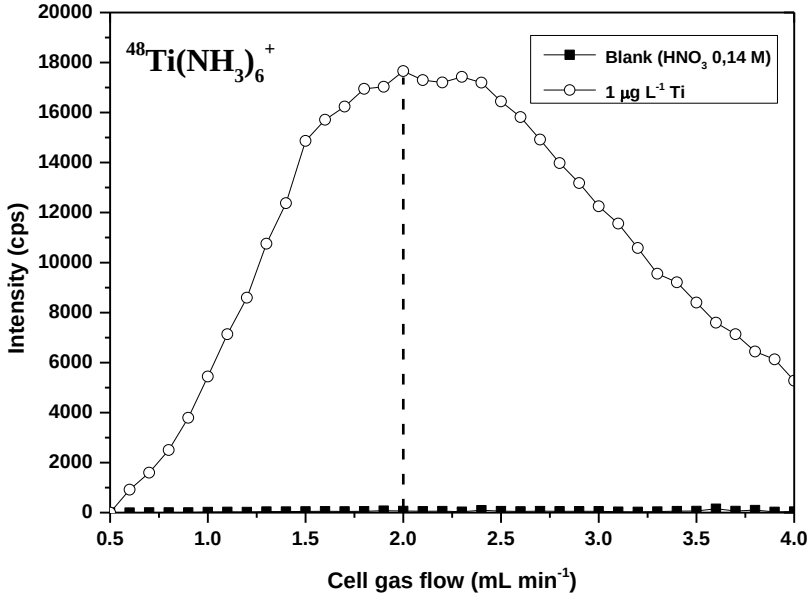

Figure 2.3. Optimization of the NH_3/He reaction gas flow rate. Signal intensities are shown as a function of the cell gas flow rate for a 0.14 M HNO_3 blank solution (--■--) and a 1 µg L^{-1} Ti standard solution (--○--).

2.3.1.3. Advantages of using the MS/MS mode

Whenever a highly reactive gas is used in a "traditional" collision/reaction cell ICP-MS instrument, there is the risk of secondary reaction chemistry. That means that not only the target analyte ions, but also other ions that are simultaneously present in the reaction cell (originating from the plasma, the solvent or the sample matrix),

can react with the gas.**[24]** Moreover, with mass-shift reactions, one should always ensure that no interfering ions are present at the new masses (m/z of the reaction products) that are used for the analysis.

One method that has been used so far to limit the contribution from newly developed species (in the cell) - kinetic energy discrimination **[25]** - cannot be relied on when reaction product ions need to be monitored. Secondary reactions in ICP-MS instruments equipped with a quadrupole-based reaction cell can also be avoided by operating the cell in a bandpass mode to eject ions from the cell that are outside a certain window of ion masses (typically a rather broad window).**[24]**

However, considering the reaction between Ti and NH_3/He as described before, this approach would not entirely solve the problem, as NH_3/He gives rise to a rather complex cluster formation (**Figure 2.2B**), resulting – for each Ti isotope – in several cluster ions with only one mass unit difference. Therefore, overlap of the signals of, *e.g.,* $^{m}Ti(NH_3)_6^+$ and $^{m+1}TiNH_2(NH_3)_5^+$ at m/z=(m+102) would result in a disturbance of the Ti isotopic pattern, which, mainly for isotopic analysis, would lead to erroneous results. Moreover, when operating the instrument in the single quad mode (first quadrupole bandpass width fully open), even for HNO_3 blank solutions, rather high background signals were obtained in the m/z-range = 148 to 152. A careful investigation of the origin of these signals (by performing a precursor ion scan: scanning over the entire mass range with Q1, while Q2 is set at a fixed m/z, e.g., 150), taught us that, upon reaction with NH_3/He, both O^+ and Ar^+ ions lead to product ions at the m/z ratios of interest. Although it is not entirely understood which reactions take place between O^+/Ar^+ and NH_3 (a charge transfer reaction followed by formation of charged ammonia clusters could be hypothesized), it is clear that both O- and Ar-ions (which are always omnipresent in a wet plasma) should be prevented from entering the reaction cell, in order to obtain accurate results.

All of the problems mentioned here, can be solved easily by operating the ICP-QQQ-MS system in the MS/MS mode, with Q1 set at the precursor ion mass (m/z=46 to 50 – single mass width) and Q2 at the mass of the corresponding $Ti(NH_3)_6^+$ cluster ion. In this way, the reaction cell chemistry can be controlled to the largest possible extent and the isotopic pattern is preserved.

2.3.1.4. Calibration data and limits of detection (LODs)

To assess the analytical performance of the method described above, 5 Ti standard solutions with concentrations ranging between 0 and 5 µg L^{-1} (0, 0.5, 1, 2.5 and 5 µg L^{-1} Ti) were used to set up a calibration curve and detection limits were calculated as 3 times the standard deviation of 10 consecutive measurements of a blank solution (0.14 M HNO_3), divided by the slope of the calibration curve (**Table 2.4**).

Table 2.4. Calibration data and instrumental limits of detection (LOD) and quantification (LOQ) obtained for Ti with ICP-MS/MS.

Isotope	Abundance (%)	Q1 (amu)	Q2 (amu)	Sensitivity[a] (L µg^{-1})	Intercept[a] (counts s^{-1})	R^2	LOD[b] (µg L^{-1})	LOQ[b] (µg L^{-1})
^{46}Ti	8.25	46	148	1163 ± 9	37 ± 13	0.9997	0.010	0.032
^{47}Ti	7.44	47	149	1275 ± 18	36 ± 16	0.9998	0.008	0.028
^{48}Ti	73.72	48	150	13330 ± 130	431 ± 83	0.9997	0.003	0.009
^{49}Ti	5.41	49	151	1021 ± 10	30 ± 12	0.9996	0.010	0.034
^{50}Ti	5.18	50	152	1011 ± 22	31 ± 24	0.9996	0.016	0.054

[a] Uncertainties expressed as standard deviation (n=10)

[b] LOD and LOQ calculated as, respectively, 3 and 10 times the standard deviation on 10 consecutive measurements of a blank solution (0.14 M HNO_3), divided by the slope of the calibration curve

It should be noted that these detection limits can only be seen as instrumental detection limits as all measurements were based on non-matrix-matched blank and standard solutions (due to the complex nature of the serum matrix, the preparation of matrix-matched solutions is not straightforward). When aiming at more representative LOD values, at least the dilution factor of the serum samples (10-fold) should be taken into account. For all Ti isotopes (instrumental) LODs below 20 ng L^{-1} are obtained, with the lowest value (3 ng L^{-1}) for the most abundant isotope ^{48}Ti, at m/*z*=150. These LODs are definitely better than those reported for similar

studies with ETAAS **[26]** or ICP-QMS **[3, 12, 17]** and at least equal to those obtained via double-focusing SF-ICP-MS.**[5, 20, 27]**

2.3.2. Results obtained for Seronorm Trace Elements Serum L-1

For validation of the analytical method developed in this work, a Seronorm Trace Elements Serum Level 1 reference material with an approximate value of 11.2 µg L^{-1} Ti was obtained from Sero (Norway). The authors are aware that in the literature, the use of Seronorm Trace Elements Serum Level 1 reference material with a lower level of Ti (1.4 µg L^{-1}) has been reported.**[28]** However, the Ti concentration varies strongly from one batch of this reference material to another and *via* contact with Sero, it was ascertained that at the time of the experiments, no serum reference material with a lower Ti concentration was available. After a simple reconstitution, 10-fold dilution and addition of Ga as internal standard, the sample solutions were analyzed by means of ICP-QQQ (MS/MS mode) and calibrated against the set of external standard solutions described before. As the Ti concentration in the Seronorm material is not certified, but only an indicative value is provided (without any information on the corresponding uncertainty level), it was decided to subject the same samples to a high resolution SF-ICP-MS analysis for comparison. **Table 2.5** summarizes the results of these analyses.

Table 2.5. Results obtained for Seronorm Trace Elements Serum L-1 (indicative value: 11.2 µg L^{-1} Ti).

	Agilent 8800 ICP-QQQ-MS		**Element XR SF-ICP-MS**
	NH_3/He ($Ti(NH_3)_6^+$)	**O_2 (TiO^+)**	
^{46}Ti	12.61 ± 0.91 [a]	15.90 ± 0.25 [a]	
^{47}Ti	11.68 ± 0.58 [a]	13.28 ± 0.26 [a]	11.51 ± 0.76 [a]
^{48}Ti	11.80 ± 0.75 [a]	28.55 ± 0.50 [a]	
^{49}Ti	11.77 ± 0.54 [a]	22.34 ± 0.38 [a]	11.41 ± 0.17 [a]
^{50}Ti	11.68 ± 0.65 [a]	12.50 ± 0.11 [a]	

[a] Uncertainties expressed as standard deviation (n=5)

At a 95% confidence level, no significant differences were found between the results obtained via ICP-MS/MS and SF-ICP-MS, except for the concentration calculated via ^{46}Ti (actually measured at m/z=148 as $Ti(NH_3)_6^+$), which is markedly higher than the concentrations obtained via the other isotopes. Except for the result obtained via ^{46}Ti monitoring, all results are (within measurement uncertainty) also in good agreement with the indicative value of 11.2 µg L^{-1}. Until now, the reason for the discrepancy of the results via the ^{46}Ti-isotope in the Serum Reference Material is unclear. But as 4 out of the 5 isotopes of Ti (including the most abundant ^{48}Ti-isotope) can be measured interference-free, and in the real human serum samples under investigation this discrepancy is not very important (see paragraph 2.3.3), no further investigation was carried out on this topic.

In section 2.3.1.1., it was already stated that – for clinical matrices – NH_3/He would be the preferred reaction gas, although higher signal intensities could be obtained when adding O_2 in the reaction cell. As our initial conclusion was mainly based on the analysis of standard solutions, it was decided to also verify this conclusion by analyzing the serum reference material by means of ICP-MS/MS and using O_2 as a reaction gas. Experimental parameters have been optimized in the same way as described before (paragraph 2.3.1.2.) and the final conditions used for the analysis of the serum samples, are listed in **Table 2.2**. From **Table 2.5**, it can be easily concluded that – for clinical samples – the approach of using O_2 as a reaction gas and determining Ti via the corresponding TiO^+ ions, is not capable of dealing with all possible interferences. As described before, the main origin of the problems is the fact that not only Ti is converted into TiO^+, but also many of the interfering ions (**Table 2.3** - *e.g.*, Ca, SO^+, PO^+,...) exhibit a similar reaction, such that the original problem of spectral interferences is not solved, but just transferred to another mass region. Therefore, for the serum samples of the test populations, only NH_3/He was used as a reaction gas in the ICP-QQQ-MS system.

2.3.3. Results obtained for human serum samples

The human serum samples originating from people without (group 1) and with (group 2) Ti-based prostheses, were treated in the same way as described for the Seronorm reference material. Results are shown in **Table 2.6**.

Table 2.6. Results obtained for human serum samples.

	Agilent 8800 ICP-QQQ-MS Conc (µg L^{-1}) [a]					Element XR SF-ICP-MS Conc (µg L^{-1}) [a]	
Control samples							
	^{46}Ti	**^{47}Ti**	**^{48}Ti**	**^{49}Ti**	**^{50}Ti**	**^{47}Ti**	**^{49}Ti**
Sample 1			0.32 ± 0.01			< LOQ[b]	< LOQ[b]
Sample 2			0.27 ± 0.01			< LOQ[b]	< LOQ[b]
Sample 3			0.29 ± 0.01			< LOQ[b]	< LOQ[b]
Sample 4	0.54 ± 0.17	0.84 ± 0.21	0.80 ± 0.17	0.73 ± 0.15	0.78 ± 0.08	0.71 ± 0.08	0.71 ± 0.09
Samples of individuals with Ti-based implants							
	^{46}Ti	**^{47}Ti**	**^{48}Ti**	**^{49}Ti**	**^{50}Ti**	**^{47}Ti**	**^{49}Ti**
Sample 5	4.22 ± 0.15	4.25 ± 0.28	4.34 ± 0.21	4.24 ± 0.16	4.23 ± 0.25	4.25 ± 0.53	4.24 ± 0.02
Sample 6	5.28 ± 0.36	5.50 ± 0.19	5.64 ± 0.34	5.56 ± 0.09	5.24 ± 0.03	5.58 ± 0.27	5.71 ± 0.12
Sample 7	2.86 ± 0.27	2.66 ± 0.06	2.74 ± 0.12	2.85 ± 0.31	2.71 ± 0.12	2.57 ± 0.11	2.71 ± 0.06
Sample 8	2.27 ± 0.26	1.73 ± 0.07	1.83 ± 0.07	1.90 ± 0.09	1.71 ± 0.12	1.98 ± 0.30	1.93 ± 0.14

[a] Uncertainties expressed as standard deviation (n=3)
[b]LOQ = 50 ng L^{-1}

For the samples categorized in group 2, no significant differences are found between the results obtained via different Ti-isotopes, and those obtained via SF-ICP-MS (R=3000 - m/z=47 and 49). For the group 1 samples (control samples) on the other hand, Ti levels are much lower, and determination was only possible at m/z=150 (most abundant Ti-isotope), due to the very low basal Ti levels in serum, in combination with the 10-fold dilution factor of the samples, required to avoid clogging of the torch and cone apertures and/or severe matrix effects. Although in previous work, *e.g.*, **[20]**, it has been shown that the detection limit offered by SF-ICP-MS is sufficiently low to allow for an accurate determination of basal Ti levels in body fluids, we were not able to reproduce these very low detection limits. Since our instrument is functioning well within the specifications provided by the manufacturer, the higher instrumental detection limit obtained in this work (15 ng L^{-1}) most probably finds its origin in a little Ti contamination of our SF-ICP-MS instrument as a consequence of memory effects from previous analyses. Therefore, no SF-ICP-MS "reference" values could be obtained for comparison with the ICP-MS/MS results for most serum samples of the control group. Nevertheless, those results are in very good agreement with basal Ti levels in serum as reported on in literature.**[5, 13, 29]** Although an interpretation of the differences in Ti concentration in the serum of people with and without Ti implants and the possible reasons and consequences is beyond the scope of this work, the results of our measurements indicate that the presence of Ti implants – even if they perform well at first sight - can definitely lead to elevated Ti levels in body fluids and therefore, the availability of fast, accurate and very sensitive analytical methods for Ti determination in clinical samples, is required for further investigations in this field.

2.4. Conclusion

In this work, a method has been developed for the accurate determination of ultra-trace levels of Ti in clinical samples by means of ICP-MS/MS. An evaluation of the use of different reaction gases (O_2 and NH_3/He) showed that accurate results can be obtained with NH_3/He as a reaction gas and determination of the Ti^+ ions at the m/z of the corresponding $Ti(NH_3)_6^+$ reaction product ions. The gain of controlling the reaction cell chemistry by operating the instrument in the MS/MS mode has been clearly demonstrated. As a proof-of-concept, the newly developed method was

successfully applied to the determination of Ti in a Seronorm Trace Elements Serum Reference Material and in serum samples obtained from individuals with and without Ti-based implants. Although the determination of Ti in the control samples can be seen as a very challenging task (due to the very low basal Ti levels and the complex matrix of clinical samples), the limit of detection of the method has proven to be sufficiently low to obtain accurate results (via the most abundant isotope ^{48}Ti). Therefore, this method can be seen as a valid alternative for SF-ICP-MS, and although it has been developed for the analysis of clinical samples, it can be expected that the method can be easily transferred to other application fields. Moreover, since the method permits the accurate monitoring of 5 different Ti isotopes at the μg L^{-1} level, it opens possibilities for performing tracer experiments or for using isotope dilution for calibration, if necessary.

Acknowledgements

The authors acknowledge Dr. Luis Rello from the Miguel Servet Universitary Hospital (Zaragoza, Spain) for providing the human serum samples and Dr. Glenn Woods (Agilent Technologies) for his valuable input concerning ICP-MS/MS method development. Also, the funding from the Special Research Fund (BOF) of Ghent University, from the Spanish Ministry of Economy and Competitiveness (Project CTQ2012-33494) and the Aragón Government (Fondo Social Europeo) is acknowledged.

References

[1] J.J. Jacobs, A.K. Skipor, J. Black, R.M. Urban, J.O. Galante, J Bone Joint Surg Am 73A (1991) 1475-1486.

[2] J.J. Jacobs, A.K. Skipor, L.M. Patteson, N.J. Hallab, W.G. Paprosky, J. Black, J.O. Galante, J Bone Joint Surg Am 80A (1998) 1447-1458.

[3] S. McGarry, S.J. Morgan, R.M. Grosskreuz, A.E. Williams, W.R. Smith, J Trauma 64 (2008) 430-433.

[4] V.J. Rasquinha, C.S. Ranawat, J. Weiskopf, J.A. Rodriguez, A.K. Skipor, J.J. Jacobs, J Arthroplasty, 21 (2006) 47-52.

[5] T.D. Richardson, S.J. Pineda, K.B. Strenge, T.A. Van Fleet, M. MacGregor, J.C. Milbrandt, J.A. Espinosa, P. Freitag, Spine, 33 (2008) 792-796.

[6] D. Rodriguez, F.J. Gil, J.A. Planell, E. Jorge, L. Alvarez, R. Garcia, M. Larrea, A. Zapata, J Mater Sci Mater Med, 10 (1999) 847-851.

[7] A. Sarmiento-Gonzalez, J.R. Encinar, J.M. Marchante-Gayon, A. Sanz-Medel, Anal Bioanal Chem, 393 (2009) 335-343.

[8] IARC, IARC Monographs on the Evaluation of Carcinogenic Risks to Humans, 93, WHO Press (2010) (ISBN: 978 92 832 1293 5).

[9] J.J. Jacobs, N.J. Hallab, A.K. Skipor, R.M. Urban, Clin Orthop Relat Res (2003) 139-147.

[10] N. Lavi, Z.B. Alfassi, Analyst, 115 (1990) 817-822.

[11] J.C. Rubio, M.C. Garcia-Alonso, C. Alonso, M.A. Alobera, C. Clemente, L. Munuera, M.L. Escudero, J Mater Sci Mater Med, 19 (2008) 369-375.

[12] L.J. Yu, S.R. Koirtyohann, M.L. Rueppel, A.K. Skipor, J.J. Jacobs, J Anal At Spectrom, 12 (1997) 69-74.

[13] C.A. Engh, Jr., S.J. MacDonald, S. Sritulanondha, A. Thompson, D. Naudie, C.A. Engh, Clin Orthop Relat Res, 467 (2009) 101-111.

[14] L. Rello, A.C. Lapena, M. Aramendia, M.A. Belarra, M. Resano, Spectrochim Acta Part B At Spectrosc, 81 (2013) 11-19.

[15] J.J. Jacobs, C. Silverton, N.J. Hallab, A.K. Skipor, L. Patterson, J. Black, J.O. Galante, Clin Orthop Relat Res (1999) 173-180.

[16] J. Kunze, M.A. Wimmer, S. Koelling, E. Schneider, Fresenius J Anal Chem, 361 (1998) 496-499.

[17] A. Sarmiento-Gonzalez, J.M. Marchante-Gayon, J.M. Tejerina-Lobo, J. Paz-Jimenez, A. Sanz-Medel, Anal Bioanal Chem, 382 (2005) 1001-1009.

[18] M. Berglund, M.E. Wieser, Pure Appl Chem, 83 (2011) 397-410.

[19] T.W. May, R.H. Wiedmeyer, Atomic Spectroscopy, 19 (1998) 150-155.

[20] A. Sarmiento-Gonzalez, J.M. Marchante-Gayon, J.M. Tejerina-Lobo, J. Paz-Jimenez, A. Sanz-Medel, Anal Bioanal Chem, 391 (2008) 2583-2589.

[21] S.D. Fernandez, N. Sugishama, J.R. Encinar, A. Sanz-Medel, Anal Chem, 84 (2012) 5851-5857.

[22] L. Balcaen, G. Woods, M. Resano, F. Vanhaecke, J Anal At Spectrom, 28 (2013) 33-39.

[23] M+ chemistry database, available from York University, http://www.chem.yorku.ca/profs/bohme/research/selection_table.html, June 2013

[24] S.D. Tanner, V.I. Baranov, D.R. Bandura, Spectrochim Acta Part B At Spectrosc, 57 (2002) 1361-1452.

[25] N. Yamada, J. Takahashi, K. Sakata, J Anal At Spectrom, 17 (2002) 1213-1222.

[26] A.K. Skipor, J.J. Jacobs, J. Schavocky, J. Black, J.O. Galante, Atomic Spectroscopy, 15 (1994) 131-134.

[27] J. Riondato, F. Vanhaecke, L. Moens, R. Dams, J Anal At Spectrom, 12 (1997) 933-937.

[28] Y. Nuevo-Ordonez, M. Montes-Bayon, E. Blanco-Gonzalez, J. Paz-Aparicio, J.D. Raimundez, J.M. Tejerina, M.A. Pena, A. Sanz-Medel, Anal Bioanal Chem, 401 (2011) 2747-2754.

[29] Y. Nuevo Ordonez, M. Montes-Bayon, E. Blanco-Gonzalez, J. Paz-Jimenez, J. Maria Tejerina-Lobo, J. Miguel Pena-Lopez, A. Sanz-Medel, J Anal At Spectrom, 24 (2009) 1037-1043.

CHAPTER 3

Potential of methyl fluoride as a universal reaction gas to overcome spectral interference in the determination of ultra-trace concentrations of metals in biofluids using ICP-MS/MS

Adapted from Bolea-Fernandez et. al., Anal. Chem, 86 (2014) 7969 - 7977

3.1. Introduction

The development of suitable multi-element methodologies for the determination of ultra-trace levels in biological samples is still a challenge for analytical chemistry, especially when, as in a biomedical context, high sample throughput without compromised accuracy is required.

An increasing number of light elements (atomic mass ≤ 80 amu) are the target of clinical interest. Aluminum, e.g., has been associated with renal insufficiency and Alzheimer's disease, while its concentration in blood is also promising as a chemical marker for drowning.**[1, 2]** Titanium is increasingly determined for monitoring patients with metal prostheses. A significant increase in the Ti concentration in biological fluids may indicate prosthesis wear.**[3-5]** As a result of the various compositions of present-day prostheses and implants, also other elements (e.g., Co, Cr, Mo, Ni and V) need to be determined at ultra-trace levels in this context.**[6-8]** This is an emerging field that requires extremely low limits of detection (LoDs) to properly establish the basal levels, which may be well below 1 μg L^{-1} for some analytes. Also for other purposes, determination of these elements is of biomedical relevance. Vanadium has been suggested for treatment of diabetes, and although it is an essential element, prolonged exposure could cause a variety of health problems.**[9, 10]** The concentration of Cr is of interest as a result of its role in glucose metabolism and in cardiovascular diseases.**[11, 12]** Excessive Mn concentrations have proved to result in a neurotoxic accumulation in the brain.**[13,14]** Cobalt is a constituent of vitamin B12 and its role in red blood cell production requires the monitoring of this element.**[15, 16]** Also disproportionate levels of Ni cause disorders or pronounced sensitivity. Many of these Ni-related issues concern the skin, but also breathing problems and even cancer have been mentioned as possible consequences.**[17, 18]**

Different techniques have been used for ultra-trace element analysis of biofluids, but inductively coupled plasma-mass spectrometry (ICP-MS) can be considered as the technique of choice for this purpose, owing to its multi-element capabilities, high detection power and wide linear dynamic range. Nevertheless, even with ICP-MS, the determination of ultra-trace levels of the elements discussed above (mass < 80 amu) in biological fluids is very challenging because of the occurrence of spectral interferences (see **Table 3.1** for a list of potential interferences).**[6, 19]** Many of the

elements giving rise to interfering species (e.g., C, Ca, Cl, Fe, K, Mg, Na, P and S) are found at much higher levels in biological fluids.

Table 3.1. Different nuclides with their natural isotopic abundance and a non-restrictive list of possible isobaric and polyatomic interferences

	Abundance (%)	Isobaric interferences	Polyatomic Interferences
$^{27}Al^+$	100	---	$^{12}C^{15}N^+$, $^{13}C^{14}N^+$, $^{1}H^{12}C^{14}N^+$
$^{46}Ti^+$	8.25	Ca^+ (0.004[a])	$^{32}S^{14}N^+$, $^{14}N^{16}O_2^+$, $^{15}N_2{}^{16}O^+$
$^{47}Ti^+$	7.44	---	$^{32}S^{14}N^1H^+$, $^{30}Si^{16}O^1H^+$, $^{32}S^{15}N^+$, $^{33}S^{14}N^+$, $^{15}N^{16}O_2^+$, $^{14}N^{16}O_2{}^1H^+$, $^{12}C^{35}Cl^+$, $^{31}P^{16}O^+$
$^{48}Ti^+$	73.72	Ca^+ (0.187[a])	$^{32}S^{16}O^+$, $^{34}S^{14}N^+$, $^{33}S^{15}N^+$, $^{14}N^{16}O^{18}O^+$, $^{14}N^{17}N_2^+$, $^{12}C_4^+$, $^{36}Ar^{12}C^+$
$^{49}Ti^+$	5.41	---	$^{32}S^{17}O^+$, $^{32}S^{16}O^1H^+$, $^{35}Cl^{14}N^+$, $^{34}S^{15}N^+$, $^{33}S^{16}O^+$, $^{14}N^{17}O_2{}^1H^+$, $^{14}N^{35}Cl^+$, $^{36}Ar^{13}C^+$, $^{36}Ar^{12}C^1H^+$, $^{12}C^{37}Cl^+$, $^{31}P^{18}O^+$
$^{50}Ti^+$	5.18	Cr^+ (4.345[a]), V^+ (0.25[a])	$^{32}S^{18}O^+$, $^{32}S^{17}O^1H^+$, $^{36}Ar^{14}N^+$, $^{35}Cl^{15}N^+$, $^{36}S^{14}N^+$, $^{33}S^{17}O^+$, $^{34}S^{16}O^+$, $^{1}H^{14}N^{35}Cl^+$, $^{34}S^{15}O^1H^+$
$^{51}V^+$	99.75	---	$^{34}S^{16}O^1H^+$, $^{35}Cl^{16}O^+$, $^{38}Ar^{13}C^+$, $^{36}Ar^{15}N^+$, $^{36}Ar^{14}N^1H^+$, $^{37}Cl^{14}N^+$, $^{36}S^{15}N^+$, $^{33}S^{18}O^+$, $^{34}S^{17}O^+$
$^{52}Cr^+$	83.79	---	$^{35}Cl^{16}O^1H^+$, $^{40}Ar^{12}C^+$, $^{36}Ar^{16}O^+$, $^{37}Cl^{15}N^+$, $^{34}S^{18}O^+$, $^{36}S^{16}O^+$, $^{38}Ar^{14}N^+$, $^{36}Ar^{15}N^1H^+$, $^{35}Cl^{17}O^+$
$^{53}Cr^+$	9.50	---	$^{37}Cl^{16}O^+$, $^{38}Ar^{15}N^+$, $^{38}Ar^{14}N^1H^+$, $^{36}Ar^{17}O^+$, $^{36}Ar^{16}O^1H^+$, $^{35}Cl^{17}O^1H^+$, $^{35}Cl^{18}O^+$, $^{36}S^{17}O^+$, $^{40}Ar^{13}C^+$
$^{55}Mn^+$	100	---	$^{40}Ar^{14}N^1H^+$, $^{39}K^{16}O^+$, $^{37}Cl^{18}O^+$, $^{40}Ar^{15}N^+$, $^{38}Ar^{17}O^+$, $^{36}Ar^{18}O^1H^+$, $^{38}Ar^{16}O^1H^+$, $^{37}Cl^{17}O^1H^+$, $^{23}Na^{32}S^+$, $^{36}Ar^{17}F^+$
$^{59}Co^+$	100	---	$^{43}Ca^{16}O^+$, $^{42}Ca^{16}O^1H^+$, $^{24}Mg^{35}Cl^+$, $^{36}Ar^{23}Na^+$, $^{40}Ar^{18}O^1H^+$, $^{40}Ar^{19}F^+$
$^{58}Ni^+$	68.08	Fe^+ (0.28[a])	$^{23}Na^{35}Cl^+$, $^{40}Ar^{18}O^+$, $^{40}Ca^{18}O^+$, $^{40}Ca^{17}O^1H^+$, $^{42}Ca^{16}O^+$, $^{29}Si_2^+$, $^{40}Ar^{17}O^1H^+$, $^{23}Na^{35}Cl^+$
$^{60}Ni^+$	26.22	---	$^{44}Ca^{16}O^+$, $^{23}Na^{37}Cl^+$, $^{43}Ca^{16}O^1H^+$

[a] Isotopic abundance (%) for isobaric nuclide.

The use of high-resolution sector-field (SF)-ICP-MS is a very elegant way to deal with spectral overlap.**[19-22]** However, an increase in mass resolution is accompanied by a significant drop in ion transmission efficiency and thus, in sensitivity (one to two orders of magnitude). In addition, the cost of the equipment is still considerably higher than that of quadrupole-based (Q)-ICP-MS. Moreover, the use of Q-ICP-MS devices is typically preferred for daily operation in clinical labs owing to their robustness. However, straightforward determination of ultra-trace levels of these elements in difficult matrices has ever been a challenge for Q-ICP-MS, due to the occurrence of spectral interferences.

At the end of the 1990s, multipole collision-reaction cells were introduced in Q-ICP-MS instrumentation, thus improving the selectivity of the technique.**[23-27]** Polyatomic ions can be either slowed down more than atomic ions upon collisions with a non-reactive gas (typically He), such that they can be selectively discriminated against using a decelerating potential,**[28-30]** or the interfering ion can be removed by selective reaction with the reaction gas. Different gases have been used for the latter purpose, the most frequently used being NH_3, O_2, H_2 and CH_4.**[31-35]** In most cases, the strategy used consists of removal of the interfering ions, such that the target analyte(s) can be measured interference-free at the original mass-to-charge (m/z) ratio.**[36, 37]** Although often successful, the use of both kinetic energy discrimination and of chemical resolution in a pressurized collision/reaction cell results in a decreased sensitivity for the analyte element(s) as well. With some reactive gases, an alternative approach is also possible, whereby not the interfering ion species but the target ion reacts with gas molecules, thus forming a novel ionic species that can be measured at a different m/z ratio. This strategy is successful as long as the interfering ion(s) does not react with the gas molecules, or reacts in a different way.**[38-41]** This approach offers a way to increase selectivity, while preserving sensitivity, if the selected reaction proceeds with high efficiency. However, one of the problems of the first generation of Q-ICP-MS instruments equipped with a collision/reaction cell is that the use of very reactive gases may lead to the production of new interferences. With NH_3, e.g., many protonated clusters of various compositions (e.g., $M(NH_2)_x(NH_3)_y^+$) that give rise to signals all across the mass spectrum are formed.**[42]** As a result, very often, the methods proposed were not truly simultaneous, but needed different gases and conditions for different analytes, thus requiring a sequential monitoring. This is a

significant drawback when aiming at high sample throughput, when samples are available in small amounts or when monitoring short transient signals (e.g., when using laser ablation, electrothermal vaporization, flow injection analysis or a chromatographic technique for sample introduction).

A new generation of Q-ICP-MS instruments (**Figure 3.1)** equipped with a tandem mass spectrometry configuration (ICP-MS/MS) has been introduced in 2012 (Chapter 1). The first papers on ICP-MS/MS published, mainly focused on mono-element determinations using "conventional" gases (O_2 and NH_3).**[5, 43-48]**

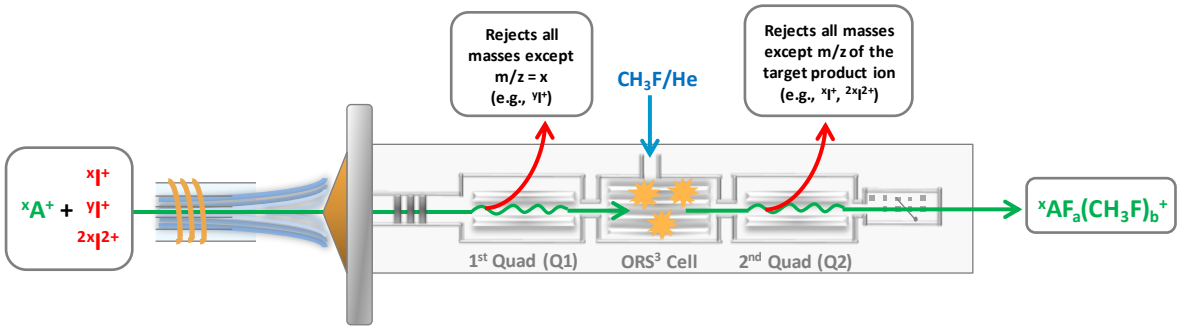

Figure 3.1. Schematic representation of ICP-MS/MS operation using CH_3F/He as reaction gas (m/z represents the mass-to-charge ratio of the corresponding analytes (A), interferences (I) and/or reaction product ions)

In this work, the capabilities of CH_3F as a reaction gas in ICP-MS/MS were evaluated. Some earlier works have investigated the reactions between CH_3F and different elements, but mostly the objective was theoretical (e.g., computational studies or studies that used inductively coupled plasma/selected-ion flow tube (ICP-SIFT) tandem mass spectrometry for studying the mechanism of reaction between CH_3F and selected atomic ions).**[49-52]** Very few papers have actually described the use of methyl fluoride as a reaction gas in Q-ICP-MS,**[53-56]** probably owing to the complex chemistry. The authors of this work selected CH_3F because it is highly reactive and is involved in different types of reactions with different elements (e.g., fluorination *versus* methyl fluoride addition), both of which are promising features for the purpose of obtaining interference-free conditions for a larger collection of elements.

The main goal of this work was to investigate the potential of ICP-MS/MS to rely on selective chemical reactions with methyl fluoride, with the aim of developing a sensitive and selective method to determine Al, Co, Cr, Mn, Ni, Ti and V in serum and urine samples.

3.2. Experimental

3.2.1. *Reagents and standards*

Purified water (resistivity > 18.2 MΩ cm) was obtained from a Milli-Q Element water purification system (Millipore, France). Pro analysis purity level 14 M HNO_3 (ChemLab, Belgium) was further purified by sub-boiling distillation. 1 g L^{-1} single-element standards solutions (Instrument Solutions, The Netherlands) were used for preparing standard solutions (Al, Co, Cr, Mn, Ni, Ti and V) and for matrix-matching (Ca, Cl, Fe, K, Mg, Na, P and S). Throughout the work, external calibration was relied on for calibration, with Ga as an internal standard. All the standards were prepared in 0.14 M HNO_3.

3.2.2. *Samples*

Two reference materials, Seronorm™ Trace Element Serum Level 1 and Seronorm™ Trace Element Urine Level 1 (Sero, Norway - Reference 201405 and 210605, respectively) were selected for method development and validation purposes. The selection was carried out based on the clinical relevance of these samples and the presence of most of the target analytes with reference values.

3.2.3. *Sample preparation*

Because of the low concentrations present in the samples, only metal-free tubes were used for standard solutions and sample preparation (15 or 50 mL polypropylene centrifuge tubes, VWR, Belgium).

Prior to analysis, Seronorm Trace Element Serum and Urine Level 1 were reconstituted in the vials. Following the instructions of the manufacturer, 3 and 5 mL of milli-Q water, respectively, were added to the vials to reconstitute the lyophilized material. To prevent contamination from the vials and the rubber stoppers (especially for Al, as indicated in the product instructions), after 30 minutes the solutions were transferred to Teflon Savillex beakers, which had been

thoroughly pre-cleaned (using HNO_3 and HCl and subsequent rinsing with Milli-Q water).

The effect of different dilutions on the extent of signal suppression was evaluated. Taking into account the magnitude of the matrix effect and the concentration of the target analytes, serum and urine samples were diluted 20- and 10-fold with 0.14 M HNO_3, respectively. Gallium was used as an internal standard (final concentration 1 µg L^{-1}). All measurements were performed immediately after the dilution to avoid problems with contamination and sample stability.

3.2.4. *Instrumentation*

An Agilent 8800 triple-quadrupole ICP-MS instrument (ICP-QQQ, Agilent Technologies, Japan) was used for all measurements. The sample introduction system consisted of a MicroMist nebulizer mounted onto a Peltier-cooled Scott-type spray chamber (2°C). The instrument is equipped with two quadrupole units, one before and one after the octopole collision/reaction cell. The cell can be pressurized with different gases, introduced via one of the four inlets, each having its own mass flow controller. The possibilities of using a mixture of CH_3F and He (10% CH_3F and 90% He) as a reaction gas was tested in this work. The CH_3F/He-mixture was introduced via the 4th inlet, normally used for O_2 (operation range of the mass flow controller: 0 – 100 %, corresponding to gas flow rates of 0 - 1 mL min^{-1} for O_2).

A Thermo Element XR sector-field ICP-MS instrument (ThermoScientific, Germany) was used for validation purposes, for those target elements for which reference values were not available or in cases of suspected contamination of the samples.

3.3. Results and discussion

As previously discussed, the determination of some elements at ultra-trace levels in complex matrices is a difficult task for Q-ICP-MS, even when using a collision/reaction cell. ICP-MS/MS allows for a more profound understanding of the chemical resolution of interferences in ICP-MS, as it permits monitoring of all the species formed.**[5, 43-48]** For that purpose, only ions with an m/z ratio of the target nuclide are allowed to enter the reaction cell by the first quadrupole, while

the second quadrupole is scanned as to detect and identify all reaction products formed (product ion scans). Also the possibility to fix the second quadrupole on a given m/z ratio and to scan the first quadrupole to unravel which ion might be at the origin of a reaction product ion is an interesting tool (precursor ion scan).

In this work, the reactions between CH_3F and Al, Co, Cr, Mn, Ni, Ti and V were studied. All the products formed were evaluated at different gas flow rates. Based on the findings thus obtained, methods were developed for mono-element determination in serum and urine samples under optimum conditions and for multi-element determination under compromise conditions.

3.3.1. *Selection of the most suited reaction products at different CH_3F flow rates*

The same protocol was applied to all the elements for investigating the different reaction products formed. Solutions containing 5 μg L^{-1} of Al, Co, Cr, Mn, Ni, Ti or V were prepared and, using the MS/MS capabilities, "product ion scans" were carried out, selecting the exact m/z ratio of every target nuclide with the first quadrupole and scanning the entire mass spectrum with the second quadrupole. The study was performed at CH_3F flow rate settings of 0.25, 0.50, 0.75 and 1.00 mL min^{-1}. The results are shown in **Figure 3.2**, which presents the signal intensity for the most prominent peaks as a function of the gas flow rate for each element. As an example, a complete product ion scan is provided in **Figure 3.3**. A careful evaluation of these results leads to the following conclusions concerning the identification of the different reaction product ions on the basis of their nominal mass, taking into account the ion-molecule reactions demonstrated in earlier work using ICP-SIFT-MS:**[51]**

i) Aluminum (^{27}Al, Figure 2a): AlF^+ (m/z 46), $AlCH_3F^+$ (m/z 61) and AlF_2^+ (m/z 65).
ii) Titanium (^{48}Ti, Figure 2b): TiF^+ (m/z 67), TiF_2^+ (m/z 86), $TiF_2(CH_3F)^+$ (m/z 120), $TiF_2(CH_3F)_2^+$ (m/z 154), $TiF_2(CH_3F)_3^+$ (m/z 188) and $TiF_2(CH_3F)_4^+$ (m/z 222).
iii) Vanadium (^{51}V, Figure 2c): VF^+ (m/z 70), VF_2^+ (m/z 89), $VF_2(CH_3F)^+$ (m/z 123), $VF_2(CH_3F)_2^+$ (m/z 157), $VF_2(CH_3F)_3^+$ (m/z 191), $VF_2(CH_3F)_4^+$ (m/z 225).

iv) Chromium (^{52}Cr, Figure 2d): CrF^+ (m/z 71), $CrCH_3F^+$ (m/z 86), $CrF(CH_3F)^+$ (m/z 105), $Cr(CH_3F)_2^+$ (m/z 120), $CrF(CH_3F)_2^+$ (m/z 139), $CrF(CH_3F)_3^+$ (m/z 173).

v) Manganese (^{55}Mn, Figure 2e): MnF^+ (m/z 74), $MnCH_3F^+$ (m/z 89), $MnF(CH_3F)^+$ (m/z 108), $Mn(CH_3F)_2^+$ (m/z 123), $MnF(CH_3F)_2^+$ (m/z 142), $MnF(CH_3F)_3^+$ (m/z 176).

vi) Cobalt (^{59}Co, Figure 2f): CoF^+ (m/z 78), $CoCH_3F^+$ (m/z 93), $CoF(CH_2F)^+$ (m/z 111), $CoF(CH_3F)^+$ (m/z 112), $Co(CH_3F)_2^+$ (m/z 127), $CoF(CH_3F)_2^+$ (m/z 146), $CoF(CH_3F)_3^+$ (m/z 180).

vii) Nickel (^{60}Ni, Figure 2g): NiF^+ (m/z 79), $NiCH_3F^+$ (m/z 94), $NiF(CH_2F)^+$ (m/z 112), $Ni(CH_3F)_2^+$ (m/z 128), $Ni(CH_3F)_3^+$ (m/z 162).

Generally speaking, the products formed at lower CH_3F flow rates are the result of fluorine addition (XF_a^+), while increasing the flow rate results in the formation of higher order reaction products, e.g., $XF_a(CH_3F)_b^+$ for Cr, Ti and V, and in methyl fluoride addition, e.g., $X(CH_3F)_b^+$ for Al, Co, Mn and Ni. It was also possible to group the target elements according to their reactions with CH_3F: (i) Ti and V, (ii) Cr and Mn, and (iii) Co and Ni - for these couples, a very similar behavior with respect to CH_3F was established. Some of our findings (Co, Cr, Mn, Ni, Ti and V) were in agreement with the results of the previously mentioned work carried out by means of ICP-SIFT-MS.**[51]**

To further test the effect of the MS/MS mode on the reactions described above, the same standard solutions were also analyzed in single quadrupole (SQ) mode, thus not prohibiting any ions on the basis of their m/z ratio to enter the octopole reaction cell using the first quadrupole. We observed that under these conditions, the results obtained were different. We hypothesize that this is due to the large amounts of various ubiquitous species that are not removed by the first quadrupole in this case (e.g., N_2^+, O_2^+, Ar^+), the presence of which seems to strongly affect the reactions with methyl fluoride.

Although all the products listed above were found, only the products showing a higher intensity were further studied for analytical purposes, as described in the forthcoming sections.

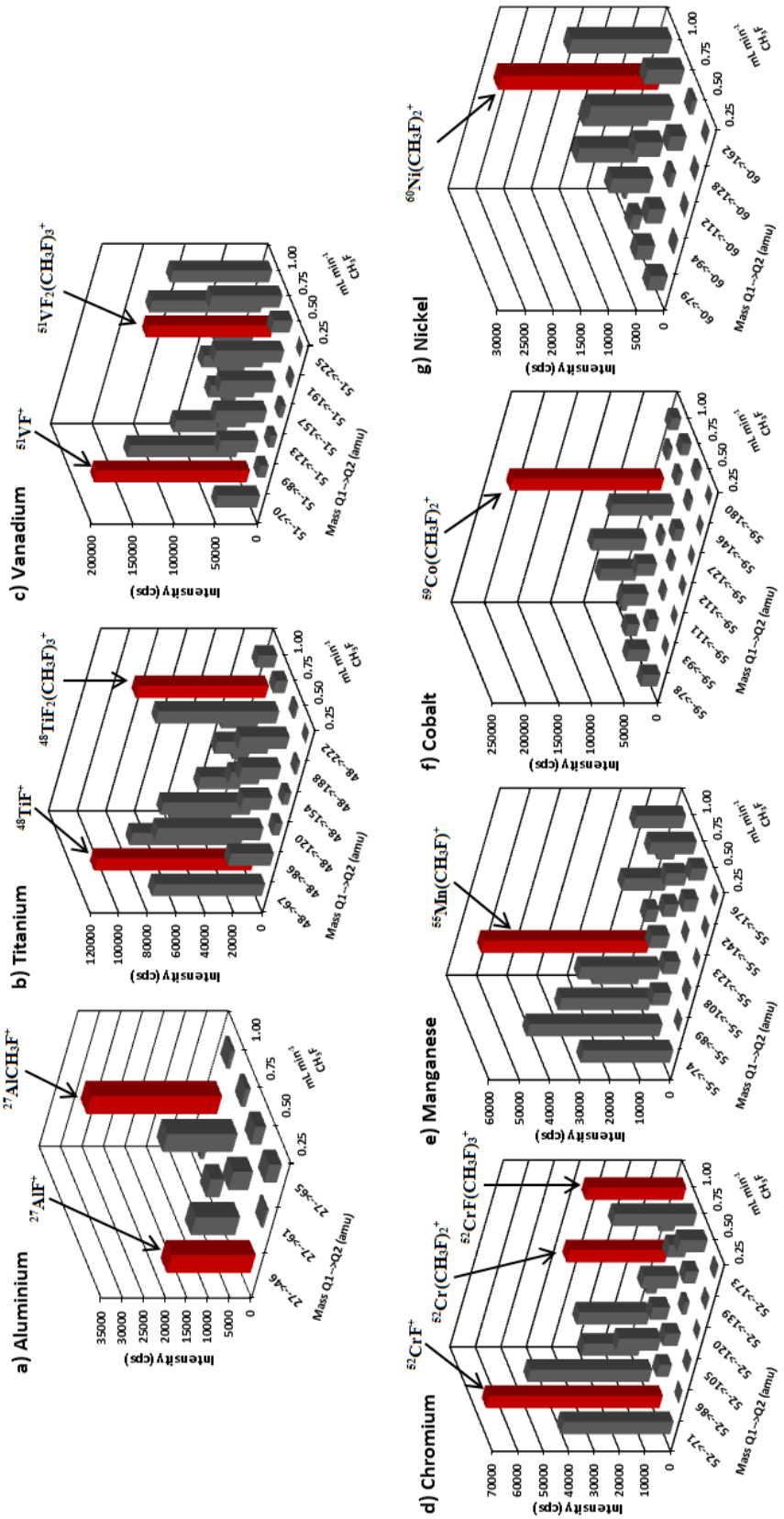

Figure 3.2. Selection of the different species formed at different methyl fluoride flow rate settings. The species ultimately used to determine the different target analytes are marked in red.

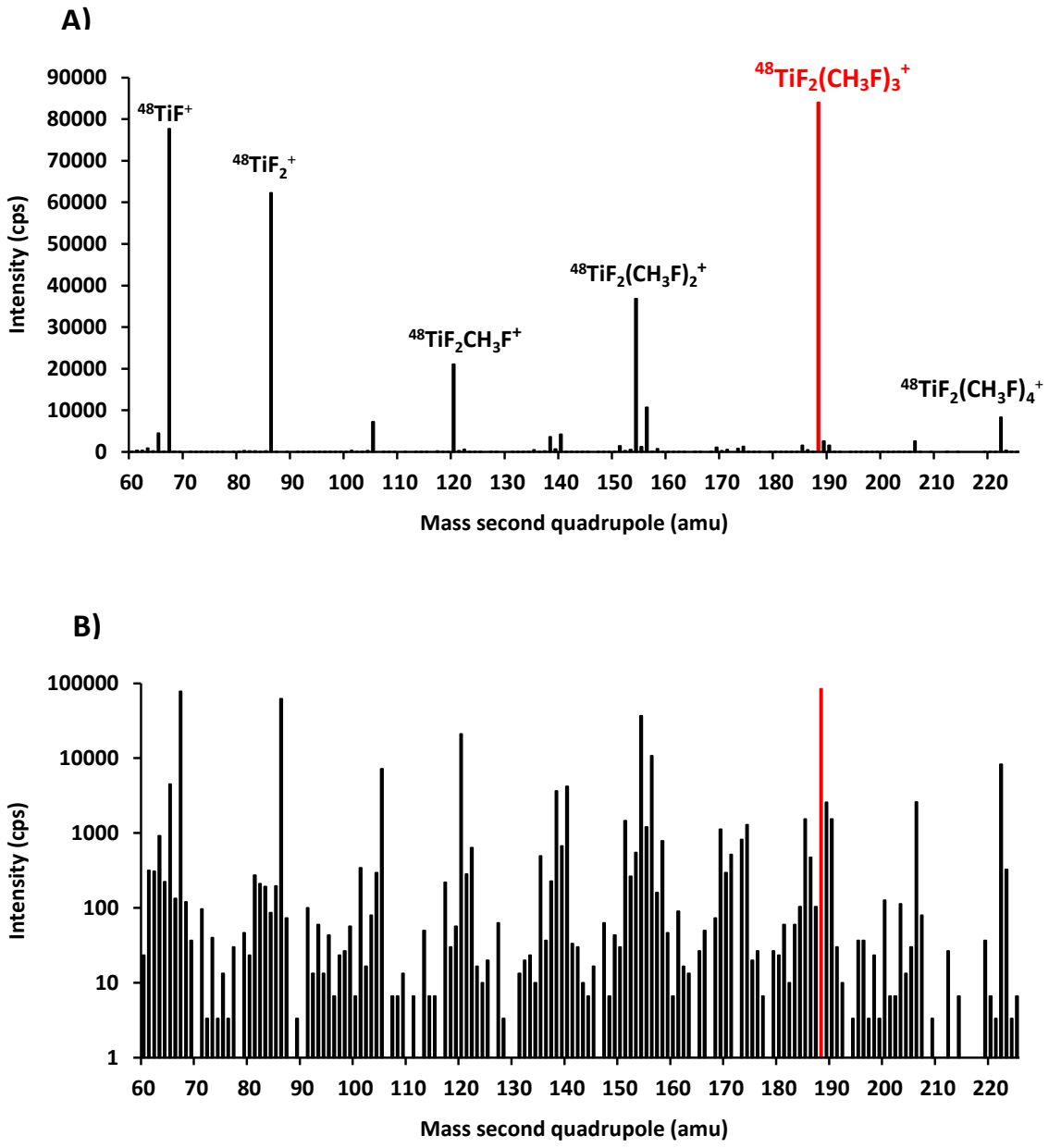

Figure 3.3. Product ion scan obtained for a standard solution containing 5 μg L^{-1} of Ti using 0.75 mL min^{-1} of CH_3F/He. Linear scale (A), Logaritmic scale (B)

3.3.2. Development of mono-element methods for the determination of each of the analyte elements under optimum conditions

For mono-element determination of the target nuclides, the reaction product ions characterized by the highest intensity were selected. The mass of the target analyte and the mass of the corresponding reaction product ion were fixed via the first and second quadrupole, respectively. The optimum gas flow rate was selected to maximize the signal-to-background ratio (Intensity for 5 μg L^{-1} in 0.14 M HNO_3). Under these optimum conditions, for every target analyte, 10 consecutive measurements of 5 standard solutions (concentrations of 0, 0.5, 1, 2.5 and 5 μg L^{-1}) were carried out. **Table 3.2** shows the different products that were finally used for quantification purposes with the corresponding methyl fluoride flow rate settings, as well as the calibration data and the instrumental limits of detection and quantification (LoDs and LoQs were calculated as $3s_{blank}$/slope and $10s_{blank}$/slope, respectively). As can be seen, the LoDs for all of the elements and nuclides are, at least for one of the reaction product ions, below 10 ng L^{-1}. It has to be stressed that these are the instrumental LoDs, such that sample dilution needs to be considered to obtain the final LoD in real-life analysis. Comparison with figures of merit obtained via other types of ICP-MS may serve to evaluate the potential of ICP-MS/MS for the determination of ultra-trace levels of these elements (**Table 3.3**).

Although it is always difficult to compare LoDs that have been obtained under different circumstances, the LoDs found with ICP-MS/MS are superior to those obtained with Q-ICP-MS (equipped with collision/reaction cell) in all cases, and are in good agreement with those obtained via SF-ICP-MS. Special attention can be paid to the case of Ti (LoDs with CH_3F, 0.9 – 3 ng L^{-1}), as it is possible to carry out a direct comparison with a previous work, based on ICP-MS/MS with NH_3 as reaction gas (chapter 2).**[5]** A 3-fold improvement (LoDs with NH_3, 3 – 10 ng L^{-1}) was found, further proving the benefits of using CH_3F.

It can be concluded that, even though sample dilution needs to be taken into account, the LODs achieved in this work are certainly fit for the purpose of analysis of biological fluids.

Table 3.2. Calibration data and instrumental limits of detection (LoD) and of quantification (LoQ) obtained for monoelemental methods in optimal conditions with ICP-MS/MS

Isotope	CH_3F/He flow rate (mL min^{-1})	Reaction product ion	Q1 (amu)	Q2 (amu)	Sensitivity[a] (L.μg^{-1})	Intercept[a] (counts.s^{-1})	R^2	LoD[b] ($\mu g.L^{-1}$)	LoQ[b] ($\mu g.L^{-1}$)
^{27}Al	0.25	$^{27}AlF^+$	27	46	3489 ± 21	686 ± 63	0.9997	0.01	0.04
	1.00	$^{27}AlCH_3F^+$		61	8021 ± 93	1401 ± 130	0.9997	0.008	0.03
^{46}Ti	0.40	$^{46}TiF^+$	46	65	1412 ± 32	98 ± 37	0.9998	0.02	0.07
	0.90	$^{46}TiF_2(CH_3F)_3^+$		186	1723 ± 19	34 ± 23	0.99996	0.003	0.01
^{47}Ti	0.40	$^{47}TiF^+$	47	66	1425 ± 26	59 ± 21	0.9998	0.003	0.009
	0.90	$^{47}TiF_2(CH_3F)_3^+$		187	1673 ± 19	39 ± 25	0.9998	0.003	0.009
^{48}Ti	0.40	$^{48}TiF^+$	48	67	15880 ± 210	2980 ± 200	0.9994	0.02	0.07
	0.90	$^{48}TiF_2(CH_3F)_3^+$		188	17920 ± 180	250 ± 200	0.99998	0.0009	0.003
^{49}Ti	0.40	$^{49}TiF^+$	49	68	1286 ± 27	46 ± 34	0.9998	0.03	0.09
	0.90	$^{49}TiF_2(CH_3F)_3^+$		189	1445 ± 20	27 ± 27	0.99998	0.003	0.01
^{50}Ti	0.40	^{50}TiF	50	69	1429 ± 25	71 ± 34	0.9997	0.007	0.02
	0.90	$^{50}TiF_2(CH_3F)_3^+$		190	1455 ± 12	29 ± 15	0.99995	0.002	0.006

Continued on next page

Continued from previous page

^{51}V	0.40	$^{51}VF^+$	51	70	39250 ± 740	420 ± 470	0.99997	0.0009	0.003
	0.80	$^{51}VF_2(CH_3F)_3^+$		191	40160 ± 330	230 ± 140	0.999997	0.0001	0.0004
^{52}Cr	0.45	$^{52}CrF^+$	52	71	12940 ± 110	61 ± 51	0.9999995	0.002	0.005
	1.00	$^{52}Cr(CH_3F)_2^+$		120	8027 ± 41	62 ± 33	0.99998	0.0009	0.003
	1.00	$^{52}CrF(CH_3F)_3^+$		173	7628 ± 55	-25 ± 43	0.999992	0.003	0.01
^{53}Cr	0.45	$^{53}CrF^+$	53	72	1495 ± 23	17 ± 17	0.99998	0.004	0.01
	1.00	$^{53}Cr(CH_3F)_2^+$		121	994 ± 18	11 ± 15	0.99994	0.006	0.02
	1.00	$^{53}CrF(CH_3F)_3^+$		174	907 ± 12	-2 ± 10	0.999994	0.01	0.03
^{55}Mn	1.00	$^{55}Mn(CH_3F)^+$	55	89	11846 ± 76	47 ± 71	0.9999997	0.001	0.004
^{59}Co	1.00	$^{59}Co(CH_3F)_2^+$	59	127	46230 ± 410	320 ± 370	0.999992	0.0003	0.0009
^{58}Ni	1.00	$^{58}Ni(CH_3F)_2^+$	58	126	14829 ± 67	85 ± 52	0.999997	0.002	0.008
^{60}Ni	1.00	$^{60}Ni(CH_3F)_2^+$	60	128	6280 ± 42	35 ± 42	0.99998	0.002	0.007

[a] Uncertainties expressed as standard deviation (n = 10)

[b] LoDs and LoQs calculated as 3 and 10 times the standard deviation on 10 consecutive measurements of a blank solution (0.14 M HNO_3), divided by the slope of the calibration curve, respectively.

Table 3.3. Comparison between the LoDs found via ICP- MS/MS and those reported in the literature based on the use of other types of ICP-MS devices (ng L^{-1}).**[1, 6, 7, 14]**

Isotopes	Q-ICP-MS[a]	SF-ICP-MS	ICP-MS/MS
^{27}Al	130	50	8
^{47}Ti	70	10	3
^{51}V	3	0.1	0.1
^{52}Cr	6	0.1	0.9
^{55}Mn	20	10	1
^{59}Co	7	0.1	0.3
^{60}Ni	30	5	2

[a]Values obtained from different papers; the gases most often used in collision-reaction cells were He, H_2, NH_3.

As most of the elements under investigation are severely affected by spectral overlap in clinical matrices, it is also important to investigate the capabilities of the methods developed to avoid these interferences. Therefore, matrix-matched standard solutions were prepared by adding 10 mg L^{-1} of the most important matrix elements present in clinical samples (Ca, Cl, Fe, K, Mg, Na, P, and S) to 5 µg L^{-1} of the analyte elements. Only in the case of Ti, the results obtained were affected by the presence of the interfering species (formation of $^{46,48}CaF^+$ and $^{48}CaF_2(CH_3F)_3^+$, overlapping with $^{46,48}TiF^+$ and, to a lesser extent, with $^{48}TiF_2(CH_3F)_3^+$, respectively). Due to the importance of this interference, especially in the case of $^{46,48}TiF^+$, and to the presence of high Ca concentrations in clinical samples, these two species were not further investigated. However, the monitoring of other reaction product ions ($^{47,49,50}TiF^+$ and $^{46,47,49,50}TiF_2(CH_3F)_3^+$) should allow interference-free Ti determination.

3.3.3. Mono-element determinations of ultra-trace elements in Seronorm Trace Elements Serum and Urine Level 1

Once all the mono-element methods were developed, two different reference materials were analyzed for validation purposes: Seronorm Trace Element Serum Level 1 and Seronorm Trace Element Urine Level 1.

Several sub-samples from one vial were analyzed with ICP-MS/MS and the results were compared with the reference values. For those target elements for which there

are not reference values and only indicative values (or even no reference values at all) are available, SF-ICP-MS was used for validation purposes (see **Table 3.4**). The results thus obtained are shown in **Table 3.5**.

Table 3.4. Instrument settings and data acquisition parameters for the Agilent 8800 and the Thermo Element XR SF-ICP-MS instruments

Agilent 8800[a]		**Element XR**	
CH_3F/He (10/90)			
Scan type	MS/MS	**Scan type**	EScan
Plasma mode	Low Matrix	**Resolution**	Medium
RF power	1550 W	**RF power**	1200 W
Carrier gas flow rate	1.11 $L.min^{-1}$	**Carrier gas flow rate**	0.975 $L.min^{-1}$
Reaction gas flow rate setting	1 $mL.min^{-1}$		
Q1 bias	-2 V	**Mass window**	125%
Octopole bias	-5 V	**Search window**	70%
Energy discrimination	-10 V	**Integration window**	60%
QP bias	-15 V	**Sample time**	0.010 s
Q2 axis offset	-0.01	**Samples/peak**	20
Q1 –> Q2 masses	27 –> 61 46 –> 186 47 –> 187 49 –> 189 50 –> 190 51 –> 191 52 –> 120 53 –> 121 55 –> 89 59 –> 127 58 –> 126 60 –> 128 71 –> 71	**Nuclides monitored**	^{27}Al ^{47}Ti ^{49}Ti ^{51}V ^{52}Cr ^{53}Cr ^{71}Ga
Wait Time Offset	2 ms		
Total analysis time / sample	163 s	**Total analysis time / sample**	86 s

[a] Instrument settings used in the multi-elemental method

Table 3.5. Results obtained for Seronorm Trace Element Serum L-1 and Seronorm Trace Element Urine L-1 same vial

Seronorm Trace Elements Serum L-1						
Analyte	**Reaction product ion**	**Mono-element ICP-MS/MS[a] (µg L^{-1})**	**Multi-element ICP-MS/MS[a] (µg L^{-1})**	**SF-ICP-MS[b] (µg L^{-1})**	**Reference value (µg L^{-1})**	**Acceptable range (µg L^{-1})**
^{27}Al	$^{27}AlF^+$	40.55 ± 0.84	—	40.73 ± 0.83	33.6 ± 1.9	29.8 – 37.4
	$^{27}AlCH_3F^+$	40.29 ± 0.73	40.00 ± 0.55			
^{46}Ti	$^{46}TiF^+$	—	—	—	11.2[c]	
	$^{46}TiF_2(CH_3F)_3^+$	12.28 ± 0.64	12.68 ± 0.71			
^{47}Ti	$^{47}TiF^+$	14.71 ± 0.69	—	11.58 ± 0.53	11.2[c]	
	$^{47}TiF_2(CH_3F)_3^+$	11.88 ± 0.38	11.83 ± 0.49			
^{48}Ti	$^{48}TiF^+$	—	—	—	11.2[c]	
	$^{48}TiF_2(CH_3F)_3^+$	14.10 ± 0.35	—			
^{49}Ti	$^{49}TiF^+$	17.46 ± 0.59	—	11.81 ± 0.33	11.2[c]	
	$^{49}TiF_2(CH_3F)_3^+$	11.44 ± 0.56	11.90 ± 0.48			
^{50}Ti	^{50}TiF	37.42 ± 1.79	—	—	11.2[c]	
	$^{50}TiF_2(CH_3F)_3^+$	11.29 ± 0.51	11.83 ± 0.55			

Continued on next page

Continued from previous page

^{51}V	$^{51}VF^{+}$	1.20 ± 0.05	—	1.19 ± 0.03	0.96[c]	
	$^{51}VF_2(CH_3F)_3^{+}$	1.23 ± 0.01	1.23 ± 0.03			
^{52}Cr	$^{52}CrF^{+}$	1.42 ± 0.04	—			
	$^{52}Cr(CH_3F)_2^{+}$	1.45 ± 0.04	1.46 ± 0.08	1.46 ± 0.06	1.5 ± 0.2	1.1 – 1.9
	$^{52}CrF(CH_3F)_3^{+}$	1.41 ± 0.03	—			
^{53}Cr	$^{53}CrF^{+}$	1.37 ± 0.07	—			
	$^{53}Cr(CH_3F)_2^{+}$	1.43 ± 0.06	1.43 ± 0.10	1.41 ± 0.10	1.5 ± 0.2	1.1 – 1.9
	$^{53}CrF(CH_3F)_3^{+}$	1.46 ± 0.10	—			
^{55}Mn	$^{55}Mn(CH_3F)^{+}$	15.14 ± 0.07	15.25 ± 0.13	—	15.0 ± 0.9	13.2 – 16.8
^{59}Co	$^{59}Co(CH_3F)_2^{+}$	1.19 ± 0.03	1.22 ± 0.05	—	1.2 ± 0.2	0.9 – 1.5
^{58}Ni	$^{58}Ni(CH_3F)_2^{+}$	5.64 ± 0.14	5.58 ± 0.08	—	5.8 ± 0.7	4.5 – 7.1
^{60}Ni	$^{60}Ni(CH_3F)_2^{+}$	5.63 ± 0.13	5.58 ± 0.20	—	5.8 ± 0.7	4.5 – 7.1

Continued on next page

Continued from previous page

Seronorm Trace Elements Urine L-1						
Analyte	**Reaction product ion**	**Mono-element ICP-MS/MS[a] (µg L^{-1})**	**Multi-element ICP-MS/MS[a] (µg L^{-1})**	**SF-ICP-MS[b] (µg L^{-1})**	**Reference value (µg L^{-1})**	**Acceptable range (µg L^{-1})**
^{27}Al	$^{27}AlF^+$	14.31 ± 0.20	—	14.62 ± 0.22	4.6 ± 3.5	1.1 – 8.1
	$^{27}AlCH_3F^+$	14.38 ± 0.33	13.88 ± 0.55			
^{46}Ti	$^{46}TiF^+$	—	—	—	13.5[c]	
	$^{46}TiF_2(CH_3F)_3^+$	13.31 ± 0.37	12.68 ± 0.35			
^{47}Ti	$^{47}TiF^+$	26.06 ± 0.86	—	12.76 ± 0.20	13.5[c]	
	$^{47}TiF_2(CH_3F)_3^+$	12.87 ± 0.50	12.38 ± 0.49			
^{48}Ti	$^{48}TiF^+$	—	—	—	13.5[c]	
	$^{48}TiF_2(CH_3F)_3^+$	14.60 ± 0.17	—			
^{49}Ti	$^{49}TiF^+$	14.88 ± 0.47	—	12.72 ± 0.21	13.5[c]	
	$^{49}TiF_2(CH_3F)_3^+$	12.82 ± 0.30	12.62 ± 0.57			
^{50}Ti	^{50}TiF	24.36 ± 0.72	—	—	13.5[c]	
	$^{50}TiF_2(CH_3F)_3^+$	12.77 ± 0.40	12.42 ± 0.31			

Continued on next page

Continued from previous page

^{51}V	$^{51}VF^{+}$	0.70 ± 0.03	—	0.74 ± 0.01	0.66 ± 0.08	0.5 – 0.9
	$^{51}VF_2(CH_3F)_3^{+}$	0.73 ± 0.02	0.77 ± 0.04			
^{52}Cr	$^{52}CrF^{+}$	1.51 ± 0.12	—			
	$^{52}Cr(CH_3F)_2^{+}$	1.66 ± 0.18	1.61 ± 0.27	1.65 ± 0.27		—
	$^{52}CrF(CH_3F)_3^{+}$	1.52 ± 0.26	—			
^{53}Cr	$^{53}CrF^{+}$	1.57 ± 0.18	—			
	$^{53}Cr(CH_3F)_2^{+}$	1.64 ± 0.20	1.63 ± 0.29	1.63 ± 0.05		—
	$^{53}CrF(CH_3F)_3^{+}$	1.66 ± 0.18	—			
^{55}Mn	$^{55}Mn(CH_3F)^{+}$	0.68 ± 0.02	0.69 ± 0.05	—	0.73 ± 0.15	0.44 – 1.02
^{59}Co	$^{59}Co(CH_3F)_2^{+}$	0.71 ± 0.01	0.72 ± 0.01	—	0.72 ± 0.15	0.43 – 1.01
^{58}Ni	$^{58}Ni(CH_3F)_2^{+}$	1.55 ± 0.03	1.56 ± 0.06	—	1.51 ± 0.30	0.91 – 2.11
^{60}Ni	$^{60}Ni(CH_3F)_2^{+}$	1.57 ± 0.07	1.58 ± 0.11	—	1.51 ± 0.30	0.91 – 2.11

[a] Uncertainties expressed as standard deviation (n = 5)

[b] Uncertainties expressed as standard deviation (n = 3)

[c] Indicative value

A good agreement between ICP-MS/MS results and the reference values was found in all cases ($t < t_{critical}$ at a 95% level of significance), with uncertainty intervals overlapping, except for Al. For this element, the value obtained by means of ICP-MS/MS was biased high (particularly for urine). However, the value obtained is in good agreement with the result obtained by means of SF-ICP-MS ($t < t_c$), thus revealing possible contamination problems during the reconstitution of the samples, which is a common issue, also indicated in the certificate of the materials. For those analytes for which indicative values are provided – Ti in serum and urine and V in serum – or for which no reference value at all is available – Cr in urine – the results were compared with those obtained via SF-ICP-MS. No significant differences were found for V and Cr ($t < t_{critical}$ for all reaction products and nuclides), nor for Ti for the reaction product ions $^{47,49}TiF_2(CH_3F)_3^+$. However, significant differences were found when considering the results obtained using the reaction product ions $^{47,49,50}TiF^+$. Unfortunately, and although a precursor ion scan was used in an attempt to identify the interferences which produce inaccuracy in the results, the species responsible were not found. In any case, the results show that an interference-free determination of at least two isotopes is possible for Cr, Ni and Ti, thus opening a way for isotopic analysis, e.g., in the context of elemental assay *via* isotope dilution or in tracer experiments with stable isotopes. This aspect is particularly remarkable for ^{58}Ni, because of the isobaric interference with ^{58}Fe and the high concentration of iron present in serum (1.39 mg L^{-1}). This indicates that, under the experimental conditions used in this work, Ni and Fe ions react differently with CH_3F or that, due to the low abundance of ^{58}Fe, the final result was not affected.

3.3.4. *Development of a multi-element method for the simultaneous determination of Al, Co, Cr, Mn, Ni, Ti and V*

As described before, the optimum instrument settings providing the highest signal intensity are different for each element, because of the influence of the CH_3F flow rate on the reactions taking place in the reaction cell. However, the development of a multi-element method, allowing for an accurate and simultaneous determination of all of the elements of interest would be of much higher value for routine analysis. Therefore, based on the results presented in **Figure 3.2**, it was investigated whether such compromise conditions could be found. Due to the significant reduction of

sensitivity found at lower CH_3F flow rates, particularly for Co, Mn and Ni, the maximum flow rate setting (1 mL min^{-1}) was selected. Once the CH_3F flow rate was chosen, the other parameters were also optimized (see **Table 3.4**). Calibration data and LoDs and LoQs obtained via measurement of 5 multi-element standard solutions (concentrations of 0, 0.5, 1, 2.5 and 5 μg L^{-1}) are shown in **Table 3.6**. Although under these conditions, a 20-30% reduction in signal intensity was observed for Al, Ti and V, the LoDs were not affected significantly and again, they were found to be below 10 ng L^{-1} in all cases.

3.3.5. *Simultaneous multi-elemental analysis of Seronorm Trace Elements Serum and Urine Level 1*

The samples analyzed via the mono-element methods were also analyzed using the multi-element method, enabling a direct comparison of the results (**Table 3.5**). At a 95% level of confidence, no significant differences were found between the results obtained under optimum conditions for every analyte and those obtained under multi-element compromise conditions ($t < t_{critical}$), except for ^{46}Ti in urine, where the difference was found to be statistically significant, although the t value is close to $t_{critical}$ (2.77 > 2.31). Also in terms of precision, no significant differences could be established at a 95% level of confidence (F-test: $F < F_{critical}$). RSD values range between 1 – 6 %, which is fit for purpose for the application intended, except for Cr in urine for which the RSD was higher, especially for the less abundant isotope ^{53}Cr (5 – 18 %).

To check the reproducibility of the method for different samples (different vials with reference material from the same batch), the same samples discussed previously and four additional samples (two vials for serum and two vials for urine) were analyzed using the multi-element method. The results are shown in **Table 3.7**, showing the average concentration and the standard deviation for three different samples (vials) from the same batch – each sample was analyzed 10 consecutive times. ANOVA indicated that there is significant variation between the results for the different samples, except for $^{47,49,50}Ti$ and ^{59}Co in serum, and ^{53}Cr and ^{60}Ni in urine ($F < F_{critical}$). These variations are particularly important in the case of Al for both serum and urine ($F_{Al,serum}$ =192.31; $F_{Al,urine}$ = 278.84 > $F_{critical}$ = 3.35) and of Ti in urine ($F_{Ti\ (46\text{-}50)}$ = 39.24 – 108.75 > $F_{critical}$ = 3.35). These results suggest that, at these

Table 3.6. Calibration data and instrumental limits of detection (LoD) and quantification (LoQ) obtained for the ICP-MS/MS multi-element method

Isotope	Reaction product ion	Q1 (amu)	Q2 (amu)	Sensitivity[a] (L.µg^{-1})	Intercept[a] (counts.s^{-1})	R^2	LoD[b] (µg.L^{-1})	LoQ[b] (µg.L^{-1})
^{27}Al	$^{27}AlCH_3F^+$	27	61	6233 ± 57	1069 ± 46	0.9990	0.01	0.03
^{46}Ti	$^{46}TiF_2(CH_3F)_3^+$	46	186	1346 ± 16	43 ± 16	0.99995	0.003	0.01
^{47}Ti	$^{47}TiF_2(CH_3F)_3^+$	47	187	1315 ± 16	52 ± 31	0.99990	0.001	0.004
^{49}Ti	$^{49}TiF_2(CH_3F)_3^+$	49	189	1026 ± 35	40 ± 29	0.99998	0.002	0.008
^{50}Ti	$^{50}TiF_2(CH_3F)_3^+$	50	190	1101 ± 18	32 ± 33	0.99993	0.003	0.01
^{51}V	$^{51}VF_2(CH_3F)_3^+$	51	191	29780 ± 220	-410 ± 220	0.99996	0.0002	0.0008
^{52}Cr	$^{52}Cr(CH_3F)_2^+$	52	120	7298 ± 79	137 ± 63	0.99998	0.004	0.01
^{53}Cr	$^{53}Cr(CH_3F)_2^+$	53	121	910 ± 27	8 ± 27	0.9999995	0.01	0.03
^{55}Mn	$^{55}Mn(CH_3F)^+$	55	89	11320 ± 110	247 ± 69	0.99997	0.001	0.005
^{59}Co	$^{59}Co(CH_3F)_2^+$	59	127	50050 ± 110	720 ± 160	0.99998	0.0006	0.002
^{58}Ni	$^{58}Ni(CH_3F)_2^+$	58	126	15180 ± 100	190 ± 130	0.999995	0.002	0.005
^{60}Ni	$^{60}Ni(CH_3F)_2^+$	60	128	5850 ± 41	94 ± 67	0.99998	0.003	0.009

[a] Uncertainties expressed as standard deviation (n=10)

[b] LoDs and LoQs calculated as 3 and 10 times the standard deviation on 10 consecutive measurements of a blank solution (0.14M HNO_3), divided by the slope of the calibration curve, respectively

concentration levels, issues like sample preparation, sample storage and contamination, become more challenging than the analysis using ICP-MS/MS itself.

3.4. Conclusion

In this work, the utility of ICP-MS/MS with methyl fluoride (a mixture of 10% CH_3F and 90 % He) as a reaction gas was demonstrated for the determination of ultra-trace levels of Al, Co, Cr, Mn, Ni, Ti and V in serum and urine samples.

In a first phase, for each target element, product ion scans have been performed at different CH_3F flow rates. Based on these results, optimized mono-element methods have been developed, allowing full exploitation of the possibilities of ICP-MS/MS for each analyte. In all cases, excellent detection limits (below 10 ng L^{-1}) could be obtained. Additionally, it was also demonstrated that a multi-element method for the simultaneous determination of all the target elements under a same set of instrument settings did not compromise the accuracy and precision of the results. Interference-free conditions were obtained for all elements studied. It has also been found that for elements such as Cr, Ni and Ti, at least two isotopes could be measured interference-free, enabling isotopic analysis.

Overall, the satisfactory results obtained suggest that the use of CH_3F is a valuable alternative for the more common reaction gases used nowadays. Finally, it has been shown that ICP-MS/MS does not only allow interference-free determination of traditionally interfered elements, but is also a versatile tool to systematically study the complex reactions taking place in a reaction cell in a very straightforward way.

Acknowledgement

The UGent authors acknowledge Agilent Technologies for providing them with an ACT-UR research project grant. MR acknowledges the funding from the Spanish Ministry of Economy and Competitiveness (Project CTQ2012-33494) and from the Aragón Government (Fondo Social Europeo).

Table 3.7. Results obtained for Seronorm Trace Elements Serum L-1 and Seronorm Trace Elements Urine L-1 in multielement conditions using three different vials

		Seronorm Trace Elements Serum L-1			**Seronorm Trace Elements Urine L-1**		
Analyte	**Reaction product ion**	**Average ± SD[a] (µg L^{-1})**	**Reference value[b] (µg L^{-1})**	**Acceptable range (µg L^{-1})**	**Average ± SD (µg L^{-1})**	**Reference value[b] (µg L^{-1})**	**Acceptable range (µg L^{-1})**
^{27}Al	$^{27}AlCH_3F^+$	40.03 ± 0.52 39.33 ± 0.50 35.14 ± 0.75	33.6 ± 1.9	29.8 – 37.4	13.75 ± 0.63 8.24 ± 0.58 9.83 ± 0.36	4.6 ± 3.5	1.1 – 8.1
^{46}Ti	$^{46}TiF_2(CH_3F)_3^+$	12.61 ± 0.66 12.71 ± 0.52 11.97 ± 0.57	11.2[c]		12.44 ± 0.36 14.26 ± 0.60 13.03 ± 0.26	13.5[c]	
^{47}Ti	$^{47}TiF_2(CH_3F)_3^+$	11.74 ± 0.50 11.63 ± 0.66 11.56 ± 0.41	11.2[c]		12.37 ± 0.42 14.59 ± 0.39 12.64 ± 0.28	13.5[c]	
^{49}Ti	$^{49}TiF_2(CH_3F)_3^+$	11.82 ± 0.49 11.70 ± 0.65 11.62 ± 0.51	11.2[c]		12.56 ± 0.58 15.16 ± 0.41 12.80 ± 0.29	13.5[c]	
^{50}Ti	$^{50}TiF_2(CH_3F)_3^+$	11.86 ± 0.72 11.41 ± 0.74 11.86 ± 0.87	11.2[c]		12.36 ± 0.28 13.96 ± 0.44 13.01 ± 0.47	13.5[c]	
^{51}V	$^{51}VF_2(CH_3F)_3^+$	1.22 ± 0.05 1.40 ± 0.06 1.31 ± 0.12	0.96[c]		0.76 ± 0.04 0.82 ± 0.03 0.83 ± 0.02	0.66 ± 0.08	0.5 – 0.9

Continued on next page

Continued from previous page

^{52}Cr	$^{52}Cr(CH_3F)_2^+$	1.44 ± 0.12 1.64 ± 0.13 1.32 ± 0.10	1.5 ± 0.2	1.1 – 1.9	1.55 ± 0.24 1.85 ± 0.47 1.97 ± 0.26	---	
^{53}Cr	$^{53}Cr(CH_3F)_2^+$	1.41 ± 0.11 1.60 ± 0.12 1.34 ± 0.15	1.5 ± 0.2	1.1 – 1.9	1.59 ± 0.28 1.82 ± 0.46 1.93 ± 0.32	---	
^{55}Mn	$^{55}Mn(CH_3F)^+$	15.34 ± 0.15 15.68 ± 0.24 15.19 ± 0.30	15.0 ± 0.9	13.2 – 16.8	0.70 ± 0.05 0.63 ± 0.03 0.72 ± 0.04	0.73 ± 0.15	0.44 – 1.02
^{59}Co	$^{59}Co(CH_3F)_2^+$	1.23 ± 0.04 1.23 ± 0.02 1.18 ± 0.13	1.2 ± 0.2	0.9 – 1.5	0.71 ± 0.01 0.71 ± 0.02 0.74 ± 0.02	0.72 ± 0.15	0.43 – 1.01
^{58}Ni	$^{58}Ni(CH_3F)_2^+$	5.56 ± 0.09 5.72 ± 0.14 5.87 ± 0.17	5.8 ± 0.7	4.5 – 7.1	1.55 ± 0.06 1.63 ± 0.06 1.60 ± 0.02	1.51 ± 0.30	0.91 – 2.11
^{60}Ni	$^{60}Ni(CH_3F)_2^+$	5.53 ± 0.17 5.76 ± 0.17 5.84 ± 0.12	5.8 ± 0.7	4.5 – 7.1	1.60 ± 0.09 1.67 ± 0.11 1.62 ± 0.06	1.51 ± 0.30	0.91 – 2.11

[a] The results show the average and the standard deviation of 10 consecutive measurements (n = 10) for samples originating from three different vials

[b] Analytical value ± 95 % confidence interval (Seronorm)

[c] Indicative values

References

[1] C. Sariego Muñiz, J. M. Marchante-Gayón, J. I. García Alonso, A. Sanz-Medel, J Anal At Spectrom, 13 (1998) 283 – 287.

[2] M. Aramendía, M. R. Flórez, M. Piette, F. Vanhaecke, M. Resano, J Anal At Spectrom, 26 (2011) 1964 – 1973.

[3] T. D. Richardson, S. J. Pineda, K. B. Strenge, T. A. Van Fleet, M. MacGregor, J. C. Milbrandt, J. A. Espinosa, P. Freitag, Spine, 33 (2008) 792 – 796.

[4] L. Rello, A. C. Lapeña, M. Aramendía, M. A. Belarra, M. Resano, Spectrochim Acta, Part B, 81 (2013) 11 – 19.

[5] L. Balcaen, E. Bolea-Fernandez, M. Resano, F. Vanhaecke, Anal Chim Acta, 809 (2014) 1 – 8.

[6] A. Sarmiento-González, J. M. Marchante-Gayón, L. M. Tejerina-Lobo, J. Paz-Jiménez, A. Sanz-Medel, Anal Bioanal Chem, 382 (2005) 1001 – 1009.

[7] A. Sarmiento-González, J. M. Marchante-Gayón, J. M. Tejerina-Lobo, J. Paz-Jiménez, A. Sanz-Medel, Anal Bioanal Chem, 391 (2008) 2583 – 2589.

[8] C. A. Engh Jr., S.J. MacDonald, S. Sritulanondha, A.Thompson, D. Naudie, C. A. Engh, Clin Orthop Relat Res, 467 (2009) 101 – 111.

[9] G. R. Willsky, A. B. Goldfine, P. J. Kostyniak, J. H. McNeill, L. Q. Yang, H. R. Khan, D. C. Crans, J Inorg Biochem, 85 (2001) 33 – 42.

[10] L. Yang, R. E. Sturgeon, D. Prince, S. Gabos, J Anal At Spectrom, 17 (2002) 1300 – 1303.

[11] C. Bonnefoy, A. Menudier, C. Moesch, G. Lachâtre, Anal Bioanal Chem,383 (2005) 167 – 173.

[12] W. Cieslak, K. Pap, D. R. Bunch, E. Reineks, R. Jackson, R. Steinle, S. Wang, Clin Biochem, 46 (2013) 266 – 270.

[13] M. Aschner, T. R. Guilarte, J. S. Schneider, W. Zheng, Toxicol Appl Pharmacol, 221 (2007) 131 – 147.

[14] B. Michalke, M. Lucio, A. Berthele, B. Kanawati, Anal Bioanal Chem, 405 (2013) 2301 – 2309.

[15] A. Schwingel Ribeiro, M. Antunes Vieira, A. Furtado da Silva, D. L. Gallindo Borges, B. Welz, U. Heitmann, A. J. Curtius, Spectrochim Acta, Part B, 60 (2005) 693 – 698.

[16] M. F. Gornet, J. K. Burkus, M. L. Harper, F. W. Chan, A. K. Skipor, J. J. Jacobs, Eur Spine J, 22 (2013) 741 – 746.

[17] S. X. Xu, L. Stuhne-Sekatec, D. M. Templeton, J Anal At Spectrom, 8 (1993) 445 – 448.

[18] S. L. C. Ferreira, W. N. L. dos Santos, V. A. Lemos, Anal Chim Acta, 445 (2001) 145 – 151.

[19] P. Schramel, I. Wendler, Fresenius J Anal Chem, 361 (1998) 487 – 491.

[20] J. Riondato, F. Vanhaecke, L. Moens, R. Dams, J Anal At Spectrom, 12 (1997) 933 – 937.

[21] N. Jakubowski, L. Moens, F. Vanhaecke, Spectrochim Acta, Part B, 53 (1998) 1739 – 1763.

[22] M. Krachler, C. Heisel, J. P. Kretzer, J Anal At Spectrom, 24 (2009) 605 – 610.

[23] S. D. Tanner, V. I. Baranov, At Spectrosc, 20 (1999) 45 – 52.

[24] V. I. Baranov, S. D. Tanner, J Anal At Spectrom, 14 (1999) 1133 – 1142.

[25] S. D. Tanner, V. I. Baranov, J Am Soc Mass Spectrom, 10 (1999) 1083 – 1094.

[26] S. D. Tanner, V. I. Baranov, U. Vollkopf, J Anal At Spectrom, 15 (2000) 1261 – 1269.

[27] S. D. Tanner, V. I. Baranov, D. R. Bandura, Spectrochim Acta, Part B, 57 (2002) 1361 – 1452.

[28] I. Feldmann, N. Jakubowski, D. Stuewer, Fresenius J Anal Chem, 365 (1999) 415 – 421.

[29] I. Feldmann, N. Jakubowski, D. Stuewer, Fresenius J Anal Chem, 365 (1999) 422 – 428.

[30] S. F. Boulyga, J. S. Becker, Fresenius J Anal Chem, 370 (2001) 618 – 623.

[31] D. R. Bandura, V. I. Baranov, S. D. Tanner, Fresenius J Anal Chem, 370 (2001) 454 – 470.

[32] B. Hattendorf, D. Günther, Spectrochim Acta, Part B, 58 (2003) 1 – 13.

[33] D. W. Koppenaal, G. C. Eiden, C. J. Barinaga, J Anal At Spectrom, 19 (2004) 561 – 570.

[34] J. W. Olesik, D. R. Jones, J Anal At Spectrom, 21 (2006) 141 – 159.

[35] M. Grotti, F. Soggia, J. L. Todolì, Analyst, 133 (2008) 1388 – 1394.

[36] L. A. Simpson, M. Thomsen, B. J. Alloway, A. Parker, J Anal At Spectrom, 16 (2001) 1375 – 1380.

[37] M. Resano, E. Garcia-Ruiz, F. Vanhaecke, Spectrochim Acta, Part B, 60 (2005) 1472 – 1481.

[38] D. R. Bandura, V. I. Baranov, S. D. Tanner, Anal Chem, 74 (2002) 1497 – 1502.

[39] D. R. Bandura, O. I. Ornatsky, L. Liao, J Anal At Spectrom, 19 (2004) 96 – 100.

[40] C. H. Yang, S. J. Jiang, Spectrochim Acta, Part B, 59 (2004) 1389 – 1394.

[41] D. R. Bandura, V. Baranov, A. E. Litherland, S. D. Tanner, Int J Mass Spectrom, 255-256 (2006) 312 – 327.

[42] B. Hattendorf, D. Günther, J Anal At Spectrom, 15 (2000) 1125 – 1131.

[43] S. Diez Fernández, N. Sugishama, J. Ruiz Encinar, A. Sanz-Medel, Anal Chem, 84 (2012) 5851 – 5857.

[44] L. Balcaen, G. Woods, M. Resano, F. Vanhaecke, J Anal At Spectrom, 28 (2013) 33 – 39.

[45] T. Ohno, Y. Muramatsu, Y. Shikamori, C. Toyama, N. Okabe, H. Matsuzaki, J Anal At Spectrom, 28 (2013) 1283 – 1287.

[46] M. Tanimizu, N. Sugiyama, E. Ponzevera, G. Bayon, J Anal At Spectrom, 28 (2013) 1372 – 1376.

[47] T. Ohno, Y. Muramatsu, J Anal At Spectrom, 29 (2014) 347 – 351.

[48] K. Böting, S. Treu, P. Leonhard, C. Heiß, N. H. Bings, J Anal At Spectrom, 29 (2014) 578 – 582.

[49] U. Mazurek, H. Schwarz, Chem Commun (2003) 1321 – 1326.

[50] G. K. Koyanagi, X. Zhao, V. Blagojevic, M. J. Y. Jarvis, D. K. Bohme, Int J Mass Spectrom, 241 (2005) 189 – 196.

[51] X. Zhao, G. K. Koyanagi, D. K. Bohme, J Phys Chem A, 110 (2006) 10607 – 10618.

[52] P. Redondo, A. Varela-Álvarez, V. M. Rayón, A. Largo, J. A. Sordo, C. Barrientos, J Phys Chem A, 117 (2013) 2932 – 2943.

[53] L. J. Moens, F. Vanhaecke, D. R. Bandura, V. I. Baranov, S. D. Tanner, J Anal At Spectrom, 16 (2001) 991 – 994.

[54] F. Vanhaecke, L. Balcaen, I. Deconinck, I. De Schrijver, C. M. Almeida, L. Moens, J Anal At Spectrom, 18 (2003) 1060 – 1065.

[55] N. Nonose, M. Ohata, T. Narukawa, A. Hioki, K. Chiba, J Anal At Spectrom, 24 (2009) 310 – 319.

[56] S. D'Ilio, N. Violante, C. Majorani, F. Petrucci, Anal Chim Acta, 698 (2011) 6 – 13.

CHAPTER 4

Determination of ultra-trace amounts of prosthesis-related metals in whole blood using volumetric absorptive micro-sampling and ICP-MS/MS

Adapted from Bolea-Fernandez et. al., Anal. Chim. Acta, 941 (2016) 1 - 9

4.1. Introduction

The most common and well-known method of sampling blood is venipuncture. However, if regular monitoring of a patient's blood is required or only limited amounts of blood can be taken, more straightforward ways of blood sampling would be helpful. The use of "dry sampling" approaches, such as the already widely used dried blood spot (DBS) method, and the more recently introduced volumetric absorptive micro-sampling (VAMS), are considered potential alternatives to overcome the problems related with the traditional venipuncture approach.**[1, 2]** These sampling methods offer inherent advantages, such as (i) minimally invasive collection of capillary blood *via* a finger or heel prick, (ii) improved sample conservation under ambient conditions due to the stabilizing effect of DBS and VAMS, and (iii) easier transport of the samples to the laboratory.**[3]** In a very short period of time, these benefits have drawn the attention of both the pharmaceutical and medical communities. The low amount of sample required in comparison with the venipuncture approach could be advantageous in animal studies during the early stage of drug discovery, and the simplicity of the procedure may facilitate unsupervised sample collection, thus reducing the number of mandatory visits to the doctor or hospital for those patients that need a regular follow-up. Nowadays, DBS sampling is widely used for many applications (e.g., neonatal screening,**[4, 5]** drug development,**[6]** pharmacokinetic studies,**[7]** medical diagnosis,**[8]** and toxicological **[9]** and forensic **[10]** studies). However, the use of DBS still suffers from a number of pitfalls that need to be addressed. Despite the development of several strategies for coping with the differences in hematocrit content (i.e. the fraction of red blood cells in the blood sample, expressed as the percentage of the total volume), this variability can still be considered as the most important factor hampering a wider application of DBS, as it influences viscosity and spreadability of blood spotted on filter paper.**[11-13]** In addition, issues related with difficulties for sample deposition and DBS formation, e.g., influence of the substrate, blood volume spotted and blood temperature, have been reported in literature too.**[14]** Recently, VAMS has been suggested as a promising alternative for the DBS method.**[15, 16]** The VAMS device consists of a holder on which an absorptive porous substrate is attached. This substrate takes up a fixed volume of blood when exposed to a liquid blood sample (see **Figure 4.1**). This sampler is designed to be simple and ergonomic, and resembles a pipette tip, which enables it to be integrated

into an automated sample preparation procedure. VAMS shares the benefits of DBS sampling in terms of easiness, sample stability, and transport efficiency, while in contrast to DBS, VAMS has been proven to overcome the issue of the variable HCT level.**[17-19]** However, VAMS is still in its infancy, and although some works reported on the successful use of VAMS for bioanalysis (especially in the context of drug analysis and pharmacokinetics),**[20-22]** to the best of the authors' knowledge no works to date have reported on the use of VAMS for subsequent (ultra-)trace element analysis in biofluids. We have evaluated the use of VAMS in the context of determination of prosthesis-related metals in whole blood.

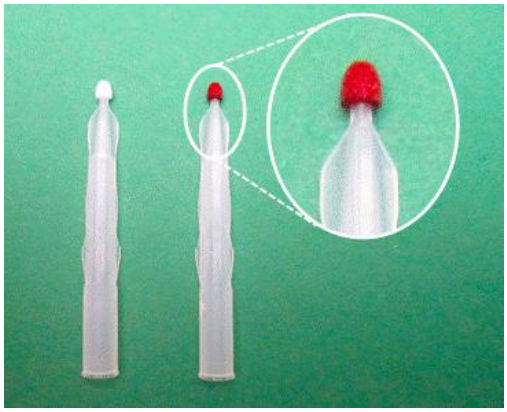

Figure 4.1. Volumetric absorptive micro-sampling (VAMS) device (Mitra™), before and after sampling blood.

The increasing use of metal-on-metal (MoM) prostheses has aroused serious concern about the elevated metal concentrations released in case of degradation and/or malfunction of these devices. Regular monitoring of the blood of implanted patients is required, which necessitates the development of efficient, fast and reliable analytical approaches for ultra-trace determination of various prosthesis-related metals (e.g., Al, Ti, V, Cr, Co, Ni, Sr and Zr) in biofluids.**[23-27]** Recent clinical works aiming to assess prosthesis-related problems reported concentrations of ~2 µg L^{-1} of Co and Cr in well-functioning devices, while concentrations as high as ~400 and 200 µg L^{-1} of Co and Cr, respectively, were reached in patients with clear malfunctions of their prosthesis. Although there are important knowledge gaps about the level of metal concentrations that should raise medical concern, and

there is not a clear consensus about critical values, in the case of Co and Cr, 7 μg L^{-1} was selected as the clinical action level that requires a follow-up of the patient's status.**[28, 29]** The use of dry approaches for sample collection may help in the periodic control of patients with reduced mobility. Dry sampling approaches also bring about specific challenges, such as the very low sample volume available, and the necessity to develop very sensitive (and preferably multi-element) analytical methodologies.**[30-33]**

Inductively coupled plasma-mass spectrometry (ICP-MS) is the technique of choice for the determination of (ultra-)trace concentrations of many elements in biological fluids owing to its low detection limits, multi-element capabilities, high sample throughput and low sample consumption. However, ICP-MS is strongly affected by the occurrence of spectral interference, i.e. overlap of the signals of the target analyte ions with those of other atomic (isobaric nuclides, doubly charged ions) or polyatomic ions with the same nominal mass-to-charge (m/z) ratio.**[34]** Thus, interference-free measurement of prosthesis-related metals is not self-evident for a blood sample, which contains many matrix elements at high concentrations (e.g., C, Ca, Cl, K, Mg, Na, P and S), while the levels of the analyte elements are often extremely low. The use of high resolution sector field ICP-MS (HR-SF-ICP-MS) is an elegant option to deal with spectral overlap, but the increase in mass resolution is also accompanied by a significant reduction in sensitivity (1 – 2 orders of magnitude).**[35, 36]** Alternately, quadrupole-based ICP-MS instruments equipped with a collision-reaction cell (ICP-CRC-QMS) can be used to separate analyte and interfering ions with the same m/z ratio *via* gas phase ion-molecule processes.**[37-40]** ICP – tandem mass spectrometry (ICP-MS/MS) is a powerful tool that should be capable to deal with these complex situations,**[41-43]** as it offers enhanced control over the reactions taking place in the cell, enabling the use of very reactive gases to monitor the target analytes as molecular reaction product ions at a mass-to-charge ratio that is free from interference.**[44-46]**

This study aimed at the development and evaluation of an analytical approach whereby VAMS is used for whole blood sampling, with subsequent ICP-MS/MS analysis for the determination of prosthesis-related metals at ultra-trace levels.

4.2. Experimental

4.2.1. Instrumentation

All measurements were carried out using an Agilent 8800 ICP-MS/MS instrument (ICP-QQQ, Agilent Technologies, Japan). The sample introduction system consisted of a MicroMist nebulizer (400 µL min^{-1}) mounted onto a Peltier-cooled (2 °C) Scott-type spray chamber. This instrument is equipped with two quadrupole units (Q1 and Q2) with an octopole collision/reaction cell system (ORS^3) located in-between. In this work, both quadrupoles were used as mass filters (MS/MS mode) and the cell was pressurized with a methyl fluoride/helium (CH_3F/He - 10:90) mixture as reaction gas. The mass flow controller can be adjusted from 0 to 100%, corresponding to gas flow rates of 0 to 1 mL min^{-1} (mass flow controller calibrated for O_2). The reaction product ions selected for both methods (100-fold dilution and VAMS) are indicated in **Table 4.1**.

A Thermo Element XR sector-field ICP-MS instrument (Thermo Scientific, Germany) was used for validation purposes for those target analytes for which reference values were not available (or in the case of suspected contamination). **Table 4.1** shows the instrument settings and data acquisition parameters for ICP-MS/MS and SF-ICP-MS measurements.

4.2.2. Samples and reagents

Only high-purity reagents were used throughout this work. Ultrapure water (resistivity > 18.2 MΩ.cm) was obtained using a Milli-Q element water purification system (Millipore, France). Pro-analysis 12 M HCl (ChemLab, Belgium) was further purified by sub-boiling distillation. 1 g/L single-element standard solutions of Al, Co, Cr, Ni, Sr, Ti, V and Zr (Instrument solutions, The Netherlands) were appropriately diluted and used for method development, validation and calibration purposes. External calibration was relied on for quantification, with Rh (Inorganic Ventures, The Netherlands) as an internal standard. Standards and samples were prepared in 0.3 M HCl. The VAMS devices (lot: 41106A) were obtained from Phenomenex (Torrance, USA) and are available under the brand name Mitra™. Such a sampling device consists of a hydrophilic polymer with an absorption volume of ~10 µL (10.5 µL for whole blood according to the instructions of the manufacturer). This absorption volume has been experimentally validated and the

Table 4.1. Instrument settings and data acquisition parameters for ICP-MS/MS and SF-ICP-MS measurements

Agilent 8800			Element XR	
	100-fold dilution method	**VAMS method**		**100-fold dilution method**
Reaction gas	CH_3F/He		Scan type	Escan
Scan type	MS/MS		Resolution	Medium m/Δm ≈ 4000
Plasma mode	Low matrix		RF power (W)	1200
RF power (W)	1550		Carrier gas flow rate (L min^{-1})	0.975
Carrier gas flow rate (L min^{-1})	1.11		Mass window (%)	125
Reaction gas flow rate (mL min^{-1}, MFC calibrated for O_2)	1.0		Search window (%)	50
Extract 1 (V)	-6.0		Integration window (%)	60
Q1 bias (V)	-1.0		Sample time (s)	0.01
Octopole bias (V)	-5.0		Samples / peak	20
Energy discrimination (V)	-8.0		Nuclides monitored	^{27}Al, ^{47}Ti,^{49}Ti, ^{51}V, ^{52}Cr, ^{53}Cr, ^{59}Co, ^{58}Ni, ^{60}Ni, ^{86}Sr, ^{87}Sr, ^{88}Sr, ^{90}Zr, ^{91}Zr,^{103}Rh
Extract 2 (V)	-195.0			
Q2 QP bias (V)	-13.0			
Q1 →Q2 masses	27 → 61	27 → 61		
	47 → 187	47 → 187		
	49 → 189	51 → 191	Total analysis time / sample (s)	142
	51 → 191	52 → 120		
	52 → 120	59 → 127		
	53 → 121	60 → 128		
	59 → 127	88 → 107		
	58 → 126	90 → 109		
	60 → 128	103 → 103		
	86 → 105			
	87 → 106			
	88 → 107			
	90 → 109			
	91 → 110			
	103 → 103			
Wait time offset (ms)	10			
Sweeps / replicate	100			
Integration time / mass (s)	1			
Replicates	10	5		
Total analysis time / sample (s)	150	45		

sampling reproducibility of these devices for blood collection has been systematically assessed under different circumstances by Denniff *et al.***[2]** Two blood reference materials, Seronorm Trace Elements Whole Blood Level 1 and Level 3 (Sero, Norway; Reference 210105 and 210305, respectively), with reference or indicative values for the elements targeted in this study, were analyzed for method validation purposes. In order to further evaluate the methods developed, spiking experiments were carried out with real venous blood taken from control patients at the University Hospital Miguel Servet (Zaragoza, Spain). The blood was collected in plastic tubes (BD Vacutainer, U.S.A.) containing EDTA as anti-coagulant.

4.2.3. Sample preparation

Seronorm Trace Elements Whole Blood Levels 1 and 3 reference materials are provided as a lyophilized material and were reconstituted in Milli-Q water following the instructions of the manufacturer. In addition to these reference materials, aliquots of 1 mL of real whole blood were spiked with small volumes of a multi-element solution in order to obtain added concentrations of 5, 10, 25 and 50 μg L^{-1} of the analyte elements. This concentration range was selected taking into account the critical concentration level for prosthesis-related metals in whole blood, and for evaluating the capabilities of VAMS at different levels. Both the reference materials (after reconstitution) and the real venous blood samples (with and without spiking) were subjected to the same sample preparation procedure. In this work, two different methods for sampling and analysis of blood were compared, i.e. (i) the direct measurement of the samples after appropriate dilution, and (ii) the use of VAMS for sample collection, followed by extraction and ICP-MS/MS analysis. In the first case, ~10 μL whole blood was diluted with ~1 mL Milli-Q water (in metal-free 15 mL polypropylene centrifuge tubes, VWR, Belgium) and subsequently acidified with 12 M HCl. HCl and HNO_3 were evaluated and higher contamination was observed in the case of HNO_3. Therefore, the use of HCl demonstrated to provide lower blanks and better LoDs. Rh (final concentration of 1 μg L^{-1}) was also added as an internal standard. The resulting 100-fold diluted solution (in 0.3 M HCl) was homogenized and centrifuged (Centrifuge 5702, Eppendorf AG, Germany) during 5 minutes at 4400 rpm. The supernatant was separated for subsequent ICP-MS-MS analysis to prevent possible nebulizer clogging.

For the VAMS approach, the sampler device was dipped into the sample for a couple of seconds (2-4 s; following the procedure described by the manufacturer). The VAMS device was subsequently dried under ambient conditions (>2 hours).

Thereafter, the absorption probe was removed from the sampler device and added into a metal-free polypropylene centrifuge tube. The analytes were extracted in approximately 1 mL of Milli-Q water with the aid of a vortex mixer (VWR, Belgium, 2 minutes). The solution thus obtained was acidified, as described earlier, and Rh was added as an internal standard. The final volume of 1 mL was considered as the minimum volume needed for ICP-MS measurement.

4.3. Results and discussion

4.3.1. Development of a multi-element ICP-MS/MS method for interference-free determination of (ultra-) trace amounts of prosthesis-related metals in whole blood

The determination of ultra-trace amounts of prosthesis-related metals in complex samples, such as whole blood, can be seriously hampered by the occurrence of spectral interferences from concomitant matrix elements (e.g., C, Ca, Cl, K, N, Na, Mg, P and S) present at high concentrations. Thus, the development of a multi-element method for the interference-free determination of Al, Co, Cr, Ni, Sr, Ti, V and Zr in whole blood is a challenging task. The use of ICP-MS/MS can provide interference-free conditions *via* reaction of the target analyte ions with a properly selected reaction gas, as a result of which they are converted into reaction product ions that can be measured interference-free at different m/z ratios (mass-shift). This approach has already been evaluated (and proven successful) for other applications and/or sample types.(Chapter 2)**[43, 44]** In this work, a CH_3F/He mixture was selected as reaction gas in ICP-MS/MS (Chapter 3, 5, 6, 7) **[45, 47-49]** and *via* product ion scanning (PIS) (at different flow rates of CH_3F/He within the range of 0 to 1 mL min^{-1}) the optimum reaction product ions, i.e. those giving the higher signal-to-background ratios, were identified. As the aim was to develop a multi-element method, compromise conditions were sought for and they were reached at the maximum gas flow rate (1 mL min^{-1}). Under these conditions, appropriate reaction product ions were selected for further use. In the case of Al,

Cr, Ni and Co, these reaction product ions resulted from molecular addition: $^{27}AlCH_3F^+$ (m/z = 61), $^{52,53}Cr(CH_3F)_2^+$ (m/z = 120, 121), $^{58,60}Ni(CH_3F)_2^+$ (m/z = 126, 128) and $^{59}Co(CH_3F)_2^+$ (m/z = 127). In the cases of Sr and Zr, the reaction product ions were formed *via* F atom transfer: $^{86,87,88}SrF^+$ (m/z = 105, 106, 107) and $^{90,91}ZrF^+$ (m/z = 109, 110). For Ti and V, finally, the reaction product ions were formed upon a combination of F atom transfer and multiple CH_3F addition: $^{47,49}TiF_2(CH_3F)_3^+$ (m/z = 187, 189) and $^{51}VF_2(CH_3F)_3^+$ (m/z =191). The reaction product ions selected were monitored in all subsequent method development and ICP-MS/MS analyses (instrumental parameters for ICP-MS/MS measurements are shown in **Table 4.1**) and the figures of merit obtained under these conditions are compiled in **Table 4.2**. It needs to be stressed that these LoDs and LoQs are purely instrumental LoDs/LoQs, such that the effect of sample pretreatment needs to be taken into account for assessing the final detection capabilities in the case of analysis of real samples (*vide infra*).

4.3.2. A simple dilute-and-shoot approach for the determination of (ultra-)trace amounts of prosthesis-related metals in whole blood

4.3.2.1. Results obtained for Seronorm Trace Elements Whole Blood L-1 and L-3

Seronorm Trace Elements Whole Blood L-1 and L-3 reference materials can be considered as representative for real venous blood samples, containing (ultra-)trace metal concentrations of the analyte elements in a similar matrix composition. The results obtained after a simple dilute-and-shoot approach, consisting of a 100-fold dilution of the reconstituted material, followed by ICP-MS/MS analysis, were evaluated. This dilution needs to be taken into account for assessing the LoDs and LoQs attainable (see **Table 4.2**). External calibration was used for quantification purposes, with Rh as an internal standard, to correct for matrix effects, instrument instability and signal drift. Several aliquots (n = 5) of both reference materials were analyzed.

The results are presented in **Table 4.3**, which shows the average result for 5 aliquots of both reference materials, each measurement consisting of 10 consecutive replicate measurements. The validation of the results obtained in this work was performed by comparison with reference or indicative values and results

obtained using SF-ICP-MS in the case of absence of reference values or in those cases possibly affected by contamination of the reference material (see **Table 4.1** for the instrumental parameters used in the SF-ICP-MS method).

Firstly, Seronorm Trace Elements Whole Blood L-3 was selected on the basis of the concentrations of the target analytes expected in whole blood of patients with increased concentrations owing to prosthesis-related problems. As can be seen, within the corresponding uncertainty, the results obtained using ICP-MS/MS are in agreement with the reference or indicative values reported by Seronorm, except for a minor difference in the case of both Ti isotopes (t-test, $t_{experimental}$ = 10.998 and 7.092 > $t_{critical}$ = 2.776, for ^{47}Ti and ^{49}Ti, respectively) and for a clear deviation in the case of ^{58}Ni (t-test, $t_{experimental}$ = 14.328 > $t_{critical}$ = 2.776), as indicated after statistical evaluation using a one-sample t-test at a level of confidence of 95%. For Zr, reference and/or indicative values were not available. In addition, no significant variation was noticed between the results obtained *via* ICP-MS/MS and SF-ICP-MS, respectively (except for ^{58}Ni), which further demonstrates the accuracy of the method developed for all target nuclides, including Ti and Zr. For ^{58}Ni, additional experiments with a solution containing Fe demonstrated that the results obtained using ICP-MS/MS were clearly affected by isobaric overlap of the signals of $^{58}Fe^{+}$ and $^{58}Ni^{+}$, as the reaction product ion $^{58}Fe(CH_3F)_2^{+}$ (m/z = 126) is formed in the case of whole blood samples due to the higher Fe content (343 mg L^{-1}) in comparison with serum samples (1.39 mg L^{-1} – Chaper 3). However, accurate Ni concentrations could be obtained using another isotope of Ni (e.g., ^{60}Ni).

In order to further evaluate the capabilities of the method developed under the most challenging conditions, Seronorm Trace Elements Whole Blood L-1, containing very low concentrations of the target elements, was analyzed as described above. The experimental results obtained using ICP-MS/MS are within the range of reference or indicative values in the case of Al, Ti, Co, ^{52}Cr and ^{60}Ni. The LoQ was not sufficiently low to allow for quantification of Cr *via* ^{53}Cr and isobaric overlap of the signal of ^{58}Ni with that of ^{58}Fe hindered the determination of Ni *via* this isotope.

A small discrepancy was found in the case of V (t-test, $t_{experimental}$ = 13.149 > $t_{critical}$ = 2.776), but the difference between experimental and indicative value can be considered negligible for the purpose of this work. Further validation of the ICP-MS/MS results by comparison with the SF-ICP-MS result was not possible for V

Table 4.2. Calibration data and instrumental limits of detection (LoD) and of quantification (LoQ) for the ICP-MS/MS method developed

Nuclide	Reaction product ion	Q1 (amu)	Q2 (amu)	Sensitivity[a] (L μg^{-1})	Intercept[a] (counts s^{-1})	R^2	LoD[b] (μg L^{-1})	LoQ[b] (μg L^{-1})	MDL[c] (μg L^{-1})	MQL[c] (μg L^{-1})
^{27}Al	$^{27}AlCH_3F^+$	27	61	5570 ± 50	3000 ± 86	0.997	0.02	0.06	2	6
^{47}Ti	$^{47}TiF_2(CH_3F)_3^+$	47	187	853 ± 14	80 ± 20	0.99994	0.02	0.06	2	6
^{49}Ti	$^{49}TiF_2(CH_3F)_3^+$	49	189	725 ± 15	50 ± 23	0.99990	0.03	0.09	3	9
^{51}V	$^{51}VF_2(CH_3F)_3^+$	51	191	20700 ± 120	40 ± 160	0.99998	0.0005	0.002	0.05	0.2
^{52}Cr	$^{52}Cr(CH_3F)_2^+$	52	120	6440 ± 28	80 ± 51	0.99997	0.003	0.008	0.3	0.8
^{53}Cr	$^{53}Cr(CH_3F)_2^+$	53	121	773 ± 18	60 ± 12	0.9998	0.02	0.08	2	8
^{58}Ni	$^{58}Ni(CH_3F)_2^+$	58	126	9230 ± 57	300 ± 88	0.99996	0.006	0.02	0.6	2
^{59}Co	$^{59}Co(CH_3F)_2^+$	59	127	34400 ± 120	200 ± 170	0.99998	0.0003	0.001	0.03	0.1
^{60}Ni	$^{60}Ni(CH_3F)_2^+$	60	128	3760 ± 37	100 ± 44	0.99998	0.003	0.009	0.3	0.9
^{86}Sr	$^{86}SrF^+$	86	105	15500 ± 96	96 ± 92	0.999996	0.0008	0.003	0.08	0.3
^{87}Sr	$^{87}SrF^+$	87	106	11300 ± 53	20 ± 83	0.99998	0.003	0.009	0.3	0.9
^{88}Sr	$^{88}SrF^+$	88	107	134000 ± 600	200 ± 670	0.999997	0.0005	0.002	0.05	0.2
^{90}Zr	$^{90}ZrF^+$	90	109	5990 ± 42	-20 ± 56	0.99997	0.006	0.02	0.6	2
^{91}Zr	$^{91}ZrF^+$	91	110	1304 ± 22	10 ± 25	0.99996	0.01	0.04	1	4

[a]Uncertainties expressed as standard deviation (n = 10).

[b]Instrumental LoDs and LoQs calculated as 3 and 10 times the standard deviation of 10 consecutive measurements of a blank solution (0.3 M HCl), divided by the slope of the calibration curve respectively.

[c]Method detection and quantification limits (MDL and MQL) correspond with the LoDs and LoQs after taking into account the 100-fold dilution of the sample.

due to the higher LoQ obtained *via* SF-ICP-MS, but for Sr and Zr, possible bias in the indicative results was revealed. We hypothesize that the discrepancy found in the case of Sr was related with a "typo" in the certificate of Seronorm Trace Elements Whole Blood Level 1, while for Zr, possible contamination issues may explain the difference between the experimentally obtained results and the indicative values. This hypothesis is also supported by cross-validation using different isotopes of the same element. Other inaccurate reference values have been reported in the literature for Seronorm samples (e.g., Se in Seronorm Trace Elements Serum L-2 **[50]**). These differences were hypothetically attributed to unknown factors causing variations between the batch measured and those originally prepared for evaluation and certification. Although at first sight the difference between the reference value and the ICP-MS/MS result seems quite large for Al, the ICP-MS/MS result is within the acceptable range indicated by the manufacturer, due to the high uncertainty accompanying the reference value. The positive bias may also be the result of possible Al contamination coming from the vial, as indicated by the manufacturer.

4.3.2.2. Results obtained for real venous blood samples

In order to further evaluate the method developed for the analysis of whole blood after a simple dilute-and-shoot approach, spiking experiments were carried out to simulate the condition of a prosthesis failure and the resulting increase in concentration of the target elements. Therefore, small amounts of a multi-element standard solution were added to 4 aliquots of a real blood sample to obtain spike concentrations of 5, 10, 25 and 50 μg L^{-1} of all the elements studied. The sample without spike ("blank blood" – containing concentrations below the LoQ for the elements targeted in this study) and the spiked samples were measured after 100-fold dilution following the procedure described in the previous section for the Seronorm reference materials; the results thus obtained are shown in **Figure 4.2**. The recoveries were calculated after subtracting the intensity for the "blank blood" sample from the intensity of the corresponding spiked sample. The results were within the range of 91% – 109%; 97% – 109%; 96% – 103% and 98% – 106% for spike concentrations of 5, 10, 25 and 50 μg L^{-1}, respectively. Generally speaking, the results obtained are in excellent agreement with the amounts added (within the typical acceptance criterion of a bias <15% for clinical QC analysis).**[51, 52]**

Table 4.3. Results obtained for Seronorm Trace Elements Whole Blood L-1 and L-3 using a simple dilute-and-shoot approach followed by ICP-MS/MS analysis in comparison with reference values and experimental SF-ICP-MS results

Nuclide	Seronorm Trace Elements Whole Blood Level 1			Seronorm Trace Elements Whole Blood Level 3		
	Reference value (µg L^{-1})	ICP-MS/MS[a] (µg L^{-1})	SF-ICP-MS[a] (µg L^{-1})	Reference value (µg L^{-1})	ICP-MS/MS[a] (µg L^{-1})	SF-ICP-MS[a] (µg L^{-1})
^{27}Al	9.20 ± 6.40	15.47 ± 1.12	< LoQ	105.00 ± 21.00	103.13 ± 6.52	103.18 ± 3.44
^{47}Ti	14.00 ± 2.00	16.45 ± 0.78	14.93 ± 1.56	12.80 ± 0.40	11.11 ± 0.34	11.36 ± 1.30
^{49}Ti	14.00 ± 2.00	16.14 ± 1.22	14.48 ± 1.66	12.80 ± 0.40	10.82 ± 0.63	10.89 ± 1.38
^{51}V	1.30 ± 0.20	0.87 ± 0.07	< LoQ	5.70 ± 1.10	5.75 ± 0.48	5.22 ± 0.72
^{52}Cr	0.86 ± 0.38	0.91 ± 0.19	< LoQ	23.20 ± 4.70	22.20 ± 0.96	21.55 ± 0.70
^{53}Cr	0.86 ± 0.38	< LoQ	< LoQ	23.20 ± 4.70	22.89 ± 1.49	21.82 ± 2.18
^{58}Ni	1.18 ± 0.48	12.92 ± 0.25	---[b]	12.60 ± 2.50	25.03 ± 1.94	---[b]
^{59}Co	0.16 ± 0.06	0.25 ± 0.10	< LoQ	11.40 ± 1.20	11.18 ±0.74	11.31 ± 0.87
^{60}Ni	1.18 ± 0.48	1.48 ± 0.49	< LoQ	12.60 ± 1.20	12.52 ±1.57	< LoQ
^{86}Sr	15.30 ± 1.10	36.78 ± 0.49	37.71 ± 1.00	15.00 ± 0.20	14.86 ± 1.05	14.54 ± 0.30
^{87}Sr	15.30 ± 1.10	36.60 ± 0.60	---[b]	15.00 ± 0.20	14.94 ± 1.08	---[b]
^{88}Sr	15.30 ± 1.10	36.78 ± 0.58	36.63 ± 1.61	15.00 ± 0.20	14.85 ± 1.08	15.38 ± 0.17
^{90}Zr	0.27 ± 0.03	5.44 ± 0.78	5.43 ± 0.96	---[c]	4.61 ± 0.86	4.55 ± 0.32
^{91}Zr	0.27 ± 0.03	5.59 ± 0.64	5.55 ± 1.02	---[c]	4.88 ± 0.79	4.73 ± 0.02

[a]Uncertainties expressed as standard deviation (n = 5).

[b]Not measured.

[c]Not available

Furthermore, no significant differences were found as a function of the spike concentration, which demonstrates the accuracy of the method developed at levels as low as 5 µg L^{-1}. The fact that, in the case of Ti, Cr, Sr and Zr, accurate results can be obtained, relying on different isotopes of the same element indicates that also isotope dilution could be used for calibration purposes, if necessary. As described before, the signals obtained for ^{58}Ni are affected by isobaric overlap with ^{58}Fe; nevertheless, the results for both Ni isotopes - in terms of spike recovery - are in good agreement. This finding supports the aforementioned hypothesis about spectral overlap of the signals of ^{58}Ni with ^{58}Fe. Also, special attention needs to be paid to the uncertainty of those measurements, and clearly, it can be seen that a higher standard deviation was found in the case of the low abundant Cr isotope (^{53}Cr), while better precisions were obtained for Co and V. These variations are related with the different sensitivities and detection capabilities of the method developed for the different target nuclides (see **Table 4.2**). Overall, the satisfactory results obtained using the simple dilute-and-shoot approach followed by ICP-MS/MS analysis suggest that it could be used in the case of a small sample volume, as obtained using VAMS.

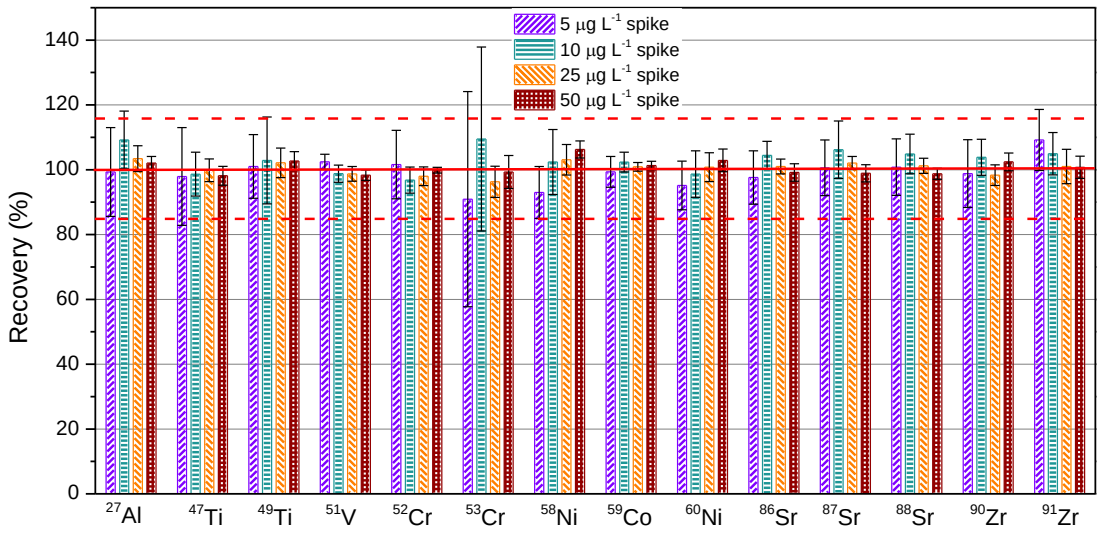

Figure 4.2. Recoveries obtained for the spiking experiments with real venous blood using a simple dilute-and-shoot approach. The error bars indicate the standard deviation of 10 consecutive measurement replicates. The solid and dashed red lines indicate 100% recovery and ±15% bias as clinical QC analysis criterion, respectively.

4.3.3. *Volumetric absorptive micro-sampling (VAMS) followed by ICP-MS/MS analysis for the determination of (ultra-) trace amounts of prosthesis-related metals in whole blood*

Once the ICP-MS/MS method was successfully developed and validated using whole blood reference materials and real samples (spiking experiments), the capabilities and limitations of VAMS were evaluated in the context of ultra-trace determination of prosthesis-related metals in whole blood. Therefore, special attention was paid to (i) the optimization of a procedure to extract the blood from the VAMS devices, and (ii) the reduction of the total sample volume needed for analysis (as only ~ 10 µL of whole blood is retained in the VAMS sampling devices). For the extraction of blood from the VAMS, a simple extraction method, allowing one to obtain accurate results without compromising the sample throughput, was aimed at. The samples were extracted from the VAMS devices with ~1 mL of Milli-Q water, followed by addition of Rh as an internal standard and subsequent acidification with HCl (25 µL of 12 M HCl). After centrifugation, the supernatant was subjected to ICP-MS/MS analyses. Thus, the blood sample was diluted ~100-fold, resulting in a final volume of 1 mL (0.3 M HCl and 1 µg L^{-1} of Rh). For measuring the VAMS samples, the method was adapted to lower measurement times due to the low volume available, and thus, only 1 isotope per element (that leading to accurate results with the lowest LoQ possible) was monitored, while 5 measurement replicates were selected (see **Table 4.1**).

4.3.3.1. VAMS contamination

An important issue when measuring ultra-trace concentrations is to control the level of contamination introduced during sample collection and/or preparation. In this method, metal-free material and high-purity reagents were used, and sample preparation steps were reduced to the minimum. However, contamination originating from the sampler device cannot be excluded, and therefore, a careful evaluation of the level of the target elements extracted from blank VAMS devices was required. Five blank VAMS devices were subjected to the complete sample preparation procedure, and the resulting solutions were analyzed *via* ICP-MS/MS. The corresponding results are shown in **Table 4.4**, which provides the average and the standard deviation (n = 5) for Al, Ti, V, Cr, Co, Ni, Sr and Zr in blank VAMS

devices, also taking into account the 100-fold dilution. The results for Ti, V, Co and Sr show very low contamination levels, below the LoQ in the case of Ti, V and Co, thus the measurement of these elements using VAMS should not be affected to a large extent by contamination issues. In the case of Zr, the concentration was considered relatively high for a "blank" device. As however the contamination seems to remain constant within the different VAMS devices, blank subtraction still provided accurate results. However, the situation is different in the case of Cr, Ni and Al. The high levels of Al and Ni could be tentatively explained by the introduction of those elements during the manufacturing, as the absorptive probe is stated to be made of a hydrophilic polyolefin, which may involve the use of Al and Ni catalysts for the polymerization process. Consequently, Al, Cr and Ni could not be measured accurately using the VAMS approach and these 3 target analytes were not taken into account in further experiments with the VAMS devices. Further investigation is required in order to improve the manufacturing process of the VAMS devices and/or to develop cleaning steps under controlled conditions prior to the sampling, thus avoiding contamination.

Table 4.4. Results obtained for blank VAMS devices

Isotope	ICP-MS/MS[a] (µg L^{-1})	ICP-MS/MS x 100[b] (µg L^{-1})
^{27}Al	33 ± 12	3300 ± 1200
^{47}Ti	< LoQ	< LoQ
^{51}V	< LoQ	< LoQ
^{52}Cr	0.30 ± 0.11	30 ± 11
^{59}Co	< LoQ	< LoQ
^{60}Ni	4.9 ± 3.9	490 ± 390
^{88}Sr	0.02 ± 0.01	1.7 ± 0.8
^{90}Zr	0.11 ± 0.01	11 ± 1

[a]Uncertainties expressed as standard deviation (n = 5).

[b]Concentration after taking into account the 100-fold dilution. Uncertainties expressed as standard deviation (n = 5).

4.3.3.2. Results obtained for Seronorm Trace Elements Whole Blood L-1 and L-3 using VAMS followed by ICP-MS/MS analysis

The capabilities and limitations of the VAMS approach in the case of prosthesis-related metals in whole blood were also evaluated by measuring the reference materials Seronorm Trace Elements Whole Blood Level 1 and Level 3. **Table 4.5** shows the average concentrations obtained for 3 replicate analyses (reference material sampled with 3 different VAMS devices) for both reference materials (every analysis consisting of 5 consecutive measurements). The average and standard deviation of 3 different analyses may provide an idea on the variability due to contamination issues. Blank VAMS were also analyzed every measurement session in order to assess contamination. The results obtained using VAMS followed by ICP-MS/MS analysis were compared to the recommended values, i.e. the reference/indicative values provided by the manufacturer or the results of the measurements using SF-ICP-MS in the case of absence of reference values, possible contamination, or suspect reference values (as indicated in section 4.3.2.1). As can be seen, the experimental results are within the recommended range in all cases. However, although no significant differences were found for Co in the Level 1 material (t-test, $t_{experimental} = 2.706 < t_{critical} = 4.303$), high uncertainty was observed, which needs to be attributed to the low amount of Co in the reference material. Under such conditions, the small contribution of contamination becomes more important due to the closeness of the concentration level to the LoQ, which probably indicates the limitation of the method developed. However, concentrations below 1 μg L^{-1} can be considered as normal levels in whole blood and do not indicate any metal release. In addition, the VAMS-based method only shows slight differences in precision compared to the simple dilute-and-shoot approach, except in the case of Zr, for which the deviation seems to be higher as a consequence of the contamination described in the previous section and indicated in **Table 4.4**.

4.3.3.3. Results obtained for real venous blood samples using VAMS followed by ICP-MS/MS analysis

Aiming at a further evaluation of the method developed using VAMS followed by ICP-MS/MS analysis, the same spiked real venous blood samples as analyzed in section 4.3.2.2 (5, 10, 25 and 50 μg L^{-1} of the target elements selected for this method) were also measured following the VAMS approach.

Table 4.5. Results obtained for Seronorm Trace Elements Whole Blood L-1 and L-3 using the VAMS approach followed by ICP-MS/MS analysis compared to recommended values

	VAMS Seronorm L-1		VAMS Seronorm L-3	
Isotope	**Recommended value[a] (µg L^{-1})**	**ICP-MS/MS[b] (µg L^{-1})**	**Recommended value[a] (µg L^{-1})**	**ICP-MS/MS[b] (µg L^{-1})**
^{47}Ti	14.00 ± 2.00	16.46 ± 2.46	12.80 ± 0.40	12.88 ± 1.36
^{51}V	1.30 ± 0.20	0.92 ± 0.24	5.70 ± 1.10	5.61 ± 0.39
^{59}Co	0.16 ± 0.06	0.89 ± 0.62	11.40 ± 1.20	10.82 ±0.48
^{88}Sr	36.63 ± 1.61*	38.82 ± 1.40	15.00 ± 0.20	14.59 ± 0.56
^{90}Zr	5.43 ± 0.96*	5.20 ± 2.64	4.55 ± 0.32*	4.90 ± 1.01

[a]Reference values provided by the manufactures or experimental results determined using SF-ICP-MS (*).

[b]Uncertainties expressed as standard deviation (n = 3).

Three replicate analyses were performed for every spiked sample. The results are shown in **Figure 4.3**, which represents the recoveries resulting after subtracting the contribution from the "blank" real venous blood. The precision (indicated as error bars in **Figure 4.3**) corresponds with the standard deviation of 3 replicate analyses for every sample (3 VAMS devices). As can be seen, within the experimental uncertainty, no significant differences were found between the results obtained using the VAMS approach followed by ICP-MS/MS analysis and the expected results (bias <15% as clinical QC analysis criterion). The accuracy and precision improved with the increase in concentration, which is clearly related with possible slight contamination of the VAMS devices and/or introduced during the sample preparation steps, although the closeness to the LoQ cannot be excluded as possible source of uncertainty. For samples containing 25 and 50 µg L^{-1} spikes, the results are accurate and precise for all target nuclides, without significant differences compared to the simple dilute-and-shoot approach. In addition, for Co and V, the results are not even affected at lower concentration levels, which can be related with the lower contamination in the VAMS devices and the better LoQ for both target elements. In the case of Ti and Zr, higher uncertainty was obtained for lower concentrations, i.e. 5 and 10 µg L^{-1}, which is in good agreement with the

results obtained for the analysis of the reference materials following the same procedure, and definitively seems to point to the relatively high contamination, already described in section 4.3.3.1 for Zr. However, based on the accuracy and precision of the results obtained for all elements at the different concentration levels of the spike, it may be assumed that the VAMS approach could be used for sampling of whole blood with the aim of diagnosing failing prostheses based on increased metal levels in the patient's blood.

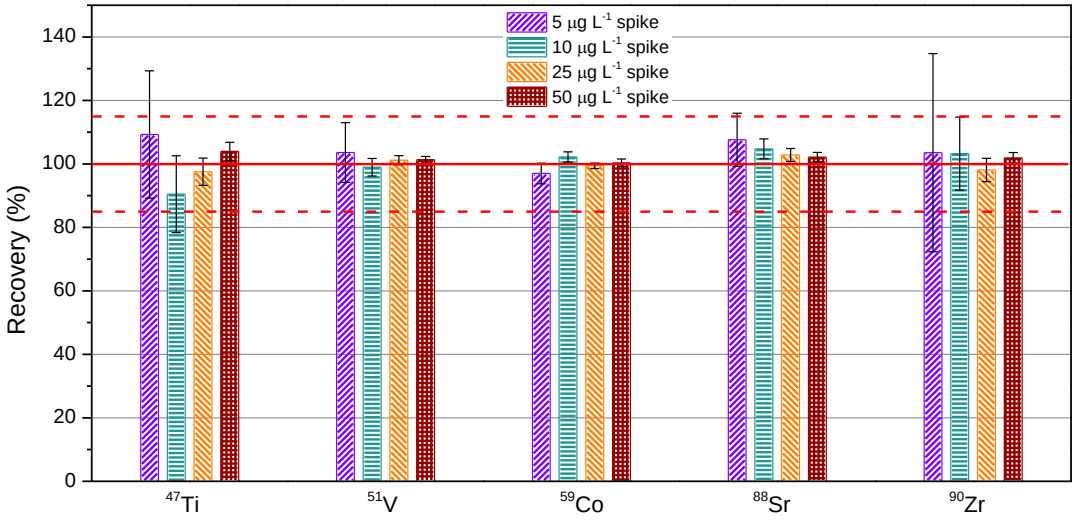

Figure 4.3. Recoveries obtained for the spiking experiments with real venous blood using the VAMS approach. The error bars indicate the standard deviation of 3 replicate analyses. The solid and dashed red lines indicate 100% recovery and ±15% bias as clinical QC analysis criterion, respectively.

4.4. Conclusion

In this work, the capabilities and limitations of a novel volumetric absorptive micro-sampling (VAMS) approach combined with tandem ICP – mass spectrometry for the determination of (ultra-)trace amounts of prosthesis-related metals in whole blood were evaluated. Firstly, a method enabling the simultaneous and interference-free measurement of ^{27}Al, $^{47,49}Ti$, ^{51}V, $^{52,53}Cr$, ^{59}Co, ^{60}Ni, $^{86,87,88}Sr$ and $^{90,91}Zr$ was developed, relying on chemical resolution (mass-shift approach) using CH_3F/He in

the CRC of an ICP-MS/MS instrument, with attainable (instrumental) LoDs ranging from 0.3 to 30 ng L^{-1}. Subsequently, a simple dilute-and-shoot approach (100-fold dilution of the samples – ICP-MS/MS analysis with external calibration and Rh as internal standard), was successfully applied to the analysis of two reference materials (Seronorm Trace Elements Whole Blood Level 1 and Level 3) and to that of spiked real venous blood samples with different spike concentrations (in the range of 5 to 50 µg L^{-1}). In the last stage, it was evaluated whether the method developed can be combined with VAMS as an alternative sample collection approach. Except for the elements inherently affected by the contamination of such devices, i.e. Al, Cr and Ni, VAMS was demonstrated to be suitable in the context of the determination of (ultra-)trace concentrations of the selected elements in whole blood. The possibility to successfully determine ultra-trace amounts of metals in such small sample volumes is owing to the high detection power and multi-element capabilities and the creation of interference-free conditions using chemical resolution in an MS/MS approach of ICP-MS. Future efforts have to aim at the development of metal-free devices when aiming at determining such low concentration levels for the analytes currently affected by contamination. To the best of the authors' knowledge, this is the first work in which VAMS is studied as a sampling approach for whole blood with the aim of (ultra-)trace element determination, and the potential suitability of this approach for future real life and/or routine applications has been demonstrated.

Acknowledgments

The authors thank Prof. Dr. C. Stove and Prof. Dr. A. Verstraete for introducing us to VAMS. Dr. Luis Rello is also thanked for the samples. MR acknowledges the funding from CTQ2015-64684-P (MINECO/FEDER) and from the Aragón Government (Fondo Social Europeo). FV acknowledges funding from the Ghent University Special Research Fund (BOF-UGent).

References

[1] P.A. Demirev, Anal Chem, 85 (2013) 779 - 789.

[2] P. Denniff, N. Spooner, Anal Chem, 86 (2014) 8489 - 8495.

[3] T.W. McDade, S. Williams, J.J. Snodgrass, Demography, 44 (2007) 899 - 925.

[4] R. Guthrie, A. Susi, Pediatrics, 32 (1963) 338 -343.

[5] J.J. Pitt, Clin. Biochem Rev, 31 (2010) 57 - 68.

[6] P. Edelbroek, J. van der Heijden, L.M.L. Stolk, Ther Drug Monit, 31 (2009) 327 - 336.

[7] P. Beaudette, K.P. Bateman, J Chromatogr, B: Anal Technol Biomed Life Sci, 809 (2004) 153 - 158.

[8] M. Resano, M. Aramendía, L. Rello, M.L. Calvo, S. Bérail, C. Pécheyran, J Anal At Spectrom, 28 (2013) 98 - 106.

[9] C.P. Stove, A.-S.M.E. Ingels, P.M.M. De Kesel, W.E. Lambert, Crit Rev Toxicol, 42 (2012) 230 - 243.

[10] M. Resano, L. Rello, E. García-Ruiz, M.A. Belarra, J Anal. At Spectrom, 22 (2007) 1250 - 1259.

[11] P. Denniff, N. Spooner, Bioanalysis, 2 (2010) 1385 - 1395.

[12] N. Youhnovski, A. Bergeron, M. Furtado, F. Garofolo, Rapid Commun Mass Spectrom, 25 (2011) 2951 - 2958.

[13] P.M.M. De Kesel, S. Capiau, V.V. Stove, W.E. Lambert, C.P. Stove, Anal Bioanal Chem, 406 (2014) 6749 - 6755.

[14] N. Spooner, R. Lad, M. Barfield, Anal Chem, 81 (2009) 1557 - 1563.

[15] N. Spooner, P. Denniff, L. Michielsen, R. De Vries, Q.C. Ji, M.E. Arnold, K. Woods, E.J. Woolf, Y. Xu, V. Boutet, P. Zane, S. Kushon, J.B. Rudge, Bioanalysis, 7 (2015) 653 - 659.

[16] Y. Luo, W. Korfmacher, S. Ho, L. Shen, J. Wang, Z. Wu, Y. Guo, G. Snow, T. O'Shea, Bioanalysis, 7 (2015) 2345 - 2359.

[17] P.M.M. De Kesel, S. Capiau, W.E. Lambert, C.P. Stove, Bioanalysis, 6 (2014) 1871 - 1874.

[18] P.M.M. De Kesel, W.E. Lambert, C.P. Stove, Anal Chim Acta, 881 (2015) 65 - 73.

[19] Y. Mano, K. Kita, K. Kusano, Bioanalysis, 7 (2015) 1821 - 1829.

[20] P. Denniff, S. Parry, W. Dopson, N. Spooner, J Pharma Biomed Anal, 108 (2015) 61 - 69.

[21] L. Mercolini, M. Protti, M.C. Catapano, J. Rudge, A.E. Sberna, J Pharma Biomed Anal, 123 (2016) 186 - 194.

[22] Z. Miao, J.G. Farnham, G. Hanson, T. Podoll, M.J. Reid, Bioanalysis, 7 (2015) 2071 - 2083.

[23] A. Sarmiento-González, J.M. Marchante-Gayón, J.M. Tejerina-Lobo, J. Paz-Jiménez, A. Sanz-Medel, Anal Bioanal Chem, 391 (2008) 2583 - 2589.

[24] L. Rello, A.C. Lapeña, M. Aramendía, M.A. Belarra, M. Resano, Spectrochim Acta Part B, 81 (2013) 11 - 19.

[25] G. Ring, J. O'Mullane, A. O'Riordan, A. Furey, Clin Biochem, 49 (2016) 617 - 635.

[26] J.J. Jacobs, A.K. Skipor, P.A. Campbell, N.J. Hallab, R.M. Urban, H.C. Amstutz, J Arthroplasty, 19 (2004) 59 - 65.

[27] M.S. Patton, T.D.B. Lyon, G.P. Ashcroft, Acta Orthop, 79 (2008) 820 - 825.

[28] B. Sampson, A. Hart, Ann Clin Biochem, 49 (2012) 118 - 131.

[29] O. Lainiala, A. Reito, P. Elo, J. Pajamäki, T. Puolakka, A. Eskelinen, Clin Orthop Relat Res, 473 (2015) 2305 - 2313.

[30] P. Abu-Rabie, P. Denniff, N. Spooner, J. Brynjolffssen, P. Galluzzo, G. Sanders, Anal Chem, 83 (2011) 8779 - 8786.

[31] P. Abu-Rabie, Bioanalysis, 3 (2011) 1675 - 1678.

[32] M. Aramendía, L. Rello, F. Vanhaecke, M. Resano, Anal Chem, 84 (2012) 8682 - 8690.

[33] M. Aramendía, L. Rello, S. Bérail, A. Donnard, C. Pécheyran, M. Resano, J Anal At Spectrom, 30 (2015) 296 - 309.

[34] R.F.J. Dams, J. Goossens, L. Moens, Mikrochim Acta, 119 (1995) 277 - 286.

[35] L. Moens, N. Jakubowski, Anal Chem, 70 (1998) 251A - 256A.

[36] N. Jakubowski, L. Moens, F. Vanhaecke, Spectrochim Acta, Part B, 53 (1998) 1739 - 1763.

[37] D.J. Douglas, Can J Spectrosc, 34 (1989) 38 - 49.

[38] S.D. Tanner, V.I. Baranov, At Spectrosc, 20 (1999).

[39] S.D. Tanner, V.I. Baranov, D.R. Bandura, Spectrochim Acta, Part B, 57 (2002) 1361 - 1452.

[40] V.I. Baranov, S.D. Tanner, J Anal At Spectrom, 14 (1999) 1133 - 1142.

[41] S. Diez Fernández, N. Sugishama, J.R. Encinar, A. Sanz-Medel, Anal Chem, 84 (2012) 5851 - 5857.

[42] L. Balcaen, G. Woods, M. Resano, F. Vanhaecke, J Anal At Spectrom, 28 (2013) 33 - 39.

[43] L. Balcaen, E. Bolea-Fernandez, M. Resano, F. Vanhaecke, Anal Chim Acta, 894 (2015) 7 - 19.

[44] L. Balcaen, E. Bolea-Fernandez, M. Resano, F. Vanhaecke, Anal Chim Acta, 809 (2014) 1 - 8.

[45] E. Bolea-Fernandez, L. Balcaen, M. Resano, F. Vanhaecke, Anal Chem, 86 (2014) 7969 - 7977.

[46] N. Sugiyama, Y. Shikamori, J Anal At Spectrom, 30 (2015) 2481 - 2487.

[47] E. Bolea-Fernandez, L. Balcaen, M. Resano, F. Vanhaecke, Anal Bioanal Chem, 407 (2015) 919 - 929.

[48] E. Bolea-Fernandez, L. Balcaen, M. Resano, F. Vanhaecke, J Anal At Spectrom, 31 (2016) 303 - 310.

[49] E. Bolea-Fernandez, S.J.M.V. Malderen, L. Balcaen, M. Resano, F. Vanhaecke, J Anal At Spectrom, 31 (2016) 464- 472.

[50] A. Townsend, A. Featherstone, C.C. Chéry, F. Vanhaecke, J. Kirby, F. Krikowa, B. Maher, G. Jacobson, G. Peterson, Clin Chem, 50 (2004) 1481 - 1482.

[51] V.P. Shah, K.K. Midha, J.W.A. Findlay, H.M. Hill, J.D. Hulse, I.J. McGilveray, G. McKay, K.J. Miller, R.N. Patnaik, M.L. Powell, A. Tonelli, C.T. Viswanathan, A. Yacobi, Pharmaceu Res, 17 (2000) 1551 - 1557.

[52] G. Tiwari, R. Tiwari, Pharm Methods, 1 (2010) 25 - 38.

CHAPTER 5

Interference-free determination of ultra-trace concentrations of As and Se using CH_3F as reaction gas in ICP-MS/MS

Adapted from Bolea-Fernandez et. al., Anal. Bioanal. Chem., 407 (2015) 919 – 929

5.1. Introduction

The determination of ultra-trace concentrations of As and Se in a large variety of samples has been the objective of numerous studies during many years. Arsenic is a toxic element that has been classified in Category 1 by the International Agency for Research on Cancer (IARC), which means that it is carcinogenic for humans.**[1]** Selenium is one of the minor elements that, due to its presence in several proteins and enzymes, is essential for biological processes. However, already at concentrations slightly higher than optimum, it becomes toxic to humans.**[2]** In addition, the antagonistic metabolic effect between As and Se **[3]** has been typically used to reduce As poisoning effects, and different As-related diseases are linked with Se deficiency.**[4-6]** For this reason, and although the toxicity and/or beneficial effects of these elements strongly depend(s) on the chemical form,**[7-10]** the determination of the total concentration of As and Se gives invaluable and fast information concerning the associated risks.**[11]** As a result, analysis of biological and environmental samples for their As and/or Se content(s) is of interest from a biomedical point of view. However, the determination of these metalloids at ultra-trace levels is not simple by means of any atomic spectroscopy technique.**[12-16]** Inductively coupled plasma - mass spectrometry (ICP-MS) can be considered as the technique of choice for the monitoring of these elements. However, despite its detection power, the determination of As and Se by ICP-MS is seriously hampered by the occurrence of both spectral and non-spectral interferences.**[17]**

Matrix effects (non-spectral interferences **[18]**) are more pronounced for As and Se than for many other elements, due to their high ionization energy (9.81 eV and 9.75 eV, respectively), and the so-called "*carbon effect*", which means that a high amount of carbon, dissolved in the sample or admixed into the ICP, leads to a signal enhancement for both As and Se. Although this effect has been widely described in the literature,**[19-21]** there is no clear consensus concerning the mechanism responsible for it. The carbon effect is hypothesized to result from charge transfer between C^+ or CH^+ (ionization energy 11.26 eV and 10.64 eV, respectively)**[22,23]** to atoms of elements with a high ionization energy. However, other characteristics need to be involved, because not for all elements with a high ionization energy, such an enhancement is observed. In addition, extremely high amounts of carbon could

also result in a signal intensity decrease due to a reduction of the plasma temperature.

Non-spectral interferences **[24,25]** can be tackled in different ways (e.g., use of a suitable internal standard,**[26]** or quantification by means of standard addition,**[27]** or by means of isotope dilution **[28-31]**), but the issue of spectral interferences remains a serious one, due to the formation of Ar-based polyatomic ions **[32,33]** that affect the determination of $^{75}As^+$ ($^{40}Ar^{35}Cl^+$ and $^{38}Ar^{37}Cl^+$) and $^{77,78,80}Se^+$ ($^{40}Ar^{36}Ar^1H^+$, $^{40}Ar^{37}Cl^+$, $^{40}Ar^{38}Ar^+$ and $^{40}Ar^{40}Ar^+$). While in the case of Se, ^{82}Se can often be monitored interference-free, no such possibility exists for the mono-isotopic As.

Different options have been explored to overcome the influence of these interferences, such as the use of analyte/matrix separation (which obviously represents additional work and degrades sample throughput),**[34]** of mathematical equations (which may not work efficiently if the ratio between the signal of the interferent and that of the analyte is too high),**[35]** of cool plasma conditions (which results in a significant drop in sensitivity for these elements owing to their poor ionization efficiency under such working conditions),**[36]** and, of vapor generation systems (the use of which also involves some additional sample pretreatment).**[37]**

Additionally, more advanced ICP-MS devices permit these spectral interferences to be overcome in a more straightforward way. The use of a sector-field ICP-MS (SF-ICP-MS) instrument, operated at higher mass resolution, is an elegant choice to resolve spectral interferences.**[38]** However, the maximum resolution setting ($m/\Delta m$ ~ 10,000) should be used in the case of As and Se, which involves a reduction in sensitivity of about two orders of magnitude, which is sometimes too much for the targeted concentrations. Also, and even using the maximum resolution setting, some polyatomic interferences still cannot be completely resolved (e.g., interference-free measurement of $^{80}Se^+$ is hard to accomplish due to the very high intensity of the $^{40}Ar_2^+$ dimer).

The most widespread approach to deal with the spectral overlap affecting the determination of As and Se nowadays is probably the use of a quadrupole based ICP-MS (Q-ICP-MS) instrument equipped with a collision/reaction cell.**[39]** Different gases can be used to pressurize the cell and ameliorate the conditions for As and/or Se determination. For instance, the combination of a collision gas **[40]** (typically He) and kinetic energy discrimination can be used to reduce the interferences as, due to

their larger size, polyatomic ions lose a larger fraction of their kinetic energy than do mono-atomic ions. However, this strategy is incapable of removing doubly charged interferences and is accompanied by a substantial reduction in sensitivity. Also, reactive gases (e.g., NH_3, H_2, CH_4, O_2) can be used to selectively react with the interfering ions,**[41-43]** aiming at the monitoring of the analyte ions at their original mass-to-charge ratio. Alternately, also a selective reaction between the analyte ions and the gas molecules,**[44,45]** resulting in the formation of a reaction product ion that can be measured interference-free at another m/z ratio, is sometimes viable. The efficacy of the latter approach strongly depends on the efficiency and rate of the reaction involved.

Recently, a new configuration of Q-ICP-MS instrumentation was introduced, the so-called triple quadrupole ICP-MS/MS **[46-49]** setup, which consists of a tandem mass spectrometer with an octopole collision/reaction cell located in-between two quadrupole mass analyzers. This new configuration enables the application of non-typical, but highly reactive gases.

Methyl fluoride is a reaction gas that has only been used scarcely in ICP-MS before.**[50,51]** However, in a previous work (Chapter 3),**[49]** we have demonstrated the possibilities of this reaction gas to resolve spectral overlap in the determination of light metals (Al, Co, Cr, Mn, Ni, Ti and V) in clinical samples using ICP-MS/MS. The main goal of the current project was to investigate the potential of methyl fluoride as a reaction gas in ICP-MS/MS for dealing with the interferences affecting ultra-trace determination of both As and Se in diverse sample types.

5.2. Experimental

5.2.1. Instrumentation

All measurements were carried out using an Agilent 8800 triple quadrupole ICP-MS/MS instrument (Agilent Technologies, Japan). The sample introduction system comprises a MicroMist nebulizer (400 µL/min) and a Peltier-cooled Scott-type spray chamber (2 °C). The instrument is equipped with two quadrupole mass analyzers (Q1 and Q2) and an octopole collision/reaction cell (ORS^3) mounted in-between the two quadrupole units (Q1 - ORS^3 - Q2). The instrument can be used in different operation modes, (i) with the first quadrupole fully open (single quadrupole mode,

SQ) or (ii) using both quadrupoles as mass filters (MS/MS mode). The cell can be pressurized with different inert or reactive gases, typically He, H_2, O_2 and NH_3, but in this work, the merits of CH_3F (a mixture of 10% CH_3F and 90% He) were evaluated. The CH_3F/He mixture was introduced *via* the 4th line (typically used for O_2) and with the flow controller calibrated for this gas. As a result, the flow rates given below are expressed in O_2-equivalent mL min^{-1}.

A Thermo Element XR sector-field ICP-MS instrument (ThermoScientific, Germany) was used with the aim of comparing the capabilities of both techniques for ultra-trace determination of As and Se.

5.2.2. Reagents and standards

Only high purity reagents were used during all of the experiments. Water was purified using a Milli-Q Element water purification system (Millipore, France). Pro-analysis 14 M HNO_3 (ChemLab, Belgium) was further purified via sub-boiling distillation. Ultra-pure 28 M HF (Fisher Chemicals, Great Britain) and 9.8 M H_2O_2 (Fluka, Belgium) were chosen for sample digestion. Trace select 25 M MeOH for studying the carbon effect was acquired from Sigma Aldrich, Germany. Throughout the work, appropriate dilutions of 1 g L^{-1} single-element standard solutions (Instrument Solutions, The Netherlands) were carried out for optimization (As and Se), for internal standardization (Te), for external calibration (standard solutions with concentrations of 0, 0.5, 1, 2.5 and 5 µg L^{-1} of As and Se) and for matrix-matching (Ca, Cl, Gd, Mo, Nb, Nd, Ru, Sm, Y, Zr).

5.2.3. Samples

Reference materials were analyzed for method validation purposes. The list comprises NIST SRM 1515 (Apple Leaves), NBS SRM 1575 (Pine Needles), NBS SRM 1573 (Tomato Leaves), NIST SRM 1568a (Rice Flour), BCR CRM 526 (Tuna Fish Tissue), NCR - CNRC DORM-4 (Fish Protein), BCR CRM 414 (Plankton), NBS SRM 1646 (Estuarine Sediment), NIST SRM 1566a (Oyster Tissue) and NRC-CNRC TORT-3 (Lobster Hepatopancreas).

5.2.4. Sample preparation

To avoid contamination, only metal-free tubes were used for standard and sample preparation (15 or 50 mL polypropylene centrifuge tubes, VWR, Belgium). The

samples were digested *via* acid digestion in Teflon Savillex beakers, which had been pre-cleaned with HNO_3 and HCl and subsequently rinsed with Milli-Q water. To complete the mineralization, between 0.1 and 0.2 g of the respective reference materials (except for the apple leaves reference material, for which 0.5 g was digested due to the low concentration of both As and Se) were digested with 4 mL of 14 M HNO_3 and 1 mL of 9.8 M H_2O_2 and, only in the case of NBS SRM 1646 (Estuarine Sediment), an additional 1 mL of 28 M HF. The procedure was completed after heating at 110 °C on a hot plate overnight.

Prior to ICP-MS/MS analysis, the digested materials were diluted 40- and 20-fold for As and Se, respectively, with Milli-Q water.

The final results were calculated on a dry mass basis, taking into account the water content of the reference materials, previously calculated after drying until constant weight.

5.3. Results and discussion

As discussed in the introduction, the determination of ultra-trace levels of As and Se using ICP-MS is still a challenge. Different problems are encountered when addressing determination of ultra-trace concentrations of these elements, and there is no straightforward method to deal with all the problems encountered without sacrificing some analytical properties. The objective of this work was to investigate the capabilities of ICP-MS/MS with CH_3F/He as a reaction gas in this context.

5.3.1. Selection of the main product ions formed upon reaction between As and Se and CH_3F/He

In order to study the reactions between CH_3F/He and As and Se, product ion scanning was used to identify the main reaction products. Standard solutions of 5 µg L^{-1} of As and of Se were measured using different CH_3F/He flow rates to find the most suitable reaction product ions, in terms of sensitivity and limits of detection (LoDs). Due to the mono-isotopic character of As, the mass-to-charge ratio of the first quadrupole was fixed at 75, while for Se, an m/z setting of 80 was selected because this is the most abundant nuclide. The results are summarized in **Figure 5.1**.

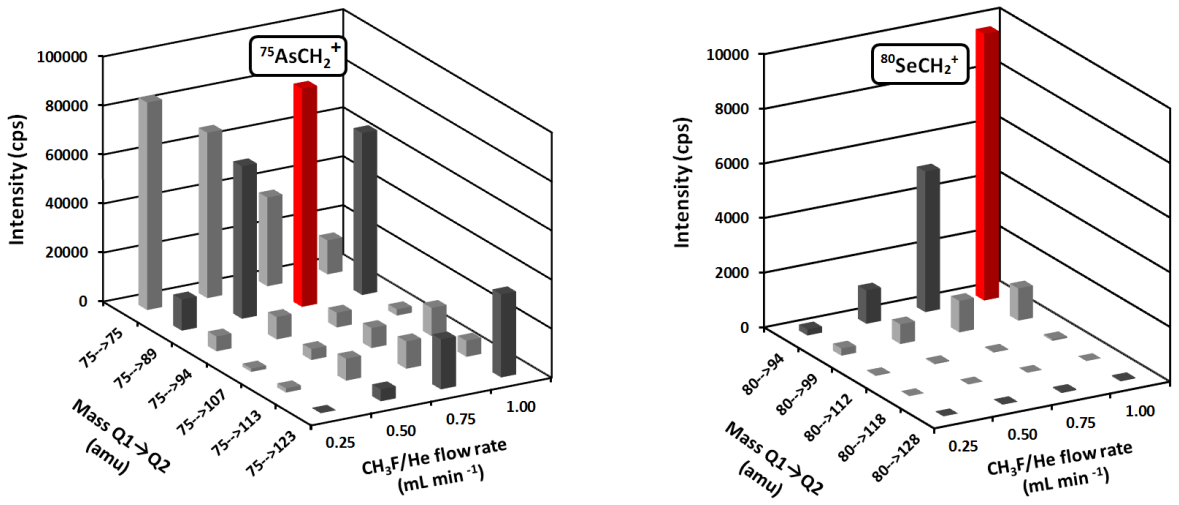

Figure 5.1. Identification of the different species formed at different CH_3F/He flow rate settings *via* product ion scanning. The main reaction product ions are highlighted in red.

In both cases, it is clear that a single product ion shows the highest sensitivity; for both As and Se, there is a selective and efficient reaction with CH_3F/He, consisting of CH_3F addition and subsequent HF elimination, resulting in the formation of $AsCH_2^+$ and $SeCH_2^+$. This reaction was studied in a previous work using ICP-SIFT-MS,**[52]** where the same behavior was found for As, but not for Se. With ICP-SIFT-MS, no reaction was seen to take place between Se and CH_3F, which indicates that some differences in reactivity can occur when other types of devices are used. **Figure 5.1** also provides valuable information concerning the optimum CH_3F/He flow rate settings. For As, the $AsCH_2^+$ signal intensity reaches a maximum at approximately 0.75 mL min^{-1} and then decreases, while the maximum sensitivity for Se is obtained at the highest flow rate setting attainable. It can be assumed that the use of higher flow rates could increase the $SeCH_2^+$ signal sensitivity even further. In any case, these reaction product ions seem promising to develop interference-free methods for As and Se determination in complex matrices using the MS/MS mode, and they were selected for further work. A schematic representation of the ICP-MS/MS operation using CH_3F/He for As and Se is shown in **Figure 5.2**.

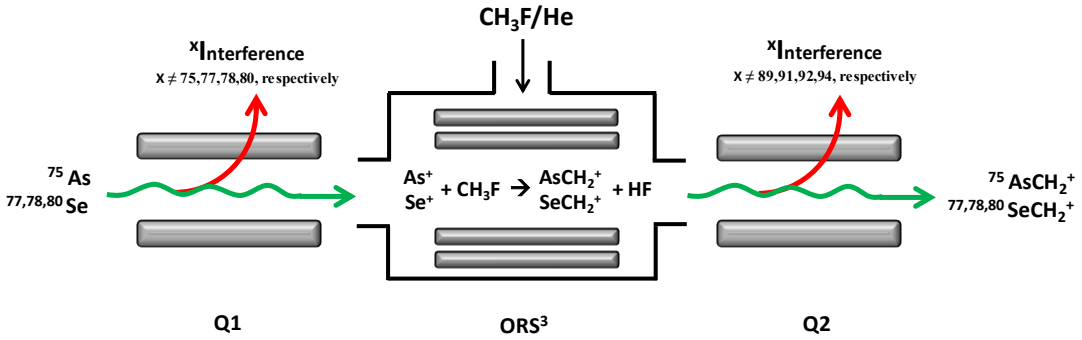

Figure 5.2. Schematic representation of ICP-MS/MS operation in the determination of As or Se using CH_3F/He as reaction gas.

5.3.2. Method development and optimum instrumental parameters for $AsCH_2^+$ and $SeCH_2^+$ monitoring

Once the most suited reaction product ions were identified, the corresponding analytical methods were developed. To further optimize the CH_3F/He flow rate settings, the signal intensity of a standard solution containing 5 μg L^{-1} of As and of Se, and a blank solution (0.14 M HNO_3) were measured at different flow rates, adjusting the first quadrupole for transition of the mass of the target nuclide (75 and 80 for ^{75}As and ^{80}Se, respectively) and the second for transmission of the mass of the selected reaction product ion (89 and 94 for $^{75}AsCH_2^+$ and $^{80}SeCH_2^+$, respectively). The results obtained are shown in **Figure 5.3**, indicating an optimum CH_3F/He flow rate setting of 0.72 (range between 0.60 - 0.80 mL min^{-1}) and 1.00 mL min^{-1} for $^{75}AsCH_2^+$ and $^{80}SeCH_2^+$, respectively. As previously said, it can be hypothesized that at an even higher CH_3F/He flow rate, the results for Se could even be better.

Despite of this limitation, the two methods were fully optimized, resulting in the instrument parameters summarized in **Table 5.1**. Under the optimum conditions for each of the target elements, a set of standard solutions (concentrations of 0, 0.5, 1, 2.5 and 5 μg L^{-1}) were measured 10 consecutive times, in order to obtain the calibration data and the instrumental limits of detection and of quantification (LoDs and LoQs were calculated as 3 and 10 times s_{blank}/slope, respectively).

The results are given for ^{75}As and for three different nuclides of Se (^{77}Se, ^{78}Se and ^{80}Se) in **Table 5.2**.

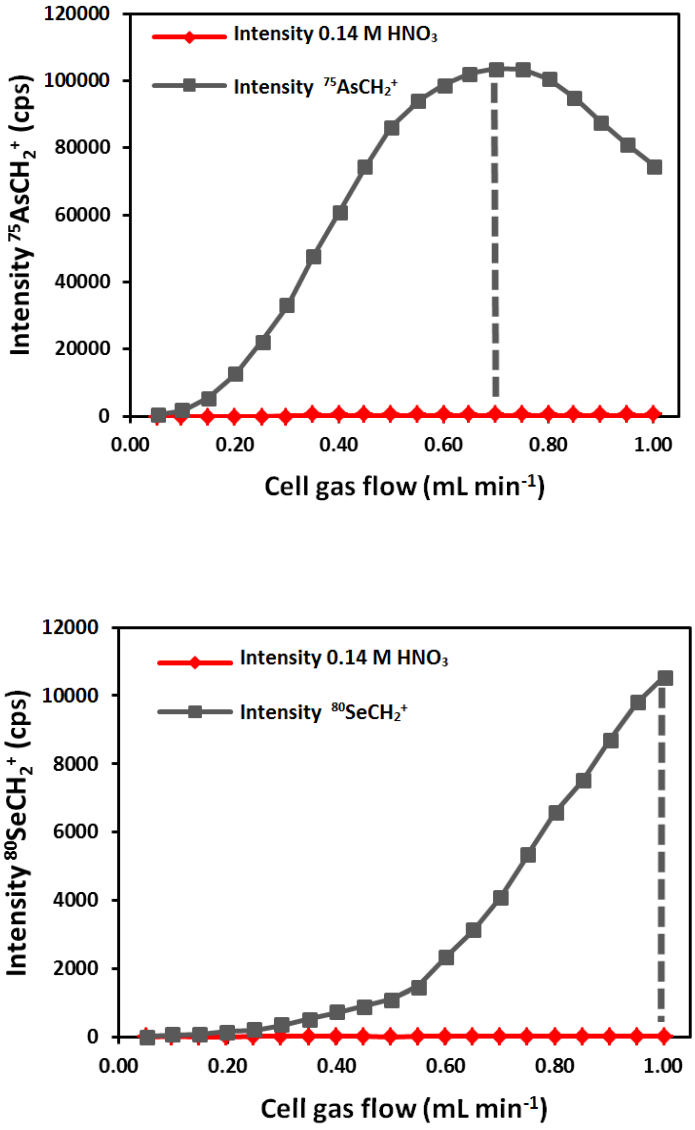

Figure 5.3. Selection of CH_3F/He flow rate settings for the selected species ($^{75}AsCH_2^+$ and $^{80}SeCH_2^+$).

Table 5.1. Instrument settings for the Agilent 8800 ICP-MS/MS instrument

Agilent 8800		
	As	**Se**
Reaction Gas	CH_3F/He	CH_3F/He
Scan type	MS/MS	MS/MS
Plasma mode	Low matrix	Low matrix
RF power (W)	1550	1550
Extract 1 (V)	-3.0	-3.9
Q1 bias (V)	-2.0	-1.0
Reaction gas flow rate setting (mL min^{-1})	0.72	1.00
Q1 → Q2	75 → 89 125 → 125	77 → 91 78 → 92 80 → 94 125 → 125
Octopole bias (V)	-4.1	-4.1
Energy discrimination (V)	-8.4	-8.4
Extract 2 (V)	-185.0	-195.0
Q2 QP bias (V)	-12.5	-12.5
Wait time offset (ms)	2	2
Sweeps / replicate	100	100
Integration time / mass (s)	1	1
Replicates	10	10
Total analysis time / sample (s)	38	65

These nuclides were selected in view of the strong Ar-based polyatomic interferences they suffer from and thus, to further prove the robustness of the methods developed. From the data in **Table 5.2**, it is possible to appreciate the difference in sensitivity between As and Se, which cannot be due to the mono-isotopic character of As only, but probably also to the higher efficiency of the reaction between CH_3F/He and As. However, excellent instrumental LoDs that are

suitable for analysis of real samples were obtained in all cases: 0.2 ng L^{-1} for As as $^{75}AsCH_2^+$ and below 10 ng L^{-1} for Se as $^{77,78,80}SeCH_2^+$. It needs to be stressed that these are instrumental LoDs, so procedural blanks and sample dilution need to be taken into account for the final LoDs.

5.3.3. Signal intensity enhancement: addition of C and surplus addition of He

Different approaches known to enhance the signal intensity for a variety of analytes were tested in this work. Due to their high ionization energy, As and Se are poorly ionized in the plasma. As described in the introduction, high amounts of carbon can give rise to a substantial increase in the As and Se signal intensities because of the carbon effect. While on one hand, the situation can complicate quantification and necessitates matrix-matching of the external standards or the method of standard additions, it is also frequently used to improve the sensitivity. With the aim of evaluating this possibility, different amounts of MeOH (between 0 and 10%) were added to both the As and Se standards (5 µg L^{-1}). The results are shown in **Figure 5.4**. A signal enhancement is observed in both cases with increasing MeOH-concentration, reaching a maximum when between 4% and 8% of MeOH is added. This leads to, approximately, a 2- and 2.5-fold improvement for As and Se, respectively. A further increase of the MeOH-concentration in the samples leads to a decrease in the signal intensity for both elements. However, from **Figure 5.4**, it can also be seen that the signal-to-background ratios and thus, also the LoDs, were actually deteriorated by the use of MeOH, probably because of the impurities present in the solvent. For this reason, admixing MeOH was not further considered.

Table 5.2. Calibration data and instrumental limits of detection (LoD) and of quantification (LoQ) obtained for Arsenic and Selenium using methyl fluoride as reaction gas in ICP-MS/MS

Isotope	CH_3F/He flow (mL min^{-1})	Q1 (amu)	Q2 (amu)	Sensitivity[a] (L.μg^{-1})	Intercept[a] (counts.s^{-1})	R^2	LoD[b] ($\mu g.L^{-1}$)	LoQ[b] ($\mu g.L^{-1}$)
^{75}As	0.72	75	89	18160 ± 250	-90 ± 100	0.999994	0.0002	0.0007
^{77}Se		77	91	286 ± 9	2 ± 11	0.99998	0.01	0.04
^{78}Se	1.00	78	92	917 ± 20	7 ± 13	0.99998	0.007	0.02
^{80}Se		80	94	1944 ± 25	-2 ± 21	0.99997	0.004	0.01

[a]Uncertainties expressed as standard deviation (n = 10)

[b]LoDs and LoQs calculated as 3 and 10 times the standard deviation on 10 consecutive measurements of a blank solution (0.14 M HNO_3), divided by the slope of the calibration curve, respectively.

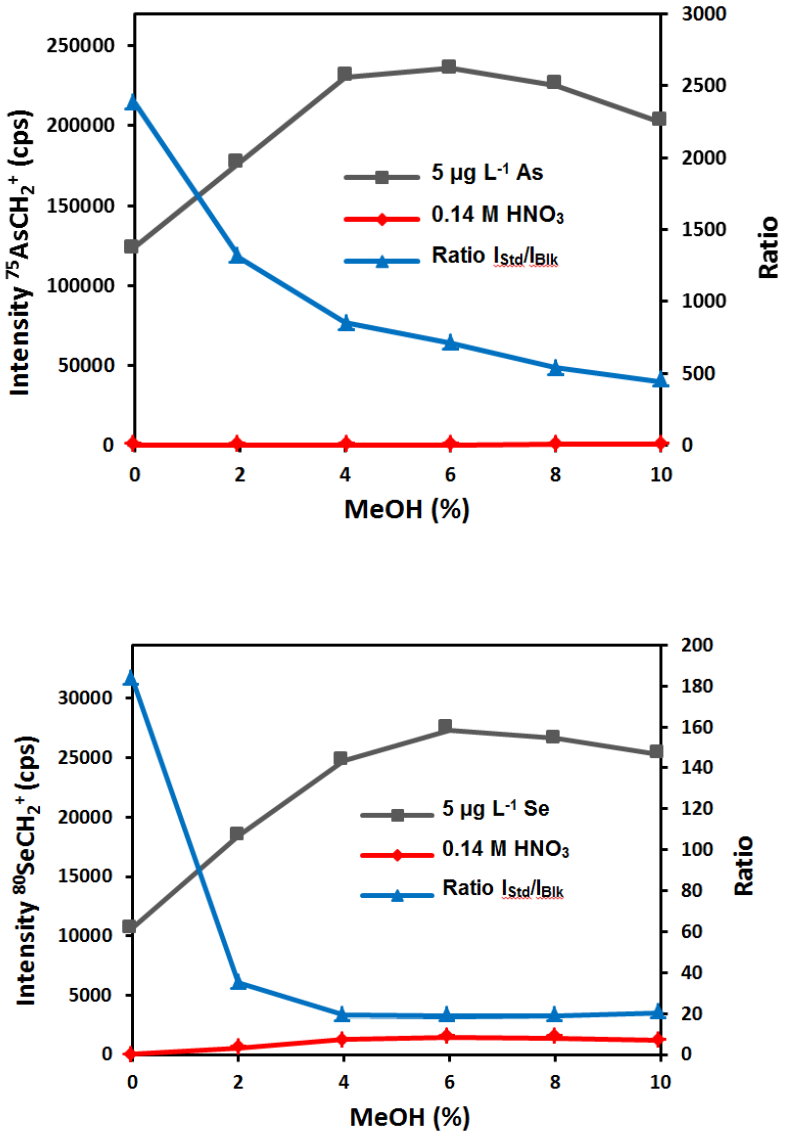

Figure 5.4. Signal enhancement produced by the addition of different amounts of MeOH *("carbon effect").*

Another experiment was conducted to investigate whether the addition of a supplemental He flow in the octopole collision/reaction cell (introduced *via* another line) could affect the reaction between CH_3F/He and the target analytes. This turned out to be the case for As. The results of this experiment are presented in **Figure 5.5**, which shows the signal intensity for 5 µg L^{-1} of As at different CH_3F/He

flow rate settings (range 0.10 - 1.00 mL min^{-1}) while the cell was also pressurized with surplus He (range 0 - 5 mL min^{-1}).

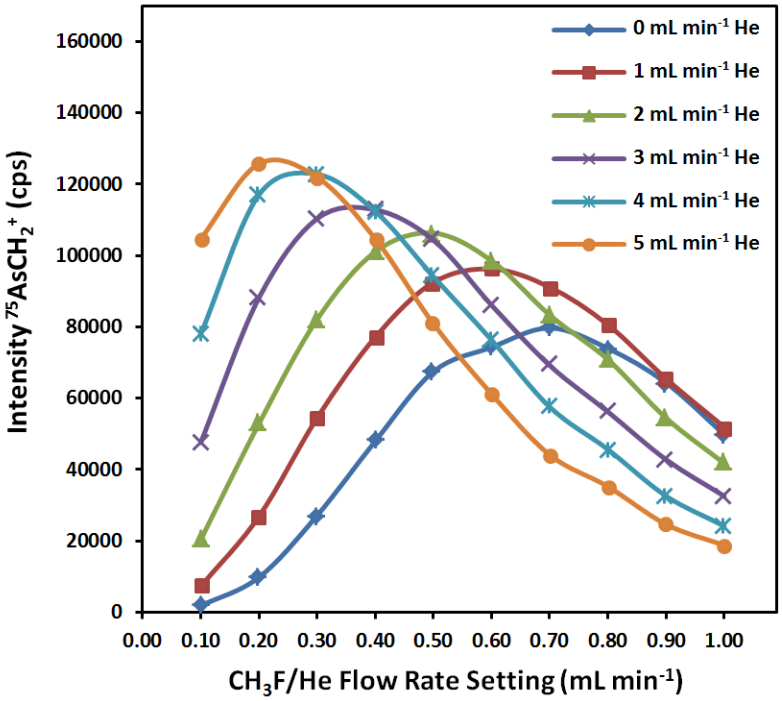

Figure 5.5. Signal enhancement produced by the addition of surplus He in the reaction of As with CH_3F/He to form $AsCH_2^+$

It can be clearly seen that a higher supplemental He flow shifts the maximum signal intensity for $^{75}AsCH_2^+$ towards lower CH_3F/He flow rates. Moreover, the net sensitivity is increased up to 3-fold, if the CH_3F/He flow rate is reduced from 0.72 to 0.20 mL min^{-1} and the He flow rate is increased from 0 to 5 mL min^{-1}. These results demonstrate that He plays an important role in the reaction between As and CH_3F. It can be hypothesized that the presence of more He slows down the As^+ ions, resulting in collisional stabilization, which improves the efficiency of the reaction between As and CH_3F. This behavior has already been mentioned in the literature for reactions between other elements and CH_3F.**[52]** The same behavior was not observed in the case of Se, for which the addition of a supplemental He flow resulted in a decreased of the signal intensity that could not be compensated with a reduction in the CH_3F/He flow rate, as was the case for As. It seems that for Se, the CH_3F/He flow rate was not high enough to observe the same phenomenon, perhaps

due to the instrumental restriction in the CH_3F/He flow rate to 1.00 mL min^{-1} and the differences in reaction efficiency, as discussed before. However, it was observed that the signal-to-background ratio also deteriorated when He was added, which in turn led to degraded LoDs. Therefore, use of an additional He flow was disregarded for further work.

5.3.4. Comparison with other cell gases

In order to better assess the potential of CH_3F/He as a reaction gas for As and Se determination, alternative cell conditions were evaluated ("vented mode", addition of He only, and addition of O_2), using both the single quadrupole mode (SQ) and the MS/MS-mode. Moreover, an SF-ICP-MS device operated in high-resolution mode was used to compare the capabilities of both techniques. The instrument settings for all the methods are provided in **Table 5.3** and **Table 5.4** for ICP-MS/MS and SF-ICP-MS, respectively.

To summarize all the data obtained, the instrumental LoDs observed under different conditions are shown in **Table 5.5**. Additionally, all the calibration data are presented in **Table 5.6**. Attention should be paid to the fact that this information is partial, because the instrumental LoDs reported are not affected by spectral interference due to the absence of the parent elements at the origin of interfering species (basically, Cl) for ^{75}As and ^{77}Se. For ^{78}Se and ^{80}Se, the overlap with $^{38}Ar^{40}Ar^{+}$ and $^{40}Ar_2^{+}$, respectively, is always affecting the signals irrespective of the matrix considered. Despite this, **Table 5.5** provides valuable information concerning the instrumental possibilities of the various methods.

Generally speaking, the use of MS/MS involves a reduction in sensitivity, which means that, for samples without spectral interferences, the SQ mode should provide a higher signal intensity.

Table 5.3. Instrument settings for the Agilent 8800 ICP-MS/MS instrument using different collision-reaction cell conditions.

	As							
	"Vented mode"		**He**		**O_2**		**CH_3F/He**	
Scan type	SQ	MS/MS	SQ	MS/MS	SQ	MS/MS	SQ	MS/MS
RF power (W)	1550	1550	1550	1550	1550	1550	1550	1550
Extract 1 (V)	0.0	0.0	0.0	0.0	0.0	0.0	-3.0	-3.0
Reaction gas flow rate setting (mL min^{-1})	---	---	4.00	4.00	0.30	0.30	0.72	0.72
Q1 → Q2	75	75 → 75	75	75 →75	91	75 → 91	89	75 → 89
Octopole bias (V)	-8.0	-8.0	-18.0	-18.0	-5.0	-5.0	-4.1	-4.1
Energy discrimination (V)	5.0	5.0	5.0	5.0	-7.0	-7.0	-8.4	-8.4
Extract 2 (V)	-180.0	-180.0	-180.0	-180.0	-170.0	-170.0	-185.0	-185.0
Wait time offset (ms)	0	0	0	0	2	2	2	2
Sweeps / replicate	100	100	100	100	100	100	100	100
Integration time / mass (s)	1	1	1	1	1	1	1	1
Replicates	10	10	10	10	10	10	10	10
Total analysis time / sample (s)[a]	37	37	37	37	38	38	38	38

Continued on the next page

Continued from the previous page

	Se							
	"Vented mode"		**He**		**O_2**		**CH_3F/He**	
Scan type	SQ	MS/MS	SQ	MS/MS	SQ	MS/MS	SQ	MS/MS
RF power (W)	1550	1550	1550	1550	1550	1550	1550	1550
Extract 1 (V)	0.0	0.0	0.0	0.0	0.0	0.0	-3.9	-3.9
Reaction gas flow rate setting (mL min^{-1})	---	---	4.00	4.00	0.30	0.30	1.00	1.00
Q1 → Q2	77	77 → 77	77 78	77 →77 78 → 78	93 94 96	77 → 93 78 → 94 80 → 96	91 92 94	77 → 91 78 → 92 80 → 94
Octopole bias (V)	-8.0	-8.0	-18.0	-18.0	-5.0	-5.0	-4.1	-4.1
Energy discrimination (V)	5.0	5.0	5.0	5.0	-7.0	-7.0	-8.4	-8.4
Extract 2 (V)	-180.0	-180.0	-180.0	-180.0	-170.0	-170.0	-195.0	-195.0
Wait time offset (ms)	0	0	0	0	2	2	2	2
Sweeps / replicate	100	100	100	100	100	100	100	100
Integration time / mass (s)	1	1	1	1	1	1	1	1
Replicates	10	10	10	10	10	10	10	10
Total analysis time / sample (s)[a]	37	37	49	49	65	65	65	65

[a]Te (as the selected internal standard) is considered for the total analysis time / sample

Table 5.4. Instrument settings for the Thermo Element XR SF-ICP-MS instrument

Element XR	
Scan type	EScan
Resolution	High (R= 10,000)
RF power (W)	1200
Carrier gas flow rate (L min^{-1})	0.975
Mass window (%)	100
Search window (%)	70
Integration window (%)	60
Nuclides monitored	^{75}As, ^{77}Se, ^{78}Se, ^{125}Te
Sample time (s)	0.01
Samples/peak	20
Total analysis time / sample (s)[a]	117

The differences in overall ion transmission efficiency between both modes could be most easily observed when the cell was used in "vented mode" or pressurized with He, because in these cases, Q1 and Q2 were set at the same mass (see **Table 5.6**). This was not the case with O_2 and CH_3F, because in these cases, Q1 is set to the mass of the target nuclide itself and Q2 to that of the corresponding reaction product ion. Under these conditions, both the reaction efficiency and the overall ion transmission efficiency govern the signal intensity. However, the LoD is also determined by the blank level at the mass of the reaction product ion, such that the LoDs when O_2 or CH_3F was used to avoid spectral overlap turned out to be better with double mass selection (MS/MS mode).

When O_2 was selected, the LoD for ^{80}Se was higher than that for ^{78}Se, despite the higher abundance of the former nuclide. The efficiency of the reaction of As and Se with O_2 is lower than that with CH_3F/He, as can be seen from the sensitivity of both methods, presented in **Table 5.6**. Additionally, the signal stability for Se was substantially deteriorated (RSD >10%) when using O_2. A final comparison between

the three pressurized cell options (He, O_2 and CH_3F/He) used to enable interference-free determinations of As and Se indicates that the use of the novel method, using CH_3F/He and the MS/MS mode, provides improved LoDs for both As and Se in all cases.

Table 5.5. Comparison of instrumental limits of detection for As and Se obtained *via* ICP-MS/MS (using different collision-reaction cell conditions) and *via* SF-ICP-MS

		Limits of detection (ng L^{-1})[a]			
ICP-MS/MS Cell conditions	**Scan type**	**^{75}As**	**^{77}Se**	**^{78}Se**	**^{80}Se**
"Vented mode"	SQ[b]	0.8	30	---[c]	---[c]
	MS/MS	0.9	50	---[c]	---[c]
He	SQ	1	20	40	----[c]
	MS/MS	2	40	60	---[c]
O_2	SQ	9	500	200	30
	MS/MS	7	500	9	30
CH_3F/He	SQ	1	200	20	10
	MS/MS	0.2	10	7	4
SF-ICP-MS	EScan[d]	10	50	500	---[c]

[a]LoDs calculated as 3 times the standard deviation on 10 consecutive measurements of a blank solution (0.14 M HNO_3), divided by the slope of the calibration curve

[b]SQ stands for single quadrupole mode

[c]Not measured (Ar-based interference was not resolved)

[d]The high resolution setting (R ~ 10,000) was used for all As and Se measurements

Table 5.6. Calibration data obtained for As and Se *via* ICP-MS/MS (using different collision-reaction cell conditions) and *via* SF-ICP-MS

Isotope	Agilent 8800							Thermo Element XR		
	Cell conditions	Scan type	Q1 (amu)	Q2 (amu)	Sensitivity[a] (L.µg^{-1})	Intercept[a] (counts.s^{-1})	R^2	Sensitivity[a] (L.µg^{-1})	Intercept[a] (counts.s^{-1})	R^2
^{75}As	"*Vented mode*"	SQ	---	75	55080 ± 420	-410 ± 360	0.999997	824 ± 18	13 ± 12	0.99996
		MS/MS	75	75	28120 ± 73	133 ± 80	0.999992			
	He	SQ	---	75	11920 ± 95	218 ± 71	0.99997			
		MS/MS	75	75	3914 ± 40	-11 ± 37	0.999997			
	O_2	SQ	---	91	13010 ± 370	650 ± 260	0.99998			
		MS/MS	75	91	7250 ± 170	290 ± 190	0.99998			
	CH_3F/He	SQ	--	89	34710 ± 580	-20 ± 170	0.99998			
		MS/MS	75	89	18160 ± 250	-90 ± 100	0.999994			
^{77}Se	"*Vented mode*"	SQ	---	77	4495 ± 56	1090 ± 210	0.99998	67 ± 5	2 ± 5	0.9999
		MS/MS	77	77	2702 ± 29	660 ± 120	0.99998			
	He	SQ	---	77	492 ± 13	11 ± 11	0.99998			
		MS/MS	77	77	300 ± 8	-0.4 ± 13	0.99995			
	O_2	SQ	---	93	153 ± 5	240 ± 14	0.998			
		MS/MS	77	93	71 ± 5	34 ± 12	0.9990			
	CH_3F/He	SQ	---	91	728 ± 26	3146 ± 72	0.9996			
		MS/MS	77	91	286 ± 10	3 ± 11	0.99998			

Continued on the next page

Continued from the previous page

^{78}Se	"*Vented mode*"	SQ	---	78	---[b]	---[b]	---[b]	223 ± 8	28 ± 17	0.9993
		MS/MS	78	78	---[b]	---[b]	---[b]			
	He	SQ	---	78	1631 ± 16	139 ± 24	0.99998			
		MS/MS	78	78	997 ± 22	99 ± 23	0.999991			
	O_2	SQ	---	94	405 ± 13	357 ± 16	0.9997			
		MS/MS	78	94	226 ± 8	4 ± 27	0.99995			
	CH_3F/He	SQ	---	92	1945 ± 20	317 ± 43	0.9997			
		MS/MS	78	92	917 ± 20	7 ± 13	0.99998			
^{80}Se	"*Vented mode*"	SQ	---	80	---[b]	---[b]	---[b]	---[b]		
		MS/MS	80	80	---[b]	---[b]	---[b]			
	He	SQ	--	80	---[b]	---[b]	---[b]			
		MS/MS	80	80	---[b]	---[b]	---[b]			
	O_2	SQ	---	96	856 ± 25	123 ± 38	0.99998			
		MS/MS	80	96	478 ± 13	54 ± 22	0.99996			
	CH_3F/He	SQ	---	94	4075 ± 30	175 ± 33	0.99997			
		MS/MS	80	94	1944 ± 25	-2 ± 22	0.99997			

[a]Uncertainties expressed as standard deviation (n = 10)

[b]Not measured: the $^{38}Ar^{40}Ar^+$ and $^{40}Ar^{40}Ar^+$ signals, were not fully resolved from the analyte signal

When comparing the figures of merit thus obtained with those obtained using SF-ICP-MS, the ICP-MS/MS approach with CH_3F/He as a reaction gas shows an improvement in the LoDs by a factor of 50, 5 and 100 for ^{75}As and $^{77,78}Se$, respectively, while the accurate monitoring of ^{80}Se is not feasible using SF-ICP-MS.

In addition, the LoDs obtained in this work using CH_3F/He in ICP-MS/MS were compared with those obtained using different setups as reported in the literature. This information is shown in **Table 5.7**, from which it can be seen that the ICP-MS/MS LoDs are superior to those obtained using SF-ICP-MS or other type of Q-ICP-MS instrumentation equipped with a collision-reaction cell.

Table 5.7. Comparison of ICP-MS/MS LoDs with those reported in the literature for other ICP-MS setups

Authors	Instrumentation	Mode	LoDs (ng L^{-1})			
			^{75}As	^{77}Se	^{78}Se	^{80}Se
A. T. Townsend et al. [38]	SF-ICP-MS	High mass resolution	95	170	---	---
J. J. Sloth [53]	Q-ICP-MS	CH_4 in quadrupole-based collision/reaction cell	---	---	---	6
C. C. Chéry et al. [54]	Q-ICP-MS	CO in quadrupole-based collision/reaction cell	---	250	---	10
J. Frank et al. [55]	SF-ICP-MS	High mass resolution	3	---	---	---
J. Darrouzès et al [33]	Q-ICP-MS	H_2/He in octopole-based collision/reaction cell	25	---	45	35
D. Pick et al. [56]	Q-ICP-MS	O_2 (As) CH_4 (Se) in quadrupole-based collision/reaction cell	30	---	---	160
X. Li et al. [57]	Q-ICP-MS	H_2/He in hexapole-based collision/reaction cell	25	---	95	---
This work	ICP-MS/MS	CH_3F/He	0.2	10	7	4

The true potential and robustness of the methods developed was subsequently assessed through the use of matrix-matched standard solutions containing elements that can give rise to interfering ions. Solutions containing 5 µg L^{-1} of As or of Se plus 100 µg L^{-1} of Ca, 500 mg L^{-1} of Cl, 100 µg L^{-1} of Gd, of Nd, and of Sm and 1 µg L^{-1} of Mo, of Nb, of Ru, of Y, and of Zr, were analyzed. While the use of He allows the polyatomic interferences (except for $^{40}Ar^{40}Ar^+$)**[40]** to be resolved, doubly charged interferences (e.g., $^{150}Nd^{2+}$, $^{150,154}Sm^{2+}$, $^{154,156,160}Gd^{2+}$) cannot be dealt with. When using O_2 or CH_3F/He, in the SQ mode, isobaric ions having the same m/z ratio as the reaction product ion (e.g., $^{89}Y^+$, $^{91,94,96}Zr^+$, $^{93}Nb^+$, $^{94,96}Mo^+$ and $^{96}Ru^+$), as well as all polyatomic interfering ions, formed either in the plasma or in the cell, still present a problem. However, in MS/MS mode, both reaction gases were able to resolve all the spectral overlaps. Moreover, CH_3F/He shows a better performance than O_2 because of the higher reaction efficiency with both As and Se, thus leading to better LoDs.

5.3.5. Results obtained for the determination of As and Se in reference materials

A number of reference materials were selected to further validate the methods relying to the use of ICP-MS/MS with CH_3F/He. The materials were of plant, animal or environmental origin, and a wide range of concentrations was covered.

External calibration was used for quantification with Te as an internal standard (selected on the basis of the closeness of its ionization energy and chemical behavior to those of the target elements) to correct for matrix effects, instrument instability and signal drift. For each reference material, several aliquots from 4 separate digestions were diluted and analyzed.

The results are presented in **Table 5.8**, which shows the average of 20 measurements, obtained from 4 different digestions, each one measured 5 consecutive times. At the 95% level of significance, all the results obtained are in good agreement with the corresponding certified value ($t < t_{critical}$), which demonstrates that the methods developed enable the straightforward determination of As and Se at different concentration levels and in various matrix types, whereby the problem of both spectral and non-spectral interferences is avoided.

Table 5.8. Results obtained for certified reference materials using CH_3F/He and ICP-MS/MS

Sample description	Arsenic		Selenium			
	Average ± SD (μg g^{-1}) [a]	Certified value (μg g^{-1})	Average ± SD (μg g^{-1}) [a]			Certified value (μg g^{-1})
	^{75}As		^{77}Se	^{78}Se	^{80}Se	
NIST SRM 1515 Apple leaves	0.038 ± 0.002	0.038 ± 0.007	0.055 ± 0.007	0.050 ± 0.003	0.049 ± 0.004	0.050 ± 0.009
NBS SRM 1575 Pine Needles	0.23 ± 0.01	0.21 ± 0.04	-----	-----	-----	-----
NBS SRM 1573 Tomato Leaves	0.30 ± 0.01	0.27 ± 0.05	-----	-----	-----	-----
NIST SRM 1568a Rice Flour	0.27 ± 0.01	0.29 ± 0.03	0.35 ± 0.04	0.35 ± 0.02	0.35 ± 0.01	0.38 ± 0.04
BCR CRM 526 Tuna Fish Tissue	5.02 ± 0.07	4.80 ± 0.30	-----	-----	-----	-----
NCR –CNRC DORM-4 Fish Protein	6.79 ± 0.06	6.80 ± 0.64	3.65 ± 0.10	3.64 ± 0.07	3.63 ± 0.03	3.56 ± 0.34
BCR – 414 Plankton	6.95 ± 0.09	6.82 ± 0.28	1.75 ± 0.09	1.72 ± 0.05	1.77 ± 0.03	1.75 ± 0.10
NBS SRM 1646 Estuarine sediment	11.07 ± 0.15	11.6 ± 1.3	0.64 ± 0.04	0.63 ± 0.03	0.65 ± 0.02	0.6[b]
NIST SRM 1566a Oyster Tissue	14.01 ± 0.20	14.0 ± 1.2	2.23 ± 0.09	2.22 ± 0.06	2.22 ± 0.04	2.21 ± 0.24
NRC – CNRC TORT-3 Lobster Hepatopancreas	60.74 ± 1.33	59.5 ± 3.8	11.03 ± 0.22	11.09 ± 0.09	11.07 ± 0.12	10.9 ± 1.0

[a]Uncertainties expressed as standard deviation (n = 20)

[b]Indicative value

Additionally, a good agreement was found among the three selected Se nuclides, thus enabling the monitoring of the most abundant isotope (^{80}Se), which is often prohibited when using other approaches (e.g., SF-ICP-MS), and also permitting isotopic analysis when required in the context of elemental assay *via* isotope dilution or tracer experiments.

The accuracy of the determination was proven for all the reference materials, including the NIST SRM 1515 (Apple Leaves), despite of its low As and Se concentrations and the presence of considerable amounts of Nd and Sm (leading to doubly charged interferences that cannot be overcome by using a collision gas (e.g., He), as discussed in the previous section).

The precision attainable was checked *via* the RSD (%), which includes the measurement precision, as well as the contribution from the sample preparation. Still, RSD values lower than 5% were found for all reference materials in the case of As. These RSD values improve down to 1-2% for reference materials with concentrations exceeding 1 μg g^{-1}. In the case of Se, RSD values better than 3% were found for ^{80}Se, better than 5% for ^{78}Se and better than 10% for ^{77}Se, except for NIST SRM 1515 (Apple Leaves), for which, due to the low concentration, the RSD values found were 13, 6 and 8% for $^{77,78,80}Se$, respectively. Except in this case, the RSDs found are in good agreement with the trend expected on the basis of the isotopic abundance of the nuclides monitored (RSD *via* $^{77}Se > ^{78}Se > ^{80}Se$).

5.4. Conclusion

In this work, the capabilities of CH_3F/He as a reaction gas in ICP-MS/MS for the ultra-trace determination of As and Se in diverse sample types have been demonstrated. This approach provides interference-free conditions, permitting As and Se determination *via* $AsCH_2^+$ and $SeCH_2^+$, respectively, with high accuracy and precision. The instrumental LoD for As was calculated to be 0.2 ng L^{-1}, while those for all of the Se nuclides studied were below 10 ng L^{-1}. For Se, the approach developed is suited for interference-free element determination *via* all of the isotopes investigated. As a result, also the utility in speciation and isotopic analysis (e.g., tracer studies and elemental assay *via* isotope dilution) can be assumed feasible.

Acknowledgements

The authors acknowledge Agilent Technologies for the ACT-UR research project grant, as well as the Spanish Ministry of Economy and Competitiveness (Project CTQ2012-33494) and the Aragón Government (Fondo Social Europeo). Elisabeth Nissen is acknowledged for her support.

References

[1] P. Roy, A. Saha, Curr Sci, 82 (2002) 38 - 45.

[2] U. Tinggi, Toxicol Lett, 137 (2003) 103 - 110.

[3] H-J. Sun, B. Rathinasabapathi, B. Wu, J. Luo, L-P. Pu, L. Q. Ma, Environ Int, 69 (2014) 148 - 158.

[4] Z. Huan, Q. Pei, G. Sun, S. Zhang, J. Liang, Y. Gao, X. Zhang, Clin Chim Acta, 387 (2008) 139 - 144.

[5] N. F. Kolachi, T. G. Kazi, S. K. Wadhwa, H. I. Afridi, J. A. Baig, S. Khan, F. Shah, Sci Total Environ, 409 (2011) 3092 - 3097.

[6] S. Sah, A. Vandenberg, J. Smits, Toxicol Appl Pharmacol, 272 (2013) 256 - 262.

[7] E. Vassileva, A. Becker, J. A. C. Broekaert, Anal Chim Acta, 441 (2001) 135 - 146.

[8] M. O. Iserte, A. F. Roig-Navarro, F. Hernádez, Anal Chim Acta, 527 (2004) 97 - 104.

[9] R-Y. Wang, Y-L. Hsu, L-F. Chang, S-J. Jiang, Anal Chim Acta, 590 (2007) 239 - 244.

[10] G. B. Tonietto, J. M. Godoy, A. C. Oliveira, M. V. de Souza, Anal Bioanal Chem, 397 (2010) 1755 - 1761.

[11] R. S. Balaba, R. B. Smart, Chemosphere, 89 (2012) 1437 - 1442.

[12] C. C. Y. Chan, R. S. Sadana, Anal Chim Acta, 270 (1992) 213 - 238.

[13] W. W. Ding, R. E. Sturgeon, Spectrochim Acta, Part B, 51 (1996) 1325 - 1334.

[14] Y. Cai, TrAC,Trends anal chem, 19 (2000) 62 - 66.

[15] E. Beccaloni, L. Musmeci, E. Stacul, Anal Bioanal Chem, 374 (2002) 1230 - 1236.

[16] M. Resano, M. dR. Flórez, E, García-Ruiz, Anal Bioanal Chem, 406 (2014) 2239 - 2259.

[17] J. Goossens, F. Vanhaecke, L. Moens, R. Dams, Anal Chim Acta, 280 (1993) 137 - 143.

[18] F. Vanhaecke, J. Riondato, L. Moens, R. Dams, Fresenius J Anal Chem, 355 (1996) 397 - 400.

[19] P. Allain, L. Jaunault, Y. Mauras, J-M. Mermet, T. Delaporte, Anal Chem, 63 (1991) 1497 - 1498.

[20] E. H. Larsen, S. Stürup, J Anal At Spectrom, 9 (1994) 1099 - 1105.

[21] M. Kovačevič, W. Goessler, N. Mikac, M. Veber, Anal Bioanal Chem, 383 (2005) 145 - 151.

[22] G. Grindlay, J. Mora, M. de Loos-Vollebregt, F. Vanhaecke, Spectrochim Acta, Part B, 86 (2013) 42 - 49.

[23] T. Nakazawa, D. Suzuki, H. Sakuma, N. Furuta, J Anal At Spectrom, 29 (2014) 1299 - 1305.

[24] Y-S. Kim, H. Kawaguchi, T. Tanaka, A. Mizuike, Spectrochim Acta, Part B, 45 (1990) 333 - 339.

[25] F. Vanhaecke, R. Dams, C. Vandecasteele, J Anal At Spectrom, 8 (1993) 433 - 438.

[26] A. S. Al-Ammar, R. K. Gupta, R. M. Barnes, Spectrochim Acta, Part B, 54 (1999) 1849 - 1860.

[27] E. D. Salin, M. Antler, G. Bort, J Anal At Spectrom, 19 (2004) 1498 - 1500.

[28] R. L. Watters Jr., K. R. Eberhardt, E. S. Beary, J. D. Fassett, Metrologia, 34 (1997) 87 - 96.

[29] L. H. Reyes, J. M. M. Gayón, J. I. G. Alonso, A. Sanz-Medel, J Anal At Spectrom, 18 (2003) 11 - 16.

[30] C. J. Park, H. Song, J Anal At Spectrom, 20 (2005) 436 - 440.

[31] A. Castillo, C. Boix, N. Fabregat, A. F. Roig-Navarro, L. A. Rodríguez-Castrillón, J Anal At Spectrom, 27 (2012) 354 - 358.

[32] S. F. Boulyga, J. S. Becker, Fresenius J Anal Chem, 370 (2001) 618 - 623.

[33] J. Darrouzès, M. Bueno, G. Lespès, M. Holeman, M. Potin-Gautier, Talanta, 71 (2007) 2080 - 2084.

[34] Z. Zhang, S. Chen, H. Yu, M. Sun, W. Liu, Anal Chim Acta, 513 (2004) 417 - 423.

[35] M. Colon, M. Hidalgo, M. Iglesias, J Anal At Spectrom, 24 (2009) 518 - 521.

[36] S. D. Tanner, J Anal At Spectrom, 10 (1995) 905 - 921.

[37] S. Musil, AsH. Pétursdóttir, A. Raab, H. Gunnlaugsdóttir, E. Krupp, J. Feldmann, Anal Chem, 86 (2014) 993 - 999.

[38] A. T. Townsend, Fresenius J Anal Chem, 364 (1999) 521 - 526.

[39] S. D'Ilio, N. Violante, C. Majorani, F. Petrucci, Anal Chim Acta, 698 (2011) 6 - 13.

[40] M. Niemelä, P. Perämäki, H. Kola, J. Piispanen, Anal Chim Acta, 493 (2003) 3 - 12.

[41] M. Resano, E. G. Ruiz, V. G. Mihuez, A. M. Móriez, G. Záray, F. Vanhaecke, J Anal At Spectrom, 22 (2007) 1158 - 1162.

[42] M. Colon, M. Hidalgo, M. Iglesias, Talanta, 85 (2011) 1941 - 1947.

[43] W. Guo, S. Hu, Y. Wang, L. Zhang, Z. Hu, J. Zhang, Microchem J, 108 (2013) 106 - 112.

[44] W. Guo, S. Hu, X. Li, J. Zhao, S. Jin, W. Liu, H. Zhang, Talanta, 84 (2001) 887 - 894.

[45] M. Grotti, R. Frache, J Anal At Spectrom, 22 (2007) 1481 - 1487.

[46] S. D. Fernández, N. Sugishama, J. R. Encinar, A. Sanz-Medel, Anal Chem, 84 (2012) 5851 - 5857.

[47] L. Balcaen, G. Woods, M. Resano, F. Vanhaecke, J Anal At Spectrom, 28 (2013) 33 - 39.

[48] L. Balcaen, E. Bolea-Fernandez, M. Resano, F. Vanhaecke, Anal Chim Acta, 809 (2014) 1 - 8.

[49] E. Bolea-Fernandez, L. Balcaen, M. Resano, F. Vanhaecke, Anal Chem, 86 (2014) 7969 - 7977.

[50] L. J. Moens, F. Vanhaecke, D. R. Bandura, V. I. Baranov, S. D. Tanner, J Anal At Spectrom, 16 (2001) 991 - 994.

[51] N. Nonose, M. Ohata, T. Narukawa, A. Hioki, K. Chiba, J Anal At Spectrom, 24 (2009) 310 - 319.

[52] X. Zhao, G. K. Koyanagi, D. K. Bohme, J Phys Chem A, 110 (2006) 10607 - 10618.

[53] J. J. Sloth, E. H. Larsen, J Anal At Spectrom, 15 (2000) 669 - 672.

[54] C. C. Chéry, D. Günther, R. Cornelis, F. Vanhaecke, L. Moens, Electrophoresis, 24 (2003) 3305 - 3313.

[55] J. Frank, M. Krachler, W. Shotyk, Anal Chim Acta, 530 (2005) 307 - 316.

[56] D. Pick, M. Leiterer, J. W. Einax, Microchem J, 95 (2010) 315 - 319.

[57] X. Li, S. Dai, W. Zhang, T. Li, X. Zheng, W. Chen, Int J Coal Geol, 124 (2014) 1 - 4.

CHAPTER 6

Tandem ICP-mass spectrometry for Sr isotopic analysis without prior Rb/Sr separation

Adapted from Bolea-Fernandez et. al., J. Anal. At. Spectrom., 31 (2016) 303 – 310

6.1. Introduction

In comparison to elements with a similar atomic number, Sr shows a relatively pronounced natural variation in its isotopic composition as a result of one of its isotopes – ^{87}Sr – being radiogenic. The consequence is a wide variety of applications for which Sr isotopic analysis is of relevance (e.g., Rb/Sr geochronological dating and other geochemical applications, provenance determination of agricultural products of plant and animal origin and migration studies).**[1-4]**

Although like for every other element with ≥ 2 isotopes, also the isotopic composition of Sr shows natural variation as a result of isotope fractionation,**[3, 5, 6]** the main process responsible for the natural variation in the isotopic composition of Sr **[7,8]** is the β^- decay of ^{87}Rb into ^{87}Sr ($T_{1/2}$ = 4.88 x 10^{10} years **[9]**). This means that, in a closed system, sub-samples containing Rb and Sr will be enriched in ^{87}Sr, and the degree of enrichment depends on the time during which the two elements have resided together and their elemental ratio Rb/Sr.**[10-12]**

However, accurate determination of the $^{87}Sr/^{86}Sr$ isotope ratio by means of inductively coupled plasma-mass spectrometry (ICP-MS) is not free from challenges. One of the most important problems is the spectral overlap of the signals of the isobaric ions $^{87}Rb^+$ and $^{87}Sr^+$, which need a mass resolution of ~ 300,000 to be resolved, which is beyond the capabilities of present-day commercially available ICP-MS instruments.**[13,14]** Additional spectral interference due to the presence of polyatomic ions, such as $ArCa^+$ and Ca_2^+ dimers, can also jeopardize the accuracy of the isotope ratio results. The use of high mass resolution,**[15]** which furthermore results in a significant drop in signal intensity and deterioration in isotope ratio precision,**[16]** is not feasible for overcoming the spectral overlap. Sr has to be isolated from the matrix, or at least separated from Rb, prior to analysis.**[17-19]** Obviously, these isolation steps negatively affect the sample throughput and make Sr isotopic analysis labor-intensive.

It has been demonstrated that chemical resolution using a quadrupole-based ICP-MS (ICP-QMS) instrument equipped with a collision/reaction cell can be an elegant option to resolve spectral overlap,**[20]** thus extending the application range of ICP-QMS to the isotopic analysis of elements that otherwise suffer from spectral interference. The use of a collision/reaction cell allows to remove spectral overlap relying on physical processes (e.g., a combination of collisions with a non-reactive

gas to slow down polyatomic ions more than atomic ions, thus enabling the former to be selectively discriminated against *via* kinetic energy discrimination),**[21]** or by selective ion/molecule reaction between an interfering ion,**[22-24]** or the target ion,**[25-27]** and a reactive gas. The latter approach is sometimes referred to as chemical resolution and allows interference-free measurement at either the original mass-to-charge (m/z) ratio of the target nuclide or at the m/z ratio of the reaction product ion formed. In this way, the sample pretreatment can be reduced or even eliminated, also facilitating the direct analysis of solid samples *via* laser ablation – ICP-MS (LA-ICP-MS).

Unfortunately, the isotope ratio precision typically offered by ICP-QMS is rather modest, with values around 0.1% RSD internal precision. Pressurizing the collision/reaction cell of an ICP-QMS instrument with an inert collision gas can lead to a slight improvement in the isotope ratio precision, by damping the fluctuations in signal intensity, through the mixing ions sampled from the plasma ion source at slightly different moments in time.**[28, 29]** However, the isotope ratio precision thus attainable is still considerably worse than that achievable with thermal ionization mass spectrometry (TIMS) or multi-collector ICP-MS (MC-ICP-MS), with an internal precision down to 0.001% RSD. Therefore, the use of ICP-QMS for the determination of isotope ratios has often been restricted to the study of induced changes in the isotopic composition of target elements in the context of tracer experiments with enriched stable isotopes,**[30, 31]** or of elemental assay using isotope dilution for calibration.**[32]** However, it has to be stressed that, the use of the more expensive MC-ICP-MS or TIMS instrumentation is not always required when natural variation in the isotopic composition of a target element needs to be studied, as for some applications, particularly those dealing with radiogenic nuclides, the precision attainable with an ICP-QMS instrument can be fit-for-purpose.**[11, 33-35]**

Additionally to the difficulties with spectral overlap mentioned above, every type of ICP-MS instrumentation suffers from mass discrimination,**[36]** a term referring to the differences in the efficiencies of ion extraction, transmission and/or detection as a function of the analyte mass. This effect results in a bias between the measured isotope ratio and the corresponding true value that needs to be adequately corrected for. Different approaches have been described in the literature for this purpose (e.g., internal correction, external correction and the combination of

both).**[37]** Also, it has been demonstrated that mass discrimination effects become more pronounced in ICP-QMS when the collision/reaction cell is pressurized with a gas, as a result of slight differences in the collisional and/or chemical behavior of the isotopes as a function of their mass.**[26, 38]**

In earlier work, the use of methyl fluoride (CH_3F) as a selective reaction gas (in combination with Ne as a non-reactive collision gas) in an ICP-QMS instrument equipped with a dynamic reaction cell (DRC) for the direct determination of Sr isotope ratios has been described.**[25]** In this approach, the selective reaction between CH_3F and Sr^+ (Rb^+ does not react with CH_3F) allows for circumventing the isobaric overlap at m/z = 87 by measuring the relative signal intensities of the Sr isotopes *via* the intensities of the corresponding SrF^+ ions. Owing to the mono-isotopic character of F, the SrF^+ ions show the same isotopic pattern as do the Sr^+ ions themselves. Despite the achievements shown in the work referred to, this did not result in a general breakthrough for Sr isotopic analysis, as it was noted that (i) interfering nuclides occurring at the m/z ratio of the selected reaction product ions (e.g., ^{103}Rh, ^{106}Cd, $^{105,106}Pd$ and ^{107}Ag) could not be removed, and (ii) that the matrix composition affects the mass discrimination to a large extent, such that the use of a matrix-matched isotopic standard for external mass bias correction was required. These important drawbacks have hindered routine application of this approach in real-life applications.

Recently, a new type of ICP-MS device was introduced onto the market. The so-called triple quadrupole ICP-MS instrumentation is equipped with a tandem mass spectrometry configuration (ICP-MS/MS), with an octopole collision/reaction cell located in-between two quadrupole analyzers. This set-up opens new possibilities for interference-free determination of ultra-trace concentrations of elements that otherwise suffer from strong spectral overlap (Chapter 2).**[39, 40]** In MS/MS-mode, only those ions with the original m/z-ratio of the analyte element pass the first quadrupole and enter the reaction cell. This results in an enhanced control over the reactions taking place in the cell and a strong reduction in matrix effects. Because of this, highly reactive gases (e.g., NH_3 and CH_3F) can be used without the risk of obtaining complex mass spectra that are difficult to interpret.**[41]** ICP-MS/MS with a CH_3F/He (10% CH_3F and 90 % He) mixture **[42]** as a reaction gas has recently been successfully used by the authors for the purpose of ultra-trace determination of several elements (Al, As, Co, Cr, Mn, Ni, Se, Ti and V)(Chapter 3 and 5),**[43, 44]**

but the possibilities of ICP-MS/MS for isotope ratio determinations have not been fully explored yet,**[45-49]** and no work to date has reported on the use of this technique for Sr isotopic analysis.

In this work, the capabilities of tandem ICP - mass spectrometry with CH_3F as a reaction gas were evaluated, with the aim to develop a method that enables the straightforward determination of the $^{87}Sr/^{86}Sr$ isotope ratio in geological materials, without previous Sr isolation or Rb/Sr separation.

6.2. Experimental

6.2.1. *Reagents and standards*

Only high-purity reagents were used throughout the work. Ultra-pure water (resistivity > 18.2 MΩ cm) was obtained from a Milli-Q Element water purification system (Millipore, France). Ultra-pure 28 M HF (Fisher Chemicals, Great Britain) and pro-analysis 14 M HNO_3 (ChemLab, Belgium), further purified by sub-boiling distillation, were used for acid digestion. Appropriate dilutions from 1 g L^{-1} single-elemental standard solutions (Ag, Ca, Cd, Pd, Rb and Sr – Instrument Solutions, The Netherlands) were made for obtaining solutions used in the context of method development. The isotopic reference material NIST SRM 987 Strontium Carbonate with a certified Sr isotopic composition ($^{87}Sr/^{86}Sr$ = 0.71034 ± 0.00026) and an in-house standard solution of Sr (Instrument solutions, The Netherlands), previously characterized *via* MC-ICP-MS ($^{87}Sr/^{86}Sr$ = 0.70753 ± 0.00006), were used for optimization, method development and validation purposes.

6.2.2. *Samples*

Five geological reference materials – USGS AGV1 Andesite and USGS G-2 Granite, USGS BHVO-1 Basalt, BCR CRM 141 Calcareous Loam Soil and BCR CRM 142 Light Sandy Soil – were analyzed for their $^{87}Sr/^{86}Sr$ isotope ratio and the results obtained were compared to values reported in the literature for the purpose of validation.

6.2.3. *Sample preparation*

Sample digestion was carried out in Savillex® beakers, that had been previously submitted to a cleaning procedure with both HNO_3 and HCl and subsequent rinsing

with Milli-Q water. Approximately 0.2 g of each reference material was accurately weighed and dissolved in 3 mL of 14 M HNO_3 and 10 mL of 28 M HF. The mixture was heated in an open beaker on a hot plate (90 °C) until dryness. For the reference materials USGS AGV1 (Andesite) and USGS G-2 (Granite), the residue was taken up in 1.4 M HNO_3. In the case of USGS BHVO-1 (Basalt), BCR CRM 141 (Calcareous Loam Soil) and BCR CRM 142 (Light Sandy Soil), an additional digestion was required to obtain a clear solution. Therefore, 5 mL of 14 M HNO_3 was added to the residue and the resulting mixture heated at 110°C in a closed beaker overnight. After digestion, the solutions thus obtained were appropriately diluted for subsequent analysis. The concentration of Sr was kept constant throughout the work (7.5 µg L^{-1} and 10 µg L^{-1} for SQ and MS/MS mode, respectively), providing approximately the same signal intensity in both modes. To avoid possible contamination, only "metal-free" tubes were used to prepare all dilutions (15 or 50 mL polypropylene centrifuge tubes, VWR, Belgium).

6.2.4. *Instrumentation*

All measurements were performed using an Agilent 8800 tandem ICP-MS instrument (ICP-QQQ, Agilent Technologies, Japan), equipped with a MicroMist nebulizer (400 µL min^{-1}) fitted onto a Peltier-cooled Scott-type spray chamber (2 °C). The octopole collision/reaction cell was pressurized with a mixture of CH_3F/He (10% CH_3F and 90% He, "Certified Master Class", Air Liquide, Belgium). The CH_3F/He mixture was introduced *via* the 4th inlet (operation range of the mass flow controller, 0 – 100 %, corresponding to gas flow rates of 0 – 1 mL min^{-1}, calibrated for O_2).

6.3. Results and discussion

6.3.1. *Method development for interference-free determination of Sr*

An important prerequisite for successful direct Sr isotopic analysis is the ability of the analytical method to monitor the signals of (at least) ^{86}Sr, ^{87}Sr and ^{88}Sr free from spectral overlap. The actual isotope ratio of interest is $^{87}Sr/^{86}Sr$, while $^{88}Sr/^{86}Sr$ is used for internal correction for mass discrimination. As measuring ^{84}Sr provides no added value, while increasing the measurement time and potentially deteriorating

the isotope ratio precision, this nuclide was not monitored. In this work, CH_3F (a mixture of 10 % CH_3F and 90 % He) was evaluated as a reaction gas in ICP-MS/MS. *Via* product ion scanning, with the cell pressurized with 1 mL min^{-1} of CH_3F/He, the mass-to-charge (m/z) ratio of each of the target nuclides ($^{86,87,88}Sr^+$) was selected in the first quadrupole, and the entire mass spectrum was scanned using the second quadrupole for identifying the reaction product ions formed. The main reaction product ions were identified as $^{86,87,88}SrF^+$. In MS/MS mode, the CH_3F/He flow rate setting was evaluated in the range of 0 - 1.0 mL min^{-1}, and a maximum signal-to-background ratio was found at 0.90 mL min^{-1}. The optimum instrument settings are summarized in **Table 6.1**.

Table 6.1. Optimum instrument settings and data acquisition parameters for the determination of the $^{87}Sr/^{86}Sr$ isotope ratio *via* the corresponding SrF^+ reaction product ions using CH_3F/He as a reaction gas in ICP-MS/MS

Agilent 8800	
Reaction Gas	CH_3F/He (10/90)
Scan type	MS/MS
Plasma mode	Low matrix
RF power (W)	1550
Extract 1 (V)	-3.0
Q1 bias (V)	0
Reaction gas flow rate setting (mL min^{-1})	0.90
Q1 → Q2	86 → 105 87 → 106 88 → 107
Octopole bias (V)	-4.7
Energy discrimination (V)	-8.4
Extract 2 (V)	-175.0
Q2 QP bias (V)	-13.1
Wait time offset (ms)	0
Sweeps / replicate	100
Acquisition time / mass (s) **[1 acquisition point per spectral peak]**	30
Number of replicates	10
Total analysis time / sample (s)	906

With the aim of demonstrating the capabilities of the MS/MS approach to avoid spectral overlap, two standard solutions were analyzed, the first one containing 10 µg L^{-1} of Sr and the second one containing the same concentration of Sr and 10 µg L^{-1} of Ag, Cd, Pd and Rb. These elements can give rise to spectral interference at the original m/z ratio of one of the target nuclides (^{87}Rb) or at the m/z ratio of the selected reaction product ions (^{105,106}Pd, ^{106}Cd, ^{107}Ag). Both standard solutions were measured in both single quadrupole mode (SQ, where the first quadrupole is not operating as a mass filter, but only as an ion guide) and MS/MS mode. The results are given in **Figure 6.1**.

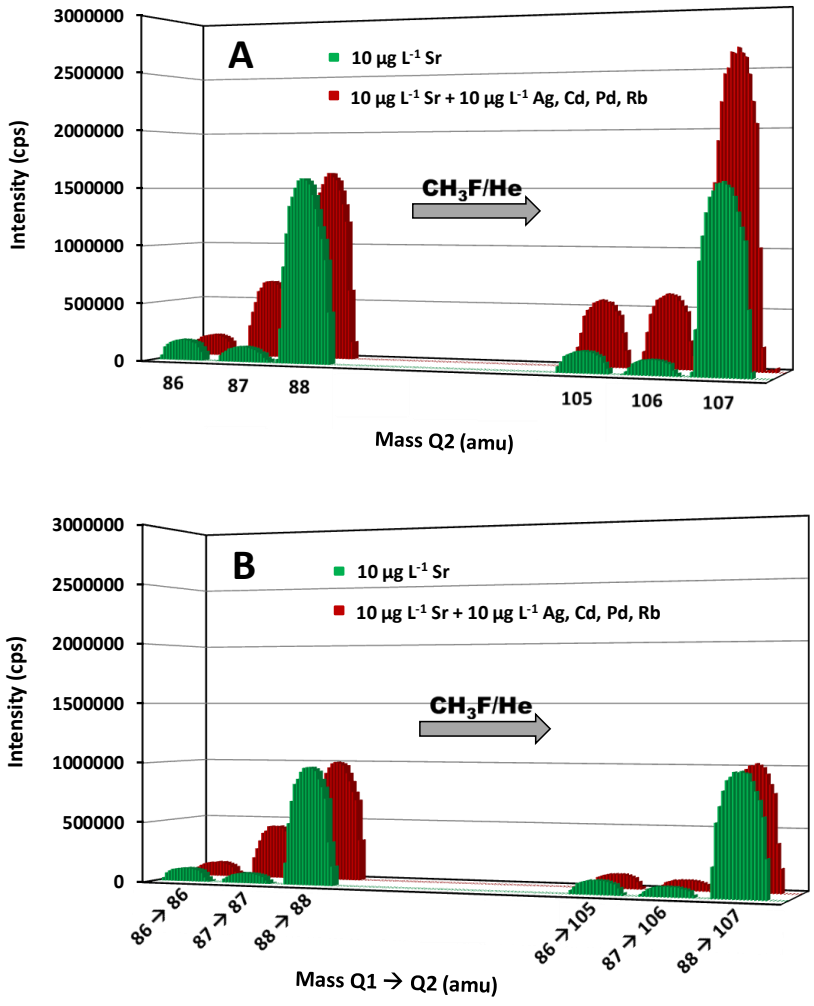

Figure 6.1. Mass spectrum, showing the isotopic composition of Sr at the original mass-to-charge ratio (m/z = 86, 87 and 88) and at the mass-to-charge ratios of the selected reaction product ion (SrF^+ m/z = 105, 106 and 107) for a standard solution of Sr (in green) and for a standard solution of Sr doped with Ag, Cd, Pd and Rb (in red) in both, single quadrupole or SQ (A) and MS/MS mode (B).

In both modes, the isotopic pattern observed for the pure Sr solution was the same without and with reaction, as a consequence of the mono-isotopic character of F, enabling the determination of the isotopic composition of Sr *via* measurement of the intensities of the SrF^+ ions. A comparison between the results for both standard solutions (without and with admixed elements) shows the effect of the overlap of the signals of ^{87}Sr and ^{87}Rb, which was resolved in both modes owing to reaction of the Sr^+ ions with CH_3F, while Rb^+ shows no reactivity towards this gas. Although a better sensitivity was achieved in SQ mode, the spectral interferences occurring in the presence of Ag, Cd and Pd ions at the m/z ratio of the selected reaction product ions prevent accurate Sr isotopic analysis in this mode. For samples containing those elements, Sr isotopic analysis without previous Sr isolation can only be successfully accomplished in MS/MS mode.

In MS/MS mode, some figures of merit (e.g., sensitivity or limits of detection and of quantification) were characterized and the corresponding results are given in **Table 6.2**.

6.3.2. Optimization of instrument settings and data acquisition parameters for the accurate and precise isotope ratio determination of Sr via SrF^+ monitoring

With the objective of achieving accurate and precise $^{87}Sr/^{86}Sr$ isotope ratio results *via* conversion of Sr^+ into the corresponding SrF^+ ions using CH_3F/He as a reaction gas in ICP-MS/MS, the detector dead time was experimentally determined and the effect of the data acquisition parameters was checked.

The detector dead time was determined according to the method proposed by Russ.**[50]** Standard solutions of Sr with concentrations of 2.5, 5.0 and 10 μg L^{-1} were measured at different detector dead times in the range of 0 to 70 ns. The $^{88}SrF^+/^{86}SrF^+$ ratios were plotted *versus* the dead time for each concentration. According to this approach, the point where the lines intersect corresponds with the correct value, which was 32.6 ± 0.3 ns in this case. Additional experiments were carried out to ascertain that the detector dead time determined using $^{88}SrF^+/^{86}SrF^+$ are also valid for $^{87}SrF^+/^{86}SrF^+$. For a range between 1 and 10 μg L^{-1}, it was evaluated whether the $^{87}SrF^+/^{86}SrF^+$ isotope ratio changes as a function of the Sr concentration. Values between 0.72497 – 0.72660 were obtained; no trend was observed and no significant differences were found, as indicated *via* ANOVA at a

Table 6.2. Calibration data and instrumental limits of detection (LoD) and of quantification (LoQ) obtained for Sr using CH_3F as a reaction gas in ICP-MS/MS

Isotope	Reaction product ion	CH_3F/He flow (mL min^{-1})	Q1 (amu)	Q2 (amu)	Sensitivity[a] (counts L μg^{-1} s^{-1})	Intercept[a] (counts s^{-1})	R^2	LoD[b] (ng L^{-1})	LoQ[b] (ng L^{-1})
^{86}Sr	$^{86}SrF^+$		86	105	21660 ± 90	48 ± 310	0.999992	1	4
^{87}Sr	$^{87}SrF^+$	0.90	87	106	14690 ± 50	68 ± 210	0.999993	1	4
^{88}Sr	$^{88}SrF^+$		88	107	172000 ± 900	340 ± 600	0.999998	0.8	3

[a]Uncertainties expressed as standard deviation (n = 10)

[b]LoDs and LoQs calculated as 3 and 10 times the standard deviation on 10 consecutive measurements of a blank solution (0.14 M HNO_3), divided by the slope of the calibration curve, respectively.

95% level of significance ($F_{experimental}$ = 1.0991 < $F_{critical}$ = 2.3861). This demonstrates that the differences in concentration (covering one order of magnitude) do not affect the accuracy of the isotope ratio results, such that it can be concluded that the dead time correction is done adequately and that the extent of instrumental mass bias does not vary within the range studied. Thus, the experimentally determined detector dead time was inserted into the software and used throughout all further work.

In addition, data acquisition parameters were optimized. The best performance is typically obtained when combining a sufficiently long acquisition time (*cf.* the role of the total number of ions detected in Poisson counting statistics) with fast scanning (to counteract the noisy character of the ICP ion source).**[29]** Different experiments were conducted with the aim of evaluating the effect of the data acquisition parameters on the accuracy and precision of the isotope ratio results. $^{87}SrF^{+}/^{86}SrF^{+}$ ratios and internal precision values, expressed as RSD (%), were determined using 10 replicates for each measurement and 100 sweeps per replicate. The results thus obtained are presented in **Figure 6.2** as a function of the total acquisition time per replicate, for both the raw data and the results after the use of an internal correction (*vide infra*). As expected, the RSD (%) decreases for longer acquisition times, down to a minimum at a total acquisition time of 90 s, corresponding with an acquisition time of 30 s for each of the isotopes selected (RSD = 0.12 and 0.09 % for the raw data and the internally corrected data, respectively). It can be seen that the $^{87}SrF^{+}/^{86}SrF^{+}$ ratio itself also changes with increasing total acquisition time, until a constant ratio is obtained for the highest values (**Figure 6.2**).

A similar trend was observed for the $^{88}SrF^{+}/^{86}SrF^{+}$ ratio, with the deviation at low acquisition times being even more pronounced. For $^{88}SrF^{+}/^{86}SrF^{+}$, however, a stable isotope ratio value is obtained as of a somewhat lower integration time than for $^{87}SrF^{+}/^{86}SrF^{+}$. This leads to an over-correction *via* internal correction, as can be seen in **Figure 6.2** for the lowest acquisition times. This tendency can most probably be explained as a result of the use of chemical reactions, where the reaction product ions typically require more time to actually reach the second quadrupole and detector and give rise to a stable ion beam, which means that a minimum dwell time (selected as a function of the acquisition time per nuclide / number of sweeps) has to be used for the measurement of the isotopic composition of Sr as SrF^{+} *via* ICP-MS/MS. More evidence for this hypothesis was found in

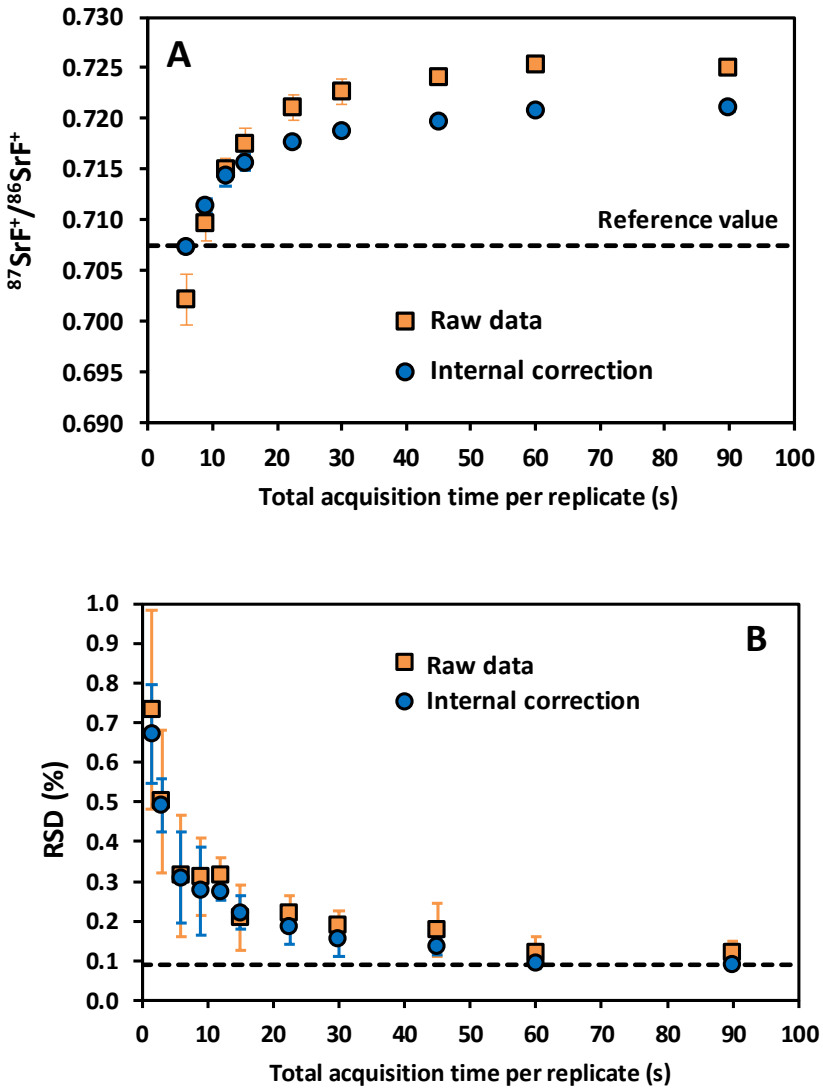

Figure 6.2. Raw and internally corrected $^{87}Sr/^{86}Sr$ isotope ratio as a function of the total acquisition time per replicate (A). Internal precision for the raw and internally corrected data expressed as RSD (%) for 10 replicate measurements as a function of the total acquisition time per replicate (B). The error bars indicate the standard deviation of 3 different analyses (each consisting of 10 replicate measurements) obtained on 3 different days.

additional experiments, where – for measurements with a short total acquisition time (3 s) - a wait time offset (WTO) was used. This WTO is an additional time on top of the quadrupole settling time, allowing the slowdown of the ions in the cell to be compensated for and giving the system time to arrive at steady state conditions. As can be seen in **Figure 6.3**, a WTO in the order of a few milliseconds (~5 ms) was

sufficient to compensate for the effect seen at low acquisition times. Additionally to the experiments explained above, also the number of sweeps per replicate was evaluated as a possible parameter affecting the precision in the isotope ratio measurements. However, although a wide range of number of sweeps was tested (50 - 1000), no reproducible effect on the accuracy or precision was noticed, probably, because longer dwell times are required when dealing with isotope ratio measurement after chemical reaction in the cell.

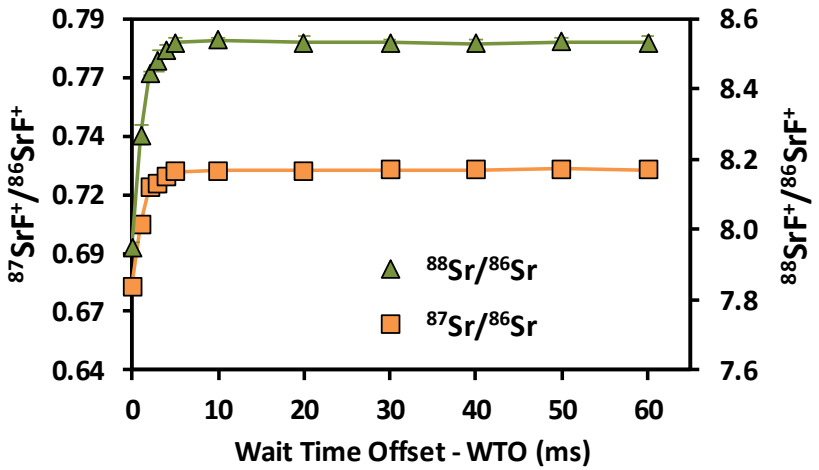

Figure 6.3. Raw $^{88}Sr/^{87}Sr$ and $^{87}Sr/^{86}Sr$ isotope ratio results (based on the corresponding SrF^+ signals) as a function of the wait time offset (WTO) obtained using a total acquisition time of 3 s.

Based on the results of these experiments, 100 sweeps and a total acquisition time of 90 s were selected as the optimum parameters, as they provide the best possible precision and stable isotope ratio results. When using these longer acquisition times, no additional measurement time was needed to obtain a constant isotope ratio result, and thus, the WTO was set at 0 ms. The optimized instrument settings and data acquisition parameters used in all further experiments are shown in **Table 6.1**.

6.3.3. Mass bias correction

As mentioned in the introduction, ICP-MS is affected by mass discrimination, such that a measured isotope ratio differs from the corresponding true value. Several approaches have been described to correct for the mass bias thus caused. The use

of internal correction, external correction and the combination of both, were evaluated with the aim of obtaining better accuracy and precision. For the internal correction approach, the $^{88}Sr/^{86}Sr$ ratio is assumed to be (sufficiently) constant in nature and used to correct the $^{87}Sr/^{86}Sr$ ratio by means of the Russell law, with the assumption that $f^{88/86} = f^{87/86}$ (see **equation 1**). Alternately, the raw data were externally corrected for the mass bias using the NIST SRM 987 as an external standard, used in a sample - standard bracketing approach (SSB). Finally, also the combination of both correction methods was tested. **Figure 6.4** and **Table 6.3** show the results for a sequence of 10 measurements of an in-house standard solution of Sr with an isotopic composition that was previously characterized *via* MC-ICP-MS ($^{87}Sr/^{86}Sr = 0.70753 \pm 0.00003$). As can be seen, the raw data are biased high, and the use of internal correction using the Russell law (**equation 1**), based on an $^{88}Sr/^{86}Sr$ isotope ratio of 8.3752 does not allow to properly correct for mass discrimination. Although internal correction leads to a significant improvement in both, internal and external precision, the results are still biased high. The bias remaining after applying internal correction most probably results from additional mass discrimination produced by collisions and reactions in the cell (not all isotopes react to exactly the same extent with the reaction gas (CH_3F), neither are they equally affected by collisions with the inert He gas). Therefore, external correction with NIST SRM 987 in a SSB approach (**equation 2**) was tested.

$$\left(\frac{^{87}Sr}{^{86}Sr}\right)_{sample,\,corrected} = \left(\frac{^{87}Sr}{^{86}Sr}\right)_{sample,\,measured} x \left(\frac{m_{^{87}Sr}}{m_{^{86}Sr}}\right)^{f} \;;\; f = \ln\left[\frac{\left(^{88}Sr/^{86}Sr\right)_{true}}{\left(^{88}Sr/^{86}Sr\right)_{measured}}\right] / \ln\left[\frac{m_{^{88}Sr}}{m_{^{86}Sr}}\right] \qquad (1)$$

$$\left(\frac{^{87}Sr}{^{86}Sr}\right)_{sample,\,corrected} = \left(\frac{\left(\frac{^{87}Sr}{^{86}Sr}\right)_{sample,\,measured}}{\frac{\left(\frac{^{87}Sr}{^{86}Sr}\right)_{std-1,measured} + \left(\frac{^{87}Sr}{^{86}Sr}\right)_{std+1,measured}}{2}}\right) x \left(\frac{^{87}Sr}{^{86}Sr}\right)_{std,true} \qquad (2)$$

Good agreement was found between the externally corrected data and the true value, but with this correction method, the external precision was not improved beyond that of the raw data. Finally, the combination of internal and external

correction was seen to provide the best results in terms of both accuracy and precision, without any significant difference between the experimentally determined isotope ratios and the true value, and with an external precision of 0.035 % RSD (n = 10). Additionally, as shown in **Figure 6.4**, also an improved internal precision (the standard deviation on 10 replicates for each measurement) was achieved when the isotope ratios were internally corrected.

In order to better assess the capabilities of the last approach for the determination of isotope ratios of Sr using CH_3F in ICP-MS/MS, longer-term studies were performed. $^{87}SrF^+/^{86}SrF^+$ isotope ratio results were collected during a period of one month and provided an average of 0.70756 ± 0.00028 and an external precision of 0.039 % RSD (n = 50). Thus, the combination of internal and external correction was used in all further work.

The Kragten approach was used in order to evaluate which factors dominate the total uncertainty.**[51]** The fractionation factor (f), nuclide masses (^{86}Sr, ^{87}Sr, ^{88}Sr), certified $^{87}Sr/^{86}Sr$ isotope ratio, and repeatability of $^{88}Sr/^{86}Sr$ and $^{87}Sr/^{86}Sr$, were taken into account as possible factors affecting the uncertainty of the results. Via this error propagation approach, it was found that the measurement precision itself dominates the total uncertainty. Inclusion of the contribution of mass bias correction results in an RSD of 0.07%.

Table 6.3. Sr isotope ratio results obtained using ICP-MS/MS with different mass bias correction approaches

Mass Bias Correction	**$^{87}SrF^+/^{86}SrF^+$ ± s**	**RSD (%)**
Raw Data	0.72542 ± 0.00049[a]	0.067[a]
Internal Correction	0.72095 ± 0.00028[a]	0.039[a]
External Correction	0.70733 ± 0.00048[a]	0.068[a]
Internal + External Correction	0.70751 ± 0.00025[a]	0.035[a]
Internal + External Correction	0.70756 ± 0.00028[b]	0.039[b]
	$^{87}Sr/^{86}Sr$	**RSD (%)**
Reference Value (MC-ICP-MS)	0.70753 ± 0.00003	0.0042

[a]Results obtained for n = 10

[b]Results obtained for n = 50 collected from different sequences during a period of one month.

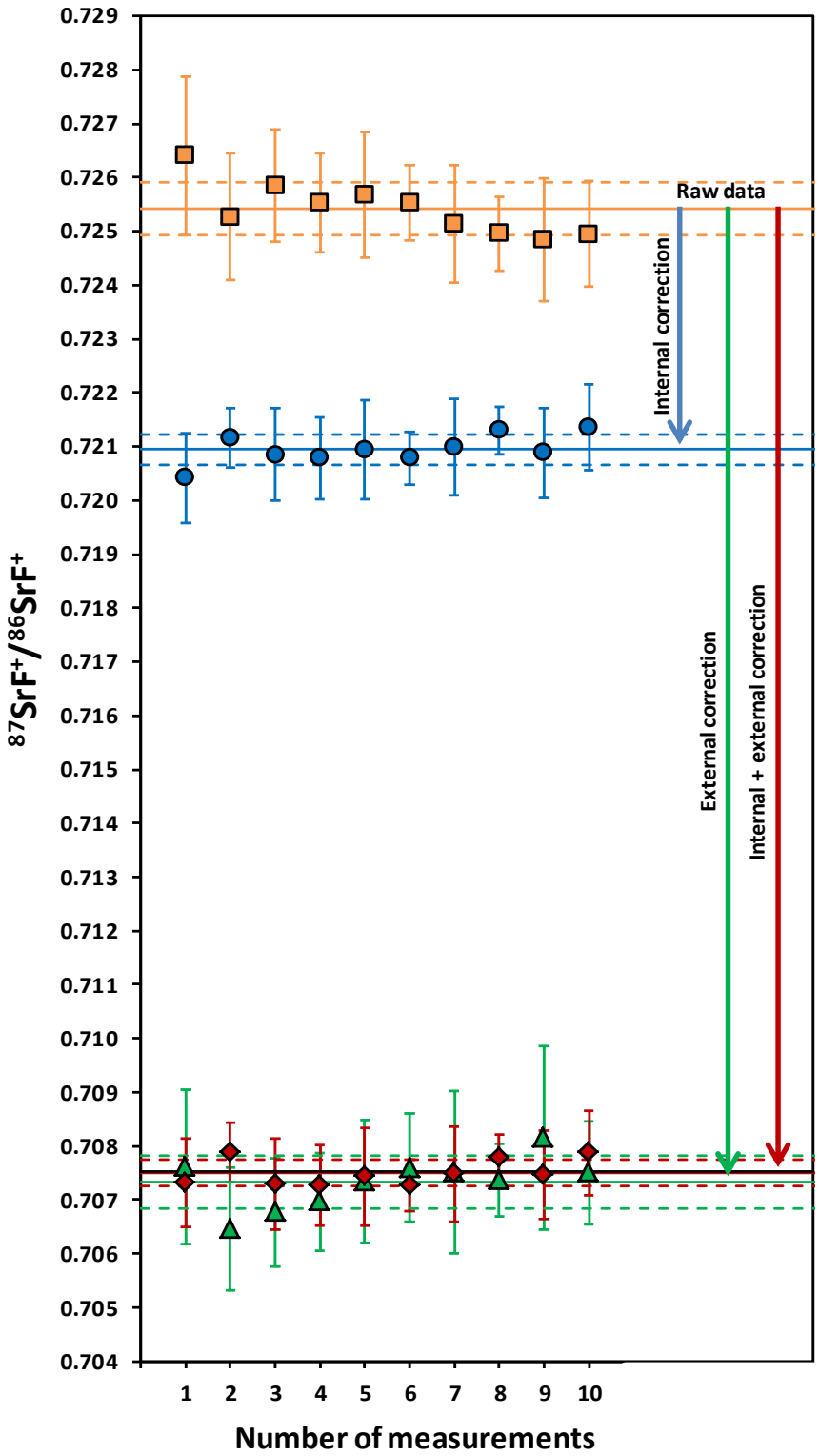

Figure 6.4. Results obtained using different mass bias correction approaches for an in-house standard solution of Sr measured in a sample-standard bracketing sequence (sample: n = 10). The error bars show the standard deviation on 10 replicates for each measurement.

6.3.4. Influence of sample matrix on isotope ratio results in SQ and MS/MS mode

In previous work,**[25]** it was shown that – even when the Sr isotopes can be measured interference-free – a good accuracy and precision of the $^{87}Sr/^{86}Sr$ isotope ratio results could not be guaranteed for geological reference materials, unless matrix-matched isotopic standards were used for external mass bias correction. This leads to the conclusion that matrix effects are responsible for the deviations obtained.

In this work, we assessed whether also with the newly developed ICP-MS/MS approach matrix effects necessitate the use of a matrix-matched standard. Therefore, the accuracy and precision of Sr isotopic analysis was assessed for pure Sr standard solutions, Sr standards with increasing concentrations of some matrix elements added (up to 1000 µg L^{-1} Ca and 200 µg L^{-1} Rb) and geological reference materials, both in SQ and MS/MS mode. The standards were measured on 3 different days in order to assess the robustness of the method under such conditions. No significant differences were found between the Sr standard solution and the different Rb- and Ca-containing solutions, neither between the results obtained in SQ and MS/MS-mode, which indicates that for these rather simple matrices, matrix effects can be neglected. For the geological reference materials, however, the situation is clearly different. For one of the reference materials, USGS AGV-1 Andesite, isotopic analysis in SQ mode (where all matrix ions are passing the first quadrupole and enter the collision/reaction cell) resulted in a $^{87}Sr/^{86}Sr$ isotope ratio of 0.65432 ± 0.00085 (after mass bias correction, based on a combination of both internal and external correction using NIST SRM 987). This result deviates strongly from the corresponding reference value of 0.70406 ± 0.00005. In MS/MS mode, however, where only a very limited selection of ions enters the cell, a good agreement was found between the results obtained and the corresponding reference value (see next section). This leads to the conclusion that for samples with a heavy matrix, matrix effects do have an influence on the final results. However, these effects can be overcome by operating the tandem mass spectrometer in the MS/MS mode, which is an additional proof of the strength of the method developed in this work.

6.3.5. Determination of the isotopic composition of Sr in geological reference materials using ICP-MS/MS

This novel method using CH_3F as a reaction gas in ICP-MS/MS for the determination of the isotopic composition of Sr without prior Sr isolation from the matrix, was used for the analysis of five reference materials of geological origin. The results are shown in **Table 6.4**. No significant differences were established between the experimental results and the corresponding reference values. In addition, the precision expressed as standard deviation for n = 5 was not significantly different ($F < F_{critical}$) from that obtained for an in-house standard solution of Sr (n=10, **Table 6.3**), except for BCR CRM 142, for which a very slight difference was found (3.66 > 3.63). Therefore, it can be stated that the approach for Sr isotopic analysis developed in this work allows accurate and precise isotope ratio results to be obtained, without the requirement of using a matrix-matched isotopic standard for mass bias correction, as was required in a similar context (CH_3F/Ne-pressurized reaction cell) with a Perkin Elmer Sciex Elan DRC ICP-MS instrument **[25]**.

Table 6.4. Results obtained using ICP-MS/MS for reference materials with geological origin

Sample description[a]	**Experimental result ± s**[b]	**Reference value ± uncertainty**
USGS AGV-1 Andesite	0.70408 ± 0.00038	0.70406 ± 0.00005
USGS G-2 Granite	0.70968 ± 0.00021	0.70983 ± 0.00006
USGS BHVO-1 Basalt	0.70337 ± 0.00029	0.70347 ± 0.00001
BCR CRM 141 Calcareous Loam Soil	0.70909 ± 0.00030	0.70924 ± 0.00007
BCR CRM 142 Light Sandy Soil	0.71513 ± 0.00048	0.71505 ± 0.00010

[a]Final concentration of Sr, after appropriate dilution of the reference materials, was 10 μg L^{-1}.

[b]Standard deviation on 5 consecutive measurements.

6.4. Conclusion

In this work, the capabilities of a novel approach for Sr isotopic analysis using CH_3F as a reaction gas in ICP-MS/MS were demonstrated. The method developed was able to remove all interfering species that could hinder Sr isotopic analysis. The removal of matrix elements, before they enter into the reaction cell provided by the MS/MS-mode, diminishes the influence of matrix effects on the final results, thus avoiding the necessity of using a matrix-matched standard, in contrast to the SQ-mode where the use of a matrix-matched standard is compulsory. The method developed enables accurate and precise (external precision better than 0.05% RSD) determination of the $^{87}Sr/^{86}Sr$ isotope ratio. It was shown that this approach can be successfully applied to the Sr isotopic analysis of reference materials of geological origin, without prior Rb/Sr separation. The robustness of the results obtained for these complex materials suggest that such method could also be deployed for the analysis of other types of samples for which Sr isotopic analysis could be of scientific interest.

Acknowledgment

The UGent authors acknowledge Agilent Technologies for providing them with an ACT-UR research project grant and the Special Research Fund of Ghent University (BOF-UGent) for research project funding. MR acknowledges the funding from the Spanish Ministry of Economy and Competitiveness (Project CTQ2012-33494) and from the Aragón Government (Fondo Social Europeo).

References

[1] C. M. Almeida, M. T. S. D. J. Vasconcelos, J Anal At Spectrom,16 (2001) 607 – 611.

[2] L. Balcaen, L. Moens, F. Vanhaecke, Spectrochim Acta, Part B, 65 (2010) 769 - 786.

[3] J. Irrgeher, T. Prohaska, R. E. Sturgeon, Z. Mester, L. Yang, Anal Methods, 5 (2013) 1687 - 1694.

[4] B. Y. Song, J. S. Ryu, H. S. Shin, K. S. Lee, J Agric Food Chem, 62 (2014) 9232 - 9238.

[5] J. Fietzke, A. Eisenhauer, Geochem Geophys Geosyst, 7 (2006) 1 - 6.

[6] F. Vanhaecke, L. Balcaen, D. Malinovsky, J Anal At Spectrom, 24 (2009) 863 - 886.

[7] J. S. Becker, H. J. Dietze, J. A. McLean, A. Montaser, Anal Chem, 71 (1999) 3077 - 3084.

[8] J. S. Becker, Int J Mass Spectrom, 242 (2005) 183 - 195.

[9] W. Neumann, E. Huster, Earth Planet Sci Lett, 33 (1976) 277 - 288.

[10] R. C. Capo, B. W. Stewart, O. A. Chadwick, Geoderma, 82 (1998) 197 - 225.

[11] F. Vanhaecke, G. De Wannemacker, L. Moens, J. Hertogen, J Anal At Spectrom, 14 (1999) 1691 - 1696.

[12] F. Begemann, K. R. Ludwig, G. W. Lugmair, K. Min, L. E. Nyquist, P. J. Patchett, P. R. Renne, C. Y. Shih, I. M. Villa, R. J. Walker, Geochim Cosmochim Acta, 65 (2001) 111 - 121.

[13] L. Moens, N. Jakubowski, Anal Chem, 70 (1998) 251A - 256A.

[14] N. Jakubowski, L. Moens, F. Vanhaecke, Spectrochim Acta, Part B, 53 (1998) 1739 - 1763.

[15] C. Latkoczy, T. Prohaska, G. Stingeder, M. Teschler-Nicola, J Anal At Spectrom, 13 (1998) 561 - 566.

[16] F. Vanhaecke, L. Moens, R. Dams, I. Papadakis, P. Taylor, Anal Chem, 69 (1997) 268 - 273.

[17] L. Balcaen, I. De Schrijver, L. Moens, F. Vanhaecke, Int J Mass Spectrom, 242 (2005) 251 – 255.

[18] P. Galler, A. Limbeck, S. F. Boulyga, G. Stingeder, T. Hirata, T. Prohaska, Anal Chem, 79 (2007) 5023 - 5029.

[19] D. De Muynck, G. Huelga-Suarez, L. Van Heghe, P. Degryse, F. Vanhaecke, J Anal At Spectrom, 24 (2009) 1498 - 1510.

[20] S. D. Tanner, V. I. Baranov, D. R. Bandura, Spectrochim Acta, Part B, 57 (2002) 1361 - 3452.

[21] S. F. Boulyga, J. S. Becker, Fresenius J Anal Chem, 370 (2001) 618 - 623.

[22] J. J. Sloth, E. H. Larsen, J Anal At Spectrom, 15 (2000) 669 - 672.

[23] Y. L. Chang, S. J. Jiang, J Anal At Spectrom, 16 (2001) 1434 - 1438.

[24] F. Vanhaecke, L. Balcaen, G. D. Wannemacker, L. Moens, J Anal At Spectrom, 17 (2002) 933 - 943.

[25] L. Moens, F. Vanhaecke, D. R. Bandura, V. I. Baranov, S. D. Tanner, J Anal At Spectrom, 16 (2001) 991 - 994.

[26] F. Vanhaecke, L. Balcaen, I. Deconinck, I. D. Schrijver, C. M. Almeida, L. Moens, J Anal At Spectrom, 18 (2003) 1060 - 1065.

[27] P. Cheng, G. K. Koyanagi, D. K. Bohme, Anal Chim Acta, 627 (2008) 148 - 153.

[28] D. R. Bandura, V. I. Baranov, S. D. Tanner, J Anal At Spectrom, 15 (2000) 921 - 928.

[29] M. Resano, P. Marzo, J. Pérez-Arantegui, M. Aramendía, C. Cloquet, F. Vanhaecke, J Anal At Spectrom, 23 (2008) 1182 - 1191.

[30] S. Stürup, Anal Bioanal Chem, 378 (2004) 273 - 282.

[31] M R. Flórez, M. Aramendía, M. Resano, A. C. Lapeña, L. Balcaen, F. Vanhaecke, J Anal At Spectrom, 28 (2013) 1005 - 1015.

[32] P. Rodríguez-González, J. M. Marchante-Gayón, J. I. García Alonso, A. Sanz-Medel, Spectrochim Acta, Part B, 60 (2005) 151 - 207.

[33] I. S. Begley, B. L. Sharp, J Anal At Spectrom, 12 (1997) 395 - 402.

[34] S. F. Boulyga, J. L. Matusevich, V. P. Mironov, V. P. Kudrjashov, L. Halicz, I. Segal, J. A. McLean, A. Montaser, J. S. Becker, J Anal At Spectrom, 17 (2002) 958 - 964.

[35] P. P. Coetzee, F. Vanhaecke, Anal Bioanal Chem, 383 (2005) 977 - 984.

[36] C. P. Ingle, B. L. Sharp, M. S. A. Horstwood, R. R. Parrish, D. J. Lewis, J Anal At Spectrom, 18 (2003) 219 - 229.

[37] L. Yang, Mass Spectrom Rev, 28 (2009) 990 - 1011.

[38] Q. Xie, R. Kerrich, J Anal At Spectrom, 17 (2002) 69 - 74.

[39] S. Díaz Fernández, N. Sigishama, J. Ruiz Encinar, A. Sanz-Medel, Anal Chem, 84 (2012) 5851 - 5857.

[40] L. Balcaen, E. Bolea-Fernandez, M. Resano, F. Vanhaecke, Anal Chim Acta, 809 (2014) 1 - 8.

[41] S. D. Tanner, V. I. Baranov, J Am Soc Mass Spectrom, 10 (1999) 1083 - 1094.

[42] X. Zhao, G. K. Koyanagi, D. K. Bohme, J Phys Chem A, 110 (2006) 10607 - 10618.

[43] E. Bolea-Fernandez, L. Balcaen, M. Resano, F. Vanhaecke, Anal Chem, 86 (2014) 7969 - 7977.

[44] E. Bolea-Fernandez, L. Balcaen, M. Resano, F. Vanhaecke, Anal Bioanal Chem, 407 (2015) 919 - 929.

[45] T. Ohno, Y. Muramatsu, Y. Shikamori, C. Toyama, N. Okabe, H. Matsuzaki, J Anal At Spectrom, 28 (2013) 1283 - 1287.

[46] M. Tanimizu, N. Sugiyama, E. Ponzevera, G. Bayon, J Anal At Spectrom, 28 (2013) 1372 - 1376.

[47] L. Balcaen, G. Woods, M. Resano, F. Vanhaecke, J Anal At Spectrom, 28 (2013) 33 - 39.

[48] T. Ohno, Y. Muramatsu, J Anal At Spectrom, 29 (2014) 347 - 351.

[49] J. Zheng, W. Bu, K. Tagami, Y. Shikamori, K. Nakano, S. Uchida, N. Ishii, Anal Chem, 86 (2014) 7103 - 7110.

[50] G. P. Russ, In. Applications of Inductively coupled Plasma Mass Spectrometry; A. R. Date, A. L. Gray, Ed.; Blackie: Glasgow, 1989.

[51] J. Kragten, Analyst, 119 (1994) 2161 - 2165.

CHAPTER 7

Laser ablation – tandem ICP – mass spectrometry (LA-ICP-MS/MS) for direct Sr isotopic analysis of solid samples with high Rb/Sr ratio

Adapted from Bolea-Fernandez et. al., J. Anal. At. Spectrom., 31 (2016) 464 – 472

7.1. Introduction

Strontium (Sr) isotopic analysis is a key tool for obtaining relevant information in many application areas – e.g., geochronological dating (Rb/Sr dating), obtaining other types of geochemical information, provenancing of, among other, agricultural products and archaeological objects, and animal and human migration studies.**[1]**

Accurate and precise determination of the isotopic composition of Sr *via* ICP-mass spectrometry is not self-evident, despite of the relatively more pronounced natural variation in its isotopic composition (coming from the radiogenic character of ^{87}Sr, i.e., β^- decay of ^{87}Rb into ^{87}Sr with a half-life $T_{1/2}$ of $4.88 \cdot 10^{10}$ years **[2]**),**[3]** in comparison to elements that only display natural variation as a result of isotope fractionation.**[4]** In fact, Sr is one of the only elements for which thermal ionization mass spectrometry (TIMS)**[5]** is preferred over multi-collector ICP-MS, as a result of the occurrence of spectral interference with the latter.**[6]** Besides the isobaric overlap of ^{87}Sr and ^{87}Rb at a mass-to-charge (m/z) ratio of 87,**[7]** the contamination of Ar with Kr will also induce isobaric overlap at m/z ratios 84 and 86. However, due to the increased sample throughput of MC-ICP-MS, the latter technique is gaining ground, compared to TIMS.**[8]** For the less demanding applications, also single-collector ICP-MS has been successfully used in this context.**[9-11]** In ICP-MS, pneumatic nebulization (PN) is the standard sample introduction system, although its use is limited to liquid or digested samples, while prior chemical separation of Sr and Rb is a must, and remaining Rb and Kr contamination of the Ar plasma gas need to be corrected for.**[12]** Laser ablation (LA) can be seen as an attractive alternative for this kind of analysis owing to the absence of sample preparation, minimal sample damage, efficient sample introduction, high sample throughput and the ability to perform spatially resolved analysis of selected sample regions.**[13-16]** However, Sr isotopic analysis by means of LA-ICP-MS is far from evident given the spectral interferences mentioned above.**[17, 18]**

Several approaches have been deployed to avoid or mitigate isobaric interference from ^{87}Rb and other spectral interferences (e.g., from Kr^+ and the polyatomic ions $ArCa^+$ and/or Ca^{2+}) affecting the measurement of the Sr isotopes.**[19]** Chemical isolation of Sr from the concomitant matrix elements can be regarded as the standard approach to overcome the spectral interferences in the isotopic analysis of Sr *via* PN-ICP-MS and it is considered imperative for samples with high Rb/Sr

ratio.**[20-22]** However, this approach is laborious and time-consuming, thus reducing sample throughput and increasing the risk of contamination. Moreover, the analysis of solid samples requires digestion, involving the use of concentrated mineral acids.

The use of high mass resolution (HR) in ICP-MS instrumentation equipped with a double-focusing sector field mass spectrometer is a powerful way to cope with spectral overlap,**[23, 24]** but, the maximum resolution attained by present-day commercially available instrumentation is limited to 10,000, which is by far insufficient to resolve the isobaric overlap of the signals of ^{87}Sr and ^{87}Rb ($R_{required}$ ~300,000),**[25]** thus limiting the applicability of LA-HR-ICP-MS to samples with a sufficiently low Rb/Sr ratio ≤ 0.2.**[26-28]** Even in those cases where the Rb/Sr ratio is low, both for PN-HR-ICP-MS (even after chemical Sr/Rb separation) and for LA-HR-ICP-MS, mathematical correction is required for the (remaining) Rb and the other spectral interferences mentioned above.**[29, 30]**

Also the use of a collision-reaction cell in quadrupole-based ICP-MS (ICP-QMS) is an elegant approach for overcoming spectral overlap and compared to HR-ICP-MS instrumentation, ICP-QMS still offers higher robustness at a lower purchase and maintenance cost. Several works to date have reported on the use of ICP-QMS for isotope ratio determination, mainly for the study of induced changes in the isotopic composition in the context of tracer experiments or elemental assay *via* isotope dilution mass spectrometry (IDMS),**[31]** but also for elements displaying a relatively large natural variation in their isotopic pattern (e.g., Li, B, Pb, Sr).**[11, 32, 33]** In modern ICP-QMS, equipped with a collison/reaction cell, isobaric overlap can be resolved *via* chemical resolution, by pressurizing the cell with a selective reactive gas that reacts differently with the interfering ion and the analyte ion, forming new reaction product ions and allowing interference-free determination.**[34, 35]** However, the number of works reporting on the use of ICP-QMS and LA-ICP-QMS using chemical resolution for interference-free isotopic analysis of elements suffering from strong spectral overlap is thus far very limited,**[36]** and no works to date have reported on their use for direct Sr isotopic analysis of solid samples with high Rb/Sr ratio. This might be attributed to the occurrence of new spectral

nterferences due to uncontrolled reactions in the cell, strong matrix effects, and the requirement of matrix-matching for mass bias correction.**[37-39]**

Recently (2012), a tandem ICP-MS device (ICP-MS/MS) has been introduced onto the market. This novel set-up allows for a better control of the reactions in the cell by removing all concomitant elements with a mass-to-charge (m/z) ratio that differs from that of the analyte ion by means of an additional quadrupole located before an octopole collision-reaction cell. After chemical reaction in the cell, the analyte ion can be measured interference-free at the original m/z ratio (conversion of the interfering ion) or at a different m/z ratio as a new reaction product ion *via* the use of a second quadrupole.**[40]** ICP-MS/MS with methyl fluoride (CH_3F) as reaction gas has been successfully applied to the interference-free determination of ultra-trace concentrations of several elements (e.g., transition metals in Chapter 3, and As and Se in Chapter 5),**[41, 42]** and more recently, for accurate and precise (0.05 % RSD) Sr isotopic analysis of digested geological materials (Chapter 6).**[43]** However, despite of the inherent benefits of tandem ICP-MS to avoid spectral overlap and the fast increase in the number of publications for elemental **[44-46]** and isotopic **[47-50]** analysis, only a few works to date have reported on the use of LA-ICP-MS/MS,**[51]** and according to the best of the authors' knowledge, no publications thus far have described the use of LA-ICP-MS/MS for isotopic analysis.

This work explores the capabilities of LA-ICP-MS/MS for Sr isotopic analysis, with the aim of obtaining direct isotopic information from solid samples with high (i.e., also > 0.2) Rb/Sr ratio.

7.2. Experimental

7.2.1. Instrumentation

An Analyte G2 (Teledyne CETAC Technologies, Omaha, USA) 193 nm ArF*excimer-based LA-unit, equipped with a HELEX 2 ablation cell, coupled to an Agilent 8800 tandem ICP-MS instrument (ICP-QQQ, Agilent Technologies, Japan) was used for all measurements. Two different sample introduction configurations, aimed at obtaining "dry" and "wet" plasma conditions, respectively, were evaluated. For "dry" plasma conditions, a standard LA-ICP-MS configuration was used. He was used as carrier gas, and Ar was added as a make-up gas downstream *via* a glass mixing

bulb between the ablation cell and the ICP torch. For "wet" plasma conditions, a Peltier-cooled Scott-type spray chamber (2°C) was inserted for the simultaneous introduction (*via* two different inlets) of the LA aerosol – previously mixed with Ar make-up gas in the glass mixing bulb – and milli-Q water aerosol, produced using a MicroMist nebulizer (400 µL min^{-1}). All connections were realized with 2 mm internal diameter PTFE tubing. See **Figure 7.1** for a detailed graphical representation of both approaches.

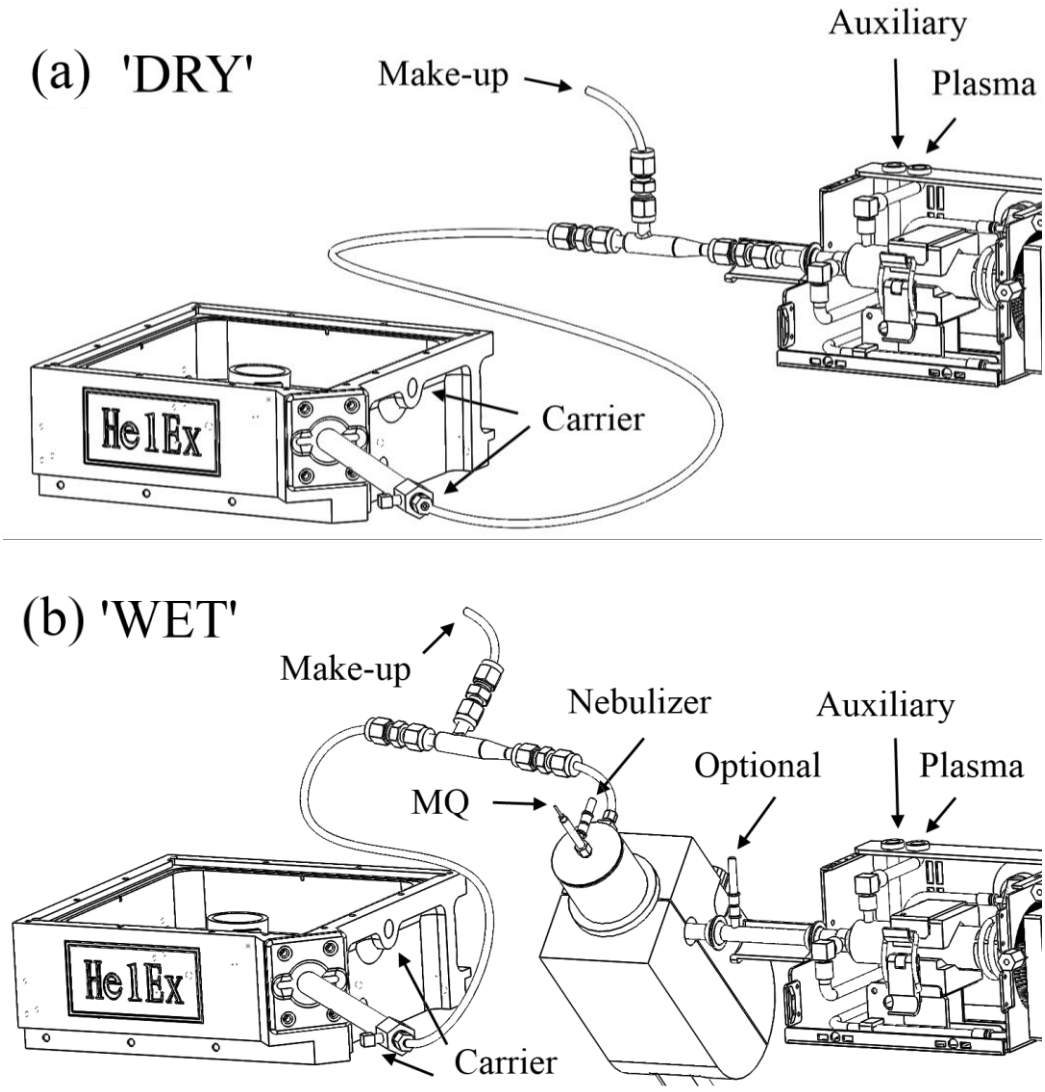

Figure 7.1. Graphic representation of the sample introduction set-ups and their gas flows for "dry" (a) and "wet" (b) plasma conditions

The octopole collision-reaction cell was pressurized with a mixture of CH_3F/He (1:9, Air Liquide, Belgium), introduced in a flow rate range of 0 - 1 mL min^{-1} (mass flow controller calibrated for O_2).

7.2.2. Samples and standards

7.2.2.1. *Standards and reagents*

The following standard reference materials (SRMs), available from NIST (National Institute of Standards and Technology, MD, USA), were selected for method development and mass bias correction purposes: SRM 610 and SRM 612 (trace elements in a glass matrix).**[52, 53]**

For "wet" plasma conditions, ultra-pure water (resistivity ≥ 18.2 MΩ cm) provided by a Milli Q Element water purification system (Millipore, France) was used.

7.2.2.2. *Samples*

7 geological reference materials (RMs) – MPI-DING (Max-Planck-Institut für Chemie, Germany) ATHO-G "rhyolite glass", MPI-DING T1-G "diorite glass", USGS (United States Geological Survey, VA, USA) BCR-2G "basalt glass", USGS BHVO-2G "basalt glass", USGS GSD-1G "basalt glass", USGS NKT-1G "nephelinite glass" and USGS TB-1G "basalt glass" were analyzed for their Sr isotopic composition. The selection was carried out in order to cover a wide range of $^{87}Sr/^{86}Sr$ isotope ratios, Sr concentrations and Rb/Sr ratios (see **Table 7.1**). The Rb/Sr ratios in the (MPI-DING, NIST and USGS) RMs used display a range from 0.02 to 0.82, the latter being considerably higher than the 0.2 maximum limit cited in earlier work. From the http://earthref.org/GERMRD **[54]** website, which summarizes data on the geochemistry of all reservoirs in the Earth, it can be seen that a Rb/Sr ratio > 1 is exceptional. The results were compared to preferred and/or compiled GeoReM reference values for validation.**[53]**

Table 7.1. Chemical composition of the reference materials (RMs) used in this work **[52, 53]**

Reference Material	Type	Sr ($\mu g\ g^{-1}$)	Rb ($\mu g\ g^{-1}$)	Al_2O_3 (% m/m)	CaO (% m/m)	FeO (% m/m)	K_2O (% m/m)	MgO (% m/m)	MnO (% m/m)	Na_2O (% m/m)	SiO_2 (% m/m)
NIST SRM 610	Silicate	515.5 ± 1	425.7 ± 1	2.039 ± 0.157	11.45 ± 0.231	0.056 ± 0.016	0.059 ± 0.002	0.065 ± 0.004	0.054 ± 0.005	13.352 ± 0.681	69.975 ± 0.391
NIST SRM 612	Silicate	78.4 ± 0.2	31.4 ± 0.4	2.11 ± 0.16	11.93 ± 0.22	0.02 ± 0.00	0.01 ± 0.00	0.00	0.01 ± 0.00	13.98 ± 0.56	71.90 ± 0.96
USGS BHVO-2G	Basalt	396 ± 1	9.2 ± 0.04	13.6 ± 0.1	11.4 ± 0.1	11.3 ± 0.1	0.51 ± 0.02	7.13 ± 0.02	0.17 ± 0.03	2.4 ± 0.1	49.3 ± 0.1
USGS NKT-1G	Nephelinite	1195 ± 57	30.7 ± 1.25	10.5	13.4	12.2	1.27	14.2	0.24	3.85	38.9
USGS TB-1G	Basalt	1352 ± 6	142 ± 0.5	17.12	6.7	8.67	4.52	3.51	0.18	3.56	54.29
USGS BCR-2G	Basalt	342 ± 4	47 ± 0.5	13.4 ± 0.4	7.06 ± 0.11	12.4 ± 0.3	1.74 ± 0.04	3.56 ± 0.09	0.19 ± 0.01	3.23 ± 0.07	54.4 ± 0.4
MPI-DING T1-G	Diorite	284 ± 6	79.7 ± 3.5	17.1 ± 0.2	7.1 ± 0.09	6.44 ± 0.06	1.96 ± 0.04	3.75 ± 0.04	0.127 ± 0.006	3.13 ± 0.09	58.6 ± 0.4
USGS GSD-1G	Basalt	69.4 ± 0.7	37.3 ± 0.4	13.4 ± 0.3	7.2 ± 0.1	13.3 ± 0.1	3 ± 0.1	3.6 ± 0.04	---	3.6 ± 0.2	53.2 ± 0.8
MPI-DING ATHO-G	Rhyolite	94.1 ± 2.7	65.3 ± 3	12.2 ± 0.02	1.7 ±0.03	3.27 ± 0.1	2.64 ± 0.09	0.103 ± 0.01	0.106 ± 0.005	3.75 ± 0.31	75.6 ± 0.7

7.2.3. *Procedure for Sr isotopic analysis via LA-ICP-MS/MS*

The instrument settings and data acquisition parameters used for Sr isotopic analysis *via* LA-ICP-MS/MS using both approaches i.e., under "dry" and "wet" plasma conditions, are summarized in **Table 7.2**.

Table 7.2. Instrument settings and data acquisition parameters for Sr isotopic analysis using LA-ICP-MS/MS in both "dry" and "wet" conditions

	"Dry" conditions	**"Wet" conditions**
Analyte G2 laser ablation system		
Energy density (J cm^{-2})	3.54	
Repetition rate (Hz)	40	
Scan speed (µm s^{-1})	15	
Beam waist diameter (µm)	20 – 85	
He carrier gas (L min^{-1})	0.42	
Agilent 8800 ICP-MS/MS		
Scan type	MS/MS	
RF power (W)	1550	
Sample depth (mm)	4.5	3.5
Ar plasma gas flow rate (L min^{-1})	15	
Ar auxiliary gas flow rate (L min^{-1})	0.90	
Ar nebulizer gas flow rate (L min^{-1})	---	1
Ar make-up gas (L min^{-1})	0.9	0.33
Water uptake rate (mL min^{-1})	---	0.30
Spray chamber temperature (°C)	---	2
CH_3F/He gas flow rate (mL min^{-1})	0.90	
Q1 →Q2 masses	86 → 105 87 → 106 88 → 107	
Energy discrimination (V)	-8.4	
Wait time offset (s)	0	
Acquisition parameters		
Dwell time per acquisition point (ms)	300	
Acquisition time per replicate measurement (s)	60	
Run time per replicate measurement (s)	60	75
Number of replicate measurements	12	
Total analysis time per sample (min)	13.55	15.55
Detector dead time (ns)	32.6 ± 0.3	

Prior to analysis, all RMs were embedded into epoxy resin (bisphenol A diglycidyl ether, Streurs, Denmark) and subsequently polished mechanically with SiC paper (P1200 to P4000) and colloidal silica suspension (40 nm grain size) to remove any surface feature.

NIST SRMs 610 and 612 were selected as the external standards for mass discrimination correction purposes. Each sample was analyzed 5 consecutive times in a standard-sample-standard sequence, corresponding to 6 and 5 analyses for standard and sample, respectively. 12 replicate measurements (line scans) were performed during each analysis. The raw ratios thus obtained were corrected for mass bias **[55]** using the double correction approach, consisting of internal correction assuming a constant $^{88}Sr/^{86}Sr$ isotope ratio (Russell law – **equation 1**), followed by sample-standard bracketing (SSB – **equation 2**).

$$R^{^{87}Sr/^{86}Sr}_{sample,corrected} = R^{^{87}Sr/^{86}Sr}_{sample,measured}\ x\ \left(\frac{m_{^{87}Sr}}{m_{^{86}Sr}}\right)^{f}\ ;\ f = \ln\left[\frac{R^{^{88}Sr/^{86}Sr}_{true}}{R^{^{88}Sr/^{86}Sr}_{measured}}\right] \Big/ \ln\left[\frac{m_{^{88}Sr}}{m_{^{86}Sr}}\right] \qquad (1)$$

$$R^{^{87}Sr/^{86}Sr}_{sample,corrected} = \left(\frac{R^{^{87}Sr/^{86}Sr}_{std,true}}{\frac{R^{^{87}Sr/^{86}Sr}_{std-1,measured} + R^{^{87}Sr/^{86}Sr}_{std+1,measured}}{2}}\right) x\ R^{^{87}Sr/^{86}Sr}_{sample,measured} \qquad (2)$$

where $m^{86,87,88}Sr$ are the atomic masses of the isotopes of interest and f is the mass bias correction factor. It has to be stressed that the $^{88}Sr/^{86}Sr$ isotope ratio is affected by natural isotope fractionation,**[56]** but the natural variation this gives rise to can be considered negligible within the precision attainable in this work. Furthermore, it has to be pointed out that no additional corrections were performed in this work (e.g., blank subtraction and/or mathematical equations for additional correction for spectral overlap), which further confirms the potential of the newly developed methodology for straightforward Sr isotopic analysis *via* LA-ICP-MS/MS.

7.3. Results and discussion

7.3.1. Optimization of conditions for Sr isotopic analysis of solid samples with high Rb/Sr ratio via LA-ICP-MS/MS

7.3.1.1. Use of chemical resolution to avoid spectral overlap

A mixture of CH_3F/He (1:9) was selected as the best suited reaction gas due to the high efficiency of the reaction with Sr – leading to the formation of SrF^+ ions – while Rb and Kr do not show reactivity towards CH_3F.**[37]** By using the capabilities provided by the MS/MS mode, all concomitant matrix ions with an m/z ratio different from that of the respective analyte ions, i.e., $^{86,87,88}Sr$, are removed by the first quadrupole (Q1), while the second quadrupole (Q2) is fixed at the m/z ratio of the new reaction product ions, i.e.,$^{86,87,88}SrF^+$ (see **Figure 7.2**).

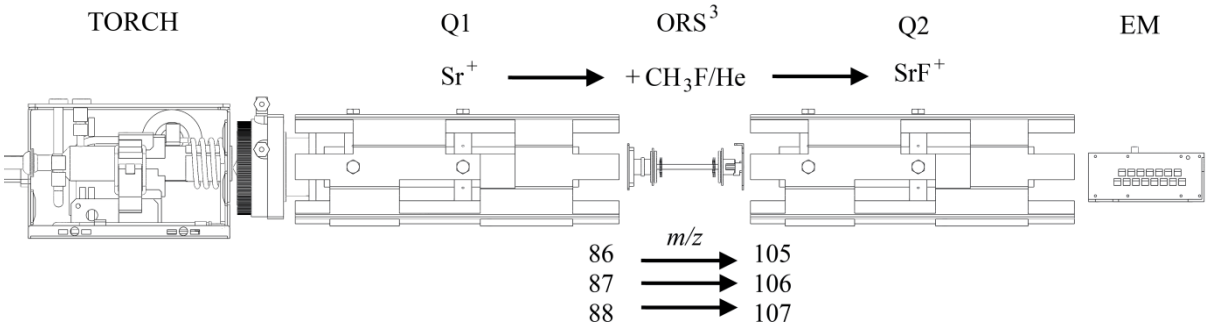

Figure 7.2. Schematic representation of the operating principle of tandem ICP–MS for interference-free Sr isotopic analysis *via* conversion of Sr into SrF^+. Q1 and Q2 represent the first and second quadrupole, while ORS^3 and EM are the acronyms for the type of collision-reaction cell (octopole reaction system 3rd generation), and detector (electron multiplier), respectively.

The CH_3F/He gas flow rate was optimized to obtain the maximum SrF^+ signal intensity, which was attained at 0.90 mL min^{-1}. The capabilities of the selected reaction gas mixture to overcome Sr/Rb isobaric overlap at m/z = 87 are documented in **Figure 7.3**, which represents the $^{87}Sr/^{86}Sr$ and $^{88}Sr/^{86}Sr$ isotope ratio results (left y-axis and right y-axis, respectively) as a function of the Rb/Sr ratio – for a set of 6 geological RMs in both, "vented" (no gas) and CH_3F/He mode.

Within the precision attainable in this work, no significant differences were found between the $^{88}Sr/^{86}Sr$ isotope ratio results in both gas modes, which indicates absence of additional fractionation produced by collisions and/or reactions in the cell, in contrast with what was observed in a previous work carried out with a quadrupole-based reaction cell.**[38]** As expected, the $^{87}Sr/^{86}Sr$ isotope ratios become increasingly biased high with rising Rb/Sr ratio in "vented" mode due $^{87}Sr/^{87}Rb$ isobaric overlap. However, the use of 0.90 mL min^{-1} of CH_3F/He suffices to remove the isobaric interference of ^{87}Rb, thus potentially allowing direct Sr isotopic analysis of solid samples with high Rb/Sr ratio *via* LA-ICP-MS/MS. Additionally, the presence of He in the gas mixture might lead to an improvement of the isotope ratio precision by the so-called collisional damping effect,**[57]** while the slowdown of the ion beam also has a positive effect on the reaction efficiency due to an increase of the residence time of the ions in the cell.**[41, 43]**

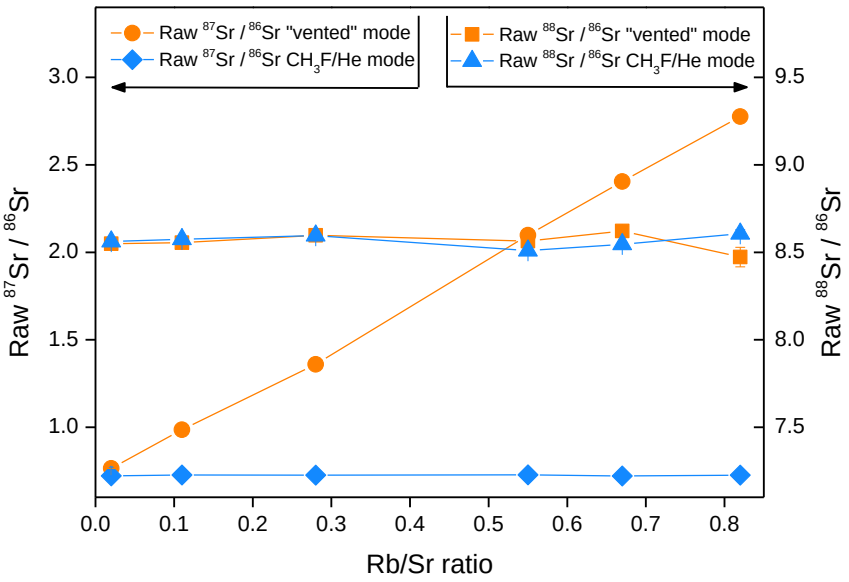

Figure 7.3. Influence of the Rb/Sr ratio on the raw $^{87}Sr/^{86}Sr$ (left y-axis) and $^{88}Sr/^{86}Sr$ (right y-axis) isotope ratios for "vented" (orange) and CH_3F/He (blue) modes

7.3.1.2. Optimization of operational conditions

Isotopic analysis *via* LA-ICP-MS has been carried out in both "dry" and "wet" mode.**[11]** The use of "wet" plasma conditions, derived by the simultaneous introduction of an aqueous solution into the ICP, brings about several advantages. An internal standard can be admixed for mass bias correction, standard solutions can be introduced for calibration purposes and overall, a higher robustness, thus better signal stability, have been reported as a result of a lighter effect of the introduction of ablated material on the plasma stability.**[58-60]**

In this work, the carrier gas transporting the aerosol produced in the ablation process was introduced into the spray chamber, *via* the make-up gas inlet (see **Figure 7.1B**). No other changes to the introduction system are required, thus facilitating transition to PN-ICP-MS/MS for other applications in routine laboratories. Of course, it has to be stressed that the use of "wet" plasma conditions involves an increase in the level of oxide species, which might aggravate the accuracy for elements suffering from oxide-based polyatomic interferences.

For both introduction system approaches (see also **Figure 7.1**), ablation conditions and data acquisition parameters were optimized in order to obtain the best transient signal stability – leading to the best internal precision – without compromising isotope ratio accuracy and/or sample throughput. NIST SRM 610 was the standard selected for optimization purposes due to its relatively high homogeneity. First, the influence of dwell time on the accuracy and precision of the Sr isotope ratios was assessed. The results obtained are presented in **Figure 7.4A**, which shows the RSD (%, left y-axis) and $^{87}Sr/^{86}Sr$ isotope ratio (right y-axis) as a function of dwell time (2 - 500 ms) for both "dry" (red) and "wet" (blue) modes. As can be seen, the RSD (%) improves clearly with the increase in dwell time until a constant value was reached at ~300 - 400 ms. The same trend was found for both plasma conditions, although better signal stability was achieved in "wet" mode, which as indicated above, can be attributed to the reduction of fluctuations in plasma load. To evaluate whether the improvement in precision observed under "wet" conditions, was truly owing to the wet plasma conditions and not merely to a change in sample aerosol trajectory, possibly affecting the particle size distribution, the "wet" setup was also assessed without co-nebulized water. The results obtained under these conditions show an RSD per replicate measurement of 2.50 ± 0.30 %,

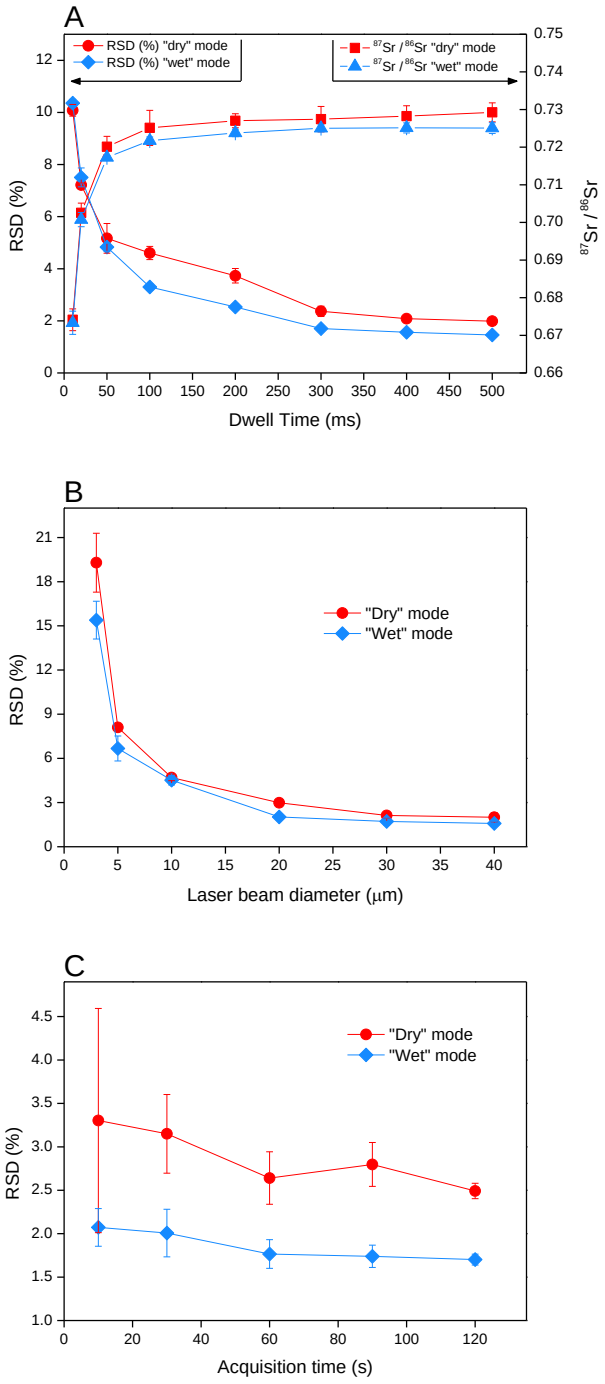

Figure 7.4. **(A)** RSD (%) – left y-axis – and $^{87}Sr/^{86}Sr$ isotope ratio – right y-axis – as a function of the dwell time in both "dry" (red) and "wet" (blue) conditions. **(B)** RSD (%) per replicate measurement as a function of laser beam diameter (μm) using NIST SRM 610 in both "dry" and "wet" conditions. **(C)** RSD (%) per replicate measurement as a function of acquisition time (s) for NIST SRM 610 analyzed in both "dry" and "wet" conditions. In all figures, each point corresponds with the average and standard deviation of 3 replicate measurements.

which is not significantly different from that obtained with the “dry” configuration, thus illustrating the added value of “wet” plasma conditions. On the other hand, variation in the $^{87}Sr/^{86}Sr$ ratio was established at low dwell times, and only at values ≥ 300 ms, the ratio appears to have stabilized. This tendency was also observed in a previous work (Chapter 6),**[43]** in which it was demonstrated that a wait time offset (WTO) of 5 ms suffices to stabilize the Sr isotope ratios at low dwell times. No such effect was observed for dwell times ≥300 ms. These observations can most probably be attributed to the additional time required for stable interaction between the ions and a reactive gas such as CH_3F in the cell. Based on these results, 300 ms was selected as dwell time and used throughout further work. It can also be seen from **Figure 7.4A**, that the raw $^{87}Sr/^{86}Sr$ isotope ratios (before mass bias correction) are clearly biased towards a higher value with respect to the reference value (recommended value for NIST SRM 610 = 0.709699 ± 0.000018 **[53]**), even more in "dry" plasma conditions.**[59]**

Another important prerequisite for successful isotopic analysis is sufficient signal intensity (cf. counting statistics). Maximum sensitivity was found when using the instrument settings summarized in **Table 7.2**. The detector dead time was experimentally determined to be 32.6 ± 0.3 ns. In both modes, the signal intensity was varied by changing the laser beam diameter. **Figure 7.4B** shows how the RSD (%) per replicate measurement (the experiment was repeated 3 times) varies as a function of the laser beam diameter. The results further confirm a better precision in "wet" mode, and in general, it can be seen that for a laser beam diameter ≤20 µm (beam waist size, corresponding to ~5 x 10^5 counts/s for NIST SRM 610), the precision is degraded due to poor counting statistics. Thus, in further experiments, the laser beam diameter was adjusted such that for all standards and samples a ^{88}Sr signal intensity of approximately 6 x 10^5 cps was obtained (the system response for NIST SRM 610 using a laser beam diameter of 25 µm) as to prevent the dual-mode discrete dynode detector from switching between counting and analog mode.

Finally, the effect of different acquisition times on the signal stability (expressed as the RSD (%) per replicate measurement) was evaluated. The results are shown in **Figure 7.4C**, from which once more, it can be seen that the precision in "wet" mode is better than that in "dry" mode. The average RSD (%) values seem to stabilize for

acquisition times ≥60 s, but the variation in RSD values obtained for different replicate measurements, is lower at higher acquisition times (**Figure 7.4C**). A compromise between precision and acquisition time was found at 60 s, although longer acquisition times can be used to increase the final precision. It has to be taken into account that although 60 s of acquisition time was selected, differences in stabilization and washout time in "dry" and "wet" mode were present, leading to run times per replicate measurement of 65 and 75 s, respectively.

7.3.1.3. Figures of merit for Sr isotope ratio measurements via LA-ICP-MS/MS

Once the instrument settings and data acquisition parameters were optimized as indicated above, the figures of merit for Sr isotopic analysis were evaluated. The accuracy and precision of the approach developed was tested by means of the determination of the $^{87}Sr/^{86}Sr$ isotope ratio in NIST SRM 610. As explained in section 2.3, 12 replicate measurements were performed for each analysis, which was repeated 5 times in a standard-sample-standard sequence. NIST SRM 612 (laser beam diameter of 85 μm) was selected as external standard for mass discrimination correction purposes – double correction approach, after internal correction *via* the Russell law (see section 7.2.3 for a detailed explanation of the mass bias correction). **Figure 7.5** represents the average value (black lines), internal precision (error bars) and external precision (black dashed lines) for the Sr isotope ratios in both “dry” and “wet” plasma modes. The green line indicates the reference value. Accurate results were obtained in both approaches, with $^{87}Sr/^{86}Sr$ isotope ratio values of 0.70945 ± 0.00121 and 0.70968 ± 0.00035 for “dry” and “wet” plasma conditions, respectively (recommended value = 0.709699 ± 0.000018,**[53]** green line in **Figure 7.5**). However, as was already expected from the conclusions drawn during optimization, the results obtained in “wet” plasma mode show a significant improvement in internal precision (expressed as within-run precision and defined as the standard deviation for 12 replicate measurements within a single analysis) and external precision (expressed as the standard deviation for 5 consecutive analyses). An internal precision in the range of 0.30 – 0.43 % (RSD) was achievable for “dry” and of 0.09 – 0.16 % (RSD) for “wet” conditions (~2.5-fold improvement for “wet” plasma mode). These values are in good agreement with those reported in the literature for LA-ICP-QMS,**[11]** and similar to the isotope

ratio precision attained using ICP-MS/MS for liquid/digested samples (Chapter 6).**[43]** Once again, it was verified whether the “wet” plasma conditions rather than the different trajectory followed by the sample aerosol were at the origin of the improvement in precision observed. The “wet” setup was also assessed without co-nebulized water. Under these conditions, the RSD (%) obtained is not significantly different from that obtained using the "dry" approach (0.30 – 0.43 %), demonstrating that the improvement in precision can be attributed to "wet" plasma conditions.

External precision values of 0.17 and 0.05 % RSD were obtained for “dry” and “wet” plasma modes, respectively (~3-fold improvement for “wet” plasma mode). It has to be pointed out that accurate and precise results were obtained in spite of the high Rb/Sr ratio in NIST SRM 610 and 612 (~0.82 and 0.40, respectively), and the differences in Sr concentration between both materials (78.4 ± 0.2 and 515.5 ± 1 μg g^{-1}, respectively). Based on those results, LA-ICP-MS/MS operated under “wet” plasma conditions was selected as the more suitable approach and was used throughout the further work.

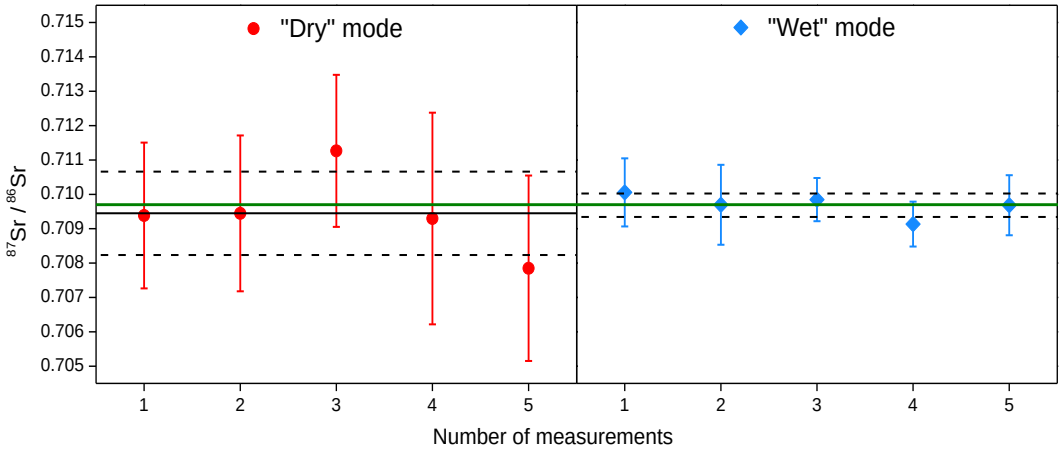

Figure 7.5. $^{87}Sr/^{86}Sr$ isotope ratio results obtained for NIST SRM 610 after double mass bias correction (Russell law followed by SSB using NIST SRM 612 as external standard) upon 5 replicate analyses in both "dry" and "wet" conditions. The error bars indicate the standard deviation of 12 replicate measurements (within-run precision). The black and dashed lines correspond with, respectively, the average and standard deviation (external precision) of 5 replicate analyses. The green line represents the recommended $^{87}Sr/^{86}Sr$ isotope ratio for NIST SRM 610.**[53]**

7.3.2. Proof-of-concept: Sr isotopic analysis of geological RMs

The same protocol for Sr isotopic analysis *via* LA-ICP-MS/MS under "wet" plasma conditions was applied to 7 geological RMs. This selection of RMs has been made in order to be able to demonstrate the capabilities of the approach developed for a wide range of (i) Rb/Sr ratio, (ii) matrix composition and (iii) Sr concentration (see **Table 7.1** and **7.3**). NIST SRM 610 was used as the external standard for mass bias correction purposes. The results are summarized in **Table 7.3**.

No significant differences were found between the $^{87}Sr/^{86}Sr$ ratios obtained in this work and the corresponding literature values, even for those materials with high Rb/Sr ratio (total range in materials studied: 0.02 – 0.82). In addition, from the comparison with the results obtained in section 7.3.1.3 for NIST SRM 610, the attainable precision does not seem to be affected by the matrix, and external precision values in the range of 0.024 – 0.054 % RSD (n = 5) are reported in **Table 7.3**. It is very important to note that no further sample/standard matrix-matching was required despite the differences in matrix composition (see **Table 7.1**). Also, no additional correction for remaining spectral overlap was required. Therefore, these results further illustrate the capabilities of the approach developed for accurate and precise Sr isotopic analysis of solid samples with high Rb/Sr ratio *via* LA-ICP-MS/MS.

Table 7.3. Results obtained upon Sr isotopic analysis *via* LA-ICP-MS/MS

Reference Material	Type	Laser beam diameter (μm)	Rb/ Sr ratio	Experimental $^{87}Sr/^{86}Sr$	RSD (%)	Recommended $^{87}Sr/^{86}Sr$ [53]
USGS BHVO-2G	Basalt	30	0.02	0.70351 ± 0.00034	0.048	0.703469 ± 0.000007
USGS NKT-1G	Nephelinite	25	0.03	0.70363 ± 0.00017	0.024	0.703509 ± 0.000019
USGS TB-1G	Basalt	20	0.11	0.70576 ± 0.00030	0.042	0.705580 ± 0.000023
USGS BCR-2G	Basalt	30	0.14	0.70486 ± 0.00038	0.054	0.705003 ± 0.000004
MPI-DING T1-G	Diorite	40	0.28	0.70990 ± 0.00035	0.049	0.710093 ± 0.000017
USGS GSD-1G	Basalt	85	0.55	0.70924 ± 0.00029	0.040	0.709416 ± 0.000050
MPI-DING ATHO-G	Rhyolite	65	0.67	0.70310 ± 0.00026	0.036	0.703271 ± 0.000015

7.4. Conclusion

For the first time ever (to the best of the authors' knowledge), this work reports on the direct Sr isotopic analysis of solid samples with high Rb/Sr ratio by means of a combination of laser ablation and tandem ICP – mass spectrometry. The use of chemical resolution – using 0.90 mL min^{-1} of a CH_3F/He mixture as reaction gas – in a LA-ICP-MS/MS system operated under "wet" plasma conditions, suffices to overcome $^{87}Sr/^{87}Rb$ isobaric overlap and to obtain accurate and precise (~0.05% RSD, external precision) isotope ratio results, independent of the matrix composition, Sr concentration and/or Rb/Sr ratio within the range of materials studied. Instrumental mass discrimination was corrected for by a combination of internal correction relying on the Russell law, followed by external correction in an SSB approach. One glass CRM (NIST SRM 610) was used as external standard for all geological RMs investigated – no closer matrix-matching or additional correction for remaining spectral overlap was required. The straightforward methodology developed in this work is a real alternative for the more common approaches dealing with Sr isotopic analysis, and the results obtained suggest its applicability in many real-life applications in routine laboratories, e.g., for pre-selecting samples for subsequent higher-precision isotopic analysis *via* TIMS or MC-ICP-MS.

Acknowledgements

The UGent authors acknowledge Agilent Technologies for providing them with an ACT-UR research project grant, the Special Research Fund of Ghent University (BOF-UGent) for providing research funding and Teledyne Cetac Technologies for financial support for their LA-ICP-MS research projects. SVM is a PhD fellow of the Flemish Research Foundation (FWO - Vlaanderen). MR acknowledges the funding from the Spanish Ministry of Economy and Competitiveness (Project CTQ2012-33494) and from the Aragón Government (Fondo Social Europeo). The authors thank Dr. Steven Goderis (VUB and UGent) for providing them with the USGS geochemical reference materials.

References

[1] R. A. Bentley, J Archaeol Method Th, 13 (2006) 135 - 187.

[2] W. Neumann, E. Huster, Earth Planet Sci Lett, 33 (1976) 277 - 288.

[3] F. Begemann, K. R. Ludwig, G. W. Lugmair, K. Min, L. E. Nyquist, P. J. Patchett, P. R. Renne, C.-Y. Shih, I. M. Villa, R. J. Walker, Geochim Cosmochim Acta, 65 (2001) 111 - 121.

[4] F. Vanhaecke, L. Balcaen, D. Malinovsky, J Anal At Spectrom, 24 (2009) 863 - 886.

[5] L. Font, G. van der Peijl, I. v. Wetten, P. Vroon, B. van der Wagt, G. DAvies, J Anal At Spectrom, 27 (2012) 719 - 732.

[6] F. Vanhaecke, L. Moens, Anal Bioanal Chem, 378 (2004) 232 - 240.

[7] P. Cheng, G. K. Koyanagi, D. K. Bohme, Anal Chim Acta, 627 (2008) 148 - 153.

[8] C. B. Douthitt, Anal Bioanal Chem, 390 (2008) 437 - 440.

[9] F. Vanhaecke, G. D. Wannemacker, L. Moens, J. Hertogen, J Anal At Spectrom, 14 (1999) 1691 - 1696.

[10] C. M. Almeida, M. T. S. D. Vasconcelos, J Anal At Spectrom, 16 (2001) 607 - 611.

[11] M. Aramendía, M. Resano, F. Vanhaecke, J Anal At Spectrom, 25 (2010) 390 - 404.

[12] S. R. Copeland, M. Sponheimer, P. J. L. Roux, V. Grimes, J. A. Lee-Thorp, D. J. de Ruiter, M. P. Richards, Rapid Commun Mass Spectrom, 22 (2008) 3187 - 3194.

[13] J. S. Becker, J Anal At Spectrom, 17 (2002) 1172 - 1185.

[14] B. Hattendorf, C. Latkoczy, D. Günther, Anal Chem (2003) 341A - 347A.

[15] M. Resano, E. García-Ruiz, F. Vanhaecke, Mass Spectrom Rev, 29 (2010) 55 - 78.

[16] R. E. Russo, X. Mao, J. J. Gonzalez, V. Zorba, J. Yoo, Anal Chem, 85 (2013) 6162 - 6177.

[17] T. Waight, J. Baker, D. Peate, Int J. Mass Spectrom, 221 (2002) 229 - 244.

[18] A. Simonetti, M. R. Buzon, R. A. Creaser, Archaeometry, 2 (2008) 371 - 385.

[19] F. C. Ramos, J. A. Wolff, D. L. Tollstrup, Chem Geol, 211 (2004) 135 - 158.

[20] P. Galler, A. Limbeck, S. F. Boulyga, G. Stingeder, T. Hirata, T. Prohaska, Anal Chem, 79 (2007) 5023 - 5029.

[21] D. D. Muynck, G. Huelga-Suarez, L. Van Heghe, P. Degryse, F. Vanhaecke, J Anal At Spectrom, 24 (2009) 1498 - 1510.

[22] S. J. Romaniello, M. P. Field, H. B. Smith, G. W. Gordon, M. H. Kim, A. D. Anbar, J Anal At Spectrom, 30 (2015) 1906 - 1912.

[23] F. Vanhaecke, L. Moens, R. Dams, I. Papadakis, P. Taylor, Anal Chem, 69 (1997) 268 - 273.

[24] N. Jakubowski, L. Moens, F. Vanhaecke, Spectrochim Acta, Part B, 53 (1998) 1739 - 1763.

[25] L. Moens, N. Jakubowski, Anal Chem, 70 (1998) 251A - 256A.

[26] J. N. Christensen, A. N. Halliday, D.-C. Lee, C. M. Hall, Earth Planet Sci Lett, 136 (1995) 79 - 85.

[27] J. Davidson, F. Tepley III, Z. Palacz, S. Meffan-Main, Earth Planet Sci Lett, 184 (2001) 427 - 442.

[28] K. P. Jochum, B. Stoll, U. Weis, D. V. Kuzmin, A. V. Sobolev, J Anal At Spectrom, 24 (2009) 1237 - 1243.

[29] L. Balcaen, I. D. Schrijver, L. Moens, F. Vanhaecke, Int J Mass Spectrom, 242 (2005) 251 - 255.

[30] P. Z. Vroon, B. van der Wagt, J. M. Koornneef, G. R. Davies, Anal Bioanal Chem, 390 (2008) 465 - 476.

[31] P. Rodríguez-González, J. M. Marchante-Gayón, J. I. García Alonso, A. Sanz-Medel, Spectrochim Acta, Part B, 60 (2005) 151 - 207.

[32] S. A. Crowe, B. J. Fryer, I. M. Samson, J. E. Gagnon, J Anal At Spectrom, 18 (2003) 1331 - 1338.

[33] P. P. Coetzee, F. Vanhaecke, Anal Bioanal Chem, 383 (2005) 977 - 984.

[34] S. D. Tanner, V. I. Baranov, J Am Soc Mass Spectrom, 10 (1999) 1083 - 1094.

[35] S. D. Tanner, V. I. Baranov, D. R. Bandura, Spectrochim Acta, Part B, 57 (2002) 1361 - 3452.

[36] J. J. Sloth, E. H. Larsen, J Anal At Spectrom, 15 (2000) 669 - 672.

[37] L. J. Moens, F. F. Vanhaecke, D. R. Bandura, V. I. Baranov, S. D. Tanner, J Anal At Spectrom, 16 (2001) 991 - 994.

[38] F. Vanhaecke, L. Balcaen, I. Deconinck, I. D. Schrijver, C. M. Almeida, L. Moens, J Anal At Spectrom, 18 (2003) 1060 - 1065.

[39] M. Resano, P. Marzo, M. Pérez-Arantegui, M. Aramendía, C. Cloquet, F. Vanhaecke, J Anal At Spectrom, 23 (2008) 1182 - 1191.

[40] L. Balcaen, E. Bolea-Fernandez, M. Resano, F. Vanhaecke, Anal Chim Acta, 894 (2015) 7 - 19.

[41] E. Bolea-Fernandez, L. Balcaen, M. Resano, F. Vanhaecke, Anal Chem, 86 (2014) 7969 - 7977.

[42] E. Bolea-Fernandez, L. Balcaen, M. Resano, F. Vanhaecke, Anal Bioanal Chem, 407 (2015) 919 - 929.

[43] E. Bolea-Fernandez, L. Balcaen, M. Resano, F. Vanhaecke, J Anal At Spectrom, 31 (2016) 303 - 310.

[44] S. Díaz Fernández, N. Sigishama, J. R. Encinar, A. Sanz-Medel, Anal Chem, 84 (2012) 5851 - 5857.

[45] L. Balcaen, E. Bolea-Fernandez, M. Resano, F. Vanhaecke, Anal Chim Acta, 809 (2014) 1 - 8.

[46] C. D. B. Amaral, R. S. Amais, L. L. Fialho, D. Schiavo, T. Amorim, A. R. A. Nogueira, F. R. P. Rocha, J. A. Nóbrega, Anal Methods, 7 (2015) 1215 - 1220.

[47] L. Balcaen, G. Woods, M. Resano, F. Vanhaecke, J Anal A. Spectrom, 28 (2013) 33 - 39.

[48] M. Tanimizu, N. Sugiyama, E. Ponzevera, G. Bayon, J Anal At Spectrom, 28 (2013) 1372 - 1376.

[49] J. Zheng, W. Bu, K. Tagami, Y. Shikamori, K. Nakano, S. Uchida, N. Ishii, Anal Chem, 86 (2014) 7103 - 7110.

[50] T. Ohno, Y. Muramatsu, J Anal At Spectrom, 29 (2014) 347 - 351.

[51] D. P. Bishop, D. Clases, f. Fryer, E. Williams, S. Wilkins, D. J. Hare, N. Cole, U. Karst, P. A. Doble, J Anal At Spectrom, 31 (2015) 197 - 202.

[52] N. J. G. Pearce, W. T. Perkins, J. A. Westgate, M. P. Gorton, S. E. Jackson, C. R. Neal, S. P. Chenery, Geostand Newsl, 21 (1996) 115 - 144.

[53] GeoReM, http://georem.mpch-mainz.gwdg.de (accessed September 2015).

[54] GERM Reservoir Database, http://earthref.org/GERMRD (accessed October 2015).

[55] L. Yang, Mass Spectrom Rev, 28 (2009) 990 - 1011.

[56] J. Irrgeher, T. Prohaska, R. E. Sturgeon, Z. Mester, L. Yang, Anal Methods, 5 (2013) 1687 - 1694.

[57] D. R. Bandura, V. I. Baranov, S. D. Tanner, J Anal At Spectrom, 15 (2000) 921 - 928.

[58] C. O'Connor, B. L. Sharp, P. Evans, J Anal At Spectrom, 21 (2006) 556 - 565.

[59] M. Resano, M. P. Marzo, R. Alloza, C. Saéz, F. Vanhaecke, L. Yang, S. Willie, R. E. Sturgeon, Anal Chim Acta, 677 (2010) 55 - 63.

[60] M. R. Flórez, M. Aramendía, M. Resano, A. C. Lapeña, L. Balcaen, F. Vanhaecke, J Anal At Spectrom, 28 (2013) 1005 - 1015.

Summary and general conclusions

In this work, a detailed description of the operating principles of a novel technique, tandem ICP – mass spectrometry, has been provided, along with a description of the analytical method development required to enable accurate, sensitive and precise (ultra)trace elemental and isotopic analysis in a variety of sample matrices. As the first commercially available ICP-MS/MS instrument (Agilent 8800) was only introduced in 2012, the aim of this work was a characterization and evaluation of the figures of merit of this technique and its application range. Throughout the work, the differences between tandem ICP-MS and the more conventional quadrupole-based ICP-MS instrumentation have been clearly indicated.

The first chapter of this PhD dissertation can be seen as a tutorial on how to operate ICP-MS/MS instruments as well as an illustration of the reasons to select this technique. Special attention has been paid to the different operation modes (SQ and MS/MS) allowed for by this novel configuration and to the different approaches that can be used to avoid spectral overlap (on-mass and mass-shift).

In the following chapters, O_2, NH_3 and CH_3F have been evaluated as potential reaction gases for the reduction of spectral overlap. From a general point of view, O_2 can be seen as one of the most common reaction gases used in CRC systems, probably owing to the easy identification of the best suited reaction product ions, i.e. MO^+ (+16 amu) and MO_2^+ (+32 amu). However, the predictable reactivity of O_2 could also be seen as a disadvantage in the case these reaction product ions are affected by spectral interference (as described in Chapter 2 for TiO^+). The use of more reactive gases, such as NH_3, may be a good alternative. In single-quadrupole instrumentation, the high reactivity of NH_3 has typically limited its applicability to on-mass approaches, in which interfering ions are removed after reaction towards NH_3 gas, while the target ions can be measured at their original m/z ratios. The introduction of ICP-MS/MS and its capability to perform product ion scans clearly opens up new possibilities. Its operation in product scanning mode also enables a straightforward systematic evaluation of the product ions formed upon reaction of the analyte ion with the reaction gas (mass-shift). This type of approach has been successfully deployed in this work for the interference-free determination of Ti via monitoring of the signal of the $Ti(NH_3)_6^+$ reaction product ions.

In some cases, however, the high reactivity of NH_3, including charge transfer reactions ($M^+ + NH_3 \rightarrow M + NH_3^+$) and the formation of sometimes many NH_3 clusters ($M(NH_3)_a^+$) could give rise to complex spectra and a spread of the original intensity over a multitude of peaks.

As an alternative, the behavior of the less common but highly reactive gas CH_3F has been carefully evaluated. While in single-quad ICP-CRC-MS systems, CH_3F has only been scarcely used as a reaction gas, the results obtained in this work show its great capabilities for dealing with spectral overlap. Different reaction pathways occur, resulting in CH_3F addition ($M(CH_3F)_a^+$), fluorination (MF^+), and the combination of both ($MF_a(CH_3F)_b^+$), as described in chapters 3 and 4. Furthermore, more selective reactions, like HF elimination after CH_3F addition (MCH_2^+), are described in Chapter 5 for As and Se determination. In chapter 6 and 7, fluorination (MF^+) has been found as a particularly useful approach to allow for an interference-free determination of the $^{87}Sr/^{86}Sr$ isotope ratio.

The methods developed in this work using different approaches and reaction gases have been successfully applied to different biomedical, environmental and geological applications, as described in detail in the different chapters.

In chapter 2, accurate and precise determination of ultra-trace levels of Ti (LoD < 3 ng L^{-1}) in human serum samples has been achieved after conversion of Ti^+ ions into $Ti(NH_3)_6^+$ ions by using NH_3/He as a reaction gas, while it was shown that the use of O_2 does not suffice to overcome all spectral interferences. The accuracy of the method developed has been evaluated by analysis of a Seronorm Trace Element Serum L-1 reference material. As a proof-of-concept, the method has been successfully applied to real samples from individuals with and without Ti-based implants. The typical basal Ti level in human serum is found to be <1 µg L^{-1}, while values in the range of 2 to 6 µg L^{-1} were observed for implanted patients.

The potential of CH_3F (a mixture of 10% CH_3F in 90% He) as a reaction gas has been evaluated for the first time in ICP-MS/MS. Via product ion scanning, the best reaction product ions formed upon reaction of CH_3F with Al, Co, Cr, Mn, Ni, Ti and V were found to be $AlCH_3F^+$, $CoCH_3F^+$, $Cr(CH_3F)_2^+$, $MnCH_3F^+$, $Ni(CH_3F)_2^+$, $TiF_2(CH_3F)_3^+$ and $VF_2(CH_3F)_3^+$. Different reaction pathways have been observed as a function of (i) target nuclide and (ii) CH_3F/He gas flow rate. Interference-free ICP-MS/MS single element assay protocols were developed for all target elements during

this work, as well as a multi-element method under compromise conditions, with LoDs for all elements below 10 ng L^{-1}. The results obtained with this method for Seronorm blood serum and urine reference materials were in excellent agreement with the corresponding reference values and/or results obtained using SF-ICP-MS. This does not only show the potential of CH_3F as a reaction gas in ICP-MS, but also the capabilities of ICP-MS/MS to systematically characterize the complex reactions taking place in a reaction cell in a very straightforward way.

The use of CH_3F as a reaction gas has been further explored in the context of the determination of ultra-trace concentrations of prosthesis-related metals (Al, Ti, V, Co, Cr, Ni, Sr and Zr) in whole blood (chapter 4). The method has been applied to evaluate the suitability of a novel sample collection approach, volumetric absorptive micro-sampling (VAMS). Instrumental LoDs between 0.3 and 30 ng L^{-1} were obtained in a multi-element approach. The accuracy of the method has been demonstrated via successful analysis of Seronorm Whole Blood L-1 and L-3 reference materials, and of real venous blood samples spiked with the target elements at different concentration levels (5 to 50 µg L^{-1}). Although from the result of this work it can be seen that the use of VAMS devices introduces contamination problems for Al, Cr and Ni, the method developed shows potential for future real-life routine application in the case of Ti, V, Co, Sr and/or Zr.

As described before, As and Se (chapter 5) undergo CH_3F addition followed by HF elimination, upon reaction with CH_3F. This renders $AsCH_2^+$ and $SeCH_2^+$ (+14 amu) as the respective favored reaction product ions. By using this approach, instrumental LoDs of 0.2 ng L^{-1} and below 10 ng L^{-1} were obtained for As and Se, respectively. The method developed is able to overcome the strong spectral overlap from $ArCl^+$ and Ar_2^+ polyatomic interferences, as well as other possible spectral interferences (as was evaluated by using synthetic matrices). Via external calibration using Te as internal standard, accurate results were obtained for reference materials from plant, animal and environmental origin, independent of the sample matrix and/or analyte concentration. The high efficiency of the reaction between As and CH_3F and the possibility to use the major isotope of Se provides enhanced detection power in comparison to other techniques, such as SF-ICP-MS.

Next to elemental analysis, another objective of this PhD thesis was the evaluation of ICP-MS/MS in the context of isotopic analysis. Although the precision attainable via quadrupole-based ICP-MS instruments is rather modest, especially when

compared to multi-collector ICP-MS, for some elements and/or for tracer studies, the precision of ICP-QMS can be fit-for-purpose. Isotopic analysis necessitates the interference-free determination of at least two isotopes of the same element. For Sr isotopic analysis, chemical resolution in ICP-MS/MS was used to avoid the isobaric interference of ^{87}Rb on ^{87}Sr. In chapter 6, it is shown that by conversion of Sr^+ ions into SrF^+ reaction product ions (Rb does not react towards CH_3F), the Sr isotopic pattern can be preserved, thus avoiding the necessity of an isolation step to separate Sr from the matrix, preceding the analysis. After mass discrimination correction by using a combination of internal (Russell law, assuming a constant $^{88}Sr/^{86}Sr$ isotope ratio) and external correction (using the isotopic reference material NIST SRM 987 $SrCO_3$ in a SSB approach), this method enables the accurate determination of $^{87}Sr/^{86}Sr$ isotope ratio in digested geological material. In contrast to previous work with a single quadrupole ICP-MS instrument with a CH_3F/Ne-pressurized cell, it was demonstrated that with an ICP-tandem mass spectrometer the use of matrix-matched standards is no longer compulsory. The precision attainable (0.05 % RSD – external precision) suffices for many applications and/or for pre-selecting samples prior to high precision isotopic analysis via MC-ICP-MS.

In the last chapter of this PhD dissertation, the combination of the method developed in chapter 6 for Sr isotopic analysis of digested samples and laser ablation sampling for direct analysis of solid samples is reported on (LA-ICP-MS/MS). For the first time ever, direct Sr isotopic analysis of solid samples with high Rb/Sr ratio has been successfully performed. Two sample introduction setups were evaluated in this work, leading to "dry" and "wet" plasma conditions, respectively. NIST SRM 610 has been used for external mass bias correction, without the requirement of a closer matrix-matching. Under "wet" plasma conditions, accurate and precise (0.02 - 0.05 % RSD) $^{87}Sr/^{86}Sr$ isotope ratio results were obtained for seven glass-type geological reference materials. The method developed is a real alternative for the more common approaches dealing with Sr isotopic analysis, as it provides results fast and without the requirement of any sample preparation steps and with minimum sample damage.

Overall, different approaches and reaction gases have been used throughout this PhD work dedicated to an exploration of the capabilities of ICP-MS/MS for accurate ultra-trace elemental and isotopic analysis. From the results of this work, it can be concluded that even for the most demanding applications (those involving very low

analyte concentrations strongly affected by spectral overlap and/or matrix effects), operation of the instrument in MS/MS mode with a mass-shift approach often provides the best results.

Future perspectives

Since its introduction in 2012, the use of ICP-MS/MS has grown very fast, as indicated by the number of scientific publications on the topic published over the years (see **Figure 1**).

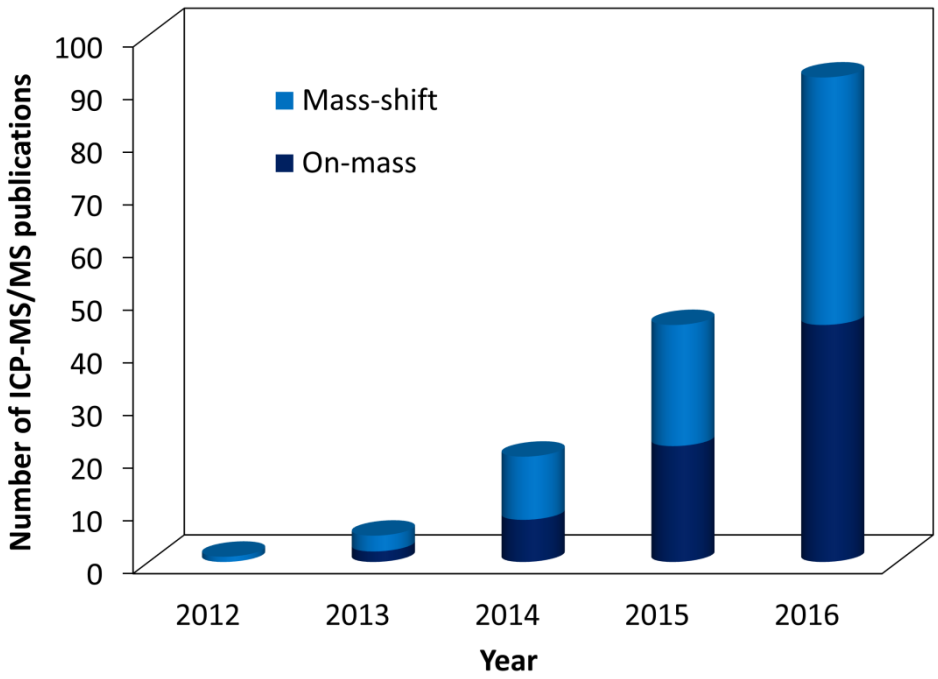

Figure 1. Number of journal publications reporting on the use of on-mass and mass-shift ICP-MS/MS approaches.

The research summarized in this PhD thesis has been carried out shortly after the introduction of the technique (from February 2013 to December 2016), during a period characterized by a strong increase in the number of papers reporting on (the use of) this technique. By means of several research papers and two tutorial reviews, this work has significantly contributed to a more widespread awareness of the attractive features and capabilities of this technique. Nowadays, ICP-MS/MS is a well-stablished and recognized technique allowing one to avoid spectral overlap

even in very complex and challenging situations. Very recently, a second generation of ICP-MS/MS instruments was launched by Agilent Technologies (Agilent 8900 ICP-MS/MS – introduced in 2016), while Thermo Scientific brought its own version of ICP-MS/MS instrumentation (iCAP TQ ICP-MS – introduced in 2017) on the market. Although the evaluation of these new tandem ICP-MS instruments is beyond the scope of this PhD thesis, it is worthwhile to mention some of their main advantages over the 8800 ICP-MS/MS instrument used in this work. One of the main benefits of these new setups is the faster detection capability, providing dwell times as low as 0.1 ms, in contrast with the minimum 3 ms dwell time offered by the Agilent 8800 ICP-MS/MS instrument. A number of applications in which detection speed is crucial, such as nanoparticle analysis and/or laser ablation (LA) ICP-MS imaging, may benefit from this improved characteristic. Another advantage is related with the knowledge acquired on the ion-molecule chemistry occurring within the CRC of an ICP-MS/MS instrument, and the development of on-mass and, especially, mass-shift approaches using different reaction gases during the past couple of years. The newest ICP-MS/MS instrument software incorporates a database enabling the user to select an appropriate approach for every target analyte, almost without requiring any additional method development. Although less interesting from a research point of view, this may allow ICP-MS/MS instrumentation to be used in routine laboratories and by non-expert users.

From the results and conclusions obtained during this PhD thesis, it is clear that tandem ICP-MS is much more than just another quadrupole-based ICP-MS. The challenge ahead now, is to build on the promising first steps of this powerful technique to achieve more universal approaches (e.g., by using other highly reactive gases) to avoid spectral overlap in ICP-MS/MS and/or to further exploit the capabilities of this novel configuration via the use of hyphenated techniques, thus allowing other information (e.g., spatial distribution and/or speciation) to be obtained in a more straightforward way.

Acknowledgments

The fact that I am writing these words means that my PhD is almost finished. I have to admit that this makes me feel strange, as this period of my life is drawing to a close. I have thanked many different people at many different times over these years, and now that it is time to acknowledge them, I even do not know how to start. Perhaps, as in every story, I should start at the beginning, writing about these people and these decisions that definitely changed my life and led me to where I am now. As life is just a series of moments, the first one that put me on this path was definitively the moment that I contacted Ángel about doing a master thesis. After more than 5 years since that decision, I can only say thanks for your kind help and for contacting Esperanza. Espe, you were the key that opened the doors of MARTE to me. I do not know how many times I have said thanks for that, but I would not be here without your help and support. Another special moment was definitely when I entered MARTE for the first time and met Martín. Martín, I have to admit that at that moment I could not imagine how important you would be for me, and in which extent you would change my future. I do not know if it is true that sometimes your signature is present in my scientific decisions, but definitely this can only be a pride for me.

I am not going to go into a lot of detail about my year in MARTE, but I took the very first step in my career there and I will always be just another "marciano". Thanks to all the members of the MARTE research group: Espe, Miguel Ángel, Ana Cris, Maite, Charo, Luis; and also to the new talents: Águeda, Raul and Diego. It was clear at that moment for me that I wanted to do a PhD, but at the same time, I was aware of the difficulties. Now it becomes relevant, but many times during that year I heard Martín talking about “his friend Frank”. I often wondered "who is Frank?", and finally you told me about your friend Frank Vanhaecke, with some anecdotes included – beyond the scope of this acknowledgements section. Another strange feeling right now, I remember that at that moment such name was weird for me, now it sounds very familiar. And this is definitely the key moment, when suddenly, on 8th October 2012, I received this email:

"Hola Eduardo,

He estado en el congreso con mi colega Frank Vanhaecke, de la Universidad de Gante (Bélgica), y él está dispuesto a ofreceros la oportunidad de hacer una tesis doctoral...

Martín”

“Hi Eduardo,

I have been in a conference with my colleague Frank Vanhaecke, from Ghent University (Belgium), and he is willing to give you the opportunity to make your PhD...

Martín"

Frank Vanhaecke? Gent? Belgium? I am still shocked!! I will never say it was easy (as it was necessary to live far from my family and friends), but I can say that it was the correct choice

and a great opportunity, and one that I have never regretted. Frank, I am sure you are the reason for that and I still remember my first time in your office. I was very nervous and doubtful, with a contract for 3 months. Then I told you, “I am not sure whether in 3 months I will be able to demonstrate that I can do my PhD”, and I still remember your answer, very quiet: "do not worry, I am not looking for experts, this is not what a PhD student should be at the beginning". Frank, at this point you already know what I think, but anyway you deserve some words and a large space in this acknowledgment section. You know me, happy and… less happy (only on a few occasions), but you have always been able to get the best out of me and motivate me to do my best. You are actually able to get the best out of everyone. It is not necessary to say that you are a great scientist and promoter, I prefer to say that you are a wonderful person. It has been a pleasure for me to be a member of the A&MS group, and even more importantly, it will be a pleasure for me to continue working with you. Now, I cannot imagine anything else.

Sometimes there are special moments that one only becomes aware of after some time. Already, during my first day in the S12, I also met Lieve. I did not know at that moment, but she would also be a very important part of this story. We shared the same office, but I would say that we bonded around a new instrument (you know, “the recently introduced (2012) Agilent 8800, ICP-MS/MS instrument”). However, it is much more than that. I have worked together with you during 4 years and I have learnt a lot from your experience. You have always been there for whatever I have needed, and this is something I will always appreciate, along with how I will always appreciate you.

These are some special moments, at least, the ones that explain why I am here. However, during these years I have received support from many people, in a large variety of ways.

First and more “official”, I would like to express my gratitude to my promoters, even if it is redundant. Frank, Martín, Lieve, it has been a great pleasure to work with all of you. We formed the ICP-MS/MS team, a nice family. I have always felt that I was one more in that family. You are the reasons why I am here now, especially from a scientific point of view but also from a personal one. There are no words to express my gratitude, I simply wish to thank you very much for everything you have done for me.

I would like to acknowledge all my co-authors and co-workers for everything you taught me and for scientific and non-scientific discussions. It has been a pleasure for me.

I would also like to acknowledge all the members of the A&MS group: Harry, Roger, Marta and Lara (muchas gracias por vuestra amistad desde el principio), Jefferson, Charo (ha pasado ya mucho tiempo desde que me preguntaste si sabía utilizar una micropipeta…, gracias por todo), Andrei, Stijn, Thibaut (my first success as supervisor, it was a pleasure), Winfried, Kris, Asha, Rosa, Steven, Ana (see below), Lana, Yulia, Sanwang, Veerle, Karen,

Agustina, Balazs, Yudi, Stepan (my Russian friend, we miss you), Sara (muchas gracias a mi compañera de oficina). You have created an atmosphere in which it is very easy to work. I wish to thank you all very much.

I also want to acknowledge all members of the Department of Analytical Chemistry, especially Karel, Chantal, Tine, Philip and Jorge, for your kind help and nice moments shared during this time.

Thanks also to all my students over these years, especially Isabel, Elisabeth, Thibaut, Kim (thanks for everything friend) and Dylan. I have learnt from all of you, and I have developed and matured as a scientist and person thanks to your help.

A todos los KAFRES, no os imagináis lo duro que se hace estar lejos de todos vosotros. Ver que pasa el tiempo y no poder disfrutar juntos de tantísimos momentos. Y a pesar del tiempo y de los cambios, vosotros mantenéis todo de la misma forma, y hacéis que cuando vamos a casa podamos sentir que el tiempo apenas ha pasado, y que todo sigue como siempre. No sabéis lo importante y lo difícil que es eso. Saber que cuando sea que volvamos vosotros vais a estar allí, como habéis estado siempre. Gracias.

Y como agradecer a mi familia por todo lo que habéis hecho por mí. Creo que es imposible, y menos aún en unas pocas palabras. Como agradecer a mis padres, Félix y Paquita, de los cuales todavía recuerdo la cara de susto que pusisteis cuando os dije que nos veníamos a Gante por 2 años (y ya van más de 4… de momento). Gracias por apoyarme en todas las decisiones que he tomado y gracias por estar cada día conmigo aunque estemos a más de 1000 Km. Gracias a mi hermano German y a mi cuñada Ana, por muchas cosas durante estos años, pero quizá la más importante, por hacer que a pesar de la distancia podamos disfrutar de Marcos casi todos los días. Gracias a Ana y a Rúa por ser, no una segunda, sino otra primera familia para mi desde hace tantos años. Muchas gracias a todos.

Y aunque ahora no lo puedas entender, también quiero dedicar un trocito de esta tesis para Marcos. Te escribo estas líneas porque sé que algún día podrás entender porque hubo un tiempo en que "tío Eduardo y tía Ana" solo estaban en una pantalla de ordenador, y aunque aparecían de vez en cuando siempre terminaban una y otra vez dentro de esa pantalla. No te imaginas lo difícil que ha sido ver cómo te hacías tan mayor sin poder estar todos los días contigo.

Ana, hay veces que no basta con decir gracias. He utilizado momentos especiales para escribir esta sección, pero los momentos más especiales de todos los vivimos y los compartimos juntos desde hace mucho tiempo. No podría haber escrito esta tesis doctoral sin ti, pero es que nada de lo que hago sería posible sin ti. Sé que un gracias nunca será suficiente, pero al menos déjame agradecerte por estar siempre conmigo.